Structure-Based Design, Synthesis and Evaluation of Novel and Selective Small-Molecule Inhibitors of the Anti-Apoptotic Protein Mcl-1

By

Fardokht Assadi Abulwerdi

A dissertation submitted in partial fulfillment
of the requirements for the degree of
Doctor of Philosophy
(Medicinal Chemistry)
in the University of Michigan
2014

Doctoral Committee:

Assistant Professor Zaneta Nikolovska-Coleska, Co-Chair
Research Professor Hollis D. Showalter, Co-Chair
Associate Professor Jason E. Gestwicki, University of California, San Francisco
Professor Duxin Sun
Professor Shaomeng Wang

*To my late **grandfather** for his love of humanity and kind heart,*

and,

*To my **dearest mother** and **sister** for their unconditional love and support.*

Acknowledgments

As my Ph.D. journey comes to an end, I look back to five years ago when I moved to Ann Arbor, Michigan from Tulsa, Oklahoma, naïve and inexperienced, but determined to do my graduate studies in Medicinal Chemistry. What I did not know was that the next fives years would be one of the most enriching, eye-opening and life-changing periods of my life both professionally and personally. Despite all the hardships, frustrations and numerous failures that I went through during my life and Ph.D. research, I cannot be happier about its outcome. Of course, this sense of satisfaction and fulfillment would have not been possible without the many individuals who have provided me with mentorship, support, friendship, and encouragement and whom I wish to thank.

First and foremost I would like to thank my two fantastic advisors and mentors, Prof. Zaneta Nikolovska-Coleska and Prof. Hollis Showalter, who are not only two scientists of high caliber but are two amazing individuals.

Zaneta, thank you for accepting me in your lab and giving me a project on which I have always wanted to work. Thank you for pushing me to try and learn new techniques and assays despite my initial reservation. I will never forget the numerous hours sometimes late into night that you spent with me discussing the project, providing feedback on my presentations or just simply discussing life matters. I admire your hard work, high standards for conducting research and passion for science and mentorship.

Hollis, thank you for generously opening your lab and agreeing to co-advise me. Thank you for always being there to answer my chemistry questions and discuss new ideas. Your vast knowledge of organic chemistry has been instrumental in moving the project forward and I thank you for sharing that with me. I admire your attention to details, sense of responsibility and your enthusiasm for organic chemistry.

My appreciation goes to three distinguished scientists and members of my dissertation committee, Prof. Jason Gestwicki, Prof. Duxin Sun and Prof. Shaomeng Wang. Your thought-provoking questions and invaluable input greatly helped the direction of the project. I would like

to specially thank Prof. Gestwicki, with whom I had the great opportunity of doing my second rotation, for providing me with several letters of support and his invaluable advice about my professional development.

I had a great fortune of working with hard-working, bright and friendly individuals. I would like to thank past and current members of both of my research labs. From the Nikolovska-Coleska lab, I am especially thankful to Ahmed Mady for all his great work in testing my synthesized compounds in biochemical and cell-based assays as well as our discussions about the project and life matters, Dr. Chenxi Shen for teaching me several biochemical techniques and our nice conversations, Dr. Chenzhong Liao for his molecular docking studies and design input of Mcl-1 inhibitors, Garret Gibbons with whom I had interesting discussion about my project and life in general, Dr. Lei Miao for his advice about chemistry and his cheerful attitude, and Dr. Andrej Perdih for his molecular docking studies as well as his friendship. My thanks also go to past members of the lab: Dr. Julie Di Bernardo, Meilan Liu and Dr. Naval Bajwa. From the Showalter lab, I am thankful to Yafei Jin for teaching me useful chemistry tricks and discussing life matters, Roderick Sorenson for his chemistry advices, Joseph Madak for our interesting conversations, and Dr. Allen Brooks for his helpful suggestions regarding my project.

I would like to thank our collaborator Prof. Tomasz Cierpicki for his help with protein assignment and NMR questions, George Lund from his lab for his great help with NMR experiment setups and questions, Dr. Jennifer Meagher and Krishnapriya Chinnaswamy for their help with protein purification, Dr. Larisa Yeomens for her help with chemistry and 1D NMR questions as well as her friendship, Dr. Hacer Karatas for her helpful advise especially during the first two years of grad school and her friendship, and Dr. Irosha Nawarathne for our interesting conversations and her friendship.

I am also thankful to the Medicinal Chemistry program for giving me an opportunity to do my Ph.D. studies, and my cohort from the program, especially Kamali Sripathi and Meghan Breen for our occasional lunches which provided a chance to catch up and vent about the difficulties of grad school and research, and Dr. Ronald Jenkins for research discussions and his help with my postdoc application.

My life would be boring without my dear friends. I would like to thank two old and dear friends, Azin Asghari and Ghazaleh Eskandari from Iran for their long-time friendships, which I cherish so much, Bedor Alwari, a great friend, I made in Tulsa and the great time I had with her

I believe that the life lessons I learned and the knowledge I gained during the past five years have made me a better person. I will continue to strive for excellence, and I hope to use my acquired skills effectively to help others and make a difference in society.

Table of Contents

Chapter 3. Development of 1*H*-pyrazolo[3,4-b]pyridine analogs as a novel class of Mcl-1 inhibitors 105

Chapter 4. Summary and future directions... 160

Appendix. Development of second-generation 59 inhibitors of Mcl-1 167

List of Figures

List of Schemes

List of Tables

Abstract

The mitochondrial pathway to apoptosis is tightly regulated through the protein-protein interactions of pro- and anti-apoptotic members of Bcl-2 family proteins. The balance of pro- and anti-apoptotic proteins is important in regulating proper cell survival. Overexpression of the anti-apoptotic members such as Mcl-1, Bcl-2 and Bcl-X_L has been observed in cancer, contributing to chemoresistance and aberrant survival. Pro-apoptotic BH3-only proteins normally serve to suppress the anti-apoptotic members. Thus, small molecules mimicking the function of BH3-only proteins, known as BH3 mimetics, have been developed and exhibited anti-cancer activity. Such compounds are being advanced in clinical trials as promising anti-cancer therapeutics. Notably, ABT-737, a selective and potent Bcl-2/Bcl-X_L inhibitor, has shown to be highly efficacious at inducing apoptosis in Bcl-2/Bcl-X_L-dependent cancers, but it is not effective in cancer cells with high Mcl-1 levels. Therefore, Mcl-1 represents an attractive molecular target for the development of a new class of anti-cancer therapy that would be synergistic with ABT-737.

High throughput screening (HTS) approaches were utilized and several small molecules capable of binding Mcl-1 and disrupting its interaction with BH3 peptides were identified. To improve the output and the quality of the HTS hits, as well as to incorporate structure-based knowledge, in silico target-based screening of identified hits was integrated and the most promising inhibitors were selected for further evaluation. In this work, two classes of novel small-molecule Mcl-1 inhibitors were developed based on two HTS leads, **59** bearing a hydroxynaphthalenylsulfonamide scaffold and **38** with a 1*H*-pyrazolo[3,4-b]pyridine scaffold.

Employing structure-based design in conjunction with protein NMR spectroscopy, new analogs were designed, synthesized and SARs were established. Two potent inhibitors, analog **21** ($K_i = 0.180\ \mu$M) from **59** class and **8** ($K_i = 2\ \mu$M) from **38** class, were developed exhibiting 9- and 12-fold improvement over their respective HTS leads. Both analogs exhibited selective inhibition of Mcl-1 over other anti-apoptotic proteins. NMR studies mapped the binding sites of **21** and **8** to the BH3-binding groove of Mcl-1. Analog **21** was further characterized in cell-based assays and

caused cell death in Mcl-1-dependant cancer cell lines through a Bak/Bax-dependent mechanism and activation of caspase-3. Additionally, another potent analog from **59** series, **10**, was used as a chemical tool to validate Mcl-1 as a potential therapeutic target in pancreatic cancer. The efficacy studies showed single-agent anti-tumor activity in a pancreatic cancer xenograft model, demonstrating for the first time the potential use of Mcl-1 inhibitors as a therapeutic strategy for the treatment of human pancreatic cancer. This work provides further understanding in the development of selective Mcl-1 inhibitors and lays a foundation for the design of more potent inhibitors which can advance the field of targeted therapies for Mcl-1-driven cancers.

Chapter 1
Introduction

"Nothing in life is to be feared, it is only to be understood."
Marie Curie (1867-1934)

1.1   Hallmarks of cancer

Cancer is a major health problem worldwide. While numerous challenges are still being faced to identify its origins and develop effective treatments, our understanding of cancer as a genetic disease over a century ago revolutionized the field of cancer research[1]. Cancer research has since turned into a logical science, where the complexities of the disease can be attributed to a number of underlying principles[2]. One set of these principles includes the molecular pathways that govern the transformation of normal cells to a neoplastic state[2]. Hanahan and Weinberg have enumerated the traits normal cells acquire during the multistage tumorigenesis process to a malignant phenotype[2, 3]. These traits or biological capabilities are termed "hallmarks of cancer" (Figure 1.1) and include 1) sustaining proliferative signaling 2) evading growth suppressors 3) resisting cell death 4) enabling replicative immortality 5) inducing angiogenesis and 6) activating invasion and metastasis. More recently and through further extensive mechanistic studies, it has been proposed that the core hallmarks of cancer cells are acquired through two enabling characteristics, namely genome instability and tumor-promoting inflammation[3]. The genome instability of cancer cells refers to the cancer cells evolving genomes being able to acquire mutations that facilitate tumorigenesis[4, 5]. The tumor-promoting inflammation characteristic of cancer cells mediated through the immune system also enhances tumorigenesis and progression by providing the tumor microenviroment with chemicals, such as reactive oxygen species, that are mutagenic to cancer cells and further facilitate their evolution toward malignancy[6, 7]. Furthermore, there are two emerging hallmarks of cancer that have been proposed, but not yet

1

proven to have generality among all cancers. These include reprogramming energy metabolism, which refers to an altered metabolism of neoplastic cells also known as "Warburg effect"[8, 9], and evasion of immune destruction, which is an ability of cancer cells to avoid recognition and elimination by the immune system[10, 11]. Both emerging hallmarks warrant further studies as it is still unclear whether they can be classified as core hallmarks or if their occurrence is a consequence of the aforementioned six core hallmarks.
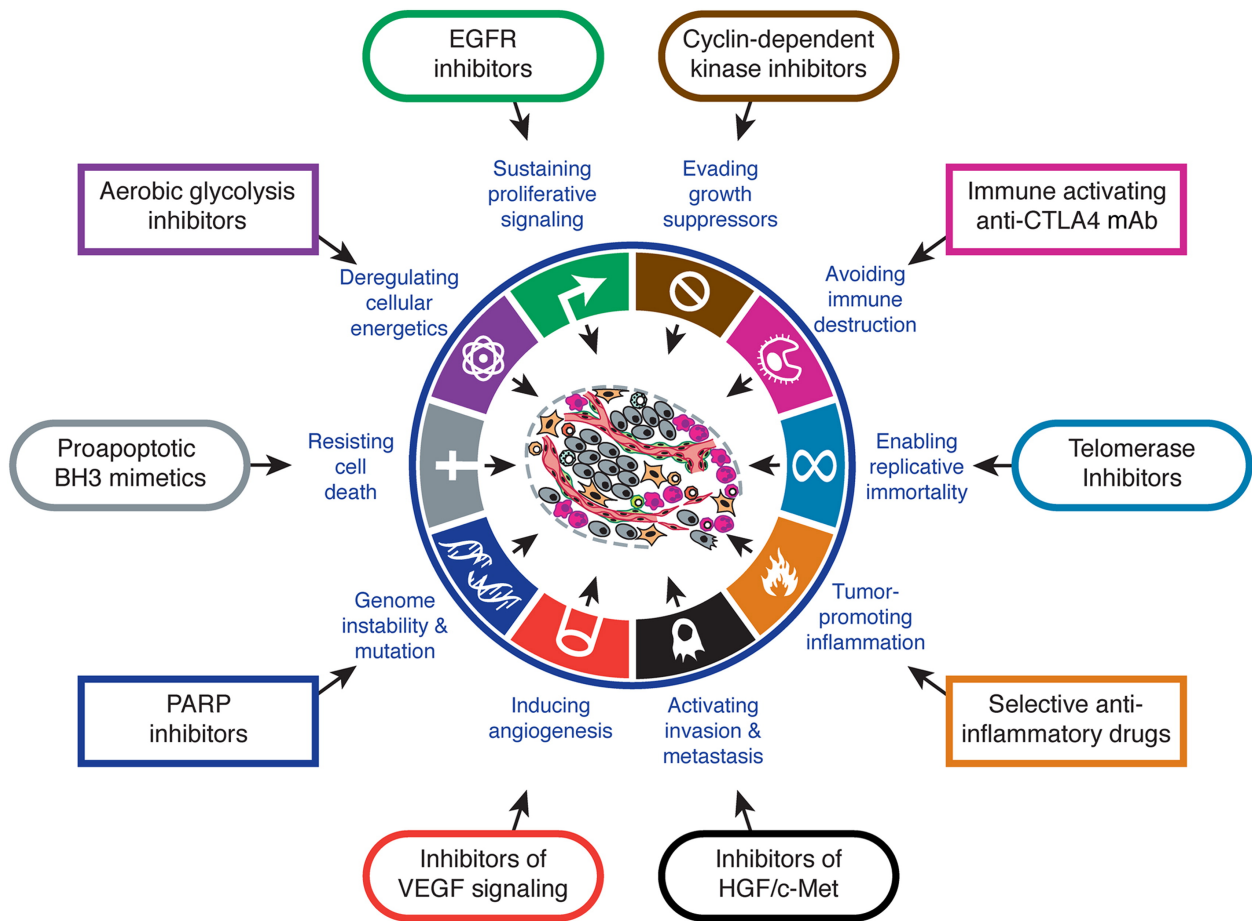
Figure 1.1. Hallmarks of cancer including the enabling ones and therapeutic targeting of the hallmarks.
Figure adapted from Hanahan, D.; Weinberg, R. A., *Cell* 2011, *144* (5), 646-74.

As a result of our increased understanding of the underlying mechanisms of cancer, increasingly more rational mechanism-based targeted therapies have been developed. Indeed, there are targeted therapies interfering with each of the acquired capabilities and even enabling characteristics, and extensive research is being done to target emerging hallmarks[3] (Figure 1.1). One of the therapeutic areas which has been an active area of research and the focus of this

dissertation is the development of molecular-targeted therapies against cancer cells resistance to apoptosis.

1.2 Programed cell death or apoptosis

Apoptosis is a genetically-regulated cell death program distinct from necrosis. The term apoptosis was first coined and described in 1972 by Kerr *et al*[12]. The morphological changes apoptotic cells undergo were described as cell shrinkage, chromatin condensation, and nuclear and cell fragmentation leading to the formation of apoptotic bodies which are eventually taken up by neighboring cells[12]. Apoptosis is essential for embryogenesis, tissue homeostasis and immunity[13] and defects in the process can cause a myriad of diseases: insufficient cell death can lead to cancer and autoimmunity disorders whereas excessive cell death can result in neurodegenerative disorders[14].

Bcl-2 (B-cell lymphoma-2) was the first protein identified to be involved in the regulation of apoptosis. The *Bcl-2* gene at the t(14;18) chromosome translocation breakpoint in B-cell follicular lymphomas was discovered in 1985[15-17]. However, it was not until 1988, that Vaux *et al.* showed that expression of *bcl-2* promoted the survival of haematopoietic cells for extended periods in the absence of growth factors and a combination of oncogene *myc* and *bcl-2* produced tumors in immunocompromised mice[18]. This and other subsequent works[19-21] showed that the mechanism regulating cell death differs from the one regulating cell survival and that overexpression of Bcl-2 inhibits cell death whose impairment is a critical step in tumor development. These key discoveries introduced a new paradigm in carcinogenesis that cancer can be driven by impairment in the process of apoptosis[22] which led to intensive investigations into the regulatory mechanisms that control apoptosis.

In mammals, the execution of apoptosis is governed by two distinct molecular programs that ultimately converge on the activation of caspases, which are intracellular cysteine proteases synthesized as inactive zymogens[22]. The two molecular pathways are the extrinsic pathway operating downstream of death receptors and the intrinsic pathway, which is regulated by the Bcl-2 family of proteins, and is activated by various stress signals[23] (Figure 1.2). The extrinsic or death-receptor pathway is triggered when the so-called death receptors (members of the TNF) such as Fas or TNF receptor-1 (TNFR1) on the cell surface bind to cognate ligands of TNF

family (Figure 1.2). The death receptors, which contain an intracellular death domain, can then activate caspase-8 through adaptor proteins that include Fas-associated death domain (FADD)[24].

Caspase-8 activation can further cause activation of effector caspases such as caspase-3, -6 or -7, without the involvement of the Bcl-2 family[22]. Instances of cross-talk between the intrinsic and extrinsic pathways have been observed in some cells such as hepatocytes in which caspase-8 mediates cleavage and activation of the pro-apoptotic BH3-only protein Bid to its active truncated form (tBid)[25] (Figure 1.2). tBid translocates to mitochondria and causes further caspase activation (caspase-9 and the effector caspases, caspase-3,-6,-7) through the intrinsic pathway[22]. Identification of cytochrome c as an apoptogenic factor released from mitochondria[26] was a key discovery in highlighting the importance of this organelle in the intrinsic pathway of apoptosis[23]. The mitochondrial outer membrane permeabilization (MOMP) is an irreversible process and is the "point of no return" in the intrinsic pathway, which results in the release of cytochrome c[23, 27]. The Bcl-2 family of proteins govern mitochondrial integrity through regulation of MOMP and thereby are the arbiters of cell fate.
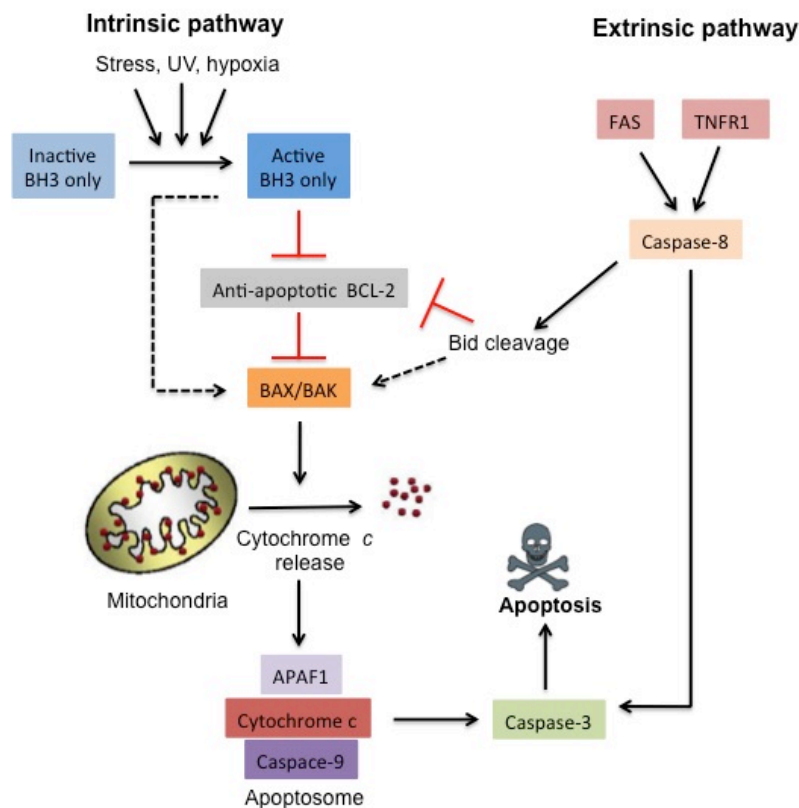
Figure 1.2. Simplified scheme of intrinsic and extrinsic pathways of apoptosis.

4

1.3 Bcl-2 family of proteins in apoptosis

Over 25 Bcl-2 family members have been identified[28, 29]. These can be divided into two classes based on their functions: anti-apoptotic proteins which inhibit apoptosis and pro-apoptotic proteins which promote apoptosis (Figure 1.3). These proteins share sequence homology within a conserved region known as Bcl-2 homology (BH) domains, which are α-helical segments and determine structure and function[23]. Anti-apoptotic members include Bcl-2, Bcl-w, Bcl-X_L, Bcl-b, Bfl-1/A1 and Mcl-1. These share sequence homology within three to four BH domains and generally function to bind and inhibit the pro-apoptotic proteins (Figure 1.3A). The pro-apoptotic Bcl-2 proteins are divided into two subclasses. The first subclass is multi-domain proteins which include Bak, Bax and Bok that share sequence homology within three to four BH domains just like anti-apoptotic proteins (Figure 1.3A). They are absolutely required for MOMP[30, 31]. The second subclass is the BH3-only proteins, including Bad, Bid, Bik, Bim, Noxa and Puma, which as the name suggests show sequence homology only within the α-helical BH3 domain (Figure 1.3B). The BH3-only proteins are expressed in response to distinct cellular stress pathways. For example, stimuli such as DNA damage results in induction of Noxa and Puma by the tumor suppressor p53[32-34]. It is important to note that the BH3 region of pro-apoptotic proteins is responsible for engaging with anti-apoptotic proteins and induction of apoptosis[35] (Figure 1.3C). In addition to BH domains, several Bcl-2 family members possess a C-terminal transmembrane (TM) domain which anchors them to subcellular membranes, including the mitochondrial outer membrane, endoplasmic reticulum (ER) and nuclear membranes[23].
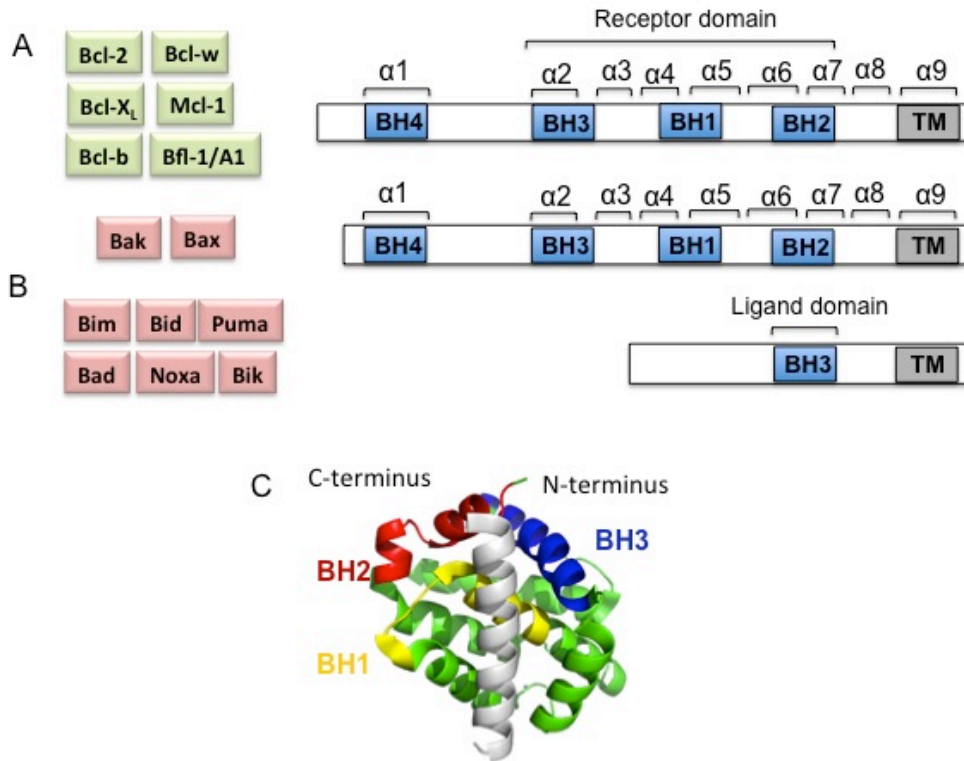
Figure 1.3. The extended Bcl-2 family of proteins. This family comprises of pro-survival proteins (shown in green boxes) and pro-apoptotic proteins (shown in red boxes). (A) Family members sharing four Bcl-2 homology (BH) domains are the multi-domain proteins. A third pro-apoptotic multi-domain protein, Bok, is not well characterized and not shown. (B) Family members displaying only the BH3 domain are the BH3-only proteins. BH3-only proteins are usually unstructured prior to binding pro-survival proteins. (C) crystal structure of Mcl-1 (green) bound to Bim BH3 peptide (white) (PDB 2PQK). Bim BH3 peptide inserts as an α-helix into the BH3-binding site (formed by BH1-BH3) of Mcl-1.

It has been shown that the mode of interaction between anti- and pro-apoptotic proteins includes the binding of the hydrophobic face of the amphipathic α-helical BH3 domain from pro-apoptotic proteins to the hydrophobic cleft formed on the surface of anti-apoptotic proteins through their BH1-3 domains[36-41] (Figure 1.3C). However, the exact nature of protein-protein interactions among the Bcl-2 family proteins that leads to mitochondrial-mediated apoptosis remains controversial.

Historically, two distinct models have been proposed for the protein interactions that regulate the process. Each model takes into account all three classes of the Bcl-2 family of proteins. In the indirect model (Figure 1.4A) of Bak and Bax activation, BH3-only proteins such as Noxa and Bad target anti-apoptotic members releasing the sequestered Bak and Bax[42-45]. These BH3-only proteins are also known as sensitizers. In the direct model (Figure 1.4B), the so-

called activator BH3-only protein, such as Bim, Bid and Puma, can still block the anti-apoptotic members while directly activating the multi-domain pro-apoptotic proteins Bak and Bax[46-52].
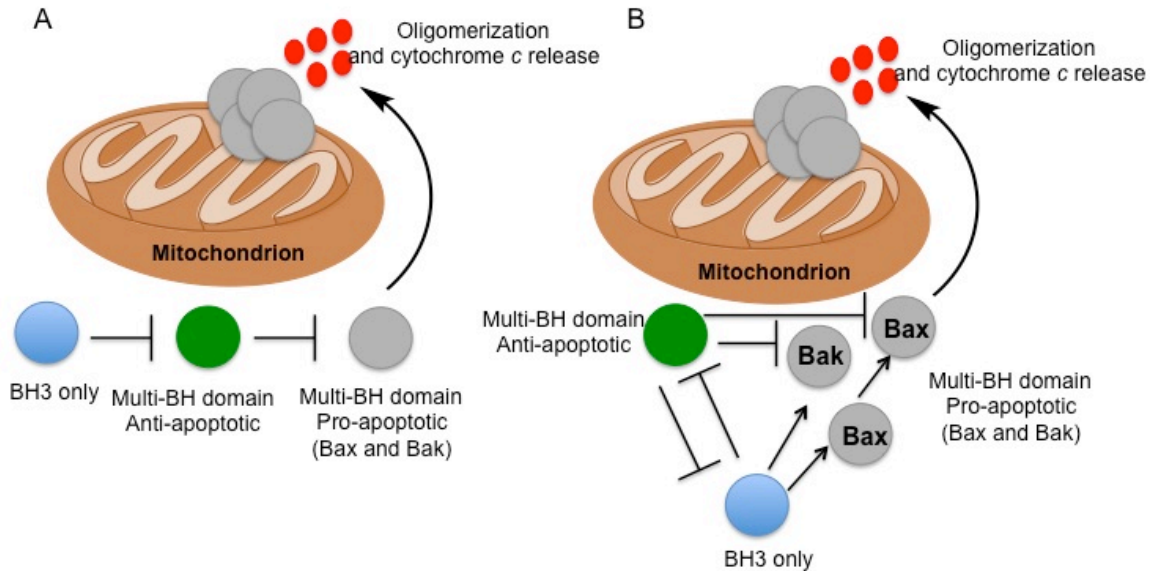
Figure 1.4. Two models by which Bcl-2 family members regulate mitochondrial apoptosis. (A) The indirect model for Bak and Bax activation in which BH3-only proteins inhibit the anti-apoptotic proteins leading to release and activation of Bak and Bax, which can oligomerize and cause MOMP. (B) The direct model for Bak and Bax activation in which BH3-only proteins directly activate Bak and Bax and inhibit the anti-apoptotic proteins to sequester activated forms of Bak and Bax, resulting in their activation and MOMP.

In either case, it is the activation and oligomerization of Bak and Bax which trigger MOMP. Upon MOMP, apoptogenic factors such as cytochrome *c* and Apaf-1 are released from the intermitochondrial membrane to the cytosol[27, 53] (Figure 1.2). Cytochrome *c* and Apaf-1 form a heptameric protein ring called an apoptosome which can bind pro-caspase-9 and activate it[54, 55]. Caspsase 9 then activates the effector caspase-3 which mediates cleavage of critical cellular proteins and execution of cell death[56].

Cancer cells shift the pro- and anti-apoptotic activities of Bcl-2 family members toward survival by genetic and epigenetic changes, altered signaling pathways and post-translational modifications[57]. For example, overexpression of anti-apoptotic Bcl-2, Bcl-X_L and Mcl-1 has been observed in human haematopoietic cancers[58, 59] and a number of solid tumors[60]. Therefore, therapeutic targeting of the Bcl-2 family proteins in cancer has been a priority. However to

develop effective therapeutics against this family, a structural understanding of the interactions between the family members are required.

1.4 Structural analysis of Bcl-2 family interactions

Structural studies of various BH3 domains bound to the BH3-binding site of anti-apoptotic proteins have identified several conserved interactions between the two interacting partners[37, 38, 41, 61-63]. These include four hydrophobic (h1-h4) and a charged residues on the BH3 ligands that form hydrophobic interactions with hydrophobic pockets (p1-p4) and an electrostatic interaction with Arg of anti-apoptotic proteins, respectively (Figure 1.5A). Furthermore, studies using synthetic BH3-only peptides encompassing BH3 domains showed that these domains promote apoptosis[42, 47, 49]. However, distinct peptides have distinct selectivity profiles and effects[42] (Figure 1.5B). While Bad BH3 peptide is selective in binding to Bcl-2, Bcl-X_L, Bcl-w and not Mcl-1, Noxa BH3 peptide selectivity binds only to Mcl-1 and Bfl-1/A1. On the other hand, Bid, Bim, and Puma BH3 peptides are promiscuous binders to all the anti-apoptotic proteins.
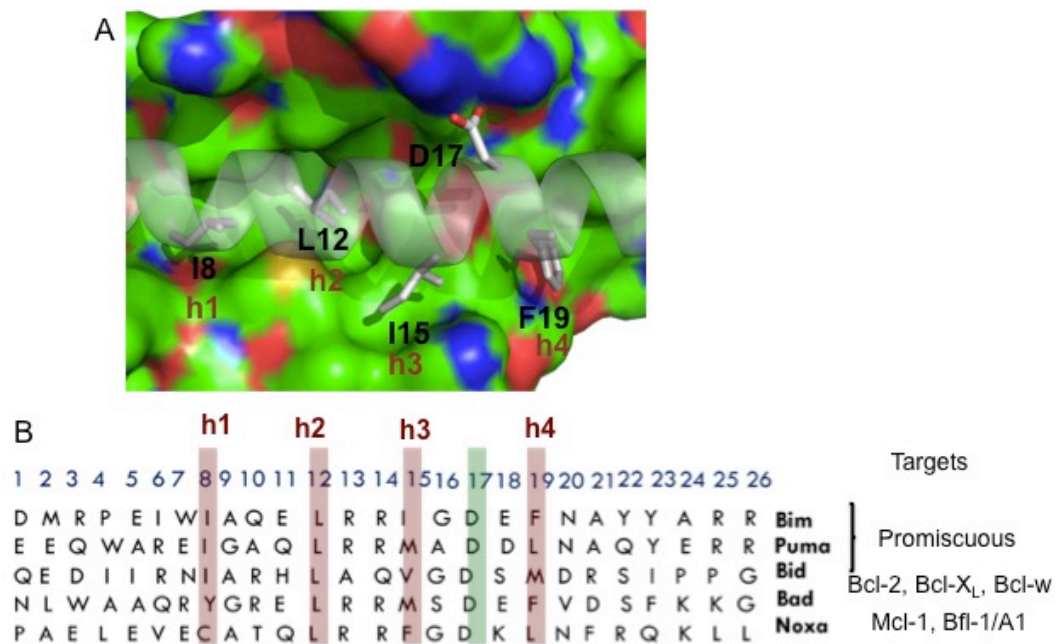
Figure 1.5. Conserved interactions of BH3-only and pro-survival proteins. (A) Bim-BH3 bound to Mcl-1 (PDB 2PQK). The residues shown are the four conserved hydrophobic residues (h1-h4) as well as the conserved aspartate of Bim-BH3 interacting with p1-p4 pockets and Arg of Mcl-1, respectively. (B) Sequences (mostly 26-mers) of BH3-only proteins used to determine their binding selectivity for anti-apoptotic proteins. The canonical four hydrophobic residues are indicated (h1–h4) in red while the conserved aspartate is shown in green.

8

The selectivity profile of the selective BH3-only peptides can be explained based on the differences in the nature of key residues within both the BH3 domain and the BH3-binding site. The Asp residue in the BH3 ligand that is involved in hydrogen bonding with Arg in the BH3-binding site seems to be more important in binding to Mcl-1 than Bcl-X$_L$ because Arg residue is less exposed in Bcl-X$_L$ [64]. Furthermore, the first two hydrophobic pockets (p1 and p2) of Mcl-1 are more constricted and less contiguous upon BH3 ligand binding than Bcl-X$_L$ because the third α-helix is well-formed and less flexible in Mcl-1 than Bcl-X$_L$ [62, 65]. Differences in the BH3 domain of Mcl-1 also change the nature of the p4 pocket making it less well-defined and more solvent-exposed than Bcl-X$_L$ [62, 65]. On the other hand, the promiscuity profile observed for Bid, Bim and Puma BH3-only peptides stems from the similarities shared between the BH3-binding sites of anti-apoptotic proteins due to the sequence homology in their BH1-3 domains as well as the plasticity of both partners to mutually undergo a conformational change upon binding [57].

The detailed structural understanding of the interactions between the pro- and anti-apoptotic proteins paved the way for development of small molecules and peptides targeting the Bcl-2 family protein-protein interactions (PPIs) for cancer therapy.

1.5 Small molecules targeting Bcl-2 family PPIs

PPIs are ubiquitous and important in biological processes such as programed cell death and present great opportunities for therapeutic intervention [66]. However, targeting PPIs by small molecules has been challenging for a number of reasons including large and extended PPI interfaces, lack of presence of defined pockets, and the hydrophobic nature of PPIs. A typical PPI interface encompasses 1500-3000 Å^2, which is a large surface area to be covered by a small molecule (surface area covered by a small molecule is ~300-1000 Å^2) [67]. Unlike enzymes, which have well-defined pockets that can be occupied by endogenous ligands, protein interfaces do not present deep and defined cavities for small molecules to bind. Additionally, due to the hydrophobic nature of protein interfaces, small molecules that tend to bind to these surfaces are large and hydrophobic with poor physicochemical properties [68]. These problems, however, have been addressed through the development of several successful PPI inhibitors.

Alanine scanning and mutagenesis studies of PPIs later showed that there are residues on each of the interacting proteins that contribute significantly to the free energy of binding between

the two partners, which are termed "hot spots" [69-72]. For a small molecule to achieve high affinity for the target and disrupt PPI, it must mimic the hot spots. Secondly, a variety of methods such as peptidomimetic approaches, virtual screening/structure-based design and screening of natural product or synthetic molecules libraries can be used in conjunction with biophysical methods such as nuclear magnetic resonance (NMR) spectroscopy, surface plasmon resonance (SPR), and x-ray crystallography to identify robust PPI small-molecule inhibitors[66, 68], which then can be further modified through medicinal chemistry for improved physicochemical properties.

Early attempts at the discovery of inhibitors of anti-apoptotic proteins included peptidomimetic[73] and high throughput screening approaches[74-76]. The premise in developing inhibitors of anti-apoptotic proteins is to mimic the function of BH3-only proteins to lower the "threshold for apoptosis", defined as the amount of stress imposed on a given cell population to trigger apoptosis. The initially identified small molecule BH3 mimetics are generally pan-inhibitors of all anti-apoptotic proteins with poor affinity for their targets and non-specific mechanism of actions[57, 64]. However, despite poor affinities and exhibition of other mechanism of actions, obatoclax (GX15-070)[77] and a gossypol derivative, TW-37[78], have progressed towards clinical trials. Selective and potent stapled peptides targeting Mcl-1[79, 80] have been developed more recently. However, they have not moved forward beyond preclinical research and have only found use for screen assay development[81].

A major breakthrough by Fesik, Rosenberg and co-workers at Abbott Laboratories came in 2005 with the development of ABT-737[82] (Figure 1.6A) and then its orally bioavailable analog ABT-263[83], also known as navitoclax. ABT-737 was shown to function like a Bad BH3-only protein as it binds and inhibits Bcl-2, Bcl-X_L and Bcl-w but not Mcl-1 or Bfl-1/A1. The first x-ray crystal structure of a non-peptidic ligand to an anti-apoptotic protein was between ABT-737 and Bcl-X_L[84] (Figure 1.6B) which provided the binding mode of the compound and explained its selectivity profile. Chlorobiphenyl and nitrophenyl along with thiophenyl of ABT-737 occupies p2 and p4 of Bcl-X_L, respectively, while the same moieties cannot be accommodated into a more constrained p2 and p4 of Mcl-1[85]. Both ABT-737 and navitoclax required Bax/Bak for cell killing, thus confirming a mechanism-based effect and exhibited potent *in vitro* and *in vivo* antitumor activity[82]. The strategy used in the development of ABT-737 was a combination of NMR-based fragment screen[86] and structure-based design. Navitoclax is currently in phase II clinical trial. However, due to lack of inhibition of Mcl-1, resistance to Mcl-1 can quickly

develop upon treatment with ABT-737[87, 88] and recently the results from phase I study of navitocalx in chronic lymphocytic leukemia (CLL) showed that treatment was not effective when high expression levels of Mcl-1 were present[89]. Therefore, Mcl-1 has become an important resistance factor and a priority for therapeutic intervention.
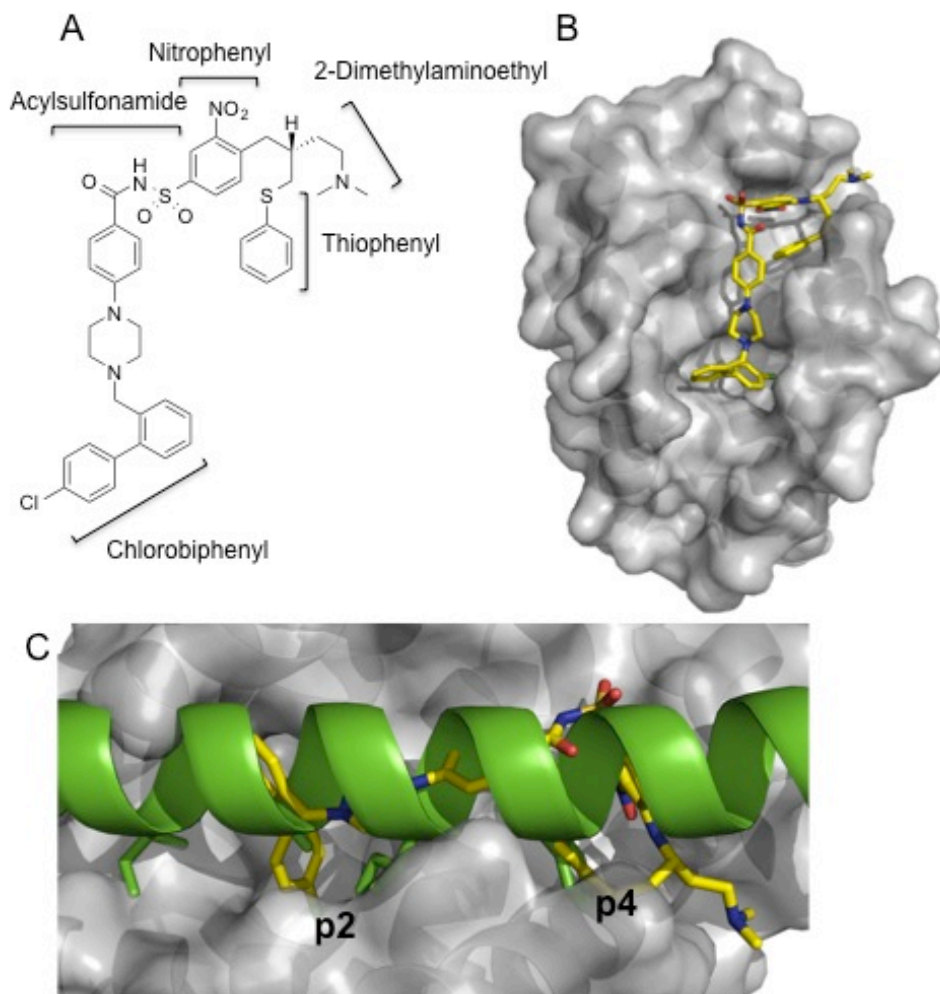
Figure 1.6. Structural studies of ABT-737. (A) Structure of ABT-737. (B) Bcl-X$_L$ bound to ABT-737 (PDB 2YXJ). (C) Overlay of Bcl-X$_L$–ABT-737 complex with Bcl-X$_L$–Bim BH3 complex (PDB 1PQ1). For clarity Bcl-X$_L$ from the BCL-X$_L$–Bim BH3 structure is not displayed in the overlay.

1.6   Targeting Mcl-1 with small molecules

Mcl-1 is among the top ten pathologic factors in a variety of cancers[60] and its overexpression in cancers has emerged as a resistance factor to anti-cancer chemotherapies[90] including ABT-737 as mentioned previously. Pharmacological[77] or genetic downregulation[91] of Mcl-1 has shown to

11

be sufficient to overcome Mcl-1-mediated resistance. Thus, Mcl-1 is an attractive therapeutic target for cancer therapy and has been the subject of intensive research over the past few years. However, development of Mcl-1 inhibitors has not been trivial due to the similarity of its BH3-binding site to other anti-apoptotic members and it's plasticity preventing its crystallization with small molecules, and despite successful attempts, nothing has entered into clinical trials.

Among several reports over the past few years on the discovery of small molecule Mcl-1 inhibitors[81, 92-98], only four can be pointed out as robust inhibitors because they have been extensively characterized. **UMI-77**[96] (Figure 1.7) with a K_i = 490 nM against Mcl-1 was developed in our lab. This compound selectively inhibits Mcl-1 over other anti-apoptotic members and is a more potent analog of a HTS lead **59** discussed in Chapter 2. **UMI-77** inhibited cell growth and induced apoptosis in pancreatic cancer cells accompanied by cytochrome *c* release and caspase-3 activation. Furthermore, studies in *in vivo* pancreatic xenograft model showed that **UMI-77** effectively inhibited tumor growth. **MIM1**[81] (Figure 1.7), identified from a HTS of a library of small molecules using a selective fluorescently-labeled Mcl-1 stapled peptide, binds Mcl-1 in low micromolar range. **MIM1** showed to bind to Mcl-1 and release Bax, trigger the death of Mcl-1- dependent cells and synergize with ABT-737 to kill cells that express both Mcl-1 and Bcl-X$_L$. Friberg *et al*. reported compound **53** (Figure 1.7) which was developed through a similar method of NMR-based fragment screen used to develop ABT-737[97]. **53** is a potent and selective inhibitor of Mcl-1 and led to the first crystal structure of Mcl-1 bound to a non-peptidic small molecule. The crystal structure of Mcl-1 bound to **53** was a significant accomplishment as flexibility of Mcl-1 has been a major hurdle for its crystallization and structure-based design of novel inhibitors. Finally, compound **11** (Figure 1.7), published recently by Takeda Pharmaceutical[98], is a dual inhibitor of Mcl-1 and Bcl-X$_L$ and was discovered by a hybridization strategy linking a Mcl-1 small-molecule inhibitor similar in structure to compound **53** to a portion of ABT-737 structure that binds the p4 of Bcl-X$_L$. A crystal structure of an analog of **11** bound to Mcl-1 and Bcl-X$_L$ confirmed its mode of binding to these anti-apoptotic proteins. The activities of both compounds **53** and **11** have been limited to *in vitro* assays and their use in cells and animal models is yet to be studied. While the development of these four Mcl-1 inhibitors clearly suggest that access to selective and potent small molecules against Mcl-1 is not out of reach, their low micromolar to high nanomolar affinities make them non-ideal for

extensive cell-based and *in vivo* efficacy studies and further optimization is needed to improve potency and selectivity of these compounds.
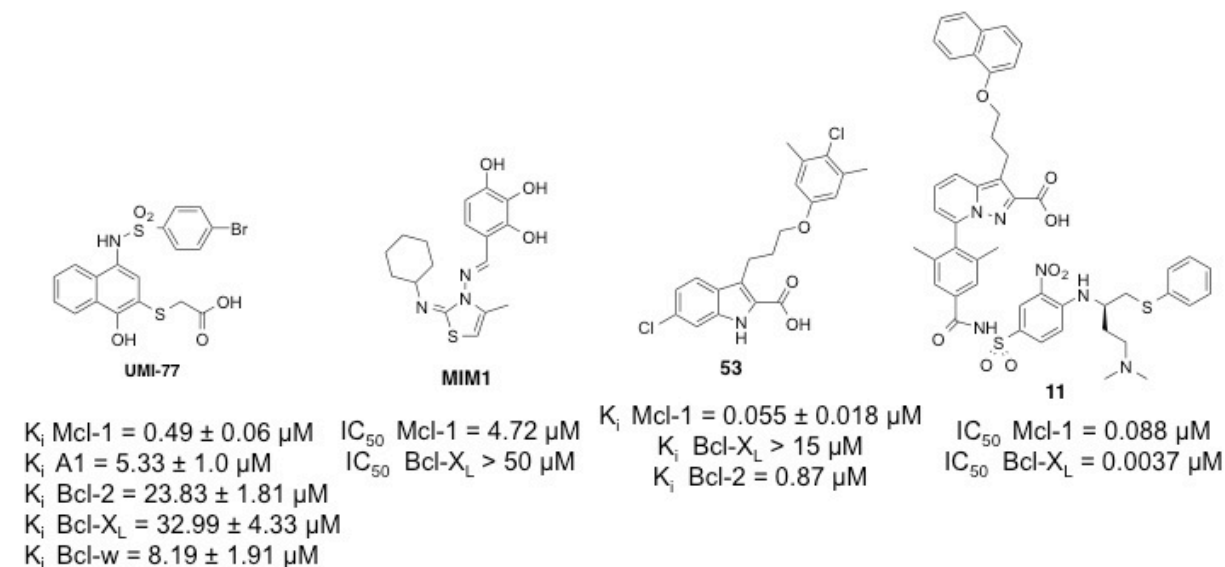
Figure 1.7. Structures and binding affinities of **UMI-77**, **MIM1**, **53**, and **11**.

It still is not clear whether targeting all anti-apoptotic family members or a subset of them is beneficial in cancer therapy. Additionally, it is still debated whether the activation model (indirect or direct) of Bak/Bax exists and if there is one which is dominant in some cancers versus others. Such questions can only be answered by having access to a wide variety of potent inhibitors with different selectivity profiles. These inhibitors can also serve as useful tools to better understand the biology and role of anti- and pro- apoptotic proteins in cancer and normal physiology.

1.7   References

1.   Marte, B. Milestone 2-cancer as a genetic disease *Nat Rev Cancer* **2006,** 6, S8.
2.   Hanahan, D.; Weinberg, R. A. The hallmarks of cancer. *Cell* **2000,** 100, 57-70.
3.   Hanahan, D.; Weinberg, R. A. Hallmarks of cancer: the next generation. *Cell* **2011,** 144, 646-74.
4.   Negrini, S.; Gorgoulis, V. G.; Halazonetis, T. D. Genomic instability--an evolving hallmark of cancer. *Nat Rev Mol Cell Biol* **2010,** 11, 220-8.
5.   Salk, J. J.; Fox, E. J.; Loeb, L. A. Mutational heterogeneity in human cancers: origin and consequences. *Annu Rev Pathol* **2010,** 5, 51-75.
6.   Colotta, F.; Allavena, P.; Sica, A.; Garlanda, C.; Mantovani, A. Cancer-related inflammation, the seventh hallmark of cancer: links to genetic instability. *Carcinogenesis* **2009,** 30, 1073-81.
7.   Grivennikov, S. I.; Greten, F. R.; Karin, M. Immunity, inflammation, and cancer. *Cell* **2010,** 140, 883-99.
8.   Warburg, O. On the origin of cancer cells. *Science* **1956,** 123, 309-14.
9.   Warburg, O. On respiratory impairment in cancer cells. *Science* **1956,** 124, 269-70.
10.   Teng, M. W.; Swann, J. B.; Koebel, C. M.; Schreiber, R. D.; Smyth, M. J. Immune-mediated dormancy: an equilibrium with cancer. *J Leukoc Biol* **2008,** 84, 988-93.
11.   Kim, R.; Emi, M.; Tanabe, K. Cancer immunoediting from immune surveillance to immune escape. *Immunology* **2007,** 121, 1-14.
12.   Kerr, J. F.; Wyllie, A. H.; Currie, A. R. Apoptosis: a basic biological phenomenon with wide-ranging implications in tissue kinetics. *Br J Cancer* **1972,** 26, 239-57.
13.   Adams, J. M.; Cory, S. The Bcl-2 apoptotic switch in cancer development and therapy. *Oncogene* **2007,** 26, 1324-37.
14.   Walensky, L. D. BCL-2 in the crosshairs: tipping the balance of life and death. *Cell Death Differ* **2006,** 13, 1339-50.
15.   Tsujimoto, Y.; Gorham, J.; Cossman, J.; Jaffe, E.; Croce, C. M. The t(14;18) chromosome translocations involved in B-cell neoplasms result from mistakes in VDJ joining. *Science* **1985,** 229, 1390-3.
16.   Cleary, M. L.; Sklar, J. Nucleotide sequence of a t(14;18) chromosomal breakpoint in follicular lymphoma and demonstration of a breakpoint-cluster region near a transcriptionally active locus on chromosome 18. *Proc Natl Acad Sci U S A* **1985,** 82, 7439-43.
17.   Bakhshi, A.; Jensen, J. P.; Goldman, P.; Wright, J. J.; McBride, O. W.; Epstein, A. L.; Korsmeyer, S. J. Cloning the chromosomal breakpoint of t(14;18) human lymphomas: clustering around JH on chromosome 14 and near a transcriptional unit on 18. *Cell* **1985,** 41, 899-906.
18.   Vaux, D. L.; Cory, S.; Adams, J. M. Bcl-2 gene promotes haemopoietic cell survival and cooperates with c-myc to immortalize pre-B cells. *Nature* **1988,** 335, 440-2.
19.   Reed, J. C.; Cuddy, M.; Slabiak, T.; Croce, C. M.; Nowell, P. C. Oncogenic potential of bcl-2 demonstrated by gene transfer. *Nature* **1988,** 336, 259-61.
20.   McDonnell, T. J.; Deane, N.; Platt, F. M.; Nunez, G.; Jaeger, U.; McKearn, J. P.; Korsmeyer, S. J. bcl-2-immunoglobulin transgenic mice demonstrate extended B cell survival and follicular lymphoproliferation. *Cell* **1989,** 57, 79-88.

21. Tsujimoto, Y. Stress-resistance conferred by high level of bcl-2 alpha protein in human B lymphoblastoid cell. *Oncogene* **1989,** 4, 1331-6.

22. Youle, R. J.; Strasser, A. The BCL-2 protein family: opposing activities that mediate cell death. *Nat Rev Mol Cell Biol* **2008,** 9, 47-59.

23. Danial, N. N. BCL-2 family proteins: critical checkpoints of apoptotic cell death. *Clin Cancer Res* **2007,** 13, 7254-63.

24. Thornberry, N. A.; Lazebnik, Y. Caspases: enemies within. *Science* **1998,** 281, 1312-6.

25. Yin, X. M.; Wang, K.; Gross, A.; Zhao, Y.; Zinkel, S.; Klocke, B.; Roth, K. A.; Korsmeyer, S. J. Bid-deficient mice are resistant to Fas-induced hepatocellular apoptosis. *Nature* **1999,** 400, 886-91.

26. Li, P.; Nijhawan, D.; Budihardjo, I.; Srinivasula, S. M.; Ahmad, M.; Alnemri, E. S.; Wang, X. Cytochrome c and dATP-dependent formation of Apaf-1/caspase-9 complex initiates an apoptotic protease cascade. *Cell* **1997,** 91, 479-89.

27. Chipuk, J. E.; Bouchier-Hayes, L.; Green, D. R. Mitochondrial outer membrane permeabilization during apoptosis: the innocent bystander scenario. *Cell Death Differ* **2006,** 13, 1396-402.

28. Adams, J. M.; Cory, S. The Bcl-2 protein family: arbiters of cell survival. *Science* **1998,** 281, 1322-6.

29. Reed, J. C. Mechanisms of apoptosis. *Am J Pathol* **2000,** 157, 1415-30.

30. Lindsten, T.; Ross, A. J.; King, A.; Zong, W. X.; Rathmell, J. C.; Shiels, H. A.; Ulrich, E.; Waymire, K. G.; Mahar, P.; Frauwirth, K.; Chen, Y.; Wei, M.; Eng, V. M.; Adelman, D. M.; Simon, M. C.; Ma, A.; Golden, J. A.; Evan, G.; Korsmeyer, S. J.; MacGregor, G. R.; Thompson, C. B. The combined functions of proapoptotic Bcl-2 family members bak and bax are essential for normal development of multiple tissues. *Mol Cell* **2000,** 6, 1389-99.

31. Wei, M. C.; Zong, W. X.; Cheng, E. H.; Lindsten, T.; Panoutsakopoulou, V.; Ross, A. J.; Roth, K. A.; MacGregor, G. R.; Thompson, C. B.; Korsmeyer, S. J. Proapoptotic BAX and BAK: a requisite gateway to mitochondrial dysfunction and death. *Science* **2001,** 292, 727-30.

32. Oda, E.; Ohki, R.; Murasawa, H.; Nemoto, J.; Shibue, T.; Yamashita, T.; Tokino, T.; Taniguchi, T.; Tanaka, N. Noxa, a BH3-only member of the Bcl-2 family and candidate mediator of p53-induced apoptosis. *Science* **2000,** 288, 1053-8.

33. Nakano, K.; Vousden, K. H. PUMA, a novel proapoptotic gene, is induced by p53. *Mol Cell* **2001,** 7, 683-94.

34. Yu, J.; Zhang, L.; Hwang, P. M.; Kinzler, K. W.; Vogelstein, B. PUMA induces the rapid apoptosis of colorectal cancer cells. *Mol Cell* **2001,** 7, 673-82.

35. Chittenden, T.; Flemington, C.; Houghton, A. B.; Ebb, R. G.; Gallo, G. J.; Elangovan, B.; Chinnadurai, G.; Lutz, R. J. A conserved domain in Bak, distinct from BH1 and BH2, mediates cell death and protein binding functions. *EMBO J* **1995,** 14, 5589-96.

36. Muchmore, S. W.; Sattler, M.; Liang, H.; Meadows, R. P.; Harlan, J. E.; Yoon, H. S.; Nettesheim, D.; Chang, B. S.; Thompson, C. B.; Wong, S. L.; Ng, S. L.; Fesik, S. W. X-ray and NMR structure of human Bcl-xL, an inhibitor of programmed cell death. *Nature* **1996,** 381, 335-41.

37. Sattler, M.; Liang, H.; Nettesheim, D.; Meadows, R. P.; Harlan, J. E.; Eberstadt, M.; Yoon, H. S.; Shuker, S. B.; Chang, B. S.; Minn, A. J.; Thompson, C. B.; Fesik, S. W.

Structure of Bcl-xL-Bak peptide complex: recognition between regulators of apoptosis. *Science* **1997,** 275, 983-6.

38. Petros, A. M.; Nettesheim, D. G.; Wang, Y.; Olejniczak, E. T.; Meadows, R. P.; Mack, J.; Swift, K.; Matayoshi, E. D.; Zhang, H.; Thompson, C. B.; Fesik, S. W. Rationale for Bcl-xL/Bad peptide complex formation from structure, mutagenesis, and biophysical studies. *Protein Sci* **2000,** 9, 2528-34.

39. Petros, A. M.; Medek, A.; Nettesheim, D. G.; Kim, D. H.; Yoon, H. S.; Swift, K.; Matayoshi, E. D.; Oltersdorf, T.; Fesik, S. W. Solution structure of the antiapoptotic protein bcl-2. *Proc Natl Acad Sci U S A* **2001,** 98, 3012-7.

40. Hinds, M. G.; Lackmann, M.; Skea, G. L.; Harrison, P. J.; Huang, D. C.; Day, C. L. The structure of Bcl-w reveals a role for the C-terminal residues in modulating biological activity. *EMBO J* **2003,** 22, 1497-507.

41. Day, C. L.; Chen, L.; Richardson, S. J.; Harrison, P. J.; Huang, D. C.; Hinds, M. G. Solution structure of prosurvival Mcl-1 and characterization of its binding by proapoptotic BH3-only ligands. *J Biol Chem* **2005,** 280, 4738-44.

42. Chen, L.; Willis, S. N.; Wei, A.; Smith, B. J.; Fletcher, J. I.; Hinds, M. G.; Colman, P. M.; Day, C. L.; Adams, J. M.; Huang, D. C. Differential targeting of prosurvival Bcl-2 proteins by their BH3-only ligands allows complementary apoptotic function. *Mol Cell* **2005,** 17, 393-403.

43. Willis, S. N.; Chen, L.; Dewson, G.; Wei, A.; Naik, E.; Fletcher, J. I.; Adams, J. M.; Huang, D. C. Proapoptotic Bak is sequestered by Mcl-1 and Bcl-xL, but not Bcl-2, until displaced by BH3-only proteins. *Genes Dev* **2005,** 19, 1294-305.

44. Willis, S. N.; Fletcher, J. I.; Kaufmann, T.; van Delft, M. F.; Chen, L.; Czabotar, P. E.; Ierino, H.; Lee, E. F.; Fairlie, W. D.; Bouillet, P.; Strasser, A.; Kluck, R. M.; Adams, J. M.; Huang, D. C. Apoptosis initiated when BH3 ligands engage multiple Bcl-2 homologs, not Bax or Bak. *Science* **2007,** 315, 856-9.

45. Uren, R. T.; Dewson, G.; Chen, L.; Coyne, S. C.; Huang, D. C.; Adams, J. M.; Kluck, R. M. Mitochondrial permeabilization relies on BH3 ligands engaging multiple prosurvival Bcl-2 relatives, not Bak. *J Cell Biol* **2007,** 177, 277-87.

46. Cheng, E. H.; Wei, M. C.; Weiler, S.; Flavell, R. A.; Mak, T. W.; Lindsten, T.; Korsmeyer, S. J. BCL-2, BCL-X(L) sequester BH3 domain-only molecules preventing BAX- and BAK-mediated mitochondrial apoptosis. *Mol Cell* **2001,** 8, 705-11.

47. Letai, A.; Bassik, M. C.; Walensky, L. D.; Sorcinelli, M. D.; Weiler, S.; Korsmeyer, S. J. Distinct BH3 domains either sensitize or activate mitochondrial apoptosis, serving as prototype cancer therapeutics. *Cancer Cell* **2002,** 2, 183-92.

48. Wei, M. C.; Lindsten, T.; Mootha, V. K.; Weiler, S.; Gross, A.; Ashiya, M.; Thompson, C. B.; Korsmeyer, S. J. tBID, a membrane-targeted death ligand, oligomerizes BAK to release cytochrome c. *Genes Dev* **2000,** 14, 2060-71.

49. Kuwana, T.; Bouchier-Hayes, L.; Chipuk, J. E.; Bonzon, C.; Sullivan, B. A.; Green, D. R.; Newmeyer, D. D. BH3 domains of BH3-only proteins differentially regulate Bax-mediated mitochondrial membrane permeabilization both directly and indirectly. *Mol Cell* **2005,** 17, 525-35.

50. Lovell, J. F.; Billen, L. P.; Bindner, S.; Shamas-Din, A.; Fradin, C.; Leber, B.; Andrews, D. W. Membrane binding by tBid initiates an ordered series of events culminating in membrane permeabilization by Bax. *Cell* **2008,** 135, 1074-84.

51. Walensky, L. D.; Pitter, K.; Morash, J.; Oh, K. J.; Barbuto, S.; Fisher, J.; Smith, E.; Verdine, G. L.; Korsmeyer, S. J. A stapled BID BH3 helix directly binds and activates BAX. *Mol Cell* **2006,** 24, 199-210.

52. Moldoveanu, T.; Grace, C. R.; Llambi, F.; Nourse, A.; Fitzgerald, P.; Gehring, K.; Kriwacki, R. W.; Green, D. R. BID-induced structural changes in BAK promote apoptosis. *Nat Struct Mol Biol* **2013,** 20, 589-97.

53. Newmeyer, D. D.; Ferguson-Miller, S. Mitochondria: releasing power for life and unleashing the machineries of death. *Cell* **2003,** 112, 481-90.

54. Shi, Y. Mechanical aspects of apoptosome assembly. *Curr Opin Cell Biol* **2006,** 18, 677-84.

55. Riedl, S. J.; Salvesen, G. S. The apoptosome: signalling platform of cell death. *Nat Rev Mol Cell Biol* **2007,** 8, 405-13.

56. Shi, Y. Mechanisms of caspase activation and inhibition during apoptosis. *Mol Cell* **2002,** 9, 459-70.

57. Juin, P.; Geneste, O.; Gautier, F.; Depil, S.; Campone, M. Decoding and unlocking the BCL-2 dependency of cancer cells. *Nat Rev Cancer* **2013,** 13, 455-65.

58. Aqeilan, R. I.; Calin, G. A.; Croce, C. M. miR-15a and miR-16-1 in cancer: discovery, function and future perspectives. *Cell Death Differ* **2010,** 17, 215-20.

59. Garzon, R.; Heaphy, C. E.; Havelange, V.; Fabbri, M.; Volinia, S.; Tsao, T.; Zanesi, N.; Kornblau, S. M.; Marcucci, G.; Calin, G. A.; Andreeff, M.; Croce, C. M. MicroRNA 29b functions in acute myeloid leukemia. *Blood* **2009,** 114, 5331-41.

60. Beroukhim, R.; Mermel, C. H.; Porter, D.; Wei, G.; Raychaudhuri, S.; Donovan, J.; Barretina, J.; Boehm, J. S.; Dobson, J.; Urashima, M.; Mc Henry, K. T.; Pinchback, R. M.; Ligon, A. H.; Cho, Y. J.; Haery, L.; Greulich, H.; Reich, M.; Winckler, W.; Lawrence, M. S.; Weir, B. A.; Tanaka, K. E.; Chiang, D. Y.; Bass, A. J.; Loo, A.; Hoffman, C.; Prensner, J.; Liefeld, T.; Gao, Q.; Yecies, D.; Signoretti, S.; Maher, E.; Kaye, F. J.; Sasaki, H.; Tepper, J. E.; Fletcher, J. A.; Tabernero, J.; Baselga, J.; Tsao, M. S.; Demichelis, F.; Rubin, M. A.; Janne, P. A.; Daly, M. J.; Nucera, C.; Levine, R. L.; Ebert, B. L.; Gabriel, S.; Rustgi, A. K.; Antonescu, C. R.; Ladanyi, M.; Letai, A.; Garraway, L. A.; Loda, M.; Beer, D. G.; True, L. D.; Okamoto, A.; Pomeroy, S. L.; Singer, S.; Golub, T. R.; Lander, E. S.; Getz, G.; Sellers, W. R.; Meyerson, M. The landscape of somatic copy-number alteration across human cancers. *Nature* **2010,** 463, 899-905.

61. Liu, X.; Dai, S.; Zhu, Y.; Marrack, P.; Kappler, J. W. The structure of a Bcl-xL/Bim fragment complex: implications for Bim function. *Immunity* **2003,** 19, 341-52.

62. Czabotar, P. E.; Lee, E. F.; van Delft, M. F.; Day, C. L.; Smith, B. J.; Huang, D. C.; Fairlie, W. D.; Hinds, M. G.; Colman, P. M. Structural insights into the degradation of Mcl-1 induced by BH3 domains. *Proc Natl Acad Sci U S A* **2007,** 104, 6217-22.

63. Fire, E.; Gulla, S. V.; Grant, R. A.; Keating, A. E. Mcl-1-Bim complexes accommodate surprising point mutations via minor structural changes. *Protein Sci* **2010,** 19, 507-19.

64. Lessene, G.; Czabotar, P. E.; Colman, P. M. BCL-2 family antagonists for cancer therapy. *Nat Rev Drug Discov* **2008,** 7, 989-1000.

65. Yang, C. Y.; Wang, S. M. Analysis of Flexibility and Hotspots in Bcl-xL and Mcl-1 Proteins for the Design of Selective Small-Molecule Inhibitors. *Acs Medicinal Chemistry Letters* **2012,** 3, 308-312.

66. Arkin, M. R.; Wells, J. A. Small-molecule inhibitors of protein-protein interactions: progressing towards the dream. *Nat Rev Drug Discov* **2004,** 3, 301-17.

67. Wells, J. A.; McClendon, C. L. Reaching for high-hanging fruit in drug discovery at protein-protein interfaces. *Nature* **2007,** 450, 1001-9.

68. Arkin, M. Protein-protein interactions and cancer: small molecules going in for the kill. *Curr Opin Chem Biol* **2005,** 9, 317-24.

69. Bogan, A. A.; Thorn, K. S. Anatomy of hot spots in protein interfaces. *J Mol Biol* **1998,** 280, 1-9.

70. Clackson, T.; Wells, J. A. A hot spot of binding energy in a hormone-receptor interface. *Science* **1995,** 267, 383-6.

71. DeLano, W. L. Unraveling hot spots in binding interfaces: progress and challenges. *Curr Opin Struct Biol* **2002,** 12, 14-20.

72. Ma, B.; Elkayam, T.; Wolfson, H.; Nussinov, R. Protein-protein interactions: structurally conserved residues distinguish between binding sites and exposed protein surfaces. *Proc Natl Acad Sci U S A* **2003,** 100, 5772-7.

73. Kutzki, O.; Park, H. S.; Ernst, J. T.; Orner, B. P.; Yin, H.; Hamilton, A. D. Development of a potent Bcl-x(L) antagonist based on alpha-helix mimicry. *J Am Chem Soc* **2002,** 124, 11838-9.

74. Wang, J. L.; Liu, D.; Zhang, Z. J.; Shan, S.; Han, X.; Srinivasula, S. M.; Croce, C. M.; Alnemri, E. S.; Huang, Z. Structure-based discovery of an organic compound that binds Bcl-2 protein and induces apoptosis of tumor cells. *Proc Natl Acad Sci U S A* **2000,** 97, 7124-9.

75. Enyedy, I. J.; Ling, Y.; Nacro, K.; Tomita, Y.; Wu, X.; Cao, Y.; Guo, R.; Li, B.; Zhu, X.; Huang, Y.; Long, Y. Q.; Roller, P. P.; Yang, D.; Wang, S. Discovery of small-molecule inhibitors of Bcl-2 through structure-based computer screening. *J Med Chem* **2001,** 44, 4313-24.

76. Degterev, A.; Lugovskoy, A.; Cardone, M.; Mulley, B.; Wagner, G.; Mitchison, T.; Yuan, J. Identification of small-molecule inhibitors of interaction between the BH3 domain and Bcl-xL. *Nat Cell Biol* **2001,** 3, 173-82.

77. Nguyen, M.; Marcellus, R. C.; Roulston, A.; Watson, M.; Serfass, L.; Murthy Madiraju, S. R.; Goulet, D.; Viallet, J.; Belec, L.; Billot, X.; Acoca, S.; Purisima, E.; Wiegmans, A.; Cluse, L.; Johnstone, R. W.; Beauparlant, P.; Shore, G. C. Small molecule obatoclax (GX15-070) antagonizes MCL-1 and overcomes MCL-1-mediated resistance to apoptosis. *Proc Natl Acad Sci U S A* **2007,** 104, 19512-7.

78. Wang, G.; Nikolovska-Coleska, Z.; Yang, C. Y.; Wang, R.; Tang, G.; Guo, J.; Shangary, S.; Qiu, S.; Gao, W.; Yang, D.; Meagher, J.; Stuckey, J.; Krajewski, K.; Jiang, S.; Roller, P. P.; Abaan, H. O.; Tomita, Y.; Wang, S. Structure-based design of potent small-molecule inhibitors of anti-apoptotic Bcl-2 proteins. *J Med Chem* **2006,** 49, 6139-42.

79. Stewart, M. L.; Fire, E.; Keating, A. E.; Walensky, L. D. The MCL-1 BH3 helix is an exclusive MCL-1 inhibitor and apoptosis sensitizer. *Nat Chem Biol* **2010,** 6, 595-601.

80. Muppidi, A.; Doi, K.; Edwardraja, S.; Drake, E. J.; Gulick, A. M.; Wang, H. G.; Lin, Q. Rational design of proteolytically stable, cell-permeable peptide-based selective Mcl-1 inhibitors. *J Am Chem Soc* **2012,** 134, 14734-7.

81. Cohen, N. A.; Stewart, M. L.; Gavathiotis, E.; Tepper, J. L.; Bruekner, S. R.; Koss, B.; Opferman, J. T.; Walensky, L. D. A competitive stapled peptide screen identifies a

selective small molecule that overcomes MCL-1-dependent leukemia cell survival. *Chem Biol* **2012,** 19, 1175-86.

82. Oltersdorf, T.; Elmore, S. W.; Shoemaker, A. R.; Armstrong, R. C.; Augeri, D. J.; Belli, B. A.; Bruncko, M.; Deckwerth, T. L.; Dinges, J.; Hajduk, P. J.; Joseph, M. K.; Kitada, S.; Korsmeyer, S. J.; Kunzer, A. R.; Letai, A.; Li, C.; Mitten, M. J.; Nettesheim, D. G.; Ng, S.; Nimmer, P. M.; O'Connor, J. M.; Oleksijew, A.; Petros, A. M.; Reed, J. C.; Shen, W.; Tahir, S. K.; Thompson, C. B.; Tomaselli, K. J.; Wang, B.; Wendt, M. D.; Zhang, H.; Fesik, S. W.; Rosenberg, S. H. An inhibitor of Bcl-2 family proteins induces regression of solid tumours. *Nature* **2005,** 435, 677-81.

83. Tse, C.; Shoemaker, A. R.; Adickes, J.; Anderson, M. G.; Chen, J.; Jin, S.; Johnson, E. F.; Marsh, K. C.; Mitten, M. J.; Nimmer, P.; Roberts, L.; Tahir, S. K.; Xiao, Y.; Yang, X.; Zhang, H.; Fesik, S.; Rosenberg, S. H.; Elmore, S. W. ABT-263: a potent and orally bioavailable Bcl-2 family inhibitor. *Cancer Res* **2008,** 68, 3421-8.

84. Lee, E. F.; Czabotar, P. E.; Smith, B. J.; Deshayes, K.; Zobel, K.; Colman, P. M.; Fairlie, W. D. Crystal structure of ABT-737 complexed with Bcl-xL: implications for selectivity of antagonists of the Bcl-2 family. *Cell Death Differ* **2007,** 14, 1711-3.

85. Liu, Q.; Moldoveanu, T.; Sprules, T.; Matta-Camacho, E.; Mansur-Azzam, N.; Gehring, K. Apoptotic regulation by MCL-1 through heterodimerization. *J Biol Chem* **2010,** 285, 19615-24.

86. Shuker, S. B.; Hajduk, P. J.; Meadows, R. P.; Fesik, S. W. Discovering high-affinity ligands for proteins: SAR by NMR. *Science* **1996,** 274, 1531-4.

87. Konopleva, M.; Contractor, R.; Tsao, T.; Samudio, I.; Ruvolo, P. P.; Kitada, S.; Deng, X.; Zhai, D.; Shi, Y. X.; Sneed, T.; Verhaegen, M.; Soengas, M.; Ruvolo, V. R.; McQueen, T.; Schober, W. D.; Watt, J. C.; Jiffar, T.; Ling, X.; Marini, F. C.; Harris, D.; Dietrich, M.; Estrov, Z.; McCubrey, J.; May, W. S.; Reed, J. C.; Andreeff, M. Mechanisms of apoptosis sensitivity and resistance to the BH3 mimetic ABT-737 in acute myeloid leukemia. *Cancer Cell* **2006,** 10, 375-88.

88. van Delft, M. F.; Wei, A. H.; Mason, K. D.; Vandenberg, C. J.; Chen, L.; Czabotar, P. E.; Willis, S. N.; Scott, C. L.; Day, C. L.; Cory, S.; Adams, J. M.; Roberts, A. W.; Huang, D. C. The BH3 mimetic ABT-737 targets selective Bcl-2 proteins and efficiently induces apoptosis via Bak/Bax if Mcl-1 is neutralized. *Cancer Cell* **2006,** 10, 389-99.

89. Roberts, A. W.; Seymour, J. F.; Brown, J. R.; Wierda, W. G.; Kipps, T. J.; Khaw, S. L.; Carney, D. A.; He, S. Z.; Huang, D. C.; Xiong, H.; Cui, Y.; Busman, T. A.; McKeegan, E. M.; Krivoshik, A. P.; Enschede, S. H.; Humerickhouse, R. Substantial susceptibility of chronic lymphocytic leukemia to BCL2 inhibition: results of a phase I study of navitoclax in patients with relapsed or refractory disease. *J Clin Oncol* **2012,** 30, 488-96.

90. Wertz, I. E.; Kusam, S.; Lam, C.; Okamoto, T.; Sandoval, W.; Anderson, D. J.; Helgason, E.; Ernst, J. A.; Eby, M.; Liu, J.; Belmont, L. D.; Kaminker, J. S.; O'Rourke, K. M.; Pujara, K.; Kohli, P. B.; Johnson, A. R.; Chiu, M. L.; Lill, J. R.; Jackson, P. K.; Fairbrother, W. J.; Seshagiri, S.; Ludlam, M. J.; Leong, K. G.; Dueber, E. C.; Maecker, H.; Huang, D. C.; Dixit, V. M. Sensitivity to antitubulin chemotherapeutics is regulated by MCL1 and FBW7. *Nature* **2011,** 471, 110-4.

91. Wei, S. H.; Dong, K.; Lin, F.; Wang, X.; Li, B.; Shen, J. J.; Zhang, Q.; Wang, R.; Zhang, H. Z. Inducing apoptosis and enhancing chemosensitivity to gemcitabine via RNA interference targeting Mcl-1 gene in pancreatic carcinoma cell. *Cancer Chemother Pharmacol* **2008,** 62, 1055-64.

92. Bernardo, P. H.; Sivaraman, T.; Wan, K. F.; Xu, J.; Krishnamoorthy, J.; Song, C. M.; Tian, L.; Chin, J. S.; Lim, D. S.; Mok, H. Y.; Yu, V. C.; Tong, J. C.; Chai, C. L. Structural insights into the design of small molecule inhibitors that selectively antagonize Mcl-1. *J Med Chem* **2010,** 53, 2314-8.

93. Rega, M. F.; Wu, B.; Wei, J.; Zhang, Z.; Cellitti, J. F.; Pellecchia, M. SAR by interligand nuclear overhauser effects (ILOEs) based discovery of acylsulfonamide compounds active against Bcl-x(L) and Mcl-1. *J Med Chem* **2011,** 54, 6000-13.

94. Doi, K.; Li, R.; Sung, S. S.; Wu, H.; Liu, Y.; Manieri, W.; Krishnegowda, G.; Awwad, A.; Dewey, A.; Liu, X.; Amin, S.; Cheng, C.; Qin, Y.; Schonbrunn, E.; Daughdrill, G.; Loughran, T. P., Jr.; Sebti, S.; Wang, H. G. Discovery of marinopyrrole A (maritoclax) as a selective Mcl-1 antagonist that overcomes ABT-737 resistance by binding to and targeting Mcl-1 for proteasomal degradation. *J Biol Chem* **2012,** 287, 10224-35.

95. Song, T.; Li, X.; Chang, X.; Liang, X.; Zhao, Y.; Wu, G.; Xie, S.; Su, P.; Wu, Z.; Feng, Y.; Zhang, Z. 3-Thiomorpholin-8-oxo-8H-acenaphtho [1,2-b] pyrrole-9-carbonitrile (S1) derivatives as pan-Bcl-2-inhibitors of Bcl-2, Bcl-xL and Mcl-1. *Bioorg Med Chem* **2013,** 21, 11-20.

96. Abulwerdi, F.; Liao, C.; Liu, M.; Azmi, A. S.; Aboukameel, A.; Mady, A. S.; Gulappa, T.; Cierpicki, T.; Owens, S.; Zhang, T.; Sun, D.; Stuckey, J. A.; Mohammad, R. M.; Nikolovska-Coleska, Z. A Novel Small-Molecule Inhibitor of Mcl-1 Blocks Pancreatic Cancer Growth In vitro and In vivo. *Mol Cancer Ther* **2013**.

97. Friberg, A.; Vigil, D.; Zhao, B.; Daniels, R. N.; Burke, J. P.; Garcia-Barrantes, P. M.; Camper, D.; Chauder, B. A.; Lee, T.; Olejniczak, E. T.; Fesik, S. W. Discovery of potent myeloid cell leukemia 1 (Mcl-1) inhibitors using fragment-based methods and structure-based design. *J Med Chem* **2013,** 56, 15-30.

98. Tanaka, Y.; Aikawa, K.; Nishida, G.; Homma, M.; Sogabe, S.; Igaki, S.; Hayano, Y.; Sameshima, T.; Miyahisa, I.; Kawamoto, T.; Tawada, M.; Imai, Y.; Inazuka, M.; Cho, N.; Imaeda, Y.; Ishikawa, T. Discovery of Potent Mcl-1/Bcl-xL Dual Inhibitors by Using a Hybridization Strategy Based on Structural Analysis of Target Proteins. *J Med Chem* **2013,** 56, 9635-45.

Chapter 2
3-Substituted-*N*-(4-hydroxynaphthalen-1-yl)arylsulfonamides as a novel class of selective Mcl-1 inhibitors

2.1   Introduction

Evasion of apoptosis or programmed cell death, a key regulator of physiological growth control and regulation of tissue homeostasis, is a hallmark of cancer and a contributor to the emergence of resistance to current therapies[1-3]. The B-cell lumphoma-2 (Bcl-2) family of proteins regulate the intrinsic (mitochondrial) pathway of apoptosis through a network of protein-protein interactions between pro- and anti-apoptotic members[4]. The anti-apoptotic proteins contain a hydrophobic surface known as the BH3-binding site, which is comprised of four contiguous hydrophobic pockets (p1-p4), that can bind to the BH3-binding domain of pro-apoptotic proteins preventing apoptosis from happening.

Overexpression of Bcl-2 survival members is observed in different types of human tumor samples and cancer cell lines, and much effort has been focused on developing therapeutics against this family of proteins for the treatment of cancers[5-7]. Selective and potent small molecule inhibitors have been successfully developed against Bcl-2[8], Bcl-X_L[9] and Bcl-2/Bcl-X_L[10-13] with Navitoclax (ABT-263) currently in phase I/II clinical trials. The efficacy of ABT-263 as a single agent has been demonstrated in tumors with low levels of the pro-survival Mcl-1. Several studies[14-18] have shown that resistance to ABT-263 and its analog ABT-737 is linked to high expression levels of Mcl-1 and in many instances this resistance can be overcome by treatment with agents that downregulate, destabilize, or inactivate Mcl-1. The biological significance of Mcl-1 protein expression in support of cell survival has been well documented in a number of cell systems, including human myeloblastic leukemia[19], myeloma[20-22], B-lymphoma[23], non-small cell lung[24], melanoma[25], pancreatic[26, 27] and prostate[28]. Furthermore, Mcl-1 is overexpressed in many human tumor specimens[26, 29-32] and metastatic tissue[33]. This

overexpression contributes to chemoresistance and disease relapse[34-36]. It has been shown that Mcl-1 down-regulation is important toward making multiple myeloma cells susceptible to BH3-only proteins and therefore to mitochondrial disruption[37, 38]. Such down-regulation can increase the sensitivity to rituximab-mediated killing of chronic and acute lymphoid leukemia (CLL and ALL)[39]. Antisense strategies targeting Mcl-1 *in vitro* and *in vivo* have provided promising results in sensitizing human melanoma and pancreatic cancer[40-42]. These data suggest that therapies specifically targeting Mcl-1, either as a single agent or in combination, can be effective in the treatment of different human cancers.

Recently, several groups including us have reported on small molecules[43-50] and stapled peptides[51, 52] as Mcl-1 inhibitors. Herein we disclose a novel series of small molecule Mcl-1 inhibitors discovered through high throughput screening (HTS) followed by the utilization of structure-based design to develop structure-activity relationships (SAR) around lead compound **59** (Figure 2.1A). Docking studies and two-dimensional ^{1}H, ^{15}N heteronuclear single quantum coherence spectroscopy (HSQC) NMR studies were employed to provide information about its binding mode which was used for the design and synthesis of additional analogs. A SAR was developed which resulted in the identification of several selective small-molecule Mcl-1 inhibitors with improved binding. Selected analogs were then tested in a series of complementary biochemical, biophysical, functional and cellular assays to evaluate their potency, specificity and mechanism of action.

2.2   Discovery of HTS lead compound 59

HTS of a 53.3K small molecule library was performed using a fluorescence polarization (FP) binding assay based on the interaction between recombinant human Mcl-1 and fluorescently labeled Bid BH3 peptide (Flu-Bid). Compound **59** (also refered to as **1**) (Figure 2.1A) was one of the validated hits and a resynthesized sample exhibited a K_i of 1.55 ± 0.18 μM against Mcl-1. To explore the binding mode of **59** with Mcl-1, *in silico* induced fit docking (IFD)[53] studies were performed using the crystal structure of Mcl-1 in complex with mNOXA BH3 peptide (PDB ID: 2NLA)[54]. The predicted binding model of **59** in the complex with Mcl-1 revealed that the thiophene and the naphthalene rings of **59** occupy two hydrophobic pockets, p2 and p3, of Mcl-1, mimicking two conserved hydrophobic residues in the BH3 binding motif represented by Leu 78 and Ile 81, respectively, in mNoxaB (Figure 2.1B). The importance of the two conserved

hydrophobic residues, Leu and Ile, in the BH3 binding motif for the high affinity interaction and selective binding to Mcl-1 has been demonstrated with structural studies of Bims2A[55], a highly selective peptide derived from Bim peptide, as well as from recently reported selective small molecule inhibitor in complex with Mcl-1[45]. The carboxylic acid group of **59** forms a network of hydrogen bonds with Arg 263 and Asn 260 of Mcl-1, mimicking the conserved Asp in BH3 peptides (Asp 83 in mNoxa). The predicted binding model also suggests that the phenolic group forms a hydrogen bond with His 224, which is one of the residues composing the p3 pocket of Mcl-1. A recent report[56] on the conformational flexibility of Mcl-1 and its binding hotspots identified His 224 as an acidic hotspot in the p3 site of Mcl-1, supporting the predicted hydrogen bonding in this region of Mcl-1.

To validate the computationally predicted binding site and confirm the binding of **59** to the BH3 groove of Mcl-1, HSQC NMR spectroscopy studies were performed. For this purpose the assignment of the backbone amides of apo human Mcl-1 was based on the work by Liu *et al.*[57], and a series of ^{1}H,^{15}N-HSQC studies were carried out. The HSQC spectra were of good quality with well-dispersed peaks, and concentration-dependent shifts of residues were observed (Figure 2.1C) indicating that **59** binds Mcl-1 specifically and causes dose-dependent perturbations of backbone amides. The chemical shift changes in the presence of a 2-fold excess of **59** were mapped and plotted against Mcl-1 residues (Figure 2.1D). Compound **59** caused moderate to significant chemical shift perturbations for residues of Met 231, Met 250, Leu 267, Phe 270, which constitute the p2 and p3 pockets and which are predicted to be occupied by the thiophene and naphthalene rings of **59**, respectively. Moderate chemical shift perturbations of Arg 263 and His 224 were also observed, which are predicted to form hydrogen bonds with the thioacidic acid and phenolic moieties of **59**, respectively. Additionally, the residues in the vicinity of the predicted binding pose (Leu 232, Val 243, Arg 248), and the ones located on an unstructured loop connecting α-helix 3 to α-helix 4 (Lys 234, Leu 235, Lys 238, Asn 239) were also perturbed. Overall analysis of the chemical shift changes of the compound **59** in complex with Mcl-1 showed that **59** affects the residues forming the BH3-binding groove, and provided conclusive evidence that **59** binds Mcl-1 protein at the same site that the conserved BH3 peptides interact with Mcl-1 protein. Therefore, based on our modeling and NMR results, the substituted-*N*-(4-hydroxynaphthalen-1-yl)arylsulfonamide represents a promising class for further optimization. A structure-based design approach supported by NMR and docking studies was

undertaken and a focused library of analogs of **59** was designed and synthesized to improve the potency of this series and validate our binding model to Mcl-1.
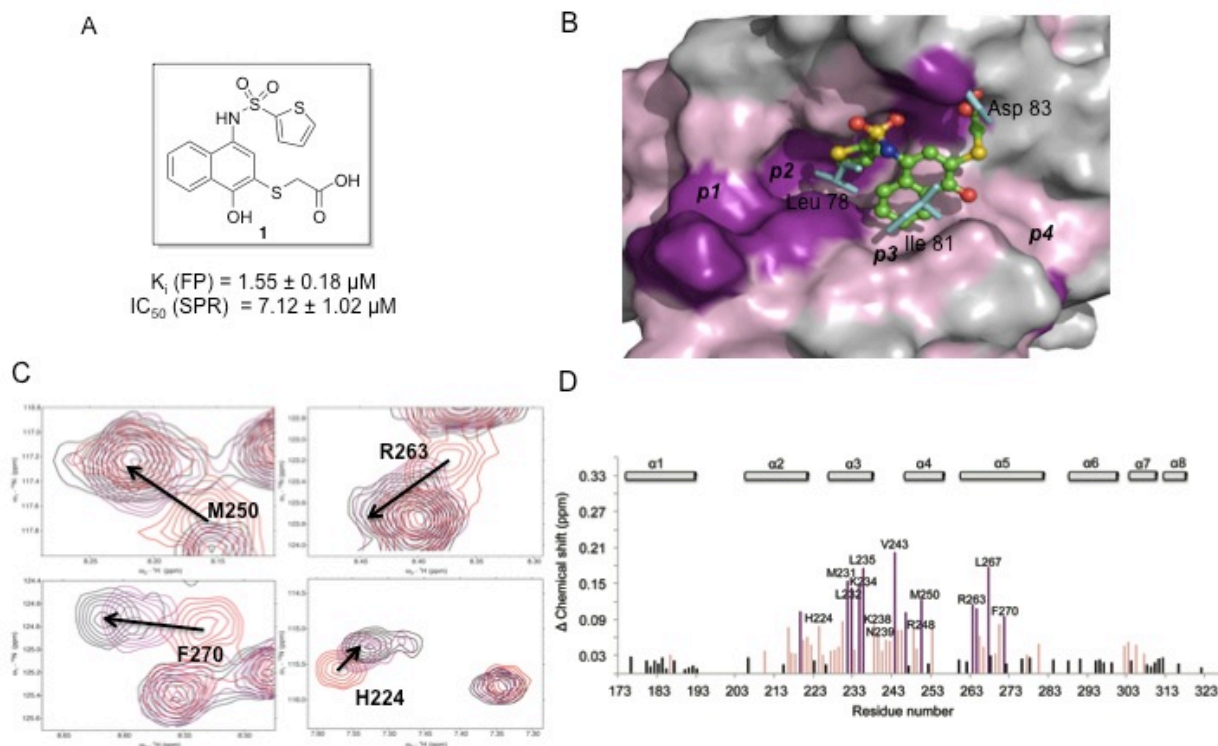

Figure 2.1. Docking and NMR studies of 59. (A) Structure of the HTS lead compound **59** or **1**. (B) Putative binding mode of **59** to Mcl-1 (2NLA). Side chains residues of mNoxa peptide are shown in blue sticks. The surface of Mcl-1 protein is colored according to the chemical shift intensity. Significant shift (> 0.09 ppm) is represented with purple, moderate shift (≥ 0.03 ppm and ≤ 0.09 ppm) represented with pink. (C) Overlaid ^{15}N-^{1}H HSQC spectra of Mcl-1 (red), and in presence of **59** (Mcl-1:**59** ratio of 1:2) (black), (Mcl-1:**59** ratio of 1:1) (purple). Arrows show the direction of chemical shift changes upon binding of **59**. (D) Plot of chemical shift changes of Mcl-1 amide upon addition of **59** (Mcl-1:**59** ratio of 1:2) as a function of Mcl-1 residue numbers.
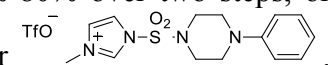
2.3   Synthesis

Except for analogs **4-8**, **15**, and **38** which were commercially available, all analogs were synthesized through a novel, modular route (Scheme 2.1), which differs from that recently reported by Ge *et al.*[58] Our route allows for facile access to a variety of analogs with variations at R_1, R_2 and R_3 and the linker region (X). It starts with the electrophilic aromatic substitution (S_EAr) of 1-methoxy-4-nitronaphthalene with *N*-iodosuccinamide to provide aryl iodide (**46**)[59]. This was subjected to Pd-catalyzed C-S or C-C cross-coupling using conditions previously

reported[60, 61], or developed in our lab based on recent literature[62-64], to provide several desired intermediates (**47**). The nitro function was reduced with iron[65] or via catalytic hydrogenation[66] to provide the corresponding amines. Reaction of the amines with appropriate sulfonyl or acyl chlorides or 3-methyl-1-((4-phenylpiperazin-1-yl)sulfonyl)-1*H*-imidazol-3-ium[67] provided the penultimate compounds (**48**), which were demethylated with BBr$_3$ followed by purification by trituration or reverse-phase HPLC to afford the target compounds (**1-3**, **9-14**, **16-23**, **25-26**, **28-29**, **31-37**) of >95% purity (Tables 2.1-2.3). In the case of analogs with an ester side chain, the BBr$_3$ step provided a convenient way to concomitantly hydrolyze the ester in a single pot. To preserve the methyl ester of analog **32** (Table 2.3), analog **40** (Table 2.4) was subjected to BBr$_3$ conditions followed by a quench with MeOH. For the synthesis of **48o**, intermediate **48k** underwent Suzuki-Miyaura coupling[68, 69] with phenyl boronic acid to provide the desired compound which was subjected to BBr$_3$ to provide **17** (Table 2.1). Aminolysis of **40** with NH$_4$OH[70] provided carboxamide **41** (Table 2.4) which was subjected to BBr$_3$ to give **33** (Table 2.3). The terminal amide of **41** was converted by a known procedure[71] to tetrazole **48bb**, which after BBr$_3$ demethylation provided **36** (Table 2.3). The thioacidic acid analogs with a methoxy at R$_3$ (**39**, **42-43**), (Table 2.4) were obtained via LiOH hydrolysis of esters **40**, **48n**, and **48o**, respectively. Acetylation of **10** (Table 2.1) with acetyl chloride[72] provided **45** (Table 2.4).

It should be mentioned that the synthetic route (Scheme 2.1) that was developed for synthesis of **59** (**1**) and its analogs was amenable to scale-up. Analog **10** (also referred to as **UMI-77**) was synthesized in 1 g utilizing this scheme for later efficacy studies in a pancreatic xenograft model.

Scheme 2.1. Synthetic route for **59** and analogs[a].

46   **47**   **48**   **1-3, 9-14, 16-23, 25-26, 28-29, 31-37**
(Tables 2.1, 2.2, 2.3)
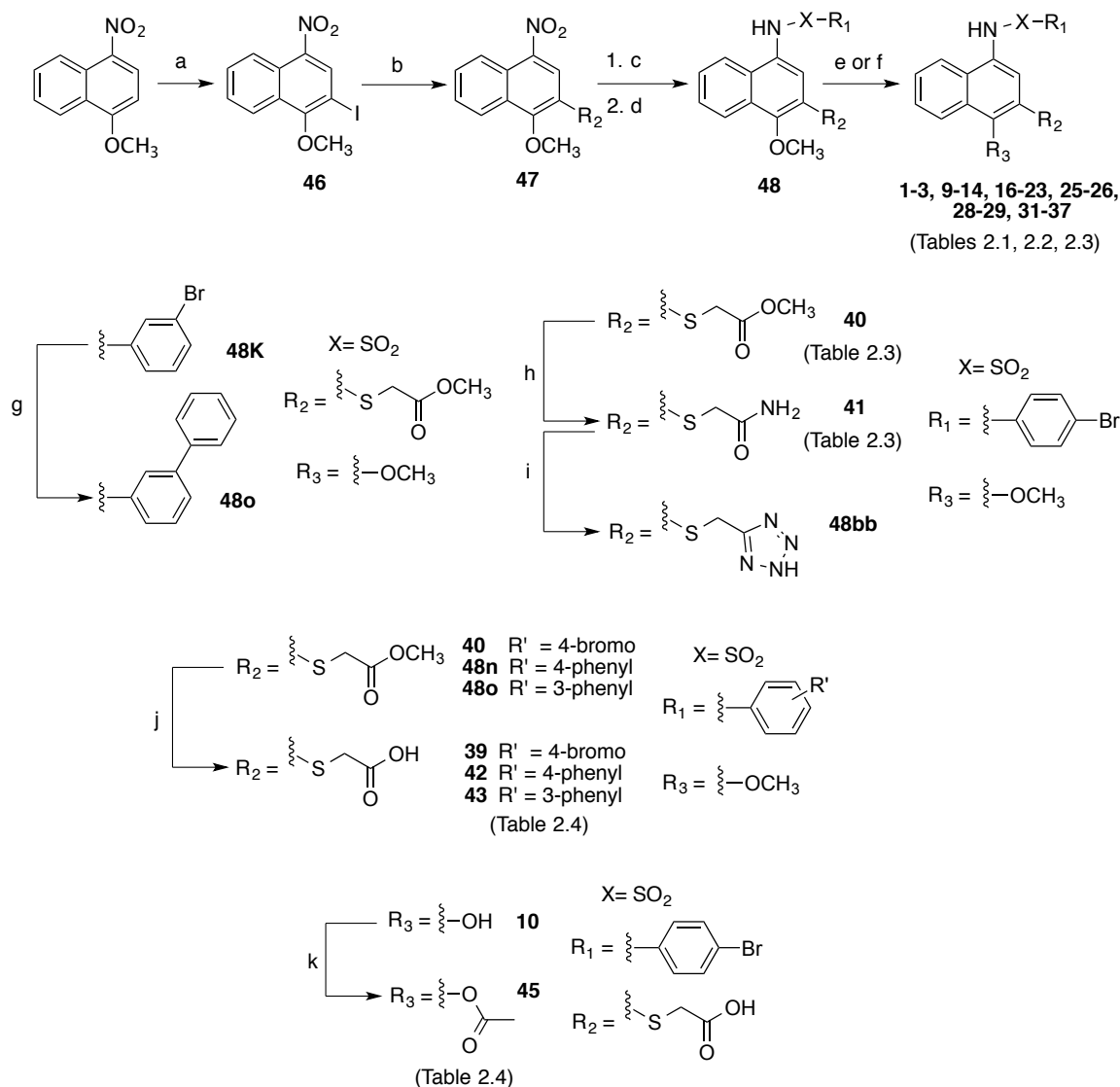
[a]Reagents and conditions: (a) NIS, TFA, reflux, 24 h, 70%; (b) $HS(CH_2)_nCOOCH_3$ (n=1, 2), $Pd(OAc)_2$, Xantphos, Cs_2CO_3, LiI, $ZnCl_2$, THF, 60 °C, overnight, 66%, or $HS(CH_2)_3CH_3$, $Pd_2(dba)_3$, Dppf, Et_3N, NMP, 80 °C, 2-3 h, 71%, or $HCC(CH_2)_nOH$ (n=1, 2), $Pd(PPh_3)_2Cl_2$, CuI, Et_3N/THF (4:1), 60 °C, 2 h, 83-97%; (c) Fe, AcOH, 70 °C, 1 h, or Pd/C, H_2 30 psi, EtOH/EtOAc (6:1), rt, overnight; (d) RSO_2Cl, pyridine, CH_2Cl_2, rt, overnight, 33%-80% over two steps, or $RCOCl$, Et_3N, CH_2Cl_2, rt, overnight, 49%-69% over two steps, or , CH_3CN, 80 °C, 15 h, 25% over three steps; (e) BBr_3, CH_2Cl_2, 0 °C to rt, 1 h, 8%-61% or BBr_3, CH_2Cl_2, 0 °C to rt, 1 h, quench with MeOH at 0 °C, 13%; (g) phenyl boronic acid, $Pd(PPh_3)_4$, Na_2CO_3, THF/H_2O, 60 °C, 2 h, 92%; (h) NH_4OH, rt, 1 h, 90%; (i) NaN_3, $SiCl_4$, CH_3CN, 80 °C, 15 h, 50%; (j) LiOH, THF, rt, 1 h, 59%-74%; (k) H_3CCOCl, Et_3N, 0 °C, rt, 30 min, 61%.

Analog **24** (Table 2.1) with a phenyl scaffold in place of naphthalene was synthesized starting from 2-iodoanisole (Scheme 2.2) which underwent S_EAr with nitric acid and acetic acid as described previously[73] to yield **49**. Aryl iodide **49** was then subjected to C-S coupling reaction with methyl thioglycolate to introduce the methyl thioacetate in **50**. The nitro group of **50** was reduced using iron and the free amine was subjected to sulfonamide coupling with 4-bromobenzene sulfonyl chloride to provide **51**. Subjection of **51** to boron tribromide conditions provided desired analog **24**.
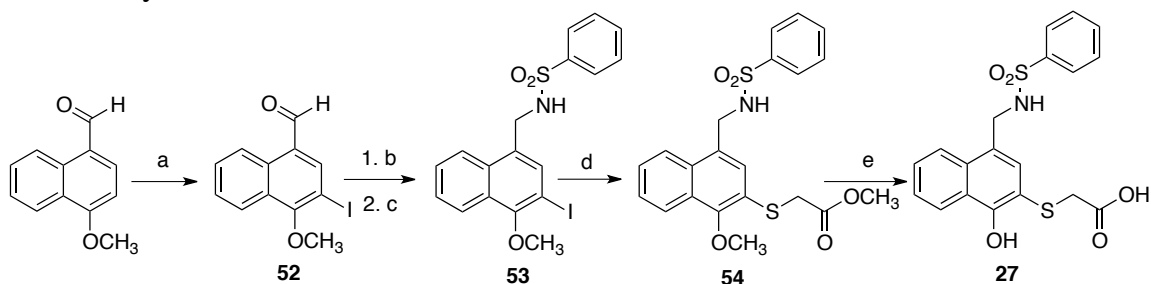
Scheme 2.2. Synthesis of **24**[a].
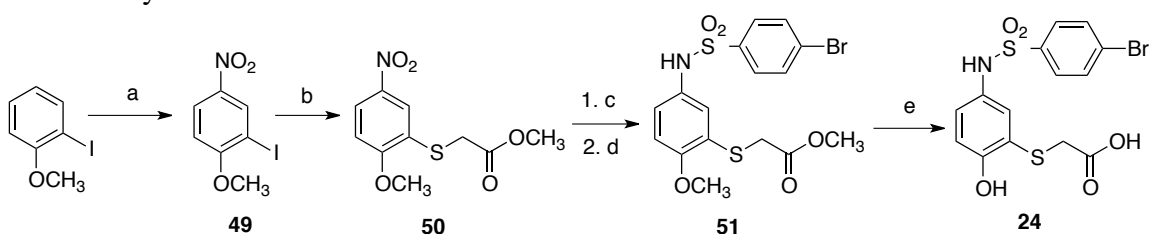
[a]Reagents and conditions: (a) HNO$_3$, AcOH, 0 $^\circ$C to 50 $^\circ$C, 1 h, 56%; (b) HSCH$_2$COOCH$_3$, Pd(OAc)$_2$, Xantphos, Cs$_2$CO$_3$, LiI, ZnCl$_2$, THF, 60 $^\circ$C, 6 h, 63%; (c) Fe, AcOH, 70 $^\circ$C, 1 h; (d) 4-bromobenzene sulfonyl chloride, pyridine, CH$_2$Cl$_2$, rt, overnight, 41% over two steps; (e) BBr$_3$, CH$_2$Cl$_2$, 0 $^\circ$C to rt, 1 h, 29%.

For the synthesis of analog **27** (Table 2.2), with a methylene linker in between the naphthalene scaffold and sulfonamide linker, Scheme 2.3 was utilized. 4-methoxy-1-naphthaldehyde was first subjected to NIS to provide **52** via S_EAr. Aldehyde **52** was treated with benzenesulfonamide in the presence of titanium chloride and triethylamine to form the corresponding sulfonimide intermediate which was reduced with sodium borohydride to sulfonaminde **53**.[74] Subjection of **53** to C-S coupling in presence of methyl thioglycoate provided **54** which was treated with boron tribromide to yield the final analog **27**.

Scheme 2.3. Synthesis of **27**[a].

[a]Reagents and conditions: (a) NIS, TFA, reflux, 8 h, 77%; (b) benzenesulfonamide, Et$_3$N, TiCl$_4$, CH$_2$Cl$_2$, 0 °C to rt, 3 h; (c) NaBH$_4$, MeOH/CH$_2$Cl$_2$ (1:1), 0 °C to rt, 45 min, 60% over two steps; (d) HSCH$_2$COOCH$_3$, Pd(OAc)$_2$, Xantphos, Cs$_2$CO$_3$, LiI, ZnCl$_2$, THF, 60 °C, 10 h, 53%; (e) BBr$_3$, CH$_2$Cl$_2$, 0 °C to rt, 1 h, 18%.

Analog **30** missing the thioacetic acid side chain was synthesized starting from 1-nitronaphthalene (Schemes 2.4) which was hydroxylated with cumene hydroperoxide in presence of a base via nucleaphilic aromatic substitution (S$_N$Ar).[75] Protection of free hydroxyl via Williamson ether synthesis with benzyl bromide provided **55**. Nitro of **55** was reduced with iron and the free amine was subjected to sulfonamide coupling with benzenesulfonyl chloride to provide sulfonamide **56**. Removal of benzyl group was achieved via catalytic hydrogenation to provide the final analog **30**.

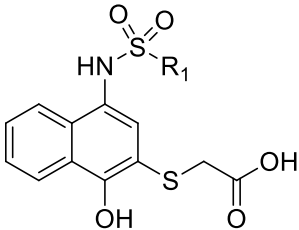**Scheme 2.4.** Synthesis of **30**[a].
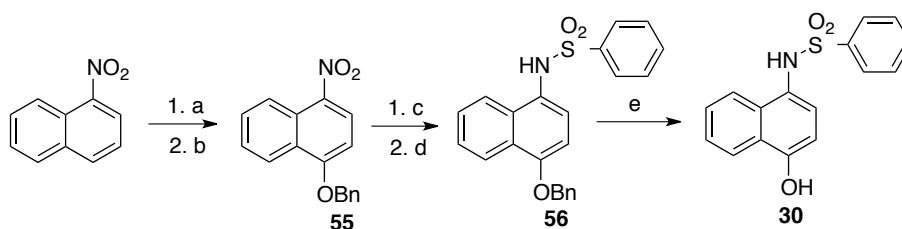
[a]Reagents and conditions: (a) cumene hydroperoxide, KOH, DMSO/H$_2$O (3:1), 0 °C to rt, 2 h, 67%; (b) benzyl bromide, NaH, DMF/THF (2:1), 0 °C to rt, 2-3 h, 64%; (c) Fe, AcOH, 70 °C, 1 h; (d) benzenesulfonyl chloride, pyridine, CH$_2$Cl$_2$, rt, overnight, 55% over two steps; (e) Pd/C, H$_2$ 30 psi, MeOH, rt, overnight, 21%.
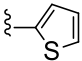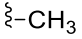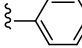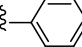
2.4 Structure-activity relationships
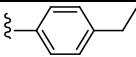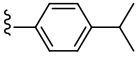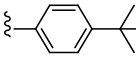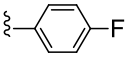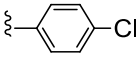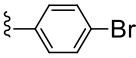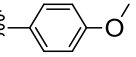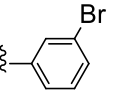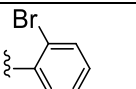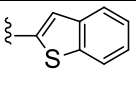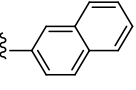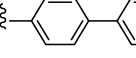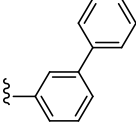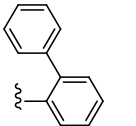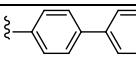
Structure-based design of analogs based on **59** yielded a focused library of compounds leading to clear SAR for this series. The binding affinities of our Mcl-1 inhibitors were determined by using competitive FP- and surface plasmon resonance (SPR)-based binding assays, which test the ability of inhibitors to disrupt interaction between Mcl-1 and two different BH3 peptides, fluorescently-labeled Bid and biotin-labeled Bim, respectively. Concurrently, HSQC NMR experiments were performed to provide structural insights of protein-bound ligand and experimental validation for the modeling studies.

The predicted binding model showed that the thiophene ring at R_1 of **59** projects into the p2 pocket (Figure 2.1B), which is the biggest and deepest pocket amongst the four hydrophobic pockets of Mcl-1[54]. To investigate the importance of hydrophobic interaction at this site and increase the binding affinity of **59**, a series of analogs with variation at R_1 was synthesized and evaluated (Table 2.1). When R_1 is changed to a methyl group in **2**, the binding affinity is significantly reduced, which is supported by the lack of chemical shift perturbations of backbone residues in the Mcl-1 BH3-binding site after addition of **2** (Figure 2.2).

Table 2.1. Binding affinities of sulfonamide analogs with variations at R_1.

Cpd	R_1	FP $K_i \pm$ SD (µM)	SPR $IC_{50} \pm$ SD (µM)
1(59)		1.55 ± 0.18	7.12 ± 1.02
2	$-CH_3$	74.92 ± 6.33	>100
3		3.56 ± 0.45	12.58 ± 3.60
4		3.13 ± 0.22	11.57 ± 7.86

5	§—⟨benzene⟩—ethyl	1.55 ± 0.37	8.68 ± 1.63
6	§—⟨benzene⟩—isopropyl	1.06 ± 0.17	4.0 ± 1.7
7	§—⟨benzene⟩—tert-butyl	0.81 ± 0.04	8.7 ± 0.95
8	§—⟨benzene⟩—F	4.23 ± 0.93	5.0 ± 1.1
9	§—⟨benzene⟩—Cl	0.82 ± 0.10	2.7 ± 0.6
10	§—⟨benzene⟩—Br	0.49 ± 0.06	2.4 ± 0.17
11	§—⟨benzene⟩—O—	9.31 ± 3.1	7.2 ± 2.8
12	§—⟨benzene⟩ Br (meta)	2.35 ± 0.19	9.68 ± 0.88
13	§—⟨benzene⟩ Br (ortho)	4.42 ± 0.86	6.2 ± 1.2
14	§—⟨benzothiophene, S⟩	1.54 ± 0.32	7.5 ± 3.0
15	§—⟨naphthalene⟩	0.73 ± 0.05	2.76 ± 1.72
16	§—⟨biphenyl (para)⟩	0.37 ± 0.10	2.03 ± 1.1
17	§—⟨biphenyl (meta)⟩	0.38 ± 0.03	2.31 ± 0.76
18	§—⟨biphenyl (ortho)⟩	2.03 ± 0.41	9.9 ± 3.5
19	§—⟨biphenyl⟩—Cl	0.17 ± 0.04	0.88 ± 0.15

20	*(structure: 2'-F, 4'-F biphenyl)*	0.24 ± 0.06	0.92 ± 0.20
21	*(structure: phenoxyphenyl)*	0.18 ± 0.05	1.45 ± 0.29
22	*(structure: 4-fluorophenoxyphenyl)*	0.29 ± 0.04	0.9 ± 0.42
23	*(structure: phenylpiperazine)*	2.22 ± 0.36	16.2 ± 5.8
24	*(structure: N-(4-bromophenylsulfonyl)amino hydroxyphenyl thioacetic acid)*	283.36 ± 81.50	>100

Figure 2.2. NMR studies of 2. Plot of chemical shift changes of Mcl-1 residues upon addition of **2** (Mcl-1:**2** ratio of 1 to 2).

As was expected, isosteric replacement of the thiophene in **59** to a phenyl in **3** maintained binding affinity. To probe the hydrophobic interactions in the p2 pocket, analogs with alkyl and halogen substituents of various sizes at the *para*-position of the phenyl ring were prepared. From this set of compounds, a trend emerged showing improved binding with increasing size and hydrophobicity of substituents. *Tert*-butyl phenyl (**7**) exhibited 4-fold (K_i = 0.8 µM) and bromo

phenyl (**10**) 7-fold (K_i = 0.5 µM) improved binding over **3**. Introduction of a more polar methoxy group in **11** was accommodated, but resulted in a 3-fold decreased binding compared to **3**. Bromine substitution at the *meta-* and *ortho-* positions of the phenyl ring was also explored and the binding results (K_i = 2.4 µM and K_i = 4.4 µM, respectively) indicated that *para*-bromo substitution is best, exhibiting the highest binding affinity to Mcl-1 amongst these three isomers. To improve the quality and accuracy of ligand-induced Mcl-1 chemical shift perturbations, resonance assignments were also determined for **10** in complex with Mcl-1 using $^{13}C,^{15}N$-Mcl-1 in the presence of a 2-fold excess of **10**. The HSQC spectrum of **10** showed a similar pattern of chemical shift perturbations as with **1**, which we attribute to the structural similarity of the two analogs. Consistent with the 7-fold improved binding of **10** in comparison with **1**, the chemical shift perturbations were larger for **10** (Figure 2.3A). In particular, significant perturbation of residues S247, R248, V253 on α-helix 4, which forms the upper rim of the p2 pocket, and residues V216, V220, Q221 located toward the C-terminus of α-helix 2, which are at the border between the p3 and p4 pockets, were observed for **10** suggesting that the Mcl-1 conformational flexibility accommodates larger R_1 substituent into the p2 pocket. Chemical shift perturbation plots derived from $^{1}H,^{15}N$-HSQC experiments of the other two bromophenyl isomers showed a similar perturbation pattern as **10** with chemical shift changes that correlate well with the binding data in which the strongest perturbation is observed for **10**, followed by **12** and **13** (Figure 2.3A-C).
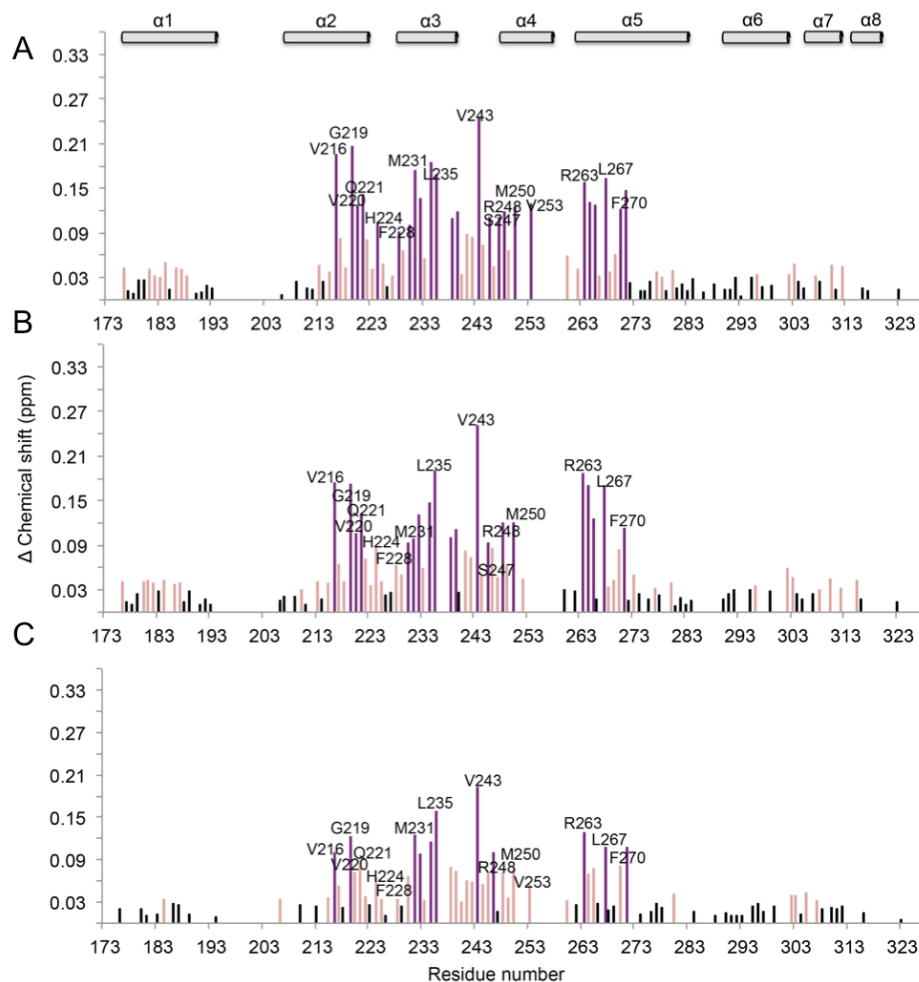
Figure 2.3. NMR studies of 10, 12, 13. Plots of chemical shift changes of Mcl-1 residues upon addition of (A) **10** (Mcl-1:**10** ratio of 1 to 2) (B) **12** (Mcl-1:**12** ratio of 1 to 2) (C) **13** (Mcl-1:**13** ratio of 1 to 2). Significant shift (> 0.09 ppm) is represented with purple, moderate shift (≥ 0.03 ppm and ≤ 0.09 ppm) represented with pink.

To further extend into the p2 pocket and gain additional interactions, analogs with biphenyl substituents were synthesized because biphenyl is considered a privileged moiety in targeting protein-protein interactions[76]. Analogs **16** and **17**, with *para-*, and *meta-*biphenyl substituents, showed a similar 9-fold improvement in binding compared to **3**, while the *ortho-*biphenyl analog, **18** showed only a 2-fold increase in binding. The predicted binding models of these compounds showed that the distal phenyl ring of **16** and **17** inserts deeper into the p2 pocket (Figures 2.4A and B, respectively). For **18**, this phenyl ring is partially solvent exposed (Figure 2.4C) which might explain its lower affinity compared to **16** and **17**. In agreement with their binding

affinities, chemical shift perturbation plots of **16** and **17** show stronger perturbation of residues involved in the binding site compared to **18** (Figure 2.4D-F).
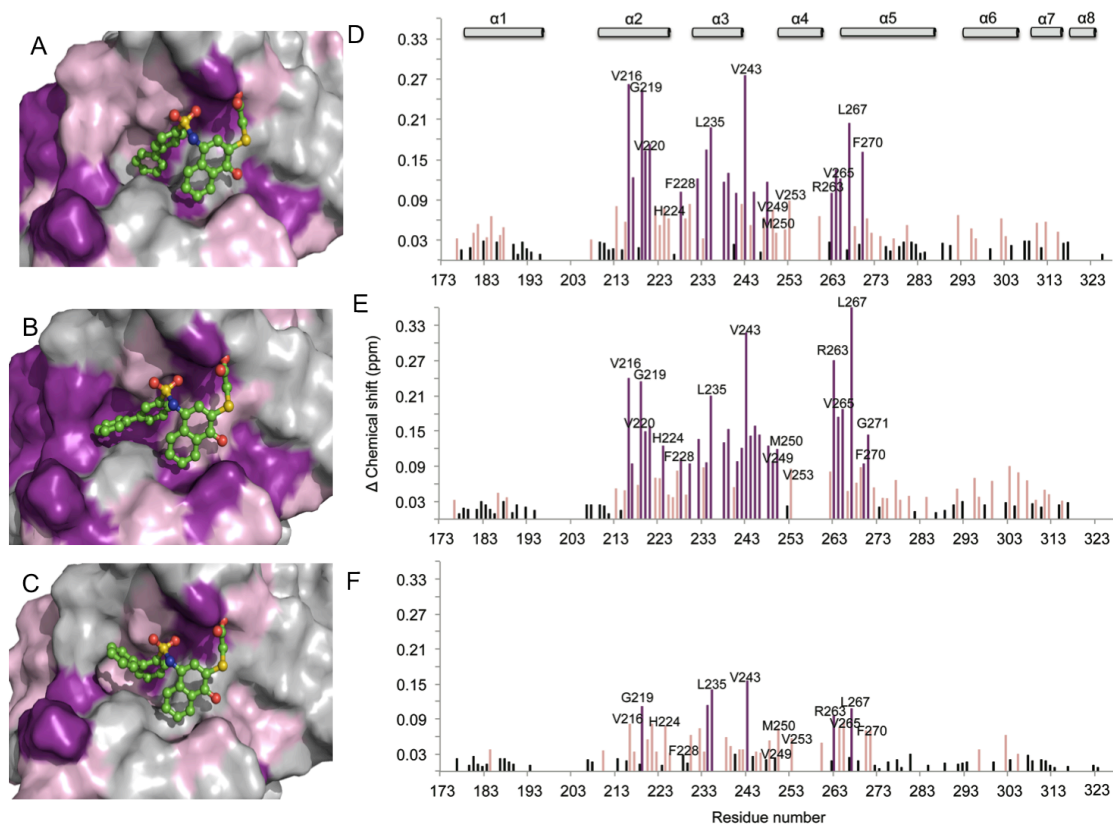
Figure 2.4 Docking and NMR studies of 16, 17, 18. Putative binding modes of (A) **16**, (B) **17**, (C) **18** to Mcl-1. Surface of Mcl-1 protein is colored according to the chemical shift intensity. Significant shift (> 0.09 ppm) is represented with purple, moderate shift (≥ 0.03 ppm and ≤ 0.09 ppm) represented with pink. Plots of chemical shift changes of Mcl-1 amide upon addition of (D) **16** (Mcl-1:**16** ratio of 1:2) (E) **17** (Mcl-1:**17** ratio of 1:2) (F) **18** (Mcl-1:**18** ratio of 1:2) as a function of Mcl-1 residue numbers.

Analysis of the HSQC spectra of analogs **16** to **18** resulted in an important finding that strongly supports their predicted binding mode. One long-standing question for us was the possibility of a flipped binding mode for this class of analogs where R_1 would occupy the p4 pocket instead of p2. The possibility of a flipped conformation has been previously documented for a different class of dual Mcl-1 and Bcl-X_L inhibitors[49]. We resorted to differential chemical shift mapping[77, 78] using the three biphenyl analogs differing only in the orientation of distal phenyl ring. The difference in the orientation of the phenyl ring would create a distinct chemical environment with the interacting residues facilitating binding site mapping. Careful analysis of

the HSQC spectra of these analogs reveals a different direction of the chemical shifts of the residues forming the p2 pocket (Phe 270, Met 250) or in its vicinity (Phe 228) as well as residues located on α-helix 4, (Val 249, Val 253) (Figures 2.5A-E). This finding provides conclusive evidence for biphenyl occupation of the p2 pocket and further supports a recently published report[56] that identifies α-helix 4 as the flexible helix of Mcl-1.
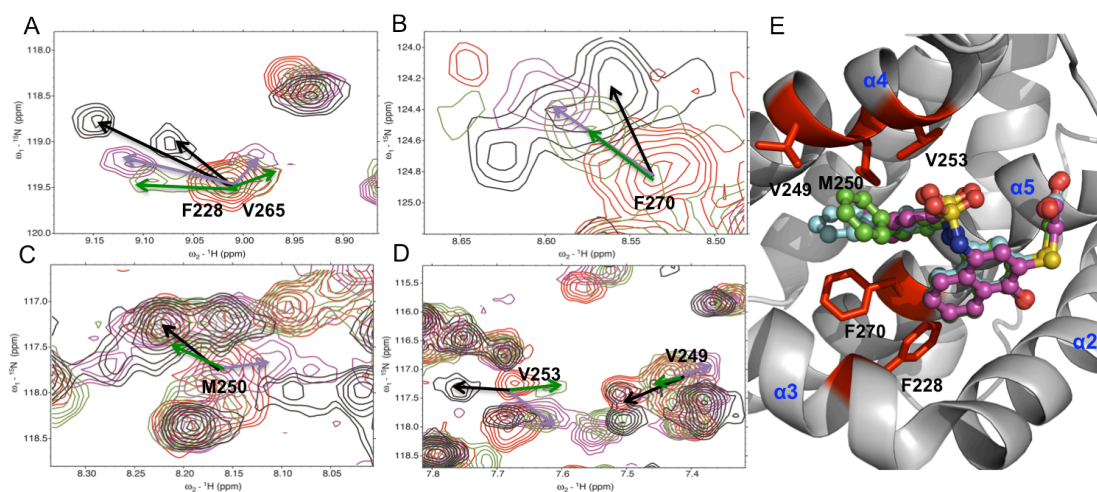
Figure 2.5. Mapping the binding site of R_1 of analogs 16, 17, 18. Overlaid ^{15}N-^1H HSQC spectra of Mcl-1 (red), and in the presence of **16** (Mcl-1:**16** ratio of 1:2) (purple), **17** (Mcl-1:**17** ratio of 1:2) (black), **18** (Mcl-1:**18** ratio of 1:2) (green) for (A) Phe 228 (B) Phe 270 (C) Met 250 (D) Val 249 and Val 253. Arrows show the direction of chemical shift changes upon binding of compounds. (E) Overlay of putative binding modes of **16** (purple), **17** (blue), **18** (green) to Mcl-1 highlighting in red Val 249, Met 250, and Val 253 on helix 4, Phe 228 on helix 3 and Phe 270 on helix 5 of Mcl-1.

Due to encouraging binding data with **16**, analogs **19** and **20** with halogenated biphenyl rings at R_1 were synthesized to further increase potency. Satisfyingly, **19** with *para*-chlorobiphenyl showed a 21-fold improved binding compared to **3**, becoming the most potent analog in our series with a K_i of 170 nM. The chemical shift perturbation plot of **19** (Figure 2.6) showed a similar pattern of perturbations to **16** suggesting a similar binding conformation but with a lower perturbation magnitude, likely due to the lower solubility of **19** in our NMR studies.
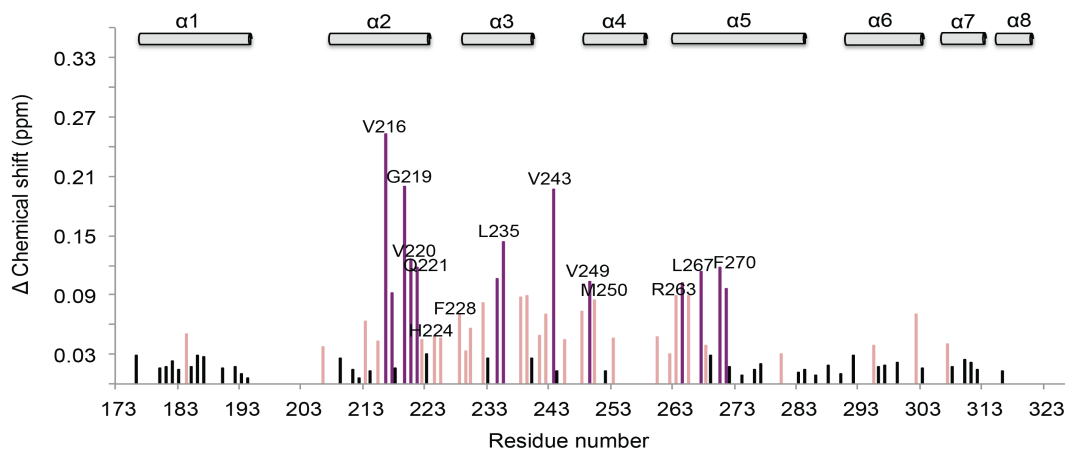
Figure 2.6. NMR studies of 19. Plot of chemical shift changes of Mcl-1 residues upon addition of **19** (Mcl-1:**19** ratio of 1 to 2). Significant shift (> 0.09 ppm) is represented with purple, moderate shift (≥ 0.03 ppm and ≤ 0.09 ppm) represented with pink.

To further improve the physicochemical properties of the biphenyl analogs, we synthesized and evaluated analogs **21** with *para*-phenoxyphenyl at R_1 and its fluorine substituted congener, **22**. Analog **21** showed a K_i of 180 nM and a 2-fold gain in potency over **16**. The chemical shift perturbation plot derived from HSQC further confirmed binding of **21** (Figure 2.7A-C). Computational docking of **21** predicted a π-π stacking of the distal phenyl of the *para*-phenoxyphenyl moiety with the phenyl of Phe 270 of Mc-1 (Figure 2.7D), which could account for its improved affinity. To increase the aqueous solubility of this class of analogs a *para*-phenylpiperazine group at R_1 was introduced in **23** which led to a 6-fold decrease in binding in comparison with the biphenyl substituent in **16**. This can be attributed to a relatively polar substitutent projecting into the hydrophobic p2 pocket and a less optimal conformational preference of phenylpiperazine versus biphenyl for the p2 pocket.
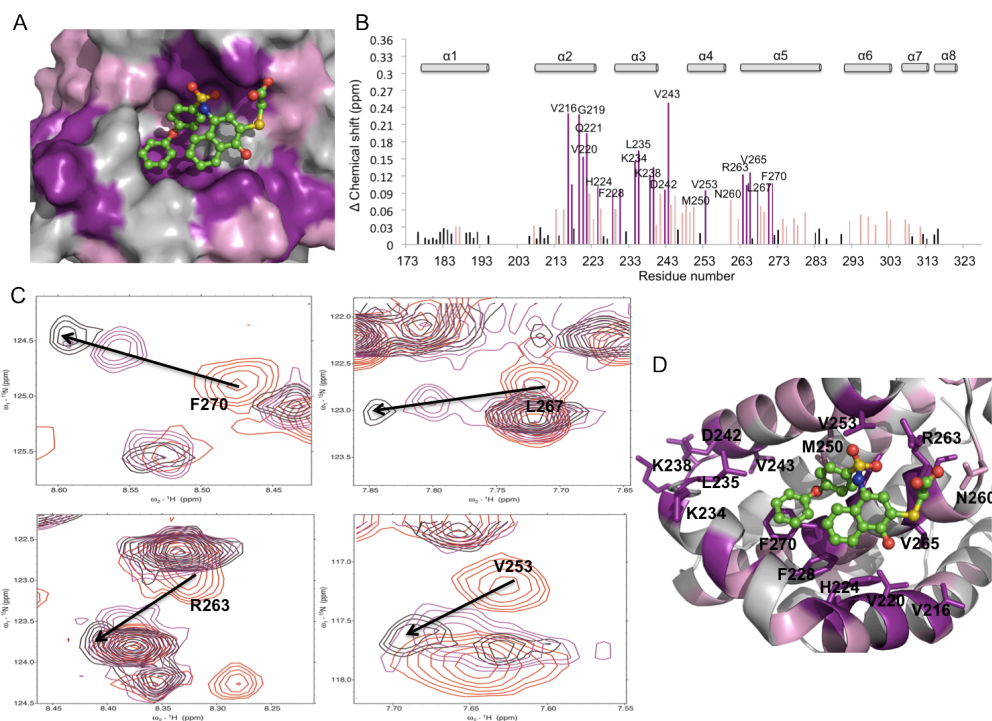
Figure 2.7. NMR and docking studies of 21. (A) Putative binding mode of **21**. Surface of the Mcl-1 protein is colored according to the chemical shift intensity. Significant shift (> 0.09 ppm) is represented with purple, moderate shift (≥ 0.03 ppm and ≤ 0.09 ppm) represented with pink. (B) Plot of chemical shift changes of Mcl-1 amide upon addition of **21** (Mcl-1:**21** ratio of 1:2) as a function of Mcl-1 residue numbers. (C) Overlaid ^{15}N-^{1}H HSQC spectra of Mcl-1 (red), and in presence of **21** (Mcl-1:**21** ratio of 1:2) (black), (Mcl-1:**21** ratio of 1:1) (purple). Arrows show the direction of chemical shift changes upon binding of **21**. (D) Mcl-1 residues shown to be perturbed in HSQC NMR in the presence of **21** (Mcl-1:**21** ratio of 1:2) (green).

To briefly explore the importance of the naphthalene core to the binding potency, analog **24** with a phenyl core was evaluated and showed a significant drop in potency (K_i = 283 µM) compared to to **10** supporting the importance of hydrophobic interaction at the p3 to the overall Mcl-1 binding.

The next focus of our SAR studies was the sulfonamide linker for which modeling suggested lack of any specific interactions with Mcl-1. To investigate the importance of the sulfonamide linker several analogs were synthesized (Table 2.2). Replacement of the sulfonamide with a carboxamide in **25** led to a significant decrease in the binding affinity with K_i value of 40.8 ± 8.50 µM compared to **10**, possibly due to an unfavorable orientation of R_1 by the carboxamide linker. The decreased binding potency was confirmed by NMR studies (Figure 2.8).

Table 2.2. Binding affinities of analogs with linker (X) variations.

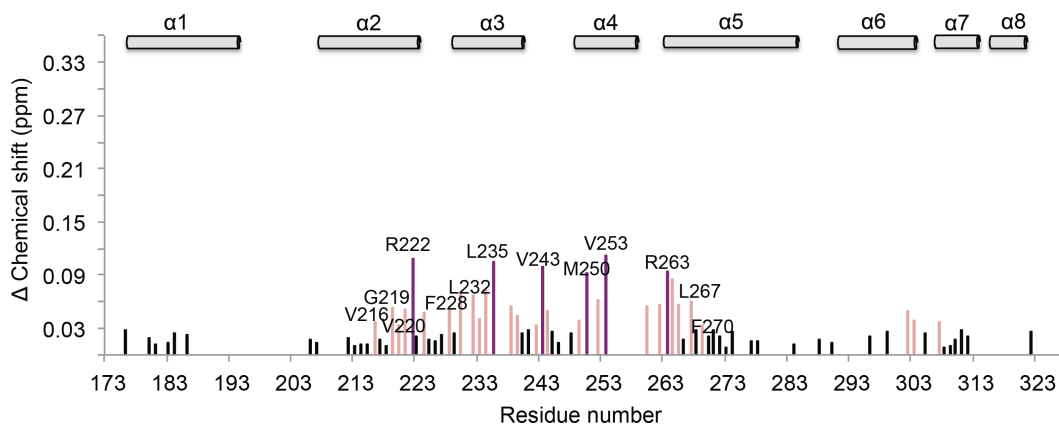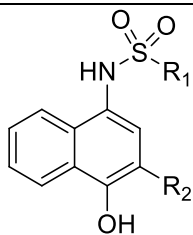| Cpd	X-R$_1$	FP $K_i \pm$ SD (μM)	SPR IC$_{50} \pm$ SD (μM)
25		40.8 ± 8.50	45.1 ± 3.9
26		5.23 ± 0.36	9.6 ± 5.1
27		64.75 ± 12.61	30.2 ± 4.0
28		12.53 ± 1.24	18.3 ± 6.6
29		59.4 ± 15.5	63.8 ± 10.8

Figure 2.8. NMR studies of 25. Plot of chemical shift changes of Mcl-1 residues upon addition of **25** (Mcl-1:**25** ratio of 1 to 2). Significant shift (> 0.09 ppm) is represented with purple, moderate shift (≥ 0.03 ppm and ≤ 0.09 ppm) represented with pink.

To explore the impact of the flexibility of the linker, a methylene linker distal (**26**) or proximal (**27**) to the naphthalene core was inserted and both analogs showed decreased binding affinity to **9** and **3** respectively. As expected, the change of the sulfonamide linker in **26** to a carboxamide in **28** decreased the potency, but only by 2-fold, suggesting that the insertion of the methylene linker between the carboxamide and the pendant aryl ring provides a degree of freedom to better orient R_1 into p2 pocket of Mcl-1.

Modeling showed that the thioacetic acid moiety at R_2 mimics the conserved Asp of BH3-only peptides and that the carboxylate is involved in electrostatic interaction with Asn 260 and Arg 263 of Mcl-1. Therefore, to further explore this site, analogs with different substituents at R_2 were synthesized (Table 2.3). Removal of the acid side chain (**30**) or its replacement with thiobutyl (**31**) did not show binding up to 100 μM. Introducing a methyl ester (**32**), or a primary carboxamide (**33**) resulted in decreased binding by 10- and 3-fold, respectively, compared to **10**, consistent with each of these functional groups forming a weaker interaction with Arg 263 compared to the carboxylic acid moiety. When the carboxylic acid was changed to an alcohol and the sulfur to methylene (**34**) or ethylene (**35**), both analogs showed decreased binding compared to parent congener **10**. As was expected, bioisosteric replacement of the carboxylic acid group with a tetrazole (**36**) maintained the binding affinity. Homologating the thioacetic acid in **37** had no detrimental effect on binding and showed a similar K_i of about 1 μM as with **15**, which might be explained with the flexibility of both the thiopropanoic acid moiety and Arg 263 side chain. However, changing the point of fusion of the naphthalene ring in **37** substantially affected the binding, and **38** with 1-naphthyl substituent did not show binding up to 100 μM. Our docking studies suggest that this might be attributed to a clash with the residues in the p2 pocket of Mcl-1.

Table 2.3. Binding affinities of sulfonamide analogs with variations at R_1 and R_2.

Cpd	R_1	R_2	FP $K_i \pm$ SD (µM)	SPR $IC_{50} \pm$ SD (µM)
30	phenyl	-H	>27*	>100
31	phenyl-Br	ξ-S-propyl	>27*	>100
32	phenyl-Br	ξ-S-CH$_2$-C(O)-OCH$_3$	5.08 ± 1.35	14.9 ± 3.3
33	phenyl-Br	ξ-S-CH$_2$-C(O)-NH$_2$	1.71 ± 0.35	3.9 ± 0.6
34	phenyl-Br	ξ-CH$_2$CH$_2$-OH	3.79 ± 0.62	11.0 ± 0.53
35	phenyl-Br	ξ-(CH$_2$)$_3$-OH	2.18 ± 0.91	19.7 ± 4.7
36	phenyl-Br	ξ-S-CH$_2$-tetrazole (NH)	1.01 ± 0.22	1.50 ± 0.30
37	naphthalen-2-yl	ξ-S-CH$_2$CH$_2$-C(O)-OH	1.13 ± 0.34	5.0 ± 1.9
38	naphthalen-1-yl	ξ-S-CH$_2$CH$_2$-C(O)-OH	>27*	64.9 ± 17.2

*Compounds were tested up to 100 µM.

Modeling showed that the phenolic group of the core naphthalene scaffold forms a hydrogen bond with His 224 of Mcl-1, consistent with the reported acidic hotspot in the p3 site of Mcl-1 close to His 224[56]. Several analogs were synthesized to probe the contribution of the phenolic group to binding to Mcl-1 (Table 2.4). When the hydroxyl group is changed to a methoxy in analog **39**, the potency decreased by 170 fold ($K_i = 86.98 \pm 15.35$ µM) compared to the phenolic

congener **10**. The analog **40**, where R_2 is methyl thioacetate and R_3 is methoxy, did not show binding up to 100 µM and the loss of the binding was confirmed with HSQC experiment as expected (Figure 2.9). Similar significant loss of binding is also apparent in compounds **41** to **44** compared to their corresponding phenolic analogs clearly indicating the importance of the phenolic group to the overall binding to Mcl-1. Compound **45** where the hydroxyl group was acetylated exhibited a K_i of 33.97 ± 15.96 µM, which is 69-fold decrease in binding compared to **10**. However, **45** showed improved binding relative to **39**, which might be attributed to the formation of a hydrogen bond between the carbonyl of the acetyl group and protonated His 224, supported by computational prediction.

Table 2.4. Binding affinities of sulfonamide analogs with variations at R_1, R_2, R_3.
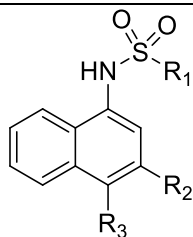
Cpd	R1	R2	R3	FP[a] $K_i \pm SD$ (µM)	SPR[a] $IC_{50} \pm SD$ (µM)
39	—Br	S—C(=O)OH	-OCH₃	86.98 ± 15.35	>100
40	—Br	S—C(=O)OCH₃	-OCH₃	>27*	>100
41	—Br	S—C(=O)NH₂	-OCH₃	>27*	>100
42	—(biphenyl)	S—C(=O)OH	-OCH₃	20.00 ± 0.79	>100
43	(meta-biphenyl)	S—C(=O)OH	-OCH₃	24.2 ± 1.9	58.4 ± 9.5
44	—Br	⌇⌇⌇OH	-OCH₃	>27*	>100
45	—Br	S—C(=O)OH	O—C(=O)CH₃	33.97 ± 15.96	26.8 ± 7.1

*Compounds were tested up to 100 µM.
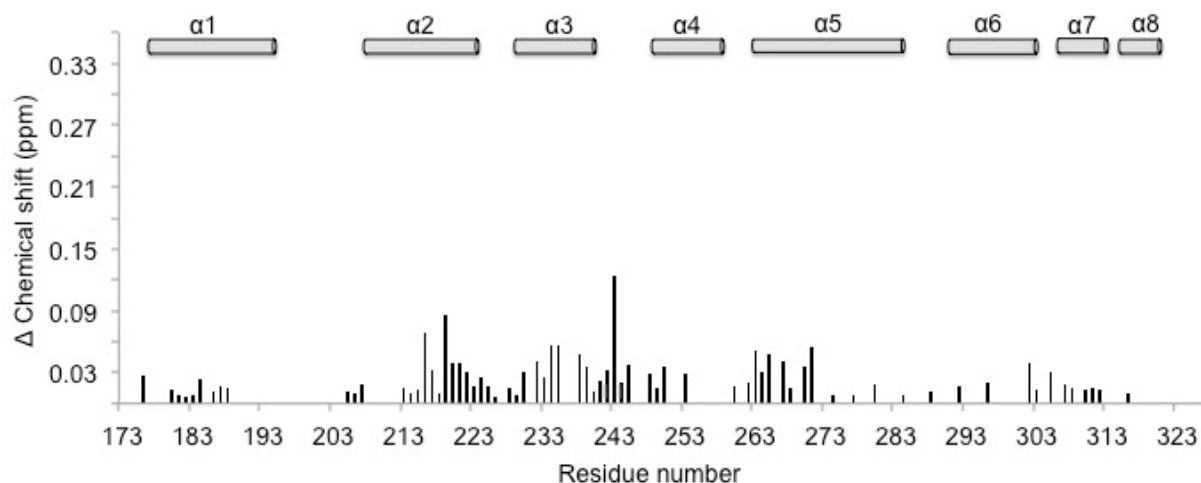
Figure 2.9. NMR studies of 40. Plot of chemical shift changes of Mcl-1 residues upon addition of **40** (Mcl-1:**40** ratio of 1 to 2).

2.5   Selectivity studies

We determined the selectivity of this class of compounds against four other Bcl-2 anti-apoptotic proteins (Bcl-2, Bcl-xL, Bcl-w, Bfl-1/A1). The most potent analogs were tested in competitive FP-based assays that were optimized for each protein, and K_i values were calculated using equations developed previously[79] (Table 2.5). In general, all the analogs inhibit Mcl-1 most potently with the following order of selectively: Bfl-1/A1 > Bcl-w > Bcl-2 > Bcl-xL. As the BH3-domain binding profile to Bfl-1/A1, as well as its BH3-binding groove, is most similar to that of Mcl-1[80], it is not surprising that the tested compounds showed less selective inhibition of A1. The most potent analogs in this series, **19** and **21**, show a profile for selectively inhibiting Mcl-1 with 7- and 19-fold versus Bfl-1/A1, 8- and 9-fold versus Bcl-w, 36- and 42-fold versus Bcl-2, and 56- and 59-fold versus Bcl-xL respectively.

Table 2.5. Selectivity of selected analogs against Bcl-2 anti-apoptotic proteins.

Cpd	Mcl-1 $K_i \pm$ SD (µM)	A1/Bfl-1 $K_i \pm$ SD (µM)	Bcl-2 $K_i \pm$ SD (µM)	Bcl-w $K_i \pm$ SD (µM)	Bcl-X$_L$ $K_i \pm$ SD (µM)
1	1.55 ± 0.18	6.14 ± 1.0	54.65 ± 9.56	37.53 ± 7.96	99.0 ± 22.63
10	0.49 ± 0.06	5.33 ± 1.0	23.83 ± 1.81	8.19 ± 1.91	32.99 ± 4.33
16	0.37 ± 0.1	2.34 ± 0.37	8.82 ± 0.65	1.92 ± 0.37	8.05 ± 0.5
17	0.38 ± 0.03	3.18 ± 0.41	7.85 ± 0.65	2.19 ± 0.45	15.14 ± 1.11
18	2.03 ± 0.41	17.26 ± 0.56	23.84 ± 3.16	4.41 ± 0.39	48.15 ± 3.28
19	0.17 ± 0.04	1.11 ± 0.19	6.11 ± 0.65	1.36 ± 0.51	9.59 ± 1.28
21	0.18 ± 0.05	3.36 ± 0.56	7.56 ± 1.08	1.58 ± 0.35	10.58 ± 1.53

2.6   Biological characterization of Mcl-1 inhibitors

To verify the specific binding of novel inhibitors to Mcl-1, we employed a pull-down assay using biotin-labeled Noxa (BL-Noxa) and whole cell lysate from the human breast cancer cell line, 2LMP. As shown in Figure 2.10, Mcl-1 was pulled down by BL-Noxa, and as was expected the Bim BH3 peptide disrupted the interaction between BL-Noxa and the Mcl-1 protein. Pre-incubation with several Mcl-1 inhibitors, **10**, **19** and **21**, completely blocked the binding of BL-Noxa to Mcl-1, similar to Bim peptide, demonstrating that these inhibitors can recognize and specifically bind to the BH3-binding groove of endogenous Mcl-1.
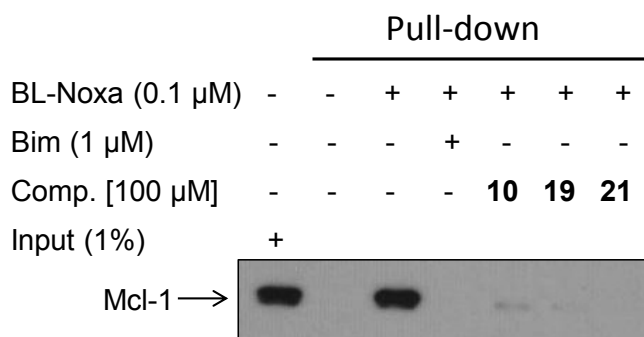

Figure 2.10. Interaction of Mcl-1 inhibitors with endogenous Mcl-1 protein and Noxa. Biotin-labeled Noxa (BL-Noxa, 0.1 µM) was incubated with whole cell lysates of 2LMP cells

with or without tested Mcl-1 inhibitors and Bim BH3 peptide as a positive control, followed by incubation with precleared streptavidin agarose beads. Eluted beads were subjected to Western blot analysis with anti-Mcl-1 antibody.

It is well established that Bax and Bak are required for the initiation of intrinsic, mitochondrial, apoptotic cell death, and they are maintained in an inactive state through interaction with the anti-apoptotic proteins[14, 81]. Therefore, cells subjected to inhibitors of anti-apoptotic proteins are expected to undergo cell death in a Bax/Bak-dependent manner[82]. To determine the contribution of Bak and Bax in the cell death induced by our Mcl-1 inhibitors, we employed murine embryonic fibroblasts (MEFs) wild type (wt) and deficient in both Bax and Bak (double knock out - DKO). Exposure of the wt MEFs to **21** resulted in a concentration-dependent cell death (assessed by PI staining), while Bax/Bak deletion significantly rescued cells from **21**-induced cell death (Figure 2.11). Although **21** induced cell death also in DKO MEFs (23% positive PI at 16 μM), it is clear that **21** is more potent in wt MEFs (61% positive PI at 16 μM), indicating that Bax and/or Bak are involved in cell death induction. Taken together, our data suggest that **21** induces cell death in a Bax/Bak-dependent manner due to its Mcl-1 inhibitory function.
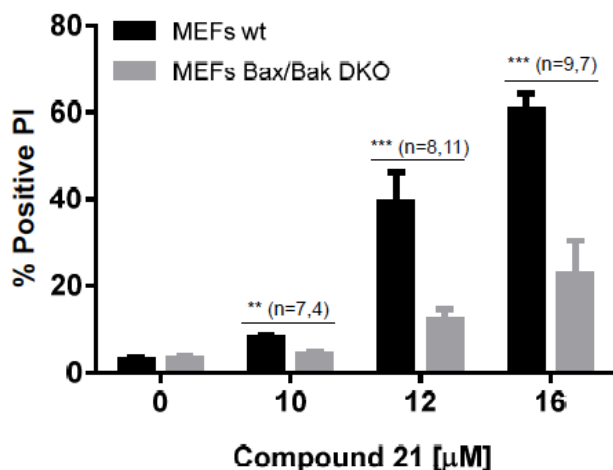
Figure 2.11. Cell death induced by 21 is Bax/Bak-dependent. MEFs deficient in Bax and Bak (gray bars) along with their wild-type counterpart (black bars) were exposed for 15 hours to different concentrations of **21** and the cell viability was assessed with PI staining. Error bars represent the mean±SEM. The significance was calculated using unpaired t test and the number of data is shown for each tested concentration with corresponding significance: (**) p<0.01 and (***) p<0.001.

To further confirm the specificity of our novel Mcl-1 inhibitors and to determine whether different pro-survival Bcl-2 proteins could suppress the apoptotic activities of novel Mcl-1 inhibitors, we used reported cell lines developed by retroviral transduction of lymphoma cells isolated from Eµ-myc transgenic mice which differ only in their expression of pro-survival Bcl-2 family proteins[83]. Lymphoma cells overexpressing Mcl-1 and Bcl-2 were treated with varying concentrations of tested compounds for 15-18 hours, and then cell viability was determined by flow cytometry using fluorescent reactive dye (LIVE/DEAD Fixable Violet Stain Kit). ABT-263 (navitoclax), a selective inhibitor of Bcl-2, Bcl-X$_L$ and Bcl-w, was used as a positive control. As predicted, lymphoma cells overexpressing Mcl-1 were sensitive to **19** and **21** as assessed by an increased percentage of cell death in a concentration-dependent manner. In contrast, cells overexpressing Bcl-2 were resistant to both Mcl-1 inhibitors (Figure 2.12). Importantly, **40** did not show any activity against both cell lines overexpressing Mcl-1 or Bcl-2, consistent with our binding studies which showed that **40** does not bind to Mcl-1. In contrast, lymphoma cells overexpressing Bcl-2 were sensitive to cell death induced by ABT-263, while cells overexpressing Mcl-1 were resistant, as expected. Collectively, these results, demonstrate that **19** and **21** specifically bind and inhibit Mcl-1 and have no effect on Bcl-2, which is consistent with our biochemical data for their selectivity profile.
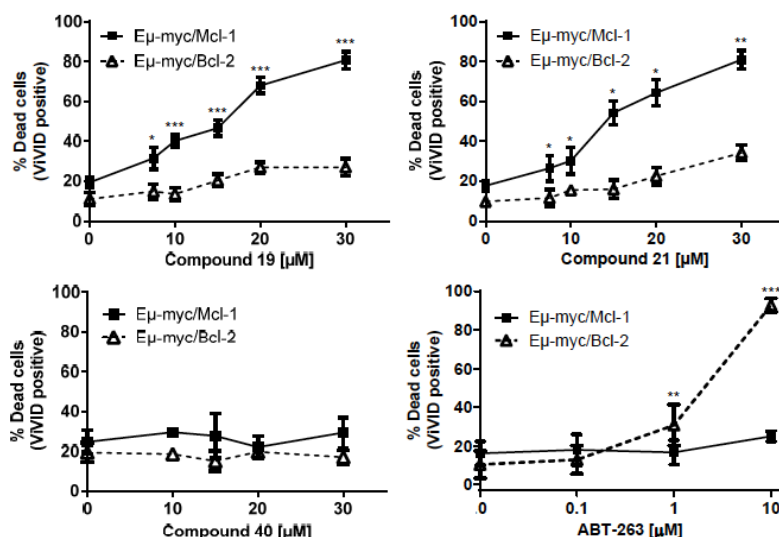
Figure 2.12. Sensitivity of Eµ-myc lymphoma cells overexpressing Mcl-1 and Bcl-2 anti-apoptotic proteins to inhibitor-induced cell death. Eµ-myc/Mcl-1 and Eµ-myc/Bcl-2 lymphomas were treated for 15-18 hours with increasing concentrations of **19**, **21**, **40** and ABT-263. Dead cells were assessed by LIVE/DEAD Fixable Dead Cell Stain Kit (ViVID). The data shown represents means ± SEM from at least 3 experiments and the significance (*) is $p<0.05$.

We next evaluated our most potent compounds for their ability to inhibit cell growth in the leukemia cell lines HL-60, MV4,11 and K-562 (Figure 2.13). It has been shown that AML-derived cell lines, HL-60 and MV4,11, are sensitive to inhibition of the anti-apoptotic protein Mcl-1, while CML-derived K-562 cell line is less sensitive to Mcl-1 inhibition[84]. Tested compounds from our series showed inhibition of the cell growth in a dose-dependent manner with similar potencies, IC_{50} values ranging from 4.24 μM to 7.56 μM against the HL-60 and MV4,11 cell lines (Figure 2.13A). Interestingly, these compounds showed decreased ability to inhibit the cell growth of K-562 with IC_{50} values of 12.5 μM to 29.9 μM. Compound **40,** which does not bind to Mcl-1, did not show inhibition up to 50 μM. Compound **21** was evaluated for its ability to induce apoptosis in the HL-60 cell line using Annexin-V and propidium iodide (PI) double staining by flow cytometry (Figure 2.13B). **21** effectively induced apoptosis in a dose-dependent manner. Treatment of the HL-60 cells by 2.5, 5.0 and 10 μM of **21** for 24 hours results in 28.9%, 37.8% and 78.4% of apoptotic cells (early + late), as compared to 7.6% of apoptotic cells in the DMSO control. Compound **40** at 40 μM has no effect on apoptosis induction just like untreated control, which is consistent with its lack of binding and inhibition of cell growth. We further tested compounds **19** and **21** in HL-60 cell line for their ability to induce caspase-3 activity, one of the important biochemical markers of apoptosis (Figure 2.13C). Both compounds induce activation of caspase-3 activity in a dose-dependent manner with **21** effectively inducing activation over a 24 h period starting at 2.5 μM. Importantly, these results correlate with the ability of **21** to induce apoposis and inhibit HL-60 cell growth.
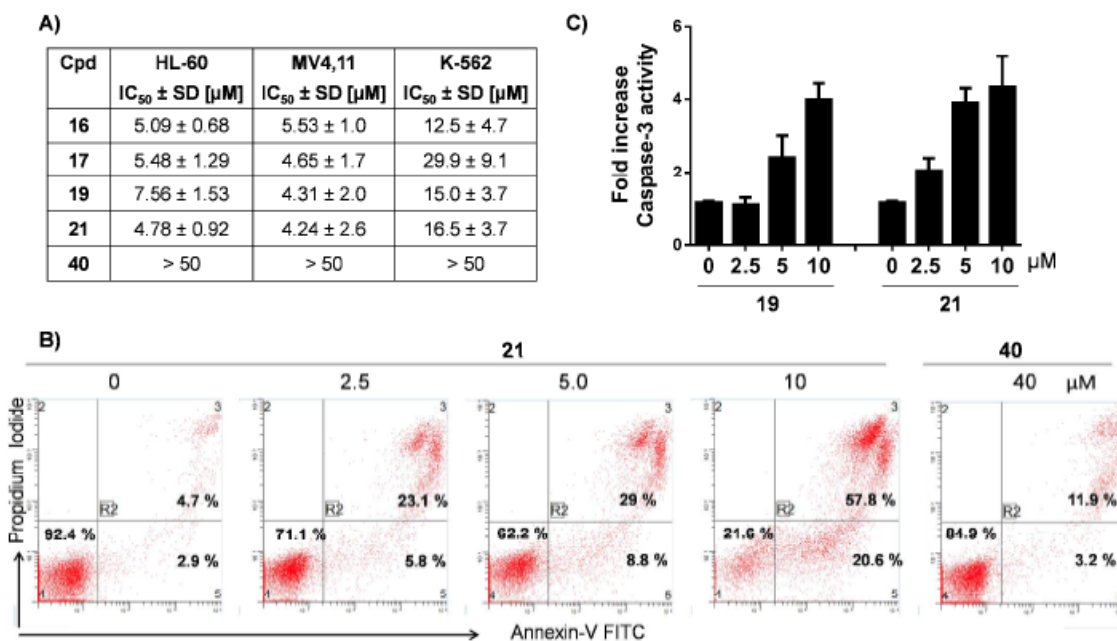
Figure 2.13. Cell-death and apoptosis induction by Mcl-1 inhibitors in human leukemic cell lines. (A) Inhibition of cell growth by designed Mcl-1 inhibitors in the HL-60, MV4,11 and K-562 leukemia cell lines. Cells were treated for 3 days and cell growth was determined using CellTiter-Glo Luminescent Cell Viability Assay. (B) Analysis of apoptosis induced by **21** in the HL-60 leukemia cell line. Cells were treated with **21** and **40** for 15 h using indicated concentrations and apoptosis was analyzed with Annexin-V and propidium Iodide (PI) double staining by flow cytometry. Early apoptotic cells were defined as Annexin-V positive/PI-negative, and late apoptotic cells as Annexin-V/PI-double positive. (C) Induction of caspase-3 by **19** and **21** in the HL-60 cell line. Cells were treated for 20 h, and caspase-3 was detected with fluorometric-based assay. Results shown are the mean and SEM from at least 3 separate experiments.

2.7 Efficacy studies of compound 10 (UMI-77) in pancreatic xenograft model

In addition to the *in vitro* cell-based studies performed with the most potent inhibitors of **59** in leukemia model cells, we have recently reported[43] on the use of analog **10** (**UMI-77**) (K_i = 0.50 μM), synthesized in 1 g scale using Scheme 2.1, in pancreatic cancer (PC) cells and xenograft mice model. Mcl-1 overexpression in PC cells is associated with resistance of cancer cells to chemotherapy and radiation making Mcl-1 an attractive molecular target for treatment of PC. It was shown that **10** inhibits PC cell growth and induces apoptosis in PC cells, but most importantly when **10** was administered at its maximum tolerated dose (MTD) of 60 mg/kg (Figure 2.14 A) to BxPC-3 xenograft model daily for 5 consecutive days a week for two weeks, it resulted in statistically significant tumor growth inhibition by 65% and 56% in comparison

with the controls in day 19 ($p < 0.0001$) and day 22 ($p < 0.003$) respectively (Figure 2.14 B). These data indicate that analog **10** exhibits single-agent antitumor activity in BxPC-3 xenograft model and highlights the potential of Mcl-1 inhibitors as novel antitumor agents in treatment of PC.
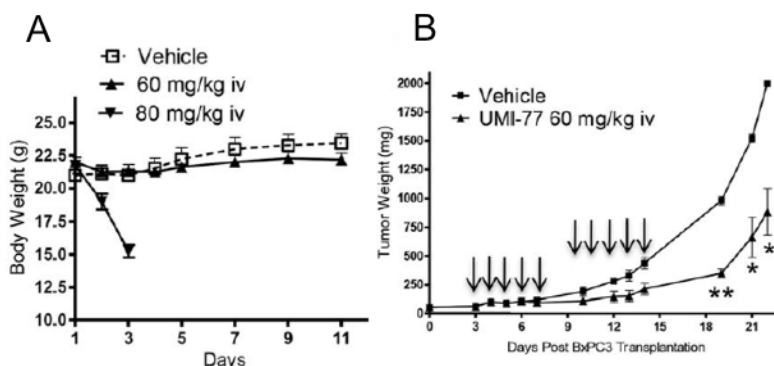

Figure 2.14. *In vivo* characterization of 10 (UMI-77). (A) Evaluation of the effect of compound **UMI-77** on weight loss of SCID mice. **UMI-77** was administrated two cycles i.v. for 5 days per week in two tested concentrations 60 and 80 mg/kg. (B) *In vivo* efficacy of UMI-77 in BxPC-3 xenograft animal model. BxPC-3 xenografts were inoculated subcutaneously in SCID mice. Once transplanted, fragments developed into palpable tumors, about 60 mg, groups of 4 animals with bi-lateral tumors were removed randomly and assigned to two treatment groups. Mice were administered **UMI-77** i.v 60 mg/kg for 5 consecutive days a week for two weeks. [■] vehicle treated group and [▼] **UMI-77** treated groups. ** indicates $p < 0.0001$, while * is $p < 0.003$ when compared to treatments with vehicle.

2.8 Conclusions

Applying HTS approach, we have identified a novel class of small molecules as selective Mcl-1 inhibitors. Employing structure-based design supported by NMR studies, we synthesized a focused library of analogs and established a SAR for binding to Mcl-1. Careful HSQC analysis of analogs **16** to **18** provided strong evidence for the predicted binding model of these compounds and further confirmation that R_1 substituent of this class of inhibitors binds to one well-defined binding pocket of Mcl-1, known as p2 pocket. Analogs **19** and **21** with K_i values of 170 nM and 180 nM, respectively, were developed as the most potent compounds in this series with an overall 9-fold increase in binding compared to **1**. Binding studies showed that **19** and **21** maintained the selectivity profile of **1**. Using wild type and Bax/Bak double knockout MEFs cells, the contribution of these two multi-domain pro-apoptotic proteins in **21** induction of cell

death was determined and demonstrated that **21** primarily cause cell death in wild type MEFs in a Bax/Bak-dependent manner. Furthermore, **19** and **21** led to sensitization of Eμ-myc lymphomas overexpressing Mcl-1, but did not show effect on cells overexpressing Bcl-2 anti-apoptotic protein, confirming their selective targeting of Mcl-1. Most potent Mcl-1 inhibitors inhibited the cell growth of AML-derived cell lines, HL-60 and MV4,11. Compounds **19** and **21** induced activation of caspase-3 in HL-60 cell line, and **21** effectively induced apoptosis starting at 2.5 μM. Finally, efficacy studies in a PC xenograft model with analog **10** demonstrated that this analog exhibited robust antitumor activity. These promising findings, for the first time, provide a proof of principle for the therapeutic potential of selective Mcl-1 inhibitors for the treatment of PC.

2.9 Experimental

Chemistry

All anhydrous reactions were run under an atmosphere of dry nitrogen. Reagents were used as supplied without further purification. Reactions were monitored by TLC using precoated silica gel 60 F254 plates. Silica gel chromatography was performed with silica gel (220–240 mesh) obtained from Silicycle. Purities of final compounds were assessed by analytical HPLC performed on a Shimadzu system with a Restek Ultra C18 (4.6 x 150 mm, 5μm particle size) column or an Agilent 1100 series with an Agilent Zorbax Eclipse Plus−C18 column and a gradient of acetonitrile with 0.1 vol% TFA (10-90%) in water with 0.1 vol% TFA. Semi-preparative HPLC was performed on a Shimadzu system with a Restek Ultra C18 (21.2 x 150 mm, 5μm particle size) column. All NMR spectra were obtained in DMSO-d_6 or CDCl$_3$ and results were recorded at 400 MHz on a Varian 400 instrument or at 500 MHz on a Varian 500 instrument. Mass spectrometry analysis was performed using a Waters LCT time-of-flight mass spectrometry instrument utilizing electrospray ionization operating in positive-ion (ESI+) or negative-ion (ESI-) modes where indicated. High-resolution mass spectrometry (HRMS) analysis was performed on an Agilent Q-TOF system. Analogs **4-8**, **15**, and **38** were purchased from commercial vendors.
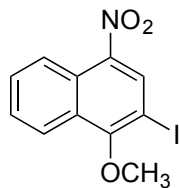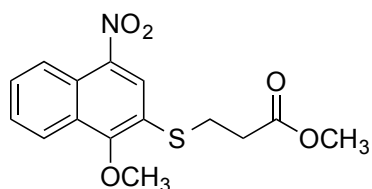
2-Iodo-1-methoxy-4-nitronaphthalene (46). Synthesized using reported procedure with modification.[59]   A mixture of 1-methoxy-4-nitronaphthalene (2.1 g, 10.4 mmol), N-iodosuccinimide (2.7 g, 12 mmol) in TFA (40 mL) was heated to reflux and stirred for 20 h under nitrogen. The reaction mixture was diluted with EtOAc (40 mL), washed with saturated aqueous $Na_2S_2O_3$ solution (30 mL), saturated aqueous $NaHCO_3$ (30 mL x 2), and brine (30 mL). The organic layer was dried ($MgSO_4$), filtered and silica was added to filtrate and the solvent was removed under reduced pressure. The adsorbed crude residue was purified by flash column chromatography (100% hexane) on silica gel to give **46** (2.4 g, 70%) as a light yellow solid. Note: R_f of starting material and product are very close and a good separation is achieved with a relatively long silica gel column and 100% hexane gradient. >95% pure product is needed for pd-catalyzed coupling step. ^{1}H NMR (400 MHz, $CDCl_3$) δ 8.59 (s, 1H), 8.58 (s, 1H), 8.21 (d, J = 8.42 Hz, 1H), 7.74 (t, J = 7.53 Hz, 1H), 7.65 (t, J = 7.53 Hz, 1H), 4.03 (s, 3H); ^{13}C NMR (100 MHz, $CDCl_3$) δ 161.69, 142.85, 134.07, 129.99, 128.55, 128.08, 126.55, 123.92, 123.02, 83.35, 62.20; ESI MS: m/z 330.0 (M+H)[+].
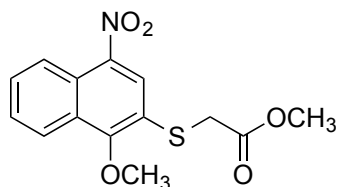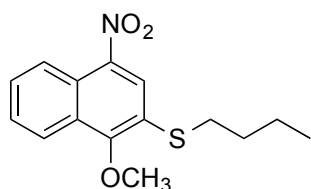

Methyl 2-((1-methoxy-4-nitronaphthalen-2-yl)thio)acetate (47a). Synthesized using reported procedures with modification.[62-64] To a solution of Cs_2CO_3 (1.5 g, 4.5 mmol) in dry THF (7 mL) under nitrogen was added methylthioglycolate (277 μL, 2.9 mmol). The mixture was stirred at room temperature for 10 min. At this time, a solution of $ZnCl_2$ (288 mg, 2.1 mmol) in dry THF (3 mL) was added and the mixture was stirred at room temperature for an additional 10 min. Meanwhile, in a separate flask $Pd(OAc)_2$ (36 mg, 0.16 mmol) and xantphos (90 mg, 0.15 mmol) were premixed in dry THF (5 mL) under nitrogen and stirred at room temperature for about 20 min. To the solution of thiol, Cs_2CO_3, and $ZnCl_2$ was added **46** (1.0 g, 3.1 mmol), LiI (200 mg, 1.5 mmol) and premixed solution of the catalyst and ligand. The mixture was stirred at 60°C under nitrogen for 20 h. The reaction mixture was filtered to remove Cs_2CO_3 and silica was

added to the mixture and the solvent was removed under reduced pressure. The adsorbed crude residue was purified by column chromatography (hexane/EtOAc 4:1) on silica gel to give **47a** (606 mg, 66%) as a yellow oil which solidified. ^{1}H NMR (400 MHz, CDCl$_3$) δ 8.59 (d, J = 8.50 Hz, 1H), 8.37 (s, 1H), 8.19 (d, J = 8.50 Hz, 1H), 7.70 (t, J = 7.57 Hz, 1H), 7.64 (t, J = 7.57 Hz, 1H), 4.07 (s, 3H), 3.77 (s, 2H), 3.70 (s, 3H); ^{13}C NMR (100 MHz, CDCl$_3$) δ 169.48, 159.95, 142.50, 129.73, 128.88, 127.85, 127.22, 125.94, 123.71, 122.93, 122.68, 61.92, 52.72, 35.10; ESI MS: m/z 308.1 (M+H)$^+$.
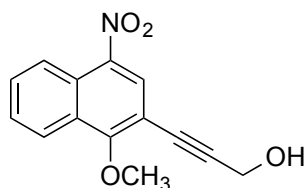

Methyl 3-((1-methoxy-4-nitronaphthalen-2-yl)thio)propanoate (47b). Synthesized using a similar procedure used to prepare **47a** except using methyl 3-mercaptopropionate. The mixture was stirred at 60°C under nitrogen for 5 h. Crude was purified using flash column chromatography (hexane/EtOAc 4:1) on silica gel with dry loading to give **47b** (194 mg, 66%) as a yellow oil. ^{1}H NMR (400 MHz, CDCl$_3$) δ 8.56 (d, J = 8.48 Hz, 1H), 8.27 (s, 1H), 8.16 (d, J = 8.48 Hz, 1H), 7.70-7.64 (m, 1H), 7.64-7.58 (m, 1H), 4.03 (s, 3H), 3.65 (s, 3H), 3.28 (t, J = 7.24 Hz, 2H), 2.65 (t, J = 7.24 Hz, 2H); ^{13}C NMR (100 MHz, CDCl$_3$) δ 171.64, 159.79, 142.48, 129.51, 128.93, 127.81, 126.94, 125.60, 123.62, 123.45, 122.57, 61.59, 51.90, 34.11, 28.11; ESI MS: m/z 322.0 (M+H)$^+$, 343.9 (M+Na)$^+$.

Butyl(1-methoxy-4-nitronaphthalen-2-yl)sulfane (47c). Syntehsized using a reported procedure.[60] A stirred mixture of **46** (300 mg, 0.91 mmol), Pd$_2$(dba)$_3$ (42 mg, 0.05 mmol), Dppf (104 mg, 0.18 mmol) and Et$_3$N (0.2 mL) in dry NMP (7 mL) was flushed with nitrogen for 15 min at room temperature. Butanethiol (83 μL, 0.77 mmol) was then added and the reaction mixture was heated to 80°C and stirred for 1.5 h. The mixture was diluted with EtOAc (10 mL) and washed with H$_2$O (10 mL x4) and brine (10 mL). The organic layer was dried (MgSO$_4$), filtered and silica was added to the filtrate and the solvent was removed under reduced pressure. The adsorbed crude residue was purified by flash column chromatography (hexane to

51

hexane/EtOAc 99:1) on silica gel to give **47c** (189 mg, 71%) as a yellow oil. ^{1}H NMR (400 MHz, CDCl$_3$) δ 8.58 (ddd, J = 0.72, 1.50, 8.36 Hz, 1H), 8.26 (s, 1H), 8.16 (ddd, J = 0.72, 1.50, 8.36 Hz, 1H), 7.68-7.59 (m, 2H), 4.03 (s, 3H), 3.03 (t, J = 7.36 Hz, 2H), 1.67 (p, J = 7.36 Hz, 2H), 1.48 (h, J = 7.36 Hz, 2H), 0.93 (t, J = 7.36 Hz, 3H); ^{13}C NMR (100 MHz, CDCl$_3$) δ 158.48, 142.53, 129.05, 128.81, 127.69, 125.69, 125.57, 125.03, 123.62, 122.34, 61.31, 32.23, 31.10, 21.92, 13.60; ESI MS: m/z 292.0 (M+H)$^+$.


3-(1-Methoxy-4-nitronaphthalen-2-yl)prop-2-yn-1-ol (47d). Syntehsized using a reported procedure.[61] A mixture of **46** (453 mg, 1.4 mmol), Pd(PPh$_3$)$_2$Cl$_2$ (48 mg, 0.07 mmol), and CuI (28 mg, 0.15 mmol) in Et$_3$N (8 mL) and dry THF (3 mL) was added dropwise to a solution of 2-propyn-1-ol (0.15 mL, 2.6 mmol) in Et$_3$N (3 mL) under nitrogen at room temperature. Reaction mixture was heated to 60°C and stirred for 2 h then diluted with EtOAc (10 mL) and washed with saturated aqueous NH$_4$Cl (15 mL x 2) and brine (15 mL). The organic layer was dried (MgSO$_4$), filtered, concentrated under reduced pressure. The crude was purified by flash column chromatography (hexane/EtOAc 3:2) on silica gel to give **47d** (342 mg, 97%) as a yellow solid. ^{1}H NMR (400 MHz, CDCl$_3$) δ 8.59 (d, J = 8.66 Hz, 1H), 8.29 (s, 1H), 8.26 (d, J = 8.66 Hz, 1H), 7.74-7.66 (m, 1H), 7.64-7.55 (m, 1H), 4.58 (s, 2H), 4.29 (s, 3H); ^{13}C NMR (100 MHz, CDCl$_3$) δ 162.40, 141.04, 130.49, 129.78, 128.26, 127.56, 126.29, 123.44, 123.24, 107.40, 93.96, 80.83, 61.95, 51.67; ESI MS: m/z 258.1 (M+H)$^+$.
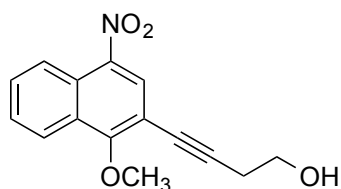
4-(1-Methoxy-4-nitronaphthalen-2-yl)but-3-yn-1-ol (47e). Synthesized using a similar procedure used to prepare **47d** except using 3-butyn-1-ol as the alkyne. The crude was purified by flash column chromatography (hexane/EtOAc 3:2) on silica gel to give **47e** (338 mg, 83%) as a yellow solid. ^{1}H NMR (400 MHz, CDCl$_3$) δ 8.53 (d, J = 8.56 Hz, 1H), 8.23 (s, 1H), 8.19 (d, J = 8.56 Hz, 1H), 7.63 (t, J = 7.59 Hz, 1H), 7.53 (t, J = 7.59 Hz, 1H), 4.23 (s, 3H), 3.87 (t, J = 6.14 Hz, 2H), 2.76 (t, J = 6.14 Hz, 2H), 2.45 (s, 1H); ^{13}C NMR (100 MHz, CDCl$_3$) δ 162.29, 141.11,

130.19, 129.91, 128.36, 127.48, 126.03, 123.43, 123.10, 109.99, 108.73, 93.90, 61.77, 60.96, 24.07; ESI MS: m/z 272.1 $(M+H)^+$.

A representative procedure for iron reduction of nitro to amine
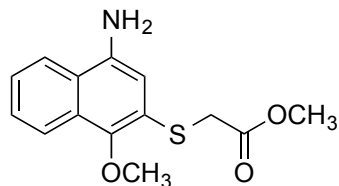
Methyl 2-((4-amino-1-methoxynaphthalen-2-yl)thio)acetate (48a). Syntehsized using a reported procedure.[65] To a suspension of iron powder (538 mg, 9.6 mmol) in glacial acetic acid (5 mL) was added **47a** (195 mg, 0.63 mmol) dissolved in glacial acetic acid (5 mL). The mixture was stirred at 70°C under nitrogen for 1 h when the mixture turned milky. The mixture was then diluted with EtOAc (15 mL) and washed with saturated aqueous $NaHCO_3$ (20 mL x 2) and brine (20 mL). Organic layer was dried ($MgSO_4$), filtered and the solvent was removed under reduced pressure to give **48a** as a crude as a purple oil. The crude was used in the next step without further purification. ^{1}H NMR (400 MHz, CDCl$_3$) δ 8.03 (d, J = 8.29 Hz, 1H), 7.76 (d, J = 8.29 Hz, 1H), 7.50 (t, J = 7.58 Hz, 1H), 7.43 (t, J = 7.58 Hz, 1H), 6.78 (s, 1H), 3.91 (s, 3H), 3.73 (s, 2H), 3.68 (s, 3H); ^{13}C NMR (100 MHz, CDCl$_3$) δ 170.48, 147.81, 138.68, 128.54, 126.54, 125.33, 124.24, 123.36, 122.45, 121.35, 111.08, 61.41, 52.53, 35.37; ESI MS: m/z 278.1 $(M+H)^+$, 300.1 $(M+Na)^+$.
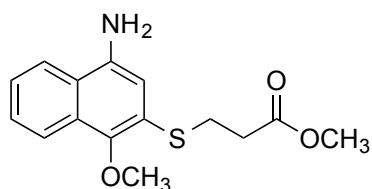
Methyl 3-((4-amino-1-methoxynaphthalen-2-yl)thio)propanoate (48b). Synthesized using the procedure for **48a** except using **47b** as the starting material. Crude was used in the next step without further purification; ^{1}H NMR (400 MHz, CDCl$_3$) δ 8.02 (d, J = 8.36 Hz, 1H), 7.75 (d, J = 8.36 Hz, 1H), 7.49 (t, J = 7.56 Hz, 1H), 7.42 (t, J = 7.56 Hz, 1H), 6.72 (s, 1H), 6.26 (s, 2H), 3.89 (s, 3H), 3.65 (s, 3H), 3.22 (t, J = 7.46 Hz, 2H), 2.64 (t, J = 7.46 Hz, 2H); ^{13}C NMR (100 MHz, CDCl$_3$) δ 172.38, 147.73, 138.77, 128.63, 126.51, 125.12, 123.92, 123.56, 122.36, 121.35, 110.85, 61.21, 51.78, 34.48, 27.90; ESI MS: m/z 292.0 $(M+H)^+$, 314.0 $(M+Na)^+$.
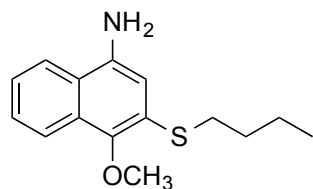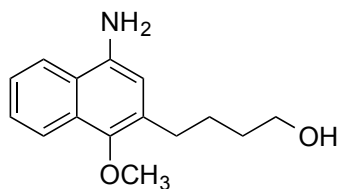
3-(Butylthio)-4-methoxynaphthalen-1-amine (48c). Synthesized using the procedure for **48a** except using **47c** as the starting material. Crude was used in the next step without further purification. ^{1}H NMR (400 MHz, CDCl$_3$) δ 8.03 (d, J = 8.30 Hz, 1H), 7.75 (d, J = 8.30 Hz, 1H), 7.49 (t, J = 7.42 Hz, 1H), 7.40 (t, J = 7.42 Hz, 1H), 6.72 (s, 1H), 6.30 (s, 2H), 3.92 (s, 3H), 2.96 (t, J = 7.33 Hz, 2H), 1.65 (p, J = 7.33 Hz, 2H), 1.47 (h, J = 7.33 Hz, 2H), 0.92 (t, J = 7.33 Hz, 3H); ^{13}C NMR (100 MHz, CDCl$_3$) δ 146.85, 138.46, 128.54, 126.42, 125.50, 124.73, 123.45, 122.20, 121.30, 110.24, 61.02, 32.29, 31.50, 22.02, 13.67; ESI MS: m/z 262.0 (M+H)$^+$.

A representative procedure for hydrogenation reaction
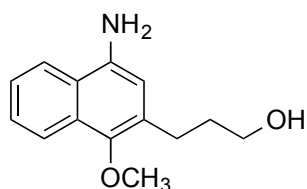
3-(4-Amino-1-methoxynaphthalen-2-yl)propan-1-ol (48d). Syntheszied using a reported procedure.[66] A stirred solution of **47d** (325 mg, 1 mmol) in a mixture of EtOH (12 mL) and EtOAc (2mL) was hydrogenated in the presence of 10% Pd/C (80 mg) at room temperature and under 30 psi of H$_2$ overnight. The suspension was filtered through a pad of celite and the filtrate was concentrated under reduced pressure. The crude was used in the next reaction without further purification. ^{1}H NMR (400 MHz, CDCl$_3$) δ 8.02 (d, J = 8.35 Hz, 1H), 7.76 (d, J = 8.35 Hz, 1H), 7.51-7.43 (m, 1H), 7.43-7.35 (m, 1H), 6.54 (s, 1H), 3.85 (s, 3H), 3.54 (t, J = 6.08 Hz, 2H), 2.80 (t, J = 7.27 Hz, 2H), 1.85 (p, J = 6.69 Hz, 2H); ^{13}C NMR (100 MHz, CDCl$_3$) δ 146.20, 138.66, 129.80, 128.24, 126.01, 124.51, 123.79, 122.41, 121.33, 111.39, 62.18, 61.32, 33.18, 25.51; ESI MS: m/z 232.1 (M+H)$^+$.


4-(4-Amino-1-methoxynaphthalen-2-yl)butan-1-ol (48e). Synthesized using the procedure for **47e** except using **47f** as the starting material. Crude was used in the next step without further

purification. ^{1}H NMR (400 MHz, CDCl$_3$) δ 7.99 (d, J = 8.39 Hz, 1H), 7.72 (d, J = 8.39 Hz, 1H), 7.43 (t, J = 7.33 Hz, 1H), 7.34 (t, J = 7.33 Hz, 1H), 6.52 (s, 1H), 3.79 (s, 3H), 3.56 (t, J = 6.43 Hz, 2H), 2.67 (t, J = 6.43 Hz, 2H), 1.65 (dt, J = 6.60, 14.36 Hz, 2H), 1.56 (dt, J = 6.60, 14.36 Hz, 2H); ^{13}C NMR (100 MHz, CDCl$_3$) δ 145.98, 138.36, 130.77, 128.39, 125.85, 124.33, 123.72, 122.34, 121.36, 111.52, 62.32, 61.97, 32.45, 29.21, 26.89.

A representative procedure for sulfonamide/amide coupling reaction of aryl amines with sulfonyl/acyl chlorides
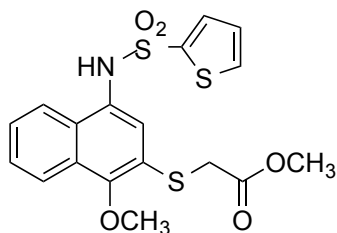
Methyl 2-((1-methoxy-4-(thiophene-2-sulfonamido)naphthalen-2-yl)thio)acetate (48f). A solution of the crude amine **48a** dissolved in dry CH$_2$Cl$_2$ (4mL) was added to 2-thiophenesulfonyl chloride (119mg, 0.65 mmol). Addition of pyridine (0.08 mL, 0.99 mmol) was followed and the mixture was stirred at room temperature under nitrogen overnight. The mixture was diluted with EtOAc (10 mL) and washed with H$_2$O (10 mL x 3) and brine (10 mL). The organic layer was dried (MgSO$_4$), filtered and the solvent was removed under reduced pressure. Crude was purified by flash column chromatography (hexane/EtOAc 7:3) on silica gel to give **48f** (176 mg, 66% over two steps) as a purple oil which solidified upon standing. ^{1}H NMR (400 MHz, CDCl$_3$) δ 8.01 (d, J = 8.40 Hz, 1H), 7.82 (d, J = 8.40 Hz, 1H), 7.49-7.43 (m, 2H), 7.42-7.39 (m, 1H), 7.39-7.34 (m, 2H), 6.92-6.88 (m, 1H), 3.95 (s, 3H), 3.68 (s, 3H), 3.65 (s, 2H); ^{13}C NMR (100 MHz, CDCl$_3$) δ 169.91, 154.12, 139.48, 133.09, 132.51, 130.06, 128.60, 127.74, 127.39, 126.96, 125.74, 123.39, 122.29, 61.49, 52.68, 35.12; ESI MS: m/z 423.9 (M+H)$^+$, 445.8 (M+Na)$^+$.
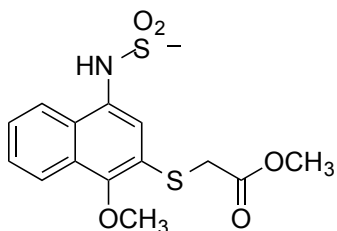
Methyl 2-((1-methoxy-4-(methylsulfonamido)naphthalen-2-yl)thio)acetate (48g).

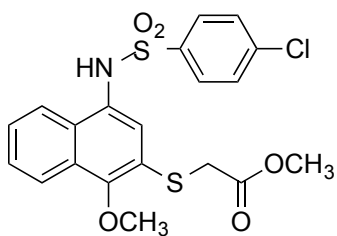Synthesized using the procedure for **48f** except using methanesulfonyl chloride, which afforded the title compound (69 mg, 39% over two steps) as a light pink solid. ^{1}H NMR (400 MHz, CDCl$_3$) δ 8.13-8.08 (m, 1H), 8.05-8.00 (m, 1H), 7.65 (s, 1H), 7.60-7.54 (m, 2H), 6.80 (s, 1H), 3.99 (s, 3H), 3.75 (s, 2H), 3.69 (s, 3H), 3.04 (s, 3H); ^{13}C NMR (100 MHz, CDCl$_3$) δ 169.98, 154.06, 129.61, 128.85, 127.84, 127.36, 127.19, 125.15, 123.67, 122.67, 122.07, 61.50, 52.64, 39.91, 35.00; ESI MS: m/z 355.9 (M+H)$^+$, 377.9 (M+Na)$^+$.
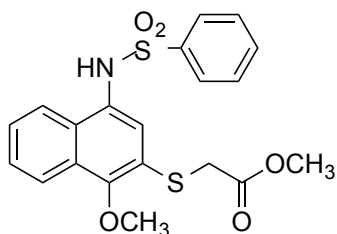
Methyl 2-((1-methoxy-4-(phenylsulfonamido)naphthalen-2-yl)thio)acetate (48h). Synthesized using the procedure for **48g** except using benzenesulfonyl chloride, which afforded the title compound (119 mg, 64% over two steps) as a purple oil which solidified upon standing. ^{1}H NMR (400 MHz, CDCl$_3$) δ 8.01 (d, *J* = 8.40 Hz, 1H), 7.74 (t, *J* = 9.06 Hz, 3H), 7.47 (q, *J* = 8.19, 8.80 Hz, 2H), 7.36 (t, *J* = 7.61 Hz, 3H), 7.29 (s, 1H), 6.93 (s, 1H), 3.95 (s, 3H), 3.68 (s, 3H), 3.61 (s, 2H); ^{13}C NMR (100 MHz, CDCl$_3$) δ 169.80, 154.02, 139.11, 132.95, 129.95, 128.98, 128.63, 127.82, 127.33, 126.95, 126.90, 125.67, 123.36, 122.31, 122.28, 61.49, 52.63, 35.06; ESI MS: m/z 417.9 (M+H)$^+$, 439.9 (M+Na)$^+$.

Methyl 2-((4-(4-chlorophenylsulfonamido)-1-methoxynaphthalen-2-yl)thio)acetate (48i). Synthesized using the procedure for **48f** except using 4-chlorobenzenesulfonyl chloride, which afforded the title compound (280 mg, 67% over two steps) as a light pink solid. ^{1}H NMR (400 MHz, CDCl$_3$) δ 8.02 (d, *J* = 8.40 Hz, 1H), 7.74 (d, *J* = 8.40 Hz, 1H), 7.66 (t, *J* = 1.96 Hz, 1H), 7.65 (t, *J* = 1.96 Hz, 1H), 7.47 (ddd, *J* = 1.17, 6.86, 8.24 Hz, 1H), 7.38 (ddd, *J* = 1.17, 6.86, 8.24 Hz, 1H), 7.35-7.33 (m, 2H), 7.32 (t, *J* = 1.94 Hz, 1H), 7.07 (s, 1H), 3.95 (s, 3H), 3.69 (s, 3H), 3.63 (s, 2H); ^{13}C NMR (100 MHz, CDCl$_3$) δ 169.84, 154.18, 139.50, 137.67, 129.86, 129.25, 128.78, 128.66, 127.49, 127.05, 125.81, 123.42, 122.41, 122.14, 61.50, 52.64, 35.02; ESI MS:

m/z 451.9 (M+H)$^+$, 473.8 (M+Na)$^+$.

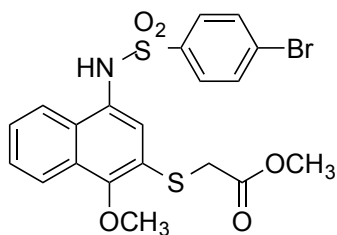**Methyl 2-((4-(4-bromophenylsulfonamido)-1-methoxynaphthalen-2-yl)thio)acetate (40).** Synthesized using the procedure for **48f** except using 4-bromobenzenesulfonyl chloride, which afforded the title compound (185 mg, 61% over two steps) as a pink/purple solid. 97% pure by HPLC. ^{1}H NMR (400 MHz, CDCl$_3$) δ 8.04 (d, J = 8.38 Hz, 1H), 7.72 (d, J = 8.38 Hz, 1H), 7.61-7.59 (m, 1H), 7.58 (t, J = 2.04 Hz, 1H), 7.54-7.47 (m, 3H), 7.44-7.38 (m, 1H), 7.34 (s, 1H), 6.76 (s, 1H), 3.97 (s, 3H), 3.71 (s, 3H), 3.64 (s, 2H); ^{13}C NMR (100 MHz, CDCl$_3$) δ 169.83, 154.25, 138.21, 132.29, 129.91, 128.89, 128.71, 128.07, 127.41, 127.12, 125.92, 123.47, 122.48, 122.17, 122.09, 61.56, 52.70, 35.03; ESI HRMS: m/z 493.9724 (M-H)$^-$.

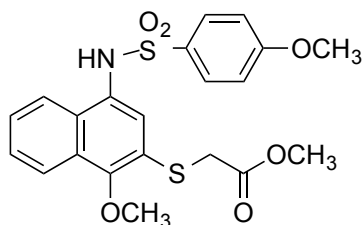**Methyl 2-((1-methoxy-4-(4-methoxyphenylsulfonamido)naphthalen-2-yl)thio)acetate (48j).** Synthesized using the procedure for **48f** except using 4-methoxybenzenesulfonyl chloride, which afforded the title compound (190 mg, 77% over two steps) as a purple oil which solidified upon standing. ^{1}H NMR (400 MHz, CDCl$_3$) δ 8.02 (d, J = 8.42 Hz, 1H), 7.80 (d, J = 8.42 Hz, 1H), 7.69-7.63 (m, 2H), 7.48 (t, J = 7.64 Hz, 1H), 7.40 (t, J = 7.64 Hz, 1H), 7.29 (s, 1H), 6.86-6.80 (m, 3H), 3.95 (s, 3H), 3.79 (s, 3H), 3.70 (s, 3H), 3.63 (s, 2H); ^{13}C NMR (100 MHz, CDCl$_3$) δ 169.82, 163.12, 153.79, 130.64, 129.85, 129.52, 128.61, 128.11, 126.95, 126.90, 125.20, 123.36, 122.31, 114.12, 61.50, 55.56, 52.65, 35.09; ESI MS: m/z 447.8 (M+H)$^+$, 469.8 (M+Na)$^+$.
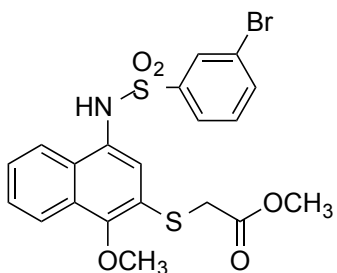
Methyl 2-((4-(3-bromophenylsulfonamido)-1-methoxynaphthalen-2-yl)thio)acetate (48k). Synthesized using the procedure for **48f** except using 3-bromobenzenesulfonyl chloride, which afforded the title compound (331 mg, 74%) as a purple/pink solid. ^{1}H NMR (400 MHz, CDCl$_3$) δ 8.04 (d, J = 8.40 Hz, 1H), 7.88 (s, 1H), 7.73 (d, J = 8.40 Hz, 1H), 7.62 (t, J = 9.41 Hz, 2H), 7.49 (t, J = 7.59 Hz, 1H), 7.40 (t, J = 7.59 Hz, 1H), 7.34 (s, 1H), 7.26-7.21 (m, 1H), 6.82 (s, 1H), 3.98 (s, 3H), 3.70 (s, 3H), 3.65 (s, 2H); ^{13}C NMR (100 MHz, CDCl$_3$) δ 169.72, 154.55, 141.06, 135.89, 130.41, 130.24, 130.03, 128.75, 127.31, 127.04, 127.02, 126.33, 125.89, 123.45, 122.90, 122.48, 122.09, 61.48, 52.55, 35.16; ESI MS: m/z 495.8, 497.8 (M+H)$^+$, 517.8, 519.8 (M+Na)$^+$.
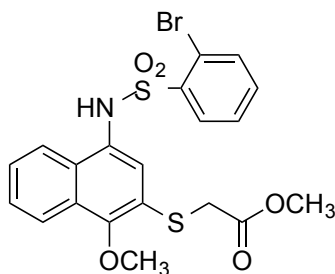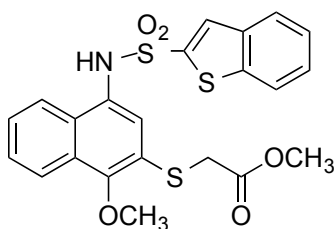

Methyl 2-((4-(2-bromophenylsulfonamido)-1-methoxynaphthalen-2-yl)thio)acetate (48l). Synthesized using the procedure for **48f** except using 2-bromobenzenesulfonyl chloride, which afforded the title compound (314 mg, 74% over two steps) as a purple oil. ^{1}H NMR (400 MHz, CDCl$_3$) δ 8.16-8.11 (m, 1H), 8.05-8.00 (m, 1H), 7.93 (d, J = 7.72 Hz, 1H), 7.78 (d, J = 7.72 Hz, 1H), 7.54-7.48 (m, 3H), 7.42-7.32 (m, 2H), 7.19 (s, 1H), 7.13 (s, 1H), 3.94 (s, 3H), 3.68 (s, 3H), 3.49 (s, 2H); ^{13}C NMR (100 MHz, CDCl$_3$) δ 169.52, 154.35, 138.58, 135.17, 133.92, 132.04, 130.52, 128.75, 127.83, 127.55, 127.11, 127.07, 125.00, 123.16, 122.90, 122.26, 119.94, 61.40, 52.50, 35.13; ESI MS: m/z 495.8, 597.8 (M+H)$^+$, 517.8, 519.8 (M+Na)$^+$.

Methyl 2-((4-(benzo[*b*]thiophene-2-sulfonamido)-1-methoxynaphthalen-2-yl)thio)acetate (48m). Synthesized using the procedure for **48f** except using 1-benzothiophene-2-sulfonyl chloride, which afforded the title compound (132 mg, 57% over two steps) as a purple oil which

solidified upon standing. ^{1}H NMR (400 MHz, CDCl$_3$) δ 8.02 (d, J = 8.40 Hz, 1H), 7.90 (d, J = 8.40 Hz, 1H), 7.79 (d, J = 7.99 Hz, 1H), 7.74 (d, J = 7.99 Hz, 1H), 7.69 (s, 1H), 7.48-7.42 (m, 2H), 7.41 (s, 1H), 7.40-7.35 (m, 2H), 7.01 (s, 1H), 3.96 (s, 3H), 3.64 (s, 3H), 3.51 (s, 2H); ^{13}C NMR (100 MHz, CDCl$_3$) δ 169.77, 154.23, 141.85, 139.53, 137.38, 130.61, 130.05, 128.66, 127.47, 127.37, 127.06, 125.72, 125.47, 125.44, 123.47, 122.62, 122.34, 122.25, 61.51, 52.58, 34.95; ESI MS: m/z 473.9 (M+H)$^+$, 495.8 (M+Na)$^+$.
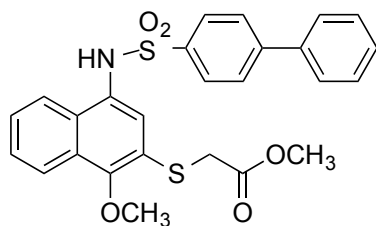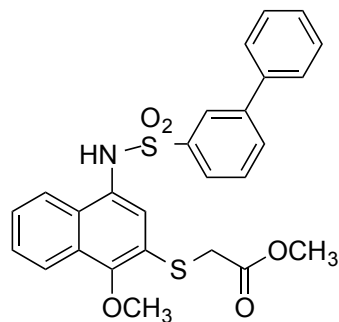

Methyl 2-((4-([1,1'-biphenyl]-4-ylsulfonamido)-1-methoxynaphthalen-2-yl)thio)acetate (48n). Synthesized using the procedure for **48f** except using 4-biphenylsulfonyl chloride, which afforded the title compound (152 mg, 71% over two steps) as a purple oil which solidified upon standing. ^{1}H NMR (400 MHz, CDCl$_3$) δ 8.02 (d, J = 8.34 Hz, 1H), 7.83-7.76 (m, 3H), 7.58 (d, J = 8.31 Hz, 2H), 7.51 (d, J = 7.14 Hz, 2H), 7.49-7.42 (m, 2H), 7.42-7.35 (m, 3H), 7.33 (s, 1H), 6.90 (s, 1H), 3.96 (s, 3H), 3.65 (s, 3H), 3.60 (s, 2H); ^{13}C NMR (100 MHz, CDCl$_3$) δ 169.75, 153.99, 145.89, 139.09, 137.68, 129.97, 128.98, 128.66, 128.50, 127.90, 127.86, 127.56, 127.23, 126.98, 126.93, 125.58, 123.43, 122.35, 122.33, 61.49, 52.58, 35.02; ESI MS: m/z 494.1 (M+H)$^+$, 516.1 (M+Na)$^+$.

Methyl 2-((4-([1,1'-biphenyl]-3-ylsulfonamido)-1-methoxynaphthalen-2-yl)thio)acetate (48o). Synthesized using reported procedures with modification.[68, 69] A stirred mixture of **48k** (307 mg, 0.62 mmol), phenylboronic acid (113 mg, 0.91 mmol), 2M aqueous Na$_2$CO$_3$ (0.93 mL), Pd(PPh$_3$)$_4$ (72 mg, 0.06 mmol) in THF (6 mL) /H$_2$O (1 mL) was heated at 60 ^{o}C under nitrogen for 2 h. Mixture was diluted with EtOAc (10 mL) and washed with H$_2$O (15 mL x 2) and brine

(15 mL). Organic layer was dried (MgSO$_4$), filtered and concentrated under reduced pressure. The crude was purified by flash column chromatography on silica to give **48o** (284 mg, 92%) as a light brown oil. ^{1}H NMR (400 MHz, CDCl$_3$/ couple of drops of D$_2$O) δ 8.00 (d, *J* = 8.39 Hz, 1H), 7.83 (s, 1H), 7.79-7.73 (m, 2H), 7.69 (dd, *J* = 7.58, 14.09 Hz, 2H), 7.47-7.40 (m, 2H), 7.37-7.31 (m, 6H), 3.92 (s, 3H), 3.62 (s, 3H), 3.58 (s, 2H); ^{13}C NMR (100 MHz, CDCl$_3$/ couple of drops of D$_2$O) δ 169.86, 154.00, 142.22, 139.49, 138.99, 133.60, 131.46, 131.02, 130.00, 129.44, 128.89, 128.63, 128.14, 127.89, 127.03, 126.98, 126.88, 125.92, 125.87, 125.80, 123.46, 122.38, 122.27, 61.43, 52.60, 34.97; ESI MS: m/z 494.1 (M+H)$^+$.
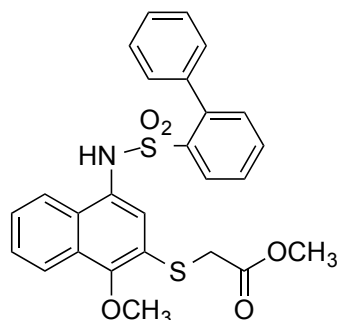

Methyl 2-((4-([1,1'-biphenyl]-2-ylsulfonamido)-1-methoxynaphthalen-2-yl)thio)acetate (48p). Synthesized using the procedure for **48f** except using 2-biphenylsulfonyl chloride which was synthesized as previously reported.[85] The title compound (57 mg, 58% over two steps) was obtained as a light orange oil. ^{1}H NMR (400 MHz, CDCl$_3$) δ 8.16 (d, *J* = 8.20 Hz, 1H), 8.00 (d, *J* = 8.20 Hz, 1H), 7.62 (t, *J* = 7.54 Hz, 1H), 7.51 (q, *J* = 7.13, 7.54 Hz, 3H), 7.44-7.37 (m, 2H), 7.37-7.29 (m, 5H), 6.93 (s, 1H), 5.86 (s, 1H), 3.91 (s, 3H), 3.67 (s, 3H), 3.44 (s, 2H); ^{13}C NMR (100 MHz, CDCl$_3$) δ 169.66, 152.79, 140.89, 138.72, 138.15, 132.77, 132.73, 129.66, 129.43, 128.59, 128.52, 128.39, 128.20, 128.11, 127.94, 127.07, 126.69, 123.16, 122.20, 122.04, 120.40, 61.44, 52.62, 34.96; ESI MS: m/z 494.0 (M+H)$^+$.
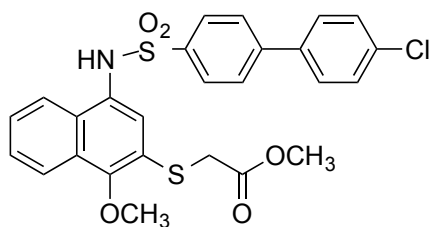
Methyl 2-((4-(4'-chloro-[1,1'-biphenyl]-4-ylsulfonamido)-1-methoxynaphthalen-2-yl)thio)acetate (48q). Synthesized using the procedure for **48f** except using 4′-chlorobiphenyl-4-sulfonyl chloride, which afforded the title compound (284 mg, 80% over two steps) as a pink oil

which solidified upon standing. ^{1}H NMR (400 MHz, CDCl$_3$) δ 8.02 (d, J = 7.14 Hz, 1H), 7.80 (d, J = 7.14 Hz, 1H), 7.78 (d, J = 7.54 Hz, 2H), 7.54 (d, J = 7.54 Hz, 2H), 7.49-7.44 (m, 2H), 7.44-7.40 (m, 3H), 7.40-7.35 (m, 1H), 7.33 (s, 1H), 6.97 (s, 1H), 3.96 (s, 3H), 3.65 (s, 3H), 3.61 (s, 2H); ^{13}C NMR (100 MHz, CDCl$_3$) δ 169.73, 154.05, 144.56, 138.08, 137.53, 134.79, 129.97, 129.19, 128.67, 128.48, 128.01, 127.80, 127.40, 126.98, 126.93, 125.64, 123.40, 122.35, 122.33, 61.50, 52.60, 35.03; ESI MS: m/z 528.1 (M+H)$^+$, 550.1 (M+Na)$^+$.

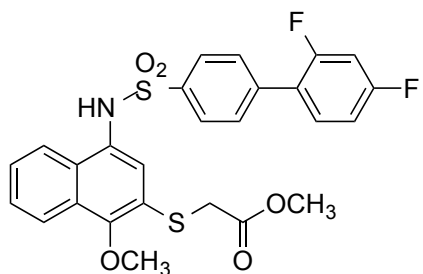**Methyl 2-((4-(2',4'-difluoro-[1,1'-biphenyl]-4-ylsulfonamido)-1-methoxynaphthalen-2-yl)thio)acetate (48r).** Synthesized using the procedure for **48f** except using 2′,4′-difluoro-biphenyl-4-sulfonyl chloride, which afforded the title compound (75 mg, 58% over two steps) as a purple oil which solidified upon standing. ^{1}H NMR (400 MHz, CDCl$_3$) δ 8.02 (d, J = 8.41 Hz, 1H), 7.83-7.76 (m, 3H), 7.50 (d, J = 8.16 Hz, 2H), 7.46 (d, J = 7.94 Hz, 1H), 7.40 (d, J = 7.94 Hz, 1H), 7.37-7.29 (m, 2H), 6.98 (s, 1H), 6.96-6.86 (m, 2H), 3.96 (s, 3H), 3.66 (s, 3H), 3.61 (s, 2H); ^{13}C NMR (100 MHz, CDCl$_3$) δ 169.84, 154.01, 139.74, 138.18, 131.40 (dd, J = 4.57, 9.75 Hz), 130.03, 129.43 (d, J = 3.03 Hz), 128.65, 127.76, 127.61, 127.02, 126.96, 125.70, 123.44, 122.37, 122.32, 111.98 (dd, J = 3.71, 21.44 Hz), 105.88-103.01 (m), 61.51, 52.63, 34.95; ESI MS: m/z 530.1 (M+H)$^+$.

Methyl 2-((1-methoxy-4-(4-phenoxyphenylsulfonamido)naphthalen-2-yl)thio)acetate (48s). Synthesized using the procedure for **48f** except using 4-phenoxybenzenesulfonyl chloride, which afforded the title compound (244 mg, 72% over two steps) as a light brown oil. ^{1}H NMR (400 MHz, CDCl$_3$) δ 8.02 (d, J = 8.43 Hz, 1H), 7.80 (d, J = 8.43 Hz, 1H), 7.66 (d, J = 8.14 Hz, 2H),

7.52-7.46 (m, 1H), 7.42-7.32 (m, 4H), 7.23 (s, 1H), 7.17 (t, J = 7.38 Hz, 1H), 6.94 (d, J = 8.52 Hz, 2H), 6.87 (d, J = 8.52 Hz, 2H), 3.95 (s, 3H), 3.69 (s, 3H), 3.66 (s, 2H); ^{13}C NMR (100 MHz, CDCl$_3$) δ 169.85, 161.65, 155.11, 153.85, 132.59, 130.09, 129.85, 129.59, 128.60, 128.03, 126.90, 126.85, 125.50, 124.81, 123.42, 122.38, 122.31, 120.02, 117.64, 61.50, 52.67, 35.05; ESI MS: m/z 509.8 (M+H)$^+$.
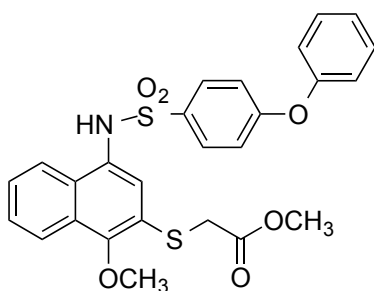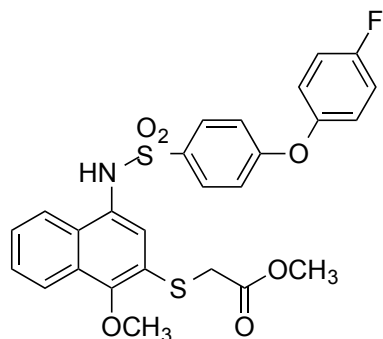

Methyl 2-((4-(4-(4-fluorophenoxy)phenylsulfonamido)-1-methoxynaphthalen-2-yl)thio)acetate (48t). Synthesized using the procedure for **48f** except using 4-(4-fluoro-phenoxy)-benzenesulfonyl chloride, which afforded the title compound (93 mg, 72% over two steps) as a yellow oil which solidified upon standing. ^{1}H NMR (400 MHz, CDCl$_3$) δ 8.02 (d, J = 8.42 Hz, 1H), 7.80 (d, J = 8.42 Hz, 1H), 7.66 (d, J = 8.72 Hz, 2H), 7.51-7.45 (m, 1H), 7.42-7.36 (m, 1H), 7.34 (s, 1H), 7.07-7.00 (m, 2H), 6.94-6.88 (m, 2H), 6.84 (d, J = 8.72 Hz, 2H), 3.95 (s, 3H), 3.69 (s, 3H), 3.66 (s, 2H); ^{13}C NMR (100 MHz, CDCl$_3$) δ 169.87, 161.82, 160.79, 158.36, 153.87, 150.83 (d, J = 2.72 Hz), 132.65, 129.83, 129.66, 128.61, 127.99, 126.88 (d, J = 4.95 Hz), 125.47, 123.39, 122.35 (d, J = 6.41 Hz), 121.67 (d, J = 8.41 Hz), 117.23, 116.86, 116.63, 61.50, 52.69, 35.06; ESI MS: m/z 528.1 (M+H)$^+$, 550.1 (M+Na)$^+$.
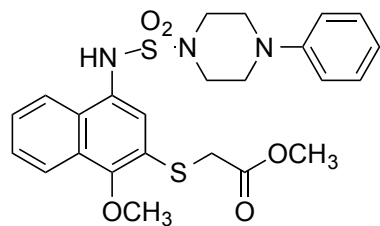
Methyl 2-((1-methoxy-4-(4-phenylpiperazine-1-sulfonamido)naphthalen-2-yl)thio)acetate (48u).

62
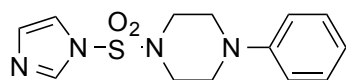
As reported previously[67], to a solution of 1,1'-sulfonyldiimidazole (1.98 g, 10 mmol) in CH_2Cl_2 (40 mL) was added methyl trifluoromethanesulfonate (1.64 g, 10 mmol) at 0 °C. The solvent was removed after 3 hours stirring. To the resulting residue in CH_3CN (40 mL) was added 1-phenylpiperazine (1.08 g, 6.67 mmol). After being stirred at room temperature overnight, the reaction mixture was concentrated under reduced pressure and the crude was purified using flash column chromatography on silica to give 1-((1H-imidazol-1-yl)sulfonyl)-4-phenylpiperazine (1.17 g, 60% yield over 2 steps) as a white solid. ^{1}H NMR (400 MHz, CDCl$_3$) δ 7.92 (s, 1H), 7.30-7.23 (m, 3H), 7.16 (s, 1H), 6.93 (t, J = 7.33 Hz, 1H), 6.89-6.84 (m, 2H), 3.37-3.30 (m, 4H), 3.26-3.20 (m, 4H); ^{13}C NMR (100 MHz, CDCl$_3$) δ 150.21, 136.62, 130.80, 129.34, 121.43, 117.64, 117.20, 48.89, 46.42; ESI MS: m/z 293.0 (M+H)$^+$.
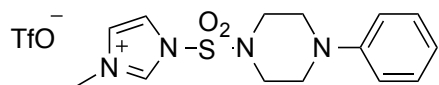
To a solution of 1-((1H-imidazol-1-yl)sulfonyl)-4-phenylpiperazine (85 mg, 0.29 mmol) in CH_2Cl_2 (3 mL) cooled at 0 °C was added methyl trifluoromethanesulfonate (0.035 mL, 0.32 mmol). After being stirred for 2h at 0 °C, the reaction mixture was concentrated under reduced pressure to give 3-methyl-1-((4-phenylpiperazin-1-yl)sulfonyl)-1H-imidazol-3-ium as a beige solid which was used in the next step without further purification.

A solution of 3-methyl-1-((4-phenylpiperazin-1-yl)sulfonyl)-1H-imidazol-3-ium (0.29 mmol) and aniline **48a** (0.29 mmol) in CH_3CN (3mL) was stirred at 80 °C for 15h. The reaction mixture was diluted with EtOAc (10 mL), washed with 1 N HCl, 1 N NaOH, H_2O, brine, dried (MgSO$_4$) and filtered. The solvent was removed under reduced pressure and the crude was purified using flash column chromatography on silica to give **48u** (36 mg, 25% over three steps) as a purple solid. ^{1}H NMR (400 MHz, CDCl$_3$) δ 8.12-8.06 (m, 1H), 8.06-8.00 (m, 1H), 7.71 (s, 1H), 7.59-7.52 (m, 2H), 7.22 (t, J = 7.94 Hz, 2H), 6.88-6.81 (m, 3H), 6.75 (s, 1H), 3.98 (s, 3H), 3.74 (s, 2H), 3.68 (s, 3H), 3.43-3.37 (m, 4H), 3.15-3.08 (m, 4H); ^{13}C NMR (100 MHz, CDCl$_3$) δ 169.86, 153.45, 150.61, 129.16, 128.93, 128.69, 128.57, 127.15, 127.07, 123.77, 123.51, 122.71, 121.71, 120.67, 116.73, 61.50, 52.59, 49.15, 46.48, 35.20; ESI MS: m/z 502.1 (M+H)$^+$, 524.1 (M+Na)$^+$.
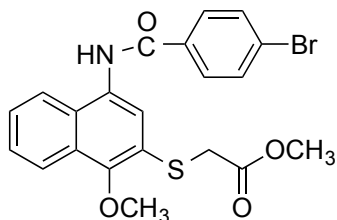
**Methyl 2-((4-(4-bromobenzamido)-1-methoxynaphthalen-2-yl)thio)acetate (48v).** Synthesized using the procedure for **48f** except using 4-bromobenzoyl chloride and Et₃N as the base, which afforded the title compound (245 mg, 66%) as a pink solid. ^{1}H NMR (400 MHz, CDCl₃) δ 8.14 (s, 1H), 8.09 (d, *J* = 8.38 Hz, 1H), 7.88 (s, 1H), 7.82- 7.73 (m, 3H), 7.63-7.56 (m, 2H), 7.56-7.43 (m, 2H), 3.98 (s, 3H), 3.74 (s, 2H), 3.68 (s, 3H); ^{13}C NMR (100 MHz, CDCl₃) δ 170.08, 165.42, 153.22, 133.17, 132.01, 131.74, 131.53, 128.82, 128.59, 128.43, 126.80, 126.77, 123.92, 123.50, 122.67, 121.57, 61.45, 52.57, 35.18; ESI MS: m/z 460.0, 462.0 (M+H)$^+$, 482.0, 484 (M+Na)$^+$.
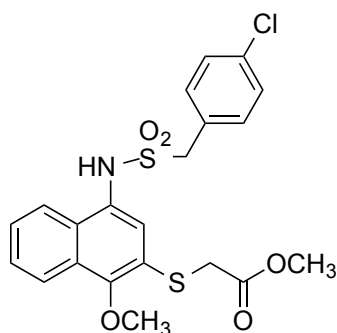
Methyl 2-((4-((4-chlorophenyl)methylsulfonamido)-1-methoxynaphthalen-2-yl)thio)acetate (48w). Synthesized using the procedure for **48f** except using 4-chlorobenzylsulfonyl chloride, which afforded the title compound (110 mg, 41% over two steps) as a light pink solid. ^{1}H NMR (400 MHz, CDCl₃) δ 8.10 (d, *J* = 8.31 Hz, 1H), 7.75 (d, *J* = 8.31 Hz, 1H), 7.65 (s, 1H), 7.57 (t, *J* = 7.54 Hz, 1H), 7.50 (t, *J* = 7.54 Hz, 1H), 7.22-7.16 (m, 4H), 6.73 (s, 1H), 4.37 (s, 2H), 4.00 (s, 3H), 3.75 (s, 2H), 3.70 (s, 3H); ^{13}C NMR (100 MHz, CDCl₃) δ 170.00, 153.34, 135.04, 132.09, 128.91, 128.74, 128.31, 127.98, 127.18, 127.08, 126.88, 123.66, 122.67, 122.59, 121.65, 61.55, 57.41, 52.66, 34.96; ESI MS: m/z 465.8 (M+H)$^+$, 487.8 (M+Na)$^+$.
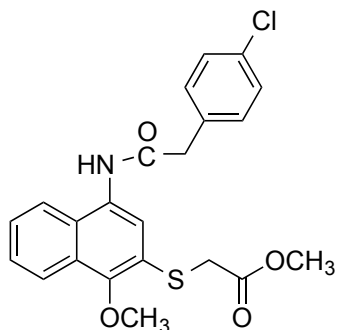

Methyl 2-((4-(2-(4-chlorophenyl)acetamido)-1-methoxynaphthalen-2-yl)thio)acetate (48x). Synthesized using the procedure for **48f** except using 4-chlorophenylacetyl chloride and Et₃N as

the base, which afforded the title compound (208 mg, 69% over two steps) as a light yellow solid. ^{1}H NMR (400 MHz, CDCl$_3$) δ 8.05 (d, J = 8.34 Hz, 1H), 7.82 (s, 1H), 7.49 (m, 1H), 7.45-7.38 (m, 4H), 7.38-7.32 (m, 3H), 3.94 (s, 3H), 3.82 (s, 2H), 3.73 (s, 2H), 3.67 (s, 3H); ^{13}C NMR (100 MHz, CDCl$_3$) δ 170.16, 169.79, 153.07, 133.95, 132.72, 130.93, 129.52, 128.47, 128.24, 127.90, 126.80, 126.72, 123.43, 123.32, 122.67, 120.80, 61.41, 52.59, 43.65, 35.14; ESI MS: m/z 429.9 (M+H)$^+$, 451.8 (M+Na)$^+$.
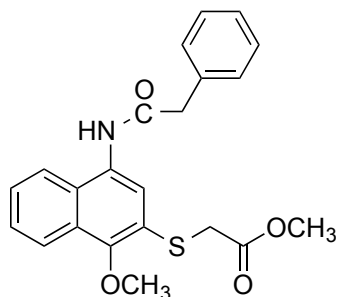
Methyl   2-((1-methoxy-4-(2-phenylacetamido)naphthalen-2-yl)thio)acetate   (48y).
Synthesized using the procedure for **48f** except using phenylacetyl chloride. Crude was triturated with cold methylene chloride to yield the title compound (154 mg, 49% over two steps) as a white solid. ^{1}H NMR (400 MHz, CDCl$_3$) δ 8.06 (d, J = 8.38 Hz, 1H), 7.94 (s, 1H), 7.53-7.44 (m, 4H), 7.40 (q, J = 7.27 Hz, 2H), 7.33 (s, 1H), 7.29-7.24 (m, 2H), 3.96 (s, 3H), 3.89 (s, 2H), 3.78 (s, 2H), 3.71 (s, 3H); ^{13}C NMR (100 MHz, CDCl$_3$) δ 170.10, 169.71, 152.55, 134.54, 129.69, 129.46, 128.70, 128.40, 127.92, 127.64, 126.59, 123.48, 122.57, 122.48, 120.78, 61.40, 52.61, 44.64, 35.16; ESI MS: m/z 396.1 (M+H)$^+$, 418.1 (M+Na)$^+$.
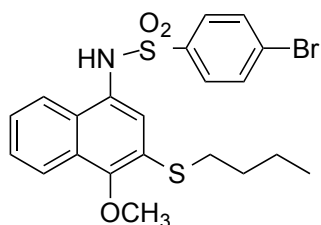
4-Bromo-*N*-(3-(butylthio)-4-methoxynaphthalen-1-yl)benzenesulfonamide   (48z).
Synthesized using the procedure for **48f** except using **48c**, and 4-bromobenzenesulfonyl chloride, which afforded the title compound (55 mg, 57% over two steps) as a light brown oil which solidified. 95% pure by HPLC. ^{1}H NMR (400 MHz, CDCl$_3$) δ 8.01 (d, J = 8.44 Hz, 1H), 7.77 (d, J = 8.44 Hz, 1H), 7.59 (d, J = 8.36 Hz, 2H), 7.49 (d, J = 8.36 Hz, 2H), 7.46 (d, J = 7.85 Hz, 1H), 7.35 (t, J = 7.85 Hz, 1H), 7.21 (s, 1H), 7.16 (s, 1H), 3.94 (s, 3H), 2.81 (t, J = 7.24 Hz, 2H), 1.58 (p, J = 7.24 Hz, 2H), 1.45 (h, J = 7.24 Hz, 2H), 0.92 (t, J = 7.24 Hz, 3H); ^{13}C NMR (100 MHz,

CDCl$_3$) δ 152.71, 138.26, 132.23, 128.92, 128.88, 128.65, 127.99, 127.25, 126.93, 126.37, 125.79, 124.49, 122.19, 122.04, 61.01, 31.92, 31.20, 21.95, 13.67; ESI MS: m/z 479.8, 481.8 (M+H)$^+$.
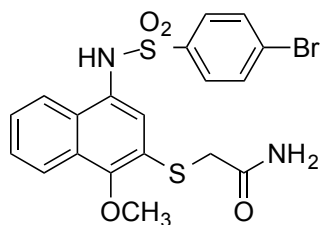
2-((4-(4-Bromophenylsulfonamido)-1-methoxynaphthalen-2-yl)thio)acetamide **(41).** Synthesized using a reported procedure.[70] Compound **40** (82 mg, 0.16 mmol) was added to aqueous NH$_4$OH (29%, 3 mL). The mixture was stirred at room temperature for 1h. Workup included diluting the mixture with EtOAc (10 mL) and washing with H$_2$O (10 mL x 2) and brine (10 mL). Organic layer was dried (MgSO$_4$), filtered and concentrated under reduced pressure to give **41** (69 mg, 90%) as a pink solid. Crude was used in the next step without further purification. 98% pure by HPLC. ^{1}H NMR (400 MHz, DMSO-d$_6$) δ 10.32 (s, 1H), 7.95 (d, J = 8.50 Hz, 1H), 7.85 (d, J = 8.50 Hz, 1H), 7.72 (d, J = 8.20 Hz, 2H), 7.60 (d, J = 8.20 Hz, 2H), 7.56-7.50 (m, 2H), 7.43-7.37 (m, 1H), 7.21 (s, 1H), 7.15 (s, 1H), 3.88 (s, 3H), 3.53 (s, 2H); ^{13}C NMR (100 MHz, DMSO-d$_6$) δ 169.76, 151.88, 139.67, 132.70, 129.69, 129.18, 129.05, 128.23, 127.46, 127.03, 126.41, 125.24, 124.89, 123.95, 121.82, 61.27, 35.91; ESI MS: m/z 480.7, 482.7 (M+H)$^+$, 502.7, 504.7 (M+Na)$^+$; ESI HRMS: m/z 478.9742 (M-H)$^-$.

4-Bromo-N-(3-(3-hydroxypropyl)-4-methoxynaphthalen-1-yl)benzenesulfonamide **(48aa).** Synthesized using the procedure for **48f** except using **48d** and 4-bromobenzenesulfonyl chloride, which afforded the title compound (163 mg, 33% over two steps) as a white solid. ^{1}H NMR (400 MHz, DMSO-d$_6$) δ 10.11 (s, 1H), 7.94 (t, J = 7.53 Hz, 2H), 7.70 (d, J = 8.53 Hz, 2H), 7.53 (d, J = 8.53 Hz, 2H), 7.51-7.45 (m, 1H), 7.42-7.35 (m, 1H), 6.86 (s, 1H), 4.47 (s, 1H), 3.79 (s, 3H), 3.37 (t, J = 5.87 Hz, 2H), 2.69-2.60 (m, 2H), 1.59-1.49 (m, 2H); ^{13}C NMR (100 MHz, DMSO-d$_6$) δ 152.33, 139.44, 132.62, 130.38, 130.34, 129.28, 128.55, 128.23, 127.00, 126.88, 126.78,

126.01, 124.09, 122.21, 62.33, 60.67, 33.79, 25.69; ESI MS: m/z 449.9, 451.9 (M+H)[+], 471.9, 473.9 (M+Na)[+].

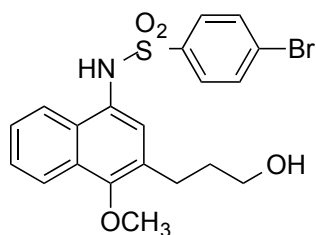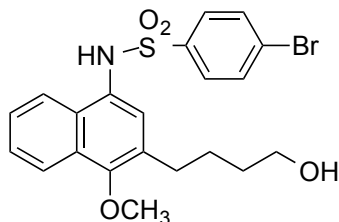**4-Bromo-*N*-(3-(4-hydroxybutyl)-4-methoxynaphthalen-1-yl)benzenesulfonamide (44).** Synthesized using the procedure for **48f** except using **48e** and 4-bromobenzenesulfonyl chloride, which afforded the title compound (226 mg, 49% over two steps) as a light pink solid. 96% pure by HPLC. ^{1}H NMR (400 MHz, DMSO-d$_6$) δ 10.09 (s, 1H), 7.99-7.91 (m, 2H), 7.70 (d, *J* = 8.43 Hz, 2H), 7.54 (d, *J* = 8.43 Hz, 2H), 7.49 (t, *J* = 7.34 Hz, 1H), 7.40 (t, *J* = 7.34 Hz, 1H), 6.81 (s, 1H), 4.33 (t, *J* = 5.42 Hz, 1H), 3.78 (s, 3H), 3.37 (q, *J* = 5.42 Hz, 2H), 2.59 (t, *J* = 7.01 Hz, 2H), 1.49-1.28 (m, 4H); ^{13}C NMR (100 MHz, DMSO-d$_6$) δ 152.35, 139.45, 132.62, 130.46, 130.42, 129.33, 128.54, 128.24, 126.97, 126.82, 126.78, 126.02, 124.16, 122.21, 62.36, 60.92, 32.66, 28.85, 26.90; ESI MS: m/z 464.1, 466.1 (M+H)[+], 486.1, 488.1 (M+Na)[+]; ESI HRMS: m/z 462.0378 (M-H)[-].
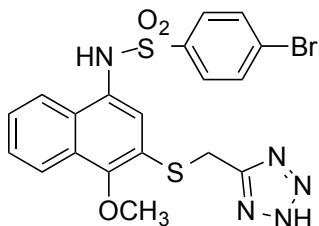
***N*-(3-(((2*H*-Tetrazol-5-yl)methyl)thio)-4-methoxynaphthalen-1-yl)-4-bromobenzenesulfonamide (48bb).** Synthesized using a reported procedure.[71] To a suspension of **40** (127mg, 0.26 mmol), sodium azide (255mg, 3.9 mmol) in dry CH$_3$CN (5mL) in a glass tube was added SiCl$_4$ (0.15mL, 1.3 mmol) via syringe. The tube was sealed and the stirring reaction mixture was heated to 80°C for 15h. The reaction was quenched with 2M Na$_2$CO$_3$. The solution was then washed with EtOAc (10 mL x 2). The aqueous phase was acidified with 1 N HCl and the mixture was extracted with EtOAc (15 mL x 5). The combined organic extracts were washed with brine (20 mL), dried (MgSO$_4$), filtered, and concentrated under reduced pressure to give **48bb** (66mg, 50%) as a tan solid. The crude was used in the next step without further purification.^{1}H NMR (400 MHz, DMSO-d$_6$) δ 10.31 (s, 1H), 7.93 (d, *J* = 8.40 Hz, 1H),

7.83 (d, J = 8.40 Hz, 1H), 7.65 (d, J = 8.04 Hz, 2H), 7.55-7.48 (m, 3H), 7.44-7.38 (m, 1H), 7.14 (s, 1H), 6.53 (s, 1H), 4.42 (s, 2H), 3.78 (s, 3H); ^{13}C NMR (100 MHz, DMSO-d$_6$) δ 153.77, 139.46, 132.64, 130.46, 129.17, 129.07, 128.36, 127.58, 127.06, 126.23, 123.97, 122.53, 122.22, 61.68, 25.09; ESI MS: m/z 505.8, 507.8 (M+H)$^+$, 527.8, 529.8 (M+Na)$^+$.

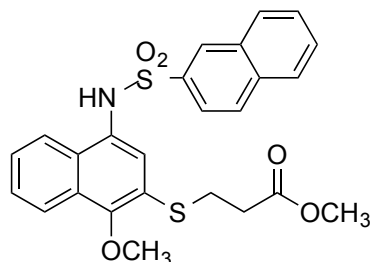**Methyl 3-((1-methoxy-4-(naphthalene-2-sulfonamido)naphthalen-2-yl)thio)propanoate (48cc).** Synthesized using the procedure for **48f** except using **48b** and 2-naphthalenesulfonyl chloride, which afforded the title compound (180 mg, 59% over two steps) as a light pink solid. ^{1}H NMR (400 MHz, CDCl$_3$) δ 8.30 (s, 1H), 7.98 (d, J = 8.39 Hz, 1H), 7.90-7.85 (m, 2H), 7.85-7.80 (m, 2H), 7.80-7.76 (m, 1H), 7.59 (t, J = 7.36 Hz, 1H), 7.53 (t, J = 7.36 Hz, 1H), 7.43 (t, J = 7.39 Hz, 1H), 7.34 (t, J = 7.39 Hz, 1H), 7.19 (s, 1H), 6.98 (s, 1H), 3.89 (s, 3H), 3.64 (s, 3H), 2.94 (t, J = 7.23 Hz, 2H), 2.40 (t, J = 7.23 Hz, 2H); ^{13}C NMR (100 MHz, CDCl$_3$) δ 171.84, 153.85, 135.99, 134.83, 131.94, 129.66, 129.43, 129.20, 129.02, 128.91, 128.75, 127.82, 127.78, 127.54, 126.95, 126.72, 125.21, 123.73, 122.39, 122.19, 109.99, 61.20, 51.79, 34.05, 27.65; ESI MS: m/z 481.9 (M+H)$^+$, 503.9 (M+Na)$^+$.
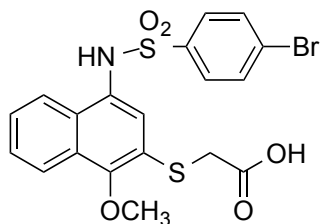
2-((4-(4-Bromophenylsulfonamido)-1-methoxynaphthalen-2-yl)thio)acetic acid (39). To a solution of **40** (425 mg, 0.85 mmol) in dry THF (2 mL) was added 1N aqueous LiOH (4 mL). The mixture was stirred at room temperature under nitrogen for 1 h. Reaction mixture was diluted with water (10 mL) and washed with EtOAc (10 mL x 2). Aqueous phase was acidified with 1N HCl and extracted with EtOAc (10 mL x 3). Combined organic extracts were washed with brine, dried (MgSO$_4$) and filtered. The solvent was removed under reduced pressure. Crude was triturated with cold CH$_2$Cl$_2$ to give **39** (305 mg, 74%) as a white/tan solid. >99% pure by

HPLC. ^{1}H NMR (400 MHz, DMSO-d$_6$) δ 10.32 (s, 1H), 7.92 (d, J = 8.38 Hz, 1H), 7.87 (d, J = 8.38 Hz, 1H), 7.68 (d, J = 8.08 Hz, 2H), 7.57 (d, J = 8.08 Hz, 2H), 7.51 (t, J = 7.56 Hz, 1H), 7.40 (t, J = 7.56 Hz, 1H), 7.09 (s, 1H), 3.84 (s, 3H), 3.65 (s, 2H); ^{13}C NMR (100 MHz, DMSO-d$_6$) δ 170.59, 152.07, 139.60, 132.69, 129.83, 129.18, 129.13, 128.28, 127.54, 127.09, 126.57, 124.60, 124.56, 124.01, 121.86, 61.30, 34.63; ESI HRMS: m/z 479.9578 (M-H)$^-$.
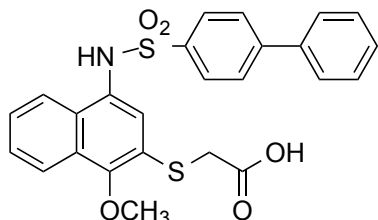
2-((4-([1,1'-Biphenyl]-4-ylsulfonamido)-1-methoxynaphthalen-2-yl)thio)acetic   acid   (42). Synthesized using the procedure for **39** except **48n** was used as the starting material. Crude was triturated with cold CH$_2$Cl$_2$ to give **42** (88 mg, 70%) as an white solid. 98% pure by HPLC. ^{1}H NMR (400 MHz, DMSO-d$_6$) δ 12.74 (s, 1H), 10.21 (s, 1H), 7.95 (d, J = 8.44 Hz, 1H), 7.91 (d, J = 8.44 Hz, 1H), 7.79-7.70 (m, 4H), 7.68-7.61 (m, 2H), 7.53-7.48 (m, 1H), 7.45 (t, J = 7.28 Hz, 2H), 7.39 (t, J = 7.28 Hz, 2H), 7.08 (s, 1H), 3.83 (s, 3H), 3.61 (s, 2H); ^{13}C NMR (100 MHz, DMSO-d$_6$) δ 170.52, 151.84, 144.73, 139.09, 138.87, 129.90, 129.50, 128.93, 128.26, 127.89, 127.78, 127.49, 126.47, 124.56, 124.21, 124.18, 121.77, 61.26, 34.56; ESI HRMS: m/z 478.0787 (M-H)$^-$.
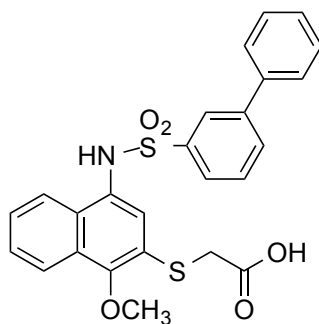
2-((4-([1,1'-Biphenyl]-3-ylsulfonamido)-1-methoxynaphthalen-2-yl)thio)acetic   acid   (43). Synthesized using the procedure for **39** except **48o** was used as the starting material. Crude was triturated with cold CH$_2$Cl$_2$ to give **43** (152 mg, 59%) as a white solid. 98% pure by HPLC. ^{1}H NMR (400 MHz, DMSO-d$_6$) δ 12.69 (s, 1H), 10.20 (s, 1H), 7.90 (d, J = 8.46 Hz, 1H), 7.86 (d, J = 8.46 Hz, 1H), 7.82 (d, J = 7.81 Hz, 1H), 7.72 (s, 1H), 7.63 (d, J = 7.81 Hz, 1H), 7.55 (t, J = 7.74 Hz, 1H), 7.50- 7.44 (m, 1H), 7.43-7.38 (m, 4H), 7.38-7.30 (m, 2H), 7.11 (s, 1H), 3.82 (s,

3H), 3.61 (s, 2H). ^{13}C NMR (100 MHz, DMSO-d$_6$) δ 170.46, 151.97, 141.49, 140.71, 138.92, 131.42, 130.33, 129.80, 129.49, 129.43, 128.66, 128.24, 127.47, 127.14, 126.43, 125.88, 125.21, 124.64, 124.59, 124.04, 121.77, 61.23, 34.56. ESI HRMS: m/z 478.0788 (M-H)$^-$.

A representative procedure for a single-pot ester hydrolysis and demethylation with BBr$_3$

2-((1-Hydroxy-4-(thiophene-2-sulfonamido)naphthalen-2-yl)thio)acetic acid (1). To a stirred solution of **48f** (48 mg, 0.12 mmol) suspended in dry CH$_2$Cl$_2$ (1.5 mL) was added BBr$_3$ (1 M in CH$_2$Cl$_2$, 0.5 mL, 0.5 mmol) dropwise at 0°C under nitrogen. The mixture was allowed to warm up to room temperature. After 1hr stir, the starting material was entirely consumed and the product formed as determined by TLC and MS (ESI$^-$). The mixture was slowly added to a stirred solution of saturated aqueous NH$_4$Cl (20 mL) at 0°C. The solution was extracted with EtOAc (15 mL x 2). The combined organic extracts were washed with brine (15 mL), dried (MgSO$_4$), filtered, and the solvent was removed under reduced pressure. The crude was purified using a C$_{18}$ reverse phase semipreparative HPLC column with solvent A (0.1% of TFA in water) and solvent B (0.1% of TFA in CH$_3$CN) as eluents to give **1 (59)** (28 mg, 59%) as a white/tan solid. 96% pure by HPLC.^{1}H NMR (400 MHz, DMSO-d$_6$) δ 10.10 (s, 1H), 8.17-8.14 (m, 1H), 7.89-7.84 (m, 2H), 7.52-7.40 (m, 2H), 7.36 (dd, J = 1.32, 3.74 Hz, 1H), 7.09 (s, 1H), 7.07 (dd, J = 3.74, 4.97 Hz, 1H), 3.56 (s, 2H); ^{13}C NMR (100 MHz, DMSO-d$_6$) δ 171.54, 152.87, 140.58, 133.57, 132.80, 131.71, 129.80, 128.03, 127.20, 126.22, 125.46, 124.33, 123.61, 122.83, 113.36, 37.25; ESI HRMS: m/z 393.9870 (M-H)$^-$.
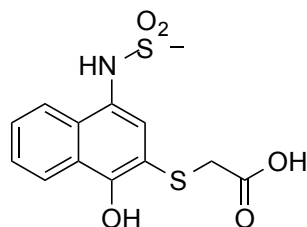
2-((1-Hydroxy-4-(methylsulfonamido)naphthalen-2-yl)thio)acetic acid (2). Synthesized using the procedure for **1** except **48t** was used as the starting material. The title compound (27 mg, 48%) as a white solid after HPLC purification. 95% pure by HPLC. ^{1}H NMR (400 MHz,

DMSO-d$_6$) δ 9.40 (s, 1H), 8.20 (d, J = 8.09 Hz, 1H), 8.14 (d, J = 8.09 Hz, 1H), 7.56 (p, J = 6.86 Hz, 2H), 7.47 (s, 1H), 3.69 (s, 2H), 2.99 (s, 3H); ^{13}C NMR (100 MHz, DMSO-d$_6$) δ 171.73, 152.58, 131.89, 129.38, 127.31, 126.30, 125.65, 125.18, 124.32, 122.82, 113.55, 39.79, 37.03; ESI HRMS: m/z 326.0164 (M-H)$^-$.
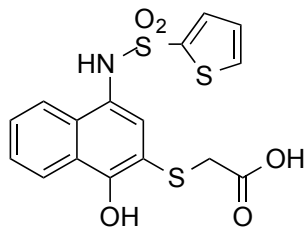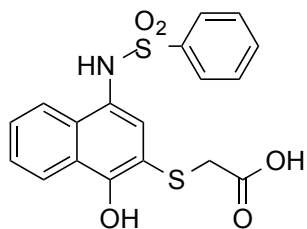

2-((1-Hydroxy-4-(phenylsulfonamido)naphthalen-2-yl)thio)acetic acid (3). Synthesized using the procedure for **1** except **48h** was used as the starting material. The title compound (21 mg, 22%) was obtained as a white solid after HPLC purification. 97% pure by HPLC. ^{1}H NMR (400 MHz, DMSO-d$_6$) δ 12.76 (s, 1H), 9.91 (s, 1H), 9.79 (s, 1H), 8.14 (d, J = 8.22 Hz, 1H), 7.88 (d, J = 8.22 Hz, 1H), 7.67-7.61 (m, 2H), 7.61-7.56 (m, 1H), 7.54-7.47 (m, 3H), 7.46-7.39 (m, 1H), 7.01 (s, 1H), 3.51 (s, 2H); ^{13}C NMR (100 MHz, DMSO-d$_6$) δ 171.46, 152.56, 140.16, 133.03, 131.56, 129.53, 129.44, 127.25, 127.05, 126.17, 125.46, 124.56, 123.76, 122.75, 113.34, 37.16; ESI HRMS: m/z 388.0319 (M-H)$^-$.

2-((4-(4-Chlorophenylsulfonamido)-1-hydroxynaphthalen-2-yl)thio)acetic   acid   (9). Synthesized using the procedure for **1** except **48i** was used as the starting material. The title compound (48 mg, 20%) was obtained as a white solid after trituration with a mixture of CH$_3$CN:H$_2$O 1:1 and cold CH$_2$Cl$_2$ and without a need for HPLC purification. 95% pure by HPLC. ^{1}H NMR (400 MHz, DMSO-d$_6$) δ 12.77 (s, 1H), 10.03 (s, 1H), 9.84 (s, 1H), 8.15 (d, J = 8.12 Hz, 1H), 7.85 (d, J = 8.12 Hz, 1H), 7.66-7.59 (m, 2H), 7.59-7.52 (m, 2H), 7.46 (dt, J = 7.28, 14.85 Hz, 2H), 7.05 (s, 1H), 3.54 (s, 2H); ^{13}C NMR (100 MHz, DMSO-d$_6$) δ 171.48, 152.72, 139.06, 137.95, 131.47, 129.66, 129.60, 129.19, 127.15, 126.25, 125.48, 124.24, 123.63, 122.84, 113.38, 37.11; ESI HRMS: m/z 421.9930 (M-H)$^-$.
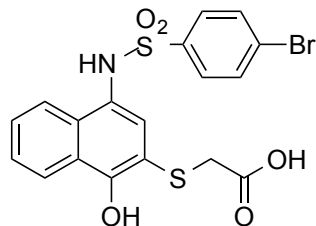
2-((4-(4-Bromophenylsulfonamido)-1-hydroxynaphthalen-2-yl)thio)acetic acid (10). Synthesized using the procedure for **1** except **39** was used as the starting material. The title compound (134 mg, 45%) was obtained as a white solid after trituration with a mixture of $CH_3CN:H_2O$ 1:1 and cold CH_2Cl_2 and without a need for HPLC purification. 99% pure by HPLC. ^{1}H NMR (400 MHz, DMSO-d_6) δ 12.80 (s, 1H), 10.05 (s, 1H), 9.87 (s, 1H), 8.14 (d, J = 8.17 Hz, 1H), 7.84 (d, J = 8.17 Hz, 1H), 7.71 (d, J = 8.48 Hz, 2H), 7.54 (d, J = 8.48 Hz, 2H), 7.48 (t, J = 7.03 Hz, 1H), 7.43 (t, J = 7.03 Hz, 1H), 7.04 (s, 1H), 3.53 (s, 2H); ^{13}C NMR (100 MHz, DMSO-d_6) δ 171.52, 152.74, 139.45, 132.56, 131.45, 129.66, 129.28, 127.18, 126.92, 126.27, 125.48, 124.21, 123.63, 122.86, 113.38, 37.10; ESI HRMS: m/z 465.9418 (M-H)$^-$.
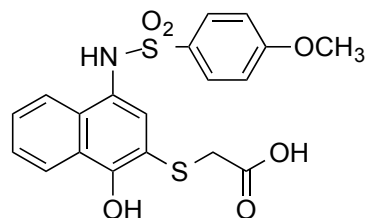
2-((1-Hydroxy-4-(4-methoxyphenylsulfonamido)naphthalen-2-yl)thio)acetic acid (11). Synthesized using the procedure for **1** except **48j** was used as the starting material. The title compound (25 mg, 29%) was obtained as a white solid after HPLC purification. 95% pure by HPLC. ^{1}H NMR (400 MHz, DMSO-d_6) δ 9.70 (s, 1H), 8.10 (d, J = 8.07 Hz, 1H), 7.89 (d, J = 7.78 Hz, 1H), 7.52 (d, J = 8.63 Hz, 2H), 7.49-7.36 (m, 2H), 7.00-6.93 (m, 3H), 3.75 (s, 3H), 3.47 (s, 2H); ^{13}C NMR (100 MHz, DMSO-d_6) δ 171.47, 162.75, 152.44, 131.81, 131.63, 129.49, 129.37, 127.05, 126.18, 125.48, 124.92, 123.93, 122.75, 114.57, 113.35, 56.02, 37.24; ESI HRMS: m/z 418.0424 (M-H)$^-$.

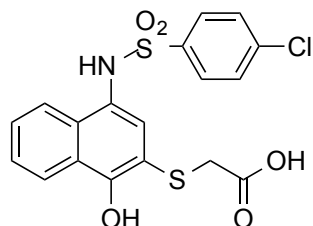**2-((4-(3-Bromophenylsulfonamido)-1-hydroxynaphthalen-2-yl)thio)acetic acid (12).** Synthesized using the procedure for **1** except **48k** was used as the starting material. The title compound (21 mg, 35%) was obtained as a white/tan solid after trituration with a mixture of $CH_3CN:H_2O$ 1:1 and cold CH_2Cl_2 and without a need for HPLC purification. 88% pure by HPLC. ^{1}H NMR (400 MHz, DMSO-d_6) δ 10.08 (s, 1H), 8.15 (d, J = 7.56 Hz, 1H), 7.87-7.78 (m, 2H), 7.75 (t, J = 1.78 Hz, 1H), 7.62-7.56 (m, 1H), 7.52-7.39 (m, 3H), 7.01 (s, 1H), 3.52 (s, 2H); ^{13}C NMR (100 MHz, DMSO-d_6) δ 171.52, 152.92, 142.07, 135.93, 131.78, 131.49, 129.77, 129.59, 127.18, 126.34, 126.28, 125.53, 124.02, 123.58, 122.89, 122.35, 113.43, 37.24; ESI HRMS: m/z 465.9414 (M-H)$^-$.
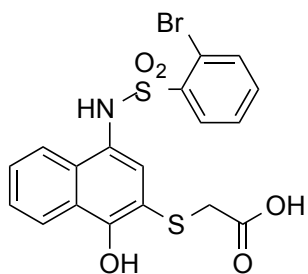
2-((4-(2-Bromophenylsulfonamido)-1-hydroxynaphthalen-2-yl)thio)acetic acid (13). Synthesized using the procedure for **1** except **48l** was used as the starting material. The title compound (34 mg, 40%) was obtained as a white solid after HPLC purification. 90% pure by HPLC. ^{1}H NMR (400 MHz, DMSO-d_6) δ 12.80 (s, 1H), 10.23 (s, 1H), 9.88 (s, 1H), 8.16-8.10 (m, 1H), 8.07-8.02 (m, 1H), 7.86 (dd, J = 1.52, 7.83 Hz, 1H), 7.78 (dd, J = 1.52, 7.83 Hz, 1H), 7.52-7.46 (m, 3H), 7.42 (td, J = 1.33, 7.60 Hz, 1H), 7.05 (s, 1H), 3.46 (s, 2H); ^{13}C NMR (100 MHz, DMSO-d_6) δ 171.42, 152.60, 139.23, 135.82, 134.64, 131.92, 131.77, 129.49, 128.52, 127.18, 126.32, 125.44, 123.98, 123.78, 122.78, 119.92, 113.54, 37.03; ESI HRMS: m/z 465.9408 (M-H)$^-$.

2-((4-(Benzo[*b*]thiophene-2-sulfonamido)-1-hydroxynaphthalen-2-yl)thio)acetic acid (14). Synthesized using the procedure for **1** except **48m** was used as the starting material. The title compound (13mg, 22%) was obtained as an orange solid after HPLC purification. 98% pure by HPLC. ^{1}H NMR (400 MHz, DMSO-d_6) δ 10.32 (s, 1H), 8.11 (d, J = 8.14 Hz, 1H), 8.02 (d, J =

8.14 Hz, 1H), 7.89 (t, *J* = 8.09 Hz, 2H), 7.72 (s, 1H), 7.47 (t, *J* = 7.56 Hz, 1H), 7.41 (t, *J* = 7.35 Hz, 2H), 7.38-7.32 (m, 1H), 7.14 (s, 1H), 3.40 (s, 2H); ^{13}C NMR (100 MHz, DMSO-d$_6$) δ 171.57, 153.29, 141.31, 141.04, 137.80, 131.73, 129.99, 129.94, 127.65, 127.22, 126.21, 125.86, 125.54, 123.96, 123.54, 123.41, 122.92, 113.33, 37.41; ESI HRMS: m/z 444.0041 (M-H)$^-$.

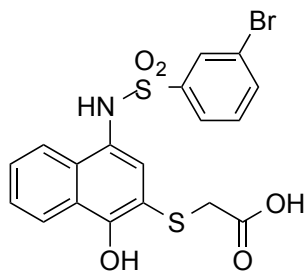**2-((4-([1,1'-Biphenyl]-4-ylsulfonamido)-1-hydroxynaphthalen-2-yl)thio)acetic acid (16).** Synthesized using the procedure for **1** except **48n** was used as the starting material. The title compound (29mg, 45%) was obtained as a white/tan solid after HPLC purification. 99% pure by HPLC. ^{1}H NMR (400 MHz, DMSO-d$_6$) δ 9.92 (s, 1H), 8.11 (d, *J* = 7.93 Hz, 1H), 7.90 (d, *J* = 7.93 Hz, 1H), 7.76 (d, *J* = 7.47 Hz, 2H), 7.72-7.62 (m, 4H), 7.50-7.42 (m, 3H), 7.43-7.36 (m, 2H), 7.02 (s, 1H), 3.46 (s, 2H); ^{13}C NMR (100 MHz, DMSO-d$_6$) δ 171.52, 152.74, 144.57, 139.00, 138.90, 131.65, 129.57, 129.52, 128.92, 128.00, 127.63, 127.46, 127.08, 126.18, 125.55, 124.53, 123.85, 122.81, 113.42, 37.27; ESI HRMS: m/z 464.0630 (M-H)$^-$.

2-((4-([1,1'-Biphenyl]-3-ylsulfonamido)-1-hydroxynaphthalen-2-yl)thio)acetic acid (17). Synthesized using the procedure for **1** except **48o** was used as the starting material. The title compound (48mg, 34%) was obtained as a white/tan solid after HPLC purification. 99% pure by HPLC. ^{1}H NMR (400 MHz, DMSO-d$_6$) δ 12.73 (s, 1H), 9.93 (s, 1H), 9.79 (s, 1H), 8.10 (d, *J* = 8.25 Hz, 1H), 7.88-7.81 (m, 2H), 7.79 (s, 1H), 7.60-7.50 (m, 2H), 7.50-7.41 (m, 4H), 7.41-7.32 (m, 3H), 7.04 (s, 1H), 3.45 (s, 2H); ^{13}C NMR (100 MHz, DMSO-d$_6$) δ 171.44, 152.66, 141.46, 140.82, 139.01, 131.50, 131.30, 130.18, 129.60, 129.55, 128.66, 127.17, 127.07, 126.23, 126.07, 125.51, 125.26, 124.59, 123.73, 122.81, 113.44, 37.16; ESI HRMS: m/z 464.0632 (M-H)$^-$.
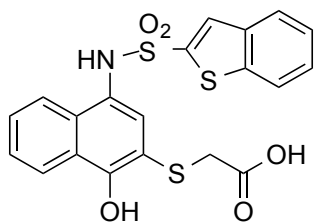
2-((4-([1,1'-Biphenyl]-2-ylsulfonamido)-1-hydroxynaphthalen-2-yl)thio)acetic   acid   (18).
Synthesized using the procedure for **1** except **48p** was used as the starting material. The title
compound (20mg, 43%) was obtained as a white/tan solid after HPLC purification. 84% pure by
HPLC. ^{1}H NMR (400 MHz, DMSO-d$_6$) δ 12.77 (s, 1H), 9.76 (s, 1H), 9.70 (s, 1H), 8.12 (d, *J* =
8.03 Hz, 1H), 7.95 (d, *J* = 8.03 Hz, 1H), 7.74 (d, *J* = 8.30 Hz, 1H), 7.58 (t, *J* = 7.46 Hz, 1H), 7.52
(t, *J* = 7.46 Hz, 1H), 7.48- 7.41 (m, 1H), 7.41-7.34 (m, 1H), 7.23 (q, *J* = 4.82, 5.81 Hz, 1H), 7.17
(t, *J* = 7.46 Hz, 3H), 7.01-6.95 (m, 1H), 6.93 (s, 1H), 6.91 (s, 1H), 3.43 (s, 2H); ^{13}C NMR (100
MHz, DMSO-d$_6$) δ 171.57, 152.24, 141.36, 139.92, 138.75, 133.21, 132.68, 131.42, 129.62,
129.37, 128.85, 128.36, 127.55, 127.48, 126.97, 126.21, 125.49, 124.57, 123.79, 122.69, 113.65,
37.07; ESI HRMS: m/z 464.0636 (M-H)⁻.

2-((4-(4'-Chloro-[1,1'-biphenyl]-4-ylsulfonamido)-1-hydroxynaphthalen-2-yl)thio)acetic
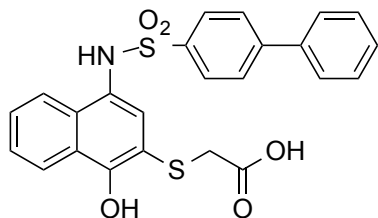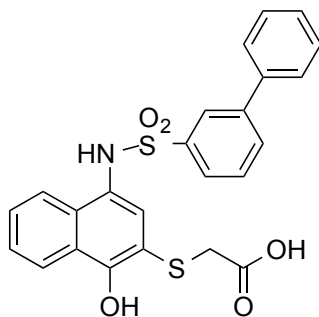**acid (19).** Synthesized using the procedure for **1** except **48q** was used as the starting material.
The title compound (36 mg, 25%) was obtained as a white solid after HPLC purification. >99%
pure by HPLC. ^{1}H NMR (400 MHz, DMSO-d$_6$) δ 12.75 (s, 1H), 9.96 (s, 1H), 9.81 (s, 1H), 8.10
(d, *J* = 8.09 Hz, 1H), 7.88 (d, *J* = 8.09 Hz, 1H), 7.77 (d, *J* = 8.24 Hz, 2H), 7.72-7.64 (m, 4H),
7.52 (d, *J* = 8.24 Hz, 2H), 7.47-7.36 (m, 2H), 6.99 (s, 1H), 3.45 (s, 2H); ^{13}C NMR (100 MHz,
DMSO-d$_6$) δ 171.45, 152.51, 143.18, 139.25, 137.67, 133.88, 131.56, 129.50, 129.39, 129.27,
128.05, 127.65, 127.09, 126.24, 125.50, 124.54, 123.84, 122.78, 113.44, 37.04; ESI HRMS: m/z
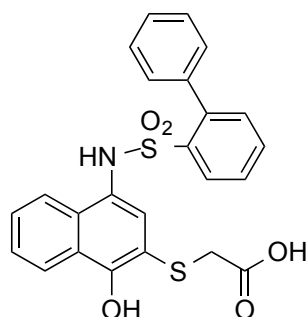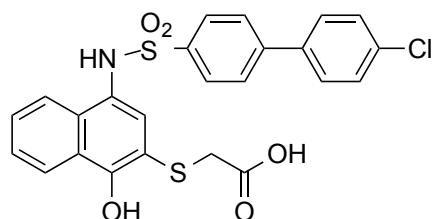498.0247 (M-H)⁻.
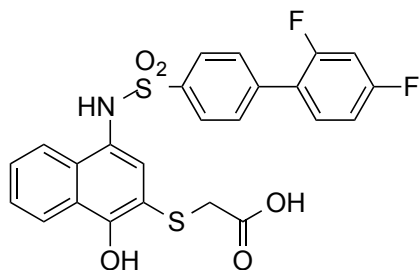
2-((4-(2',4'-difluoro-[1,1'-biphenyl]-4-ylsulfonamido)-1-hydroxynaphthalen-2-yl)thio)acetic acid (20). Synthesized using the procedure for **1** except **48r** was used as the starting material. The title compound (31 mg, 48%) as a white solid after HPLC purification. 95% pure by HPLC. ^{1}H NMR (400 MHz, DMSO-d$_6$) δ 12.71 (s, 1H), 9.97 (s, 1H), 9.80 (s, 1H), 8.10 (d, J = 8.16 Hz, 1H), 7.86 (d, J = 8.16 Hz, 1H), 7.69 (d, J = 7.72 Hz, 2H), 7.62 (d, J = 7.72 Hz, 2H), 7.59-7.53 (m, 1H), 7.47-7.34 (m, 3H), 7.19 (t, J = 8.31 Hz, 1H), 7.00 (s, 1H), 3.46 (s, 2H); ^{13}C NMR (100 MHz, DMSO-d$_6$) δ 171.46, 152.55, 139.44, 138.77, 132.51 (dd, J = 4.88, 9.80 Hz), 131.58, 129.82 (d, J = 2.86 Hz), 129.50, 127.66, 127.06, 126.23, 125.50, 124.50, 123.81, 122.78, 113.47, 112.73 (dd, J = 3.78, 21.26 Hz), 105.15 (t, J = 26.72 Hz), 37.04; ESI HRMS: m/z 500.0441 (M-H)$^-$.

2-((1-Hydroxy-4-(4-phenoxyphenylsulfonamido)naphthalen-2-yl)thio)acetic acid (21). Synthesized using the procedure for **1** except **48s** was used as the starting material. The title compound (18mg, 13%) was obtained as a white solid after HPLC purification. 96% pure by HPLC. ^{1}H NMR (400 MHz, DMSO-d$_6$) δ 12.81 (s, 1H), 9.87 (s, 1H), 9.83 (s, 1H), 8.14 (d, J = 8.31 Hz, 1H), 7.86 (d, J = 8.31 Hz, 1H), 7.59 (d, J = 8.75 Hz, 2H), 7.50 (t, J = 7.09 Hz, 1H), 7.44 (t, J = 7.81 Hz, 3H), 7.23 (t, J = 7.09 Hz, 1H), 7.05-6.98 (m, 5H), 3.55 (s, 2H); ^{13}C NMR (100 MHz, DMSO-d$_6$) δ 171.53, 160.76, 155.60, 152.58, 134.17, 131.57, 130.75, 129.84, 129.76, 127.06, 126.16, 125.48, 125.07, 124.60, 123.78, 122.80, 120.03, 118.33, 113.38, 37.15; ESI HRMS: m/z 480.0579 (M-H)$^-$.

2-((4-(4-(4-Fluorophenoxy)phenylsulfonamido)-1-hydroxynaphthalen-2-yl)thio)acetic acid (22). Synthesized using the procedure for **1** except **48t** was used as the starting material. The title compound (36 mg, 44%) as a white solid after HPLC purification. 98% pure by HPLC. ^{1}H NMR (400 MHz, DMSO-d$_6$) δ 12.78 (s, 1H), 9.83 (s, 1H), 9.79 (s, 1H), 8.11 (d, *J* = 8.21 Hz, 1H), 7.83 (d, *J* = 8.21 Hz, 1H), 7.55 (d, *J* = 8.46 Hz, 2H), 7.44 (dt, *J* = 6.92, 21.86 Hz, 2H), 7.25 (t, *J* = 8.52 Hz, 2H), 7.11-7.02 (m, 2H), 6.99-6.96 (m, 2H), 6.95 (s, 1H), 3.51 (s, 2H). ^{13}C NMR (100 MHz, DMSO-d$_6$) δ 171.53, 161.09, 152.57, 151.54 (d, *J* = 2.57 Hz), 134.14, 131.59, 129.86, 129.68, 127.08, 126.19, 125.48, 124.61, 123.80, 122.80, 122.17 (d, *J* = 8.70 Hz), 117.90, 117.45, 117.22, 113.38, 37.17; ESI HRMS: m/z 498.0485 (M-H)$^-$.

2-((1-Hydroxy-4-(4-phenylpiperazine-1-sulfonamido)naphthalen-2-yl)thio)acetic acid (23). Synthesized using the procedure for **1** except **48u** was used as the starting material. The title compound (14.5 mg, 48%) was obtained as a white solid after HPLC purification. 99% pure by HPLC. ^{1}H NMR (400 MHz, DMSO-d$_6$) δ 9.77 (s, 1H), 9.59 (s, 1H), 8.15 (t, *J* = 7.91 Hz, 2H), 7.59-7.53 (m, 1H), 7.53-7.48 (m, 2H), 7.20-7.14 (m, 2H), 6.89 (d, *J* = 7.91 Hz, 2H), 6.77 (t, *J* = 7.26 Hz, 1H), 3.64 (s, 2H), 3.24-3.16 (m, 4H), 3.14-3.04 (m, 4H); ^{13}C NMR (100 MHz, DMSO-d$_6$) δ 171.57, 152.02, 150.84, 131.08, 129.40, 128.56, 127.32, 126.28, 125.52, 125.43, 123.76, 122.95, 120.04, 116.48, 113.63, 48.54, 46.36, 37.06; ESI HRMS: m/z 472.1002 (M-H)$^-$.

2-((4-(4-Bromobenzamido)-1-hydroxynaphthalen-2-yl)thio)acetic acid (25). Synthesized using the procedure for **1** except **48v** was used as the starting material.The title compound was obtained (8.5 mg, 30%) as a white solid after HPLC purification. 98% pure by HPLC. ^{1}H NMR (400 MHz, DMSO-d$_6$) δ 10.36 (s, 1H), 8.23 (d, J = 5.36 Hz, 1H), 8.02 (d, J = 8.05 Hz, 2H), 7.83 (d, J = 5.36 Hz, 1H), 7.78 (d, J = 8.05 Hz, 2H), 7.57-7.50 (m, 3H), 3.72 (s, 2H); ^{13}C NMR (100 MHz, DMSO-d$_6$) δ 171.74, 165.71, 151.94, 133.90, 131.89, 130.66, 130.30, 128.64, 127.11, 126.17, 126.13, 125.80, 125.47, 123.80, 122.97, 113.65, 37.15; ESI HRMS: m/z 429.9747 (M-H)$^-$.

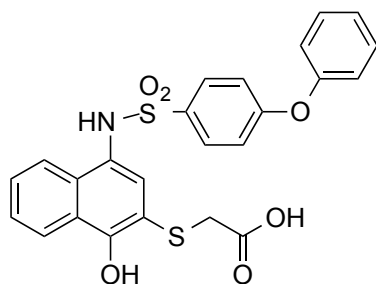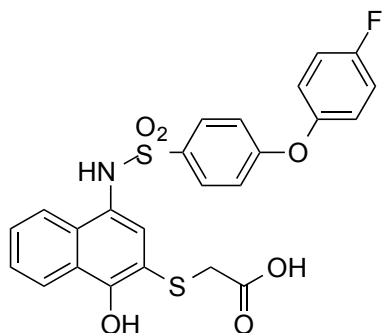**2-((4-((4-Chlorophenyl)methylsulfonamido)-1-hydroxynaphthalen-2-yl)thio)acetic acid (26).** Synthesized using the procedure for **1** except **48w** was used as the starting material. The title compound (15.5 mg, 20%) was obtained as a white solid after HPLC purification. 97% pure by HPLC. ^{1}H NMR (400 MHz, DMSO-d$_6$) δ 12.86 (s, 1H), 9.84 (s, 1H), 9.55 (s, 1H), 8.20 (d, J = 8.36 Hz, 1H), 8.07 (d, J = 8.36 Hz, 1H), 7.60-7.51 (m, 2H), 7.44 (s, 1H), 7.43-7.38 (m, 4H), 4.49 (s, 2H), 3.71 (s, 2H); ^{13}C NMR (100 MHz, DMSO-d$_6$) δ 171.81, 152.35, 133.45, 133.18, 131.79, 129.37, 128.93, 128.72, 127.23, 126.30, 125.63, 124.99, 124.28, 122.79, 113.67, 57.16, 36.96; ESI HRMS: m/z 436.0086 (M-H)$^-$.
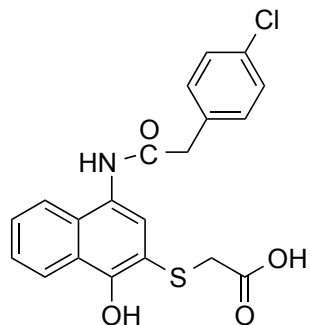
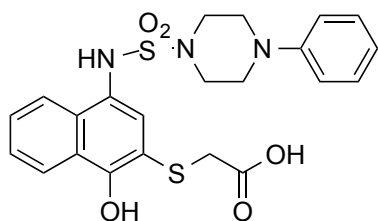**2-((4-(2-(4-Chlorophenyl)acetamido)-1-hydroxynaphthalen-2-yl)thio)acetic acid (28).** Synthesized using the procedure for **1** except **48x** was used as the starting material. The title compound (19 mg, 10%) was obtained as a white solid after trituration with a mixture of $CH_3CN:H_2O$ 1:1 and cold CH_2Cl_2 and without a need for HPLC purification. 93% pure by HPLC. ^{1}H NMR (400 MHz, DMSO-d_6) δ 9.96 (s, 1H), 8.23-8.17 (m, 1H), 7.89-7.83 (m, 1H), 7.57-7.50 (m, 3H), 7.47-7.39 (m, 4H), 3.78 (s, 2H), 3.66 (s, 2H); ^{13}C NMR (100 MHz, DMSO-d_6) δ 171.72, 169.89, 151.36, 135.73, 131.66, 131.49, 129.70, 128.69, 127.15, 127.00, 126.11, 126.07, 125.40, 123.21, 123.02, 113.51, 42.24, 37.21; ESI HRMS: m/z 400.0417 (M-H)$^-$.

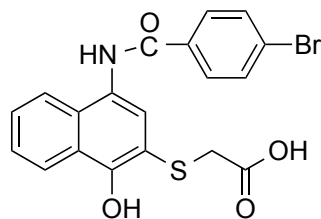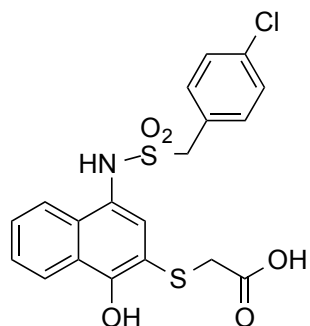**2-((1-Hydroxy-4-(2-phenylacetamido)naphthalen-2-yl)thio)acetic acid (29).** Synthesized using the procedure for **1** except **48y** was used as the starting material. The title compound (50 mg, 61%) was obtained as a white solid after trituration with a mixture of $CH_3CN:H_2O$ 1:1 and cold CH_2Cl_2 and without a need for HPLC purification. 96% pure by HPLC. ^{1}H NMR (400 MHz, DMSO-d_6) δ 12.78 (s, 1H), 9.97 (s, 1H), 9.66 (s, 1H), 8.26-8.12 (m, 1H), 7.92-7.77 (m, 1H), 7.59-7.47 (m, 3H), 7.42 (d, J = 7.64 Hz, 2H), 7.37 (t, J = 7.40 Hz, 2H), 7.31-7.24 (m, 1H), 3.77 (s, 2H), 3.67 (s, 2H); ^{13}C NMR (100 MHz, DMSO-d_6) δ 171.73, 170.25, 151.26, 136.74, 129.70, 129.58, 128.76, 127.10, 126.97, 126.92, 126.19, 126.06, 125.38, 123.22, 122.99, 113.49, 43.09, 37.13; ESI HRMS: m/z 366.0802 (M-H)$^-$.

4-Bromo-*N*-(3-(butylthio)-4-hydroxynaphthalen-1-yl)benzenesulfonamide (31). Synthesized using the procedure for **1** except **48z** was used as the starting material. The title compound (10 mg, 8%) was obtained as a white solid after HPLC purification. 99% pure by HPLC. ^{1}H NMR (400 MHz, CDCl$_3$) δ 8.23 (d, *J* = 7.40 Hz, 1H), 7.79 (d, *J* = 7.40 Hz, 1H), 7.59-7.50 (m, 4H), 7.50-7.45 (m, 1H), 7.37 (s, 1H), 7.26 (s, 1H), 6.60 (s, 1H), 3.49 (s, 1H), 2.65 (t, *J* = 7.24 Hz, 2H), 1.52-1.45 (m, 2H), 1.45-1.35 (m, 2H), 0.90 (t, *J* = 7.24 Hz, 3H); ^{13}C NMR (100 MHz, CDCl$_3$) δ 154.04, 138.33, 132.18, 131.86, 131.23, 128.98, 128.09, 127.90, 126.29, 123.80, 123.47, 122.92, 122.16, 111.25, 36.61, 31.70, 21.74, 13.60; ESI HRMS: m/z 463.9998 (M-H)$^-$.
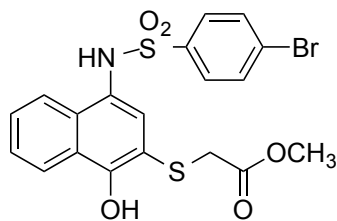
Methyl 2-((4-(4-bromophenylsulfonamido)-1-hydroxynaphthalen-2-yl)thio)acetate (32). To a suspension of **40** (122 mg, 0.25 mmol) in dry CH$_2$Cl$_2$ (2 mL) was added BBr$_3$ (1M in CH$_2$Cl$_2$, 1 mL, 1 mmol) dropwise at 0°C. The mixture was allowed to warm up to room temperature and stirred under nitrogen. The starting material was entirely consumed as determined by TLC and analytical HPLC after 1 h. The mixture was again cooled down to 0°C and MeOH (3 mL) was added. After addition, the mixture was allowed to warm up to room temperature and stirred for 1.5 h till a new spot formed as monitored by TLC. The mixture was slowly added to a stirring solution of saturated aqueous NH$_4$Cl (15 mL) at 0°C. The solution was extracted with EtOAc (15 mL x 2). The combined organic extracts were washed with brine (15 mL), dried (MgSO$_4$), and filtered. The solvent was removed under reduced pressure. The crude was triturated with cold CH$_2$Cl$_2$ to give **32** (16 mg, 13%) as a light yellow solid. 96% pure by HPLC. ^{1}H NMR (400 MHz, DMSO-d$_6$) δ 10.08 (s, 1H), 9.90 (s, 1H), 8.15 (d, *J* = 8.22 Hz, 1H), 7.85 (d, *J* = 8.22 Hz, 1H), 7.73 (d, *J* = 8.58 Hz, 2H), 7.55 (d, *J* = 8.58 Hz, 2H), 7.52-7.41 (m, 2H), 6.99 (s, 1H), 3.60 (s, 5H); ^{13}C NMR (100 MHz, DMSO-d$_6$) δ 170.21, 152.67, 139.44, 132.58, 131.45, 129.39,

129.23, 127.20, 126.93, 126.30, 125.51, 124.25, 123.67, 122.85, 113.07, 52.64, 36.18; ESI HRMS: m/z 479.9586 (M-H)⁻.

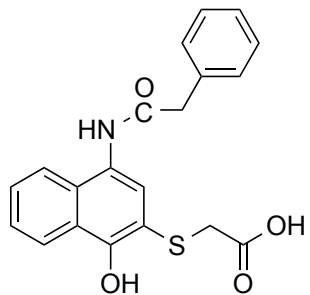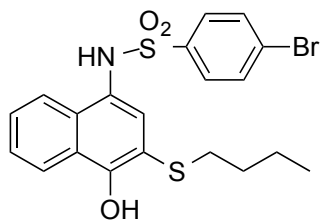**2-((4-(4-Bromophenylsulfonamido)-1-hydroxynaphthalen-2-yl)thio)acetamide (33).** Synthesized using the procedure for **1** except **41** was used as the starting material. The title compound (24 mg, 42%) as a yellow solid after trituration with a mixture of CH_3CN:H_2O 1:1 and cold CH_2Cl_2 and without a need for HPLC purification. 96% pure by HPLC. ^1H NMR (400 MHz, DMSO-d_6) δ 11.14 (s, 1H), 9.98 (s, 1H), 8.14 (d, J = 8.15 Hz, 1H), 7.87-7.78 (m, 2H), 7.69 (d, J = 8.16 Hz, 2H), 7.56-7.48 (m, 3H), 7.44 (p, J = 6.86 Hz, 2H), 6.98 (s, 1H), 3.47 (s, 2H); ^{13}C NMR (100 MHz, DMSO-d_6) δ 173.00, 154.82, 139.41, 132.55, 132.15, 131.51, 129.34, 127.54, 126.92, 126.20, 125.68, 123.58, 123.23, 112.74; ESI HRMS: m/z 464.9591 (M-H)⁻.
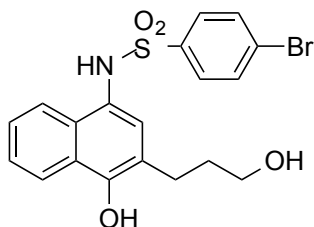
4-Bromo-*N*-(4-hydroxy-3-(3-hydroxypropyl)naphthalen-1-yl)benzenesulfonamide (34). Synthesized using the procedure for **1** except **48aa** was used as the starting material. The title compound (16 mg, 32%) was obtained as a white solid after HPLC purification. 99% pure by HPLC. ^1H NMR (400 MHz, DMSO-d_6) δ 9.87 (s, 1H), 9.17 (s, 1H), 8.11 (d, J = 8.34 Hz, 1H), 7.82 (d, J = 8.34 Hz, 1H), 7.68 (d, J = 8.50 Hz, 2H), 7.49 (d, J = 8.50 Hz, 2H), 7.38 (t, J = 7.23 Hz, 1H), 7.31 (t, J = 7.23 Hz, 1H), 6.73 (s, 1H), 3.34 (t, J = 6.35 Hz, 2H), 2.61 (t, J = 7.48 Hz, 2H), 1.54 (p, J = 6.68 Hz, 2H); ^{13}C NMR (100 MHz, DMSO-d_6) δ 149.29, 139.59, 132.49, 130.41, 129.31, 128.21, 126.80, 126.16, 125.66, 125.40, 123.69, 123.54, 122.46, 122.39, 60.51, 33.15, 26.18; ESI HRMS: m/z 434.0063 (M-H)⁻.
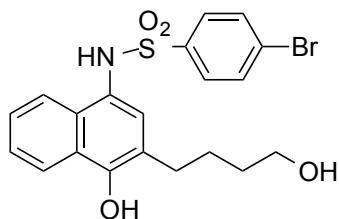
4-Bromo-*N*-(4-hydroxy-3-(4-hydroxybutyl)naphthalen-1-yl)benzenesulfonamide (35).
Synthesized using the procedure for **1** except **44** was used as the starting material. The title
compound (49 mg, 34%) was obtained as a white solid after HPLC purification. 98% pure by
HPLC. ^{1}H NMR (400 MHz, DMSO-d$_6$) δ 9.84 (s, 1H), 9.13 (s, 1H), 8.12 (d, *J* = 8.17 Hz, 1H),
7.87 (d, *J* = 8.17 Hz, 1H), 7.69 (d, *J* = 8.49 Hz, 2H), 7.51 (d, *J* = 8.49 Hz, 2H), 7.39 (t, *J* = 7.31
Hz, 1H), 7.33 (t, *J* = 7.31 Hz, 1H), 6.67 (s, 1H), 4.36 (s, 1H), 3.42-3.33 (m, 2H), 2.58 (t, *J* = 5.70
Hz, 2H), 1.45-1.26 (m, 4H); ^{13}C NMR (100 MHz, DMSO-d$_6$) δ 149.19, 139.58, 132.50, 130.54,
129.39, 128.16, 126.78, 126.20, 125.66, 125.39, 123.64, 123.61, 122.58, 122.46, 61.16, 32.47,
29.39, 26.67; ESI HRMS: m/z 448.0223 (M-H)$^-$.
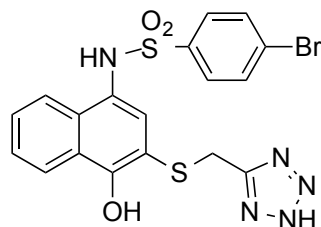
N-(3-(((2*H*-Tetrazol-5-yl)methyl)thio)-4-hydroxynaphthalen-1-yl)-4-
bromobenzenesulfonamide (36). Synthesized using the procedure for **1** except **48bb** was used
as the starting material. The title compound (3.3 mg, 10%) was obtained as a white solid after
HPLC purification. 99% pure by HPLC. ^{1}H NMR (400 MHz, DMSO-d$_6$) δ 10.00 (s, 1H), 8.13 (d,
J = 8.04 Hz, 1H), 7.75 (d, *J* = 8.04 Hz, 1H), 7.64 (d, *J* = 8.62 Hz, 2H), 7.49-7.43 (m, 3H), 7.42-
7.36 (m, 1H), 6.91 (s, 1H), 4.25 (s, 2H); ^{13}C NMR (100 MHz, DMSO-d$_6$) δ 153.78, 139.47,
132.51, 131.79, 130.43, 129.21, 127.45, 126.87, 126.27, 125.59, 124.10, 123.57, 123.08, 26.54;
ESI HRMS: m/z 489.9647 (M-H)$^-$.

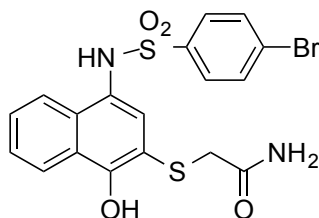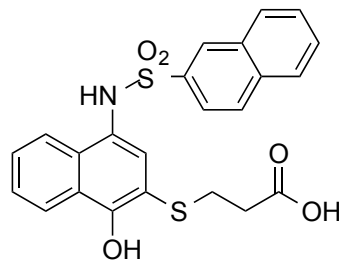**3-((1-Hydroxy-4-(naphthalene-2-sulfonamido)naphthalen-2-yl)thio)propanoic acid (37).** Synthesized using the procedure for **1** except **48cc** was used as the starting material. The title compound (23 mg, 15%) was obtained as a white solid after HPLC purification. >99% pure by HPLC. ^{1}H NMR (400 MHz, DMSO-d$_6$) δ 12.31 (s, 1H), 10.01 (s, 1H), 9.60 (s, 1H), 8.23 (s, 1H), 8.14-8.06 (m, 2H), 8.06-7.97 (m, 3H), 7.80 (d, J = 8.52 Hz, 1H), 7.68 (t, J = 7.36 Hz, 1H), 7.60 (t, J = 7.36 Hz, 1H), 7.43 (p, J = 6.84 Hz, 2H), 6.87 (s, 1H), 2.62 (t, J = 6.83 Hz, 2H), 2.17 (t, J = 6.83 Hz, 2H); ^{13}C NMR (100 MHz, DMSO-d$_6$) δ 172.97, 152.44, 137.07, 134.56, 131.90, 131.48, 129.68, 129.51, 129.23, 129.20, 128.33, 128.20, 128.00, 126.94, 126.22, 125.51, 124.61, 123.96, 122.93, 122.70, 113.33, 34.12, 29.59; ESI HRMS: m/z 452.0630 (M-H)$^-$.
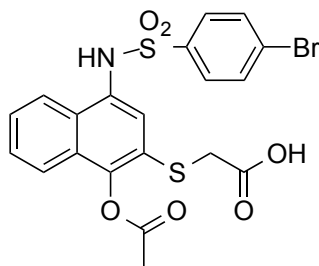
2-((1-Acetoxy-4-(4-bromophenylsulfonamido)naphthalen-2-yl)thio)acetic acid (45). Synthesized using a reported procedure.[72] A stirred solution of **10** (50 mg, 0.11 mmol) in dry THF (1.5 mL) was cooled to 0 °C. Et$_3$N (31 μL, 0.22 mmol) was added and the mixture was stirred for 5 min before acetylchloride (10 μL, 0.14 mmol) was added at 0°C. The mixture was stirred under nitrogen for an additional 20 min then diluted with EtOAc (10 mL) and washed with H$_2$O (10 mL x 3). The organic layer was dried (MgSO$_4$), filtered and concentrated under reduced pressure. The crude was subjected to flash column chromatography (hexane/EtOAc 4:1) on silica gel to afford **45** (34 mg, 61%) as a white solid. 99% pure by HPLC. ^{1}H NMR (400 MHz, CDCl$_3$) δ 8.29 (d, J = 8.10 Hz, 1H), 7.96 (d, J = 8.48 Hz, 2H), 7.76 (d, J = 8.10 Hz, 1H), 7.71 (d, J = 8.48 Hz, 2H), 7.69-7.59 (m, 2H), 7.37 (s, 1H), 3.63 (s, 2H), 1.79 (s, 3H); ^{13}C NMR (100 MHz, CDCl$_3$) δ 170.13, 161.35, 147.04, 137.50, 132.14, 131.33, 131.18, 129.73, 129.46, 128.87, 128.46, 126.94, 125.55, 122.76, 121.64, 114.58, 28.48, 24.29; ESI HRMS: m/z 507.9533 (M-H)$^-$.
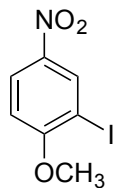
2-Iodo-1-methoxy-4-nitrobenzene (49).[73] To a stirred solution of iodoanisole (1 mL, 7.7 mmol) in AcOH (2 mL) was added fuming nitric acid (0.8 mL, 17 mmol) dropwise at 0°C. The mixture was allowed to warm up to room temperature and then heated up to 50°C and stirred for 1h under nitrogen when the color of the mixture became dark red/orange. Solid precipitate formed on cooling which was collected by filtration. Solid was washed with a 4:1 mixture of EtOH:H$_2$O (10 mL) and dried on high vacuum to give **49** (1.2g, 56%) as a light orange solid. ^{1}H NMR (400 MHz, CDCl$_3$) δ 8.66 (s, 1H), 8.24 (d, J = 8.88 Hz, 1H), 6.85 (d, J = 8.88 Hz, 1H), 3.98 (s, 3H); ^{13}C NMR (100 MHz, CDCl$_3$) δ 163.01, 141.88, 135.10, 125.69, 109.56, 85.13, 57.13; ESI MS: m/z 279.8 (M+H)$^+$.
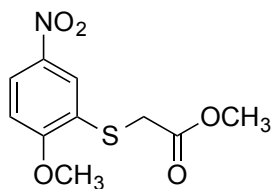
Methyl 2-((2-methoxy-5-nitrophenyl)thio)acetate (50). To a solution of Cs$_2$CO$_3$ (541 mg, 1.66 mmol) in dry THF (3 mL) under nitrogen was added methylthioglycolate (101 μL, 1.07 mmol). The mixture was stirred at room temperature for 10 min. At this time, a solution of ZnCl$_2$ (114 mg, 0.83 mmol) in dry THF (1 mL) was added and the mixture was stirred at room temperature for an additional 10 min. Meanwhile, in a separate flask Pd(OAc)$_2$ (16 mg, 0.07 mmol) and xantphos (34 mg, 0.06 mmol) were premixed in dry THF (2 mL) under nitrogen and stirred at room temperature for about 20 min. To the solution of thiol, Cs$_2$CO$_3$, and ZnCl$_2$ was added **49** (299 mg, 1.07 mmol), LiI (74 mg, 0.55 mmol) and premixed solution of the catalyst and ligand. The mixture was stirred at 60°C under nitrogen for 6.5 h. The reaction mixture was filtered to remove Cs$_2$CO$_3$ and silica was added to the mixture and the solvent was removed under reduced pressure. The adsorbed crude residue was purified by column chromatography (hexane/EtOAc 85:15) on silica gel to give **50** (178 mg, 63%) as a light yellow solid. ^{1}H NMR (400 MHz, CDCl$_3$) δ 8.20 (d, J = 2.70 Hz, 1H), 8.12 (dd, J = 2.70, 9.0 Hz, 1H), 6.90 (d, J = 9.0 Hz, 1H),

3.98 (s, 3H), 3.72 (s, 3H), 3.69 (s, 2H); ^{13}C NMR (100 MHz, CDCl$_3$) δ 169.36, 161.83, 141.62, 125.41, 124.74, 124.07, 109.73, 56.65, 52.71, 33.99; ESI MS: m/z 279.9 (M+Na)$^+$.
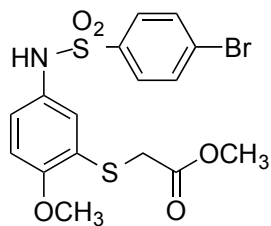
Methyl 2-((5-(4-bromophenylsulfonamido)-2-methoxyphenyl)thio)acetate (51).
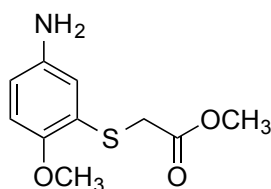
To a suspension of iron powder (374 mg, 6.7 mmol) in glacial acetic acid (5 mL) was added **50** (171 mg, 0.66 mmol). The mixture was stirred at 70°C under nitrogen for 1 h when the mixture turned milky. The mixture was then diluted with EtOAc (10 mL) and washed with saturated aqueous NaHCO$_3$ (15 mL x 2) and brine (15 mL). Organic layer was dried (MgSO$_4$), filtered and the solvent was removed under reduced pressure to give the crude as a purple oil. The crude was used in the next step without further purification. ^{1}H NMR (400 MHz, CDCl$_3$) δ 6.69 (d, J = 2.60 Hz, 1H), 6.64 (d, J = 8.58 Hz, 1H), 6.50 (dd, J = 2.60, 8.58 Hz, 1H), 3.74 (s, 3H), 3.64 (s, 3H), 3.57 (s, 2H); ^{13}C NMR (100 MHz, CDCl$_3$) δ 170.30, 150.99, 140.41, 123.27, 118.30, 115.00, 112.25, 56.34, 52.38, 34.91; ESI MS: m/z 228.0 (M+H)$^+$, 249.9 (M+Na)$^+$.

A solution of the crude amine dissolved in dry CH$_2$Cl$_2$ (4mL) was added to 4-bromobenzenesulfonyl chloride (184mg, 0.70 mmol). Addition of pyridine (0.11 mL, 1.36 mmol) was followed and the mixture was stirred at room temperature under nitrogen for 30 min when TLC did not show any starting material. The mixture was diluted with EtOAc (10 mL) and washed with H$_2$O (10 mL x 3) and brine (10 mL). The organic layer was dried (MgSO$_4$), filtered and the solvent was removed under reduced pressure. Crude was triturated with cold CH$_2$Cl$_2$ to give **51** (122 mg, 41% over two steps) as a white solid ^{1}H NMR (400 MHz, CDCl$_3$) δ 7.58-7.51 (m, 4H), 7.03 (d, J = 2.50 Hz, 1H), 6.89 (dd, J = 2.50, 8.70 Hz, 1H), 6.70 (d, J = 8.70 Hz, 1H),

6.58 (s, 1H), 3.83 (s, 3H), 3.67 (s, 3H), 3.54 (s, 2H); ^{13}C NMR (100 MHz, CDCl$_3$) δ 169.83, 156.05, 137.82, 132.26, 128.80, 128.72, 127.98, 126.06, 124.19, 123.85, 110.90, 56.04, 52.59, 34.33; ESI MS: m/z 445.9, 447.9 (M+H)$^+$, 467.8, 469.8 (M+Na)$^+$.
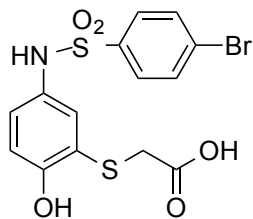
2-((5-(4-Bromophenylsulfonamido)-2-hydroxyphenyl)thio)acetic acid (24). To a stirred solution of **51** (82 mg, 0.18 mmol) suspended in dry CH$_2$Cl$_2$ (2.5 mL) was added BBr$_3$ (1 M in CH$_2$Cl$_2$, 0.55 mL, 0.55 mmol) dropwise at 0 °C under nitrogen. The mixture was allowed to warm up to room temperature. After 30 min stir, the starting material was entirely consumed and the product formed as determined by TLC and MS (ESI$^-$). The mixture was slowly added to a stirred solution of saturated aqueous NH$_4$Cl (20 mL) at 0°C. The solution was extracted with EtOAc (15 mL x 2). The combined organic extracts were washed with brine (15 mL), dried (MgSO$_4$), filtered, and the solvent was removed under reduced pressure. The crude was purified using a C$_{18}$ reverse phase semi-preparative HPLC column with solvent A (0.1% of TFA in water) and solvent B (0.1% of TFA in CH$_3$CN) as eluents to give **24** (22 mg**,** 29%) as a white solid. 97% pure by HPLC. ^{1}H NMR (400 MHz, DMSO-d$_6$) δ 12.65 (s, 1H), 9.89 (s, 2H), 7.75 (d, J = 7.98 Hz, 2H), 7.58 (d, J = 7.98 Hz, 2H), 6.93 (s, 1H), 6.69-6.66 (m, 2H), 3.58 (s, 2H); ^{13}C NMR (100 MHz, DMSO-d$_6$) δ 170.87, 153.27, 139.08, 132.62, 129.15, 126.97, 124.00, 122.38, 122.13, 115.50, 109.99, 34.26; ESI HRMS: m/z 415.9273 (M-H)$^-$.
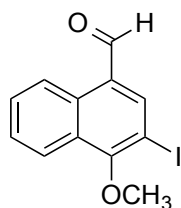
3-Iodo-4-methoxy-1-naphthaldehyde (52). A mixture of commercially available 1-methoxy-4-naphthaldehyde (504 mg, 2.7 mmol), N-iodosuccinimide (704 mg, 3.1 mmol) in TFA (10 mL) was heated to reflux and stirred for 8 h under nitrogen. The reaction mixture was diluted with EtOAc (20 mL), washed with saturated aqueous Na$_2$S$_2$O$_3$ solution (20 mL), saturated aqueous NaHCO$_3$ (20 mL x 2), and brine (20 mL). The organic layer was dried (MgSO$_4$), filtered and silica was added to filtrate and the solvent was removed under reduced pressure. The adsorbed

crude residue was purified by flash column chromatography (hexane/EtOAc 96:4) on silica gel to give **52** (648 mg, 77%) as a tan solid. ^{1}H NMR (400 MHz, CDCl$_3$) δ 10.23 (s, 1H), 9.22 (d, J = 8.48 Hz, 1H), 8.26 (s, 1H), 8.18 (d, J = 8.48 Hz, 1H), 7.71 (t, J = 7.63 Hz, 1H), 7.62 (t, J = 7.63 Hz, 1H), 4.04 (s, 3H); ^{13}C NMR (100 MHz, CDCl$_3$) δ 191.28, 162.11, 146.45, 131.97, 129.69, 129.44, 128.64, 127.75, 125.41, 122.73, 85.22, 62.06; ESI MS: m/z 313.0 (M+H)$^+$.
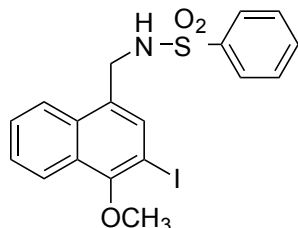
N-((3-Iodo-4-methoxynaphthalen-1-yl)methyl)benzenesulfonamide (53).
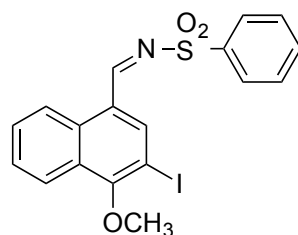
Synthesized using a reported procedure with modification.[74] To a solution of **52** (318 mg, 1 mmol) in dry CH$_2$Cl$_2$ (3.5 mL), benzenesulfonamide (209 mg, 1.3 mmol) and triethylamine (0.43 mL, 3.1 mmol) were successive added. After 5 min stir at room temperature, the reaction mixture was cooled down to 0 °C, and TiCl$_4$ (0.14 mL, 1.3 mmol) in CH$_2$Cl$_2$ (1 mL) was added dropwise. The reaction mixture was continued to stir at 0 °C for 10 min before warming up to room temperature. The reaction progress was monitoring by TLC. After 3h, the mixture was quenched saturated aqueous NaHCO$_3$ and the aqueous layer was extracted with CH$_2$Cl$_2$ (2 x 15 mL). The combined organic layers were washed with brine, dried (Na$_2$SO$_4$), and solvent was removed under reduced pressure. The crude product was used for the next step without further purification.

The previous crude product was dissolved in a mixture of MeOH (3mL) and CH$_2$Cl$_2$ (3mL). After cooling to 0°C, NaBH$_4$ (39mg, 1 mmol) was added in small portions, then brought to room temperature and stirred for 45 min. The mixture was quenched with H$_2$O, extracted with EtOAc (2 x 10 mL). The combined organic layers were washed with brine, dried (Na$_2$SO$_4$), and solvent was removed under reduced pressure. The crude product was purified by flash column

chromatography (hexane/EtOAc 85:15) on silica gel to give **53** (279 mg, 60% over two steps) as a yellow oil which solidified. ^{1}H NMR (500 MHz, CDCl$_3$) δ 8.05 (d, J = 7.7 Hz, 1H), 7.89 (d, J = 7.7 Hz, 1H), 7.86 (d, J = 8.3 Hz, 2H), 7.61-7.56 (m, 2H), 7.55-7.47 (m, 5H), 4.48 (s, 2H), 3.92 (s, 3H); ^{13}C NMR (125 MHz, CDCl$_3$) δ 156.92, 139.49, 136.02, 132.85, 132.29, 129.22, 129.13, 128.40, 127.47, 127.11, 126.88, 123.90, 122.97, 85.83, 61.65, 44.62; ESI MS: m/z 476.0 (M+Na)$^+$.
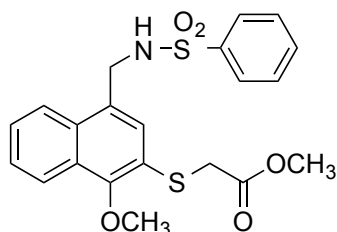
Methyl 2-((1-methoxy-4-(phenylsulfonamidomethyl)naphthalen-2-yl)thio)acetate (54). To a solution of Cs$_2$CO$_3$ (160 g, 0.49 mmol) in dry THF (2 mL) under nitrogen was added methylthioglycolate (31 μL, 0.33 mmol, 95% purity grade). The mixture was stirred at room temperature for 10 min. At this time, a solution of ZnCl$_2$ (29 mg, 0.21 mmol) in dry THF (1 mL) was added and the mixture was stirred at room temperature for an additional 10 min. Meanwhile, in a separate flask Pd(OAc)$_2$ (4 mg, 0.02 mmol) and xantphos (10 mg, 0.02 mmol) were premixed in dry THF (1 mL) under nitrogen and stirred at room temperature for about 20 min. To the solution of thiol, Cs$_2$CO$_3$, and ZnCl$_2$ was added **53** (151 mg, 0.33 mmol), LiI (20 mg, 0.15 mmol) and premixed solution of the catalyst and ligand successively. The mixture was stirred at 60°C under nitrogen for 10 h. The reaction mixture was filtered to remove Cs$_2$CO$_3$ and silica was added to the mixture and the solvent was removed under reduced pressure. The adsorbed crude residue was purified by column chromatography (hexane/EtOAc 7:3) on silica gel to give **54** (76 mg, 53%) as a yellow oil. ^{1}H NMR (400 MHz, CDCl$_3$) δ 8.00 (d, J = 8.18 Hz, 1H), 7.83 (t, J = 7.87 Hz, 3H), 7.55-7.48 (m, 2H), 7.48 -7.39 (m, 4H), 7.27 (s, 1H), 4.45 (d, J = 5.95 Hz, 2H), 3.91 (s, 3H), 3.65 (s, 2H), 3.63 (s, 3H); ^{13}C NMR (100 MHz, CDCl$_3$) δ 170.14, 155.33, 139.57, 132.66, 131.63, 129.02, 128.44, 128.17, 127.06, 127.02, 126.62, 123.71, 122.53, 122.48, 61.34, 52.59, 45.00, 35.20; ESI MS: m/z 454.1 (M+Na)$^+$.
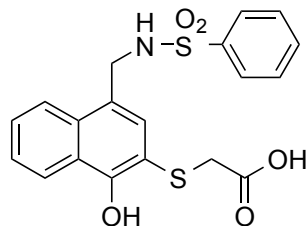
2-((1-Hydroxy-4-(phenylsulfonamidomethyl)naphthalen-2-yl)thio)acetic acid (27). To a stirred solution of **54** (76 mg, 0.18 mmol) suspended in dry CH_2Cl_2 (2 mL) was added BBr_3 (1 M in CH_2Cl_2, 0.54 mL, 0.54 mmol) dropwise at 0^oC under nitrogen. The mixture was allowed to warm up to room temperature. After 1hr stir, the starting material was entirely consumed and the product formed as determined by TLC and MS (ESI$^-$). The mixture was slowly added to a stirred solution of saturated aqueous NH_4Cl (20 mL) at 0^oC. The solution was extracted with EtOAc (15 mL x 2). The combined organic extracts were washed with brine (15 mL), dried ($MgSO_4$), filtered, and the solvent was removed under reduced pressure. The crude was purified using a C_{18} reverse phase semipreparative HPLC column with solvent A (0.1% of TFA in water) and solvent B (0.1% of TFA in CH_3CN) as eluents to give **27** (12.5 mg**,** 18%) as a white/tan solid. 94% pure by HPLC. ^{1}H NMR (400 MHz, DMSO-d_6) δ 12.78 (s, 1H), 9.64 (s, 1H), 8.16 (d, J = 7.82 Hz, 1H), 8.04 (t, J = 5.47 Hz, 1H), 7.92 (d, J = 7.82 Hz, 1H), 7.79 (d, J = 7.22 Hz, 2H), 7.63-7.57 (m, 1H), 7.57-7.47 (m, 4H), 7.32 (s, 1H), 4.24 (d, J = 5.75 Hz, 2H), 3.61 (s, 2H); ^{13}C NMR (100 MHz, DMSO-d_6) δ 171.84, 153.54, 140.78, 132.75, 132.24, 132.00, 129.53, 127.37, 126.93, 125.87, 125.44, 124.59, 124.13, 123.24, 112.76, 44.59, 37.47; ESI HRMS: m/z 402.0475 (M-H)$^-$.
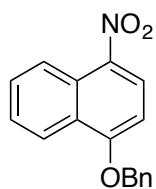
1-(benzyloxy)-4-nitronaphthalene (55).[75]
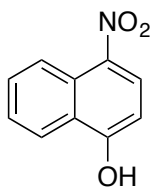
A stirred solution of 1-nitronaphthalene (1.4 g, 8 mmole) in DMSO (30 mL) was cooled down to 0^oC. KOH (1.8 g, 32 mmole) dissolved in H_2O (10 mL) was added dropwise. Color of the solution changed from yellow to dark green. Addition of cumene hydroperoxide (technical grade,

89

1.5mL, 8 mmole) dissolved in DMSO (4mL) via syringe was followed at 0°C to provide a dark brown solution which was stirred for 2 h at room temperature. Saturated aqueous $Na_2S_2O_3$ solution (10mL) was added and the mixture was stirred for another 15 min at room temperature. The mixture was diluted with H_2O (10 mL) and washed with EtOAc (30 mL x 2). Aqueous phase was acidified with 1N HCl and extracted with EtOAc (30 mL x 3). The organic extracts were washed with brine (30 mL), dried ($MgSO_4$) and filtered. The solvent was removed under reduced pressure to provide a black oil which was purified by flash column chromatography (hexane/EtOAc 3:2) on silica gel to give 4-nitronaphthalen-1-ol (1.03g, 67%) as a yellow/brown solid. ^1H NMR (400 MHz, DMSO-d_6) δ 11.89 (s, 1H), 8.64 (d, J = 8.78 Hz, 1H), 8.38 (d, J = 9.34 Hz, 1H), 8.30 (d, J = 8.16 Hz, 1H), 7.77 (t, J = 7.62 Hz, 1H), 7.61 (t, J = 7.62 Hz, 1H), 6.95 (d, J = 8.16 Hz, 1H); ^{13}C NMR (100 MHz, DMSO-d_6) δ 160.80, 137.07, 130.79, 128.95, 127.23, 126.57, 124.70, 123.54, 123.26, 107.19; ESI MS: m/z 190.0 (M+H)$^+$.

To a stirred solution of 4-nitronaphthalen-1-ol (505 mg, 2.7 mmol) in dry DMF (3 mL) was added NaH (60 wt% dispersion in oil, 193 mg, 4.8 mmol) suspended in dry DMF (3 mL) at 0°C. Benzyl bromide (0.46 mL, 3.9 mmol) in dry THF (3 mL) was added next at 0°C. The mixture was warmed up to room temperature and stirred under nitrogen for 2-3 h. Mixture was diluted with EtOAc (10 mL), washed with H_2O (10 mL x 4) and brine (10 mL). The organic layer was dried ($MgSO_4$), filtered, concentrated and purified by column chromatography on silica to give **55** (465 mg, 64%) as a light brown solid. ^1H NMR (400 MHz, CDCl$_3$) δ 8.77 (d, J = 9.40 Hz, 1H), 8.43 (d, J = 7.70 Hz, 1H), 8.36 (d, J = 7.70 Hz, 1H), 7.73 (t, J = 7.70 Hz, 1H), 7.58 (t, J = 7.70 Hz, 1H), 7.53-7.47 (m, 2H), 7.46-7.35 (m, 3H), 6.88 (d, J = 9.40 Hz, 1H), 5.34 (s, 2H); ^{13}C NMR (100 MHz, CDCl$_3$) δ 159.50, 139.36, 135.54, 130.06, 128.81, 128.50, 127.46, 127.01, 126.92, 126.60, 125.76, 123.47, 122.88, 103.15, 70.91; ESI MS: m/z 280.0 (M+H)$^+$, 302.0 (M+Na)$^+$.
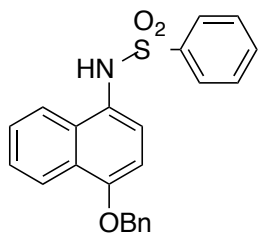
_N_-(4-(benzyloxy)naphthalen-1-yl)benzenesulfonamide (56).
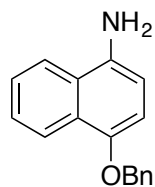
To a suspension of iron powder (601 mg, 10.7 mmol) in glacial acetic acid (6 mL) was added **55** (301 mg, 1.08 mmol). The mixture was stirred at 70 $^{\circ}$C under nitrogen for 1.5 h when the mixture turned milky. The mixture was then diluted with EtOAc (10 mL) and washed with saturated aqueous NaHCO$_3$ (15 mL x 2) and brine (15 mL). Organic layer was dried (MgSO$_4$), filtered and the solvent was removed under reduced pressure to give the crude as a purple oil. The crude was used in the next step without further purification. ^{1}H NMR (400 MHz, CDCl$_3$) δ 8.40-8.35 (m, 1H), 7.87-7.80 (m, 1H), 7.55-7.49 (m, 4H), 7.42 (t, J = 7.36 Hz, 2H), 7.39-7.31 (m, 3H), 6.78-6.69 (m, 2H), 5.18 (s, 2H); ^{13}C NMR (100 MHz, CDCl$_3$) δ 148.64, 137.56, 134.70, 128.53, 127.81, 127.38, 126.40, 125.83, 125.46, 125.39, 122.79, 120.98, 110.41, 106.12, 70.56; ESI MS: m/z 250.0 (M+H)$^+$.

A solution of the crude amine dissolved in dry CH$_2$Cl$_2$ (5mL) was added to benzenesulfonyl chloride (218mg, 1.2 mmol). Addition of pyridine (0.18 mL, 2.2 mmol) was followed and the mixture was stirred at room temperature under nitrogen overnight. The mixture was diluted with EtOAc (10 mL) and washed with H$_2$O (10 mL x 3) and brine (10 mL). The organic layer was dried (MgSO$_4$), filtered and the solvent was removed under reduced pressure. Crude was purified by flash column chromatography on silica gel to give **56** (236 mg, 55% over two steps) as a brown oil which solidified upon standing. ^{1}H NMR (400 MHz, CDCl$_3$) δ 8.30 (d, J = 7.94 Hz, 1H), 7.75-7.66 (m, 3H), 7.49 (t, J = 6.20 Hz, 3H), 7.46-7.39 (m, 4H), 7.38-7.32 (m, 3H), 7.20 (d, J = 8.22 Hz, 1H), 6.75 (d, J = 8.22 Hz, 1H), 6.60 (s, 1H), 5.21 (s, 2H); ^{13}C NMR (100 MHz, CDCl$_3$) δ 154.17, 139.41, 136.59, 132.70, 131.08, 128.83, 128.60, 128.07, 127.38, 127.30, 127.14, 126.13, 125.68, 125.61, 123.75, 122.58, 121.75, 104.42, 70.24; ESI MS: m/z 389.9 (M+H)$^+$, 411.9 (M+Na)$^+$.
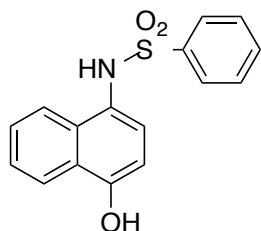
***N*-(4-hydroxynaphthalen-1-yl)benzenesulfonamide (30).** A stirred solution of **56** (200 mg, 0.51 mmol) in MeOH (15 mL) was hydrogenated in the presence of 10% Pd/C (163 mg) at room temperature and under 30 psi of H_2 for 6 h. The suspension was filtered through a pad of celite. The filtrate diluted with EtOAc (20 mL) was washed with saturated aqueous NH_4Cl (20 mL x 2). The organic layer was dried ($MgSO_4$), filtered and the solvent was removed under reduced pressure. The crude was purified using a C_{18} reverse phase semipreparative HPLC column with solvent A (0.1% of TFA in water) and solvent B (0.1% of TFA in CH_3CN) as eluents to give **30** (32 mg**,** 21%) as a white solid. 99% pure by HPLC. ^{1}H NMR (400 MHz, DMSO-d_6) δ 8.07 (d, *J* = 7.83 Hz, 1H), 7.86 (d, *J* = 7.83 Hz, 1H), 7.63 (d, *J* = 7.58 Hz, 2H), 7.60-7.53 (m, 1H), 7.48 (t, *J* = 7.37 Hz, 2H), 7.38 (p, *J* = 6.69 Hz, 2H), 6.85 (d, *J* = 7.98 Hz, 1H), 6.71 (d, *J* = 7.98 Hz, 1H); ^{13}C NMR (100 MHz, DMSO-d_6) δ 151.24, 139.13, 131.28, 130.38, 127.80, 125.58, 124.92, 124.39, 123.71, 123.55, 122.05, 122.01, 120.89, 106.09; ESI HRMS: m/z 298.0547 (M-H)$^-$.

Protein purification

His-tagged proteins containing Mcl-1 (residues 171–327), Bcl-2 (residues 1-202 with inserted Bcl-X_L sequence from residues 35 to 50), Bcl-X_L (residues 1-209 lacking its C-terminal transmembrane domain with a deletion of the flexible loop region 45 – 85), Bcl-w (residues 1-155), A1/Bfl-1 (residues 1-151), were expressed from the pHis-TEV vector (a modified pET vector) in *E. coli* BL21 (DE3) cells. Cells were grown at 37 ºC in 2×YT containing antibiotics to an OD_{600} density of 0.6. Protein expression was induced by 0.4 mM IPTG at 37 ºC for 4 hours. Cells were lysed in 50 mM Tris pH 8.0 buffer containing 500 mM NaCl, 0.1% bME and 40 μl of Leupectin/Aprotin. All proteins were purified from the soluble fraction using Ni-NTA resin (QIAGEN), following the manufacturer's instructions. Mcl-1 was further purified on a Source Q15 column (Amersham Biosciences) in 25 mM Tris pH 8.0 buffer, with NaCl gradient. Bcl-2 and Bcl-X_L were purified on a Superdex75 column (Amersham Biosciences). All proteins were stored in 25 mM Tris pH 8.0 buffers containing 150 mM NaCl and 2 mM DTT and at -80 ºC in presence of 25% Glycerol.

Determination of the K_d values of fluorescent probes to anti-apoptotic proteins

Fluorescein tagged BID BH3 (Bcl-2 Homology 3) peptide was used as a fluorescent probe in the FP-based binding assays. Two fluorescent labeled BID BH3 peptide probes were used: i)

fluorescein tagged BID peptide (Flu-BID), labeled with fluorescein on the N-terminus of the BH3 peptide (79-99); ii) the second tracer was purchased from Abgent (Catalog # SP2121a), named as FAM-BID, where the BH3 peptide (80-99) is labeled with 5-FAM. Their K_d values were determined to all members of the Bcl-2 family proteins with a fixed concentration of the tracer (2 nM of Flu-BID and FAM-BID) and different concentrations of the tested proteins, in a final volume of 125 μl in the assay buffer (100 mM potassium phosphate, pH 7.5, 100 μg/ml bovine γ-globulin, 0.02% sodium azide, Invitrogen, with 0.01% Triton X-100 and 4% DMSO). Plates were mixed and incubated at room temperature for 2 hours and the polarization values in millipolarization units (mP) were measured at an excitation wavelength of 485 nm and an emission wavelength of 530 nm. Equilibrium dissociation constants (K_d) were calculated by fitting the sigmoidal dose-dependent FP increases as a function of protein concentrations using Graphpad Prism 6.0 software. Based upon analysis of the dynamic ranges for the signals and their K_d values, Flu-BID was selected as the tracer in the Mcl-1 and Bcl-2 competitive binding assays, while FAM-BID was selected as the tracer for the rest of the proteins, A1/Bfl-1, Bcl-w and Bcl-xL. The K_d value of Flu-BID to Mcl-1 was 34 ± 3.5 nM, and to Bcl-2 was 20 ± 0.86 nM and the K_d values of FAM-BID to A1/Bfl-1 was 0.83 ± 0.06 nM, to Bcl-w was 5.5 ± 1.6 nM, and to Bcl-xL was 10 ± 4.0 nM respectively, in our saturation experiments.

Fluorescence polarization-based binding assays

Sensitive and quantitative FP-based binding assays were developed and optimized to determine the binding affinities of small-molecule inhibitors to the recombinant Mcl-1, A1/Bfl-1, Bcl-w, Bcl-2, and Bcl-xL proteins. Protocols for expression and purification of used anti-apoptotic proteins and determination of K_d values of fluorescent probes to proteins are provided in the Supporting Information. Based on the K_d values, the concentrations of the proteins used in the competitive binding experiments were 90 nM for Mcl-1, 40 nM for Bcl-w, 50 nM for Bcl-xL, 60 nM for Bcl-2, and 4 nM for A1/Bfl-1. The fluorescent probes, Flu-BID and FAM-BID were fixed at 2 nM for all assays except for A1/Bfl-1 where FAM-BID was used at 1 nM. 5 μL of the tested compound in DMSO and 120 μL of protein/probe complex in the assay buffer (100 mM potassium phosphate, pH 7.5; 100 μg/ml bovine gamma globulin; 0.02% sodium azide, purchased from Invitrogen, Life Technologies) were added to assay plates (Microfluor 2Black, Thermo Scientific), incubated at room temperature for 3 h and the polarization values (mP) were

measured at an excitation wavelength at 485 nm and an emission wavelength at 530 nm using the plate reader Synergy H1 Hybrid, BioTek. IC$_{50}$ values were determined by nonlinear regression fitting of the competition curves (GraphPad Prism 6.0 Software). The K_i values were calculated as described previously.[79]

Solution competitive surface plasmon resonance-based assay using immobilized biotin-labeled Bim BH3 peptide

The solution competitive SPR-based assay was performed on Biacore 2000. N terminal biotin-labeled Bim BH3 peptide (141 - 166 amino acids), was immobilized on streptavidin (SA) chip giving density of 1400 RU (Response Units). The pre-incubated Mcl-1 protein (20 nM) with tested small-molecule inhibitors for at least 30 minutes was injected over the surfaces of the chip. Response units were measured at 15 seconds in the dissociation phase and the specific binding was calculated by subtracting the control surface (Fc1) signal from the surfaces with immobilized biotin-labeled Bim BH3. IC$_{50}$ values were determined by non-linear least squares analysis using GraphPad Prism 6.0 software.

Molecular modeling

Crystal structure of Mcl-1 in complex with mNoxa BH3 peptide (PDB entry 2NLA) and in silico Schrödinger's IFD were used to model the binding poses of our designed compounds with Mcl-1. IFD is allowing incorporation of the protein and ligand flexibility in the docking protocol, which is consisted of the following steps: (i) constrained minimization of the protein with an RMSD cutoff of 0.18 Å; (ii) initial Glide docking of the ligand using a softened potential (Van der Waals radii scaling); (iii) one round of Prime side-chain prediction for each protein/ligand complex, on residues within defined distance of any ligand pose; (iv) prime minimization of the same set of residues and the ligand for each protein/ligand complex pose; (v) Glide re-docking of each protein/ligand complex structure within a specified energy of the lowest energy structure; (vi) estimation of the binding energy (IFDScore) for each output pose. All docking calculations were run in the extra precision (XP) mode of Glide. The center of the grid box of the Mcl-1 was defined by the Val 249 (in h1), Phe 270 (in h2), Val 220 (in h3/h4) and Val 216 (in h4). The size of the grid box was set to 15 Å. Default values were used for all other parameters. Schrödinger's MC/SD dynamic simulation performs constant temperature calculations that take advantage of

the strengths of Monte Carlo methods for quickly introducing large changes in a few degree of freedom, and stochastic dynamics for its effective local sampling of collective motions. The MC/SD dynamic simulation time in our study was set to 100 ps by allowing movement of the docked ligand and the residues which is less than 6 Å to the ligand. The force field used was set to OPLS_2001. Default values were used for all other parameters.

NMR studies

^{15}N-labeled or ^{15}N, ^{13}C-labeled Mcl-1 proteins for NMR studies were prepared and purified using the same protocol as for unlabeled protein with the exception that the bacteria were grown on M9 minimal media supported with 3 g/ L of ^{13}C-glucose and/or 1 g/L of (^{15}NH$_4$)$_2$SO$_4$. ^{15}N, ^{13}C-labeled Mcl-1 was used for backbone reassignment and 80% of residues were reassigned based on the work by Liu *et al*[57]. Protein samples were prepared in a 20 mM sodium phosphate, 150 mM NaCl and 1 mM DTT solution at pH 7 in 7% D$_2$O. The binding mode of the compounds has been characterized by recording ^{1}H,^{15}N -HSQC experiments with a 138 µL solution of uniformly ^{15}N-labeled Mcl-1 (75µM) in the absence and presence of added compounds with the indicated molar ratio concentrations. All Spectra were acquired at 30 $^{\circ}$C on a Bruker 600 MHz NMR spectrometer equipped with a cryogenic probe, processed using Bruker TopSpin and rNMR[86], and were analyzed with Sparky[87]. Plots of chemical shift changes were calculated as $((\Delta^1\text{H ppm})^2 + (0.2(\Delta^{15}\text{N ppm}))^2)^{0.5}$ of Mcl-1 amide upon addition of compound. The absence of a bar in a chemical shift plot indicates no chemical shift difference, or the presence of a proline or residue that is overlapped or not assigned.

Biotin−streptavidin pull-down experiment

Human breast cancer 2LMP cells, a subclone of the MDA-MB-231 cell line, were lysed in CHAPS buffer (10 mM HEPES (pH 7.4), 2.5 mM EDTA, 150 mM NaCl, 1.0% CHAP). Pre-cleared cell lysates were incubated with different concentrations of compounds followed by incubation with biotinylated Noxa BH3 peptide (18-43) and streptavidin−agarose beads to pull-down Mcl-1 protein bound to Noxa peptide. Beads were washed with CHAPS buffer, and Mcl-1 protein was eluted by boiling in SDS-PAGE sample buffer and analyzed by Western blotting using Mcl-1 antibody (Santa Cruz).

Cell culture and cell viability assays

MEFs cells, wild type and Bax/Bak double knock out, were gifts from Shaomeng Wang at the University of Michigan and were cultured in DMEM (Life Technologies), supplemented with 10% fetal bovine serum (FBS) (Thermo Scientific HyClone). The retroviral transduced lymphoma cells isolated from Eμ-myc transgenic mice were gifts from Ricky W. Johnstone at University of Melbourne, Melbourne, Australia and cultured as previously described.[83] Human leukemia cell lines HL-60, K-562 and MV-4-11 were obtained from American Type Culture Collection (ATCC). The cells were cultured in RPMI 1640 medium (Life Technologies), all supplemented with 10% FBS. MEFs cells were seeded in 12-well plates at 0.5×10^6 cells/well. The cells were left to adhere and then treated for 15 hours with increasing concentrations of the compounds. The cells were harvested, washed with phosphate-buffered saline (PBS) then stained with 0.025 mg/ml propidium iodide (MP Biomedicals). The percentage of propodium iodide positive population was determined by flow cytometry and calculated using WinList 3.0. The Mcl-1 and Bcl-2 retroviral transduced lymphoma Eμ-myc cells were seeded in 24-well plates at 0.5×10^6 cells/well. They were treated with different concentrations of tested compounds for 16 hrs. The cells were harvested and stained with violet LIVE/DEAD Fixable Dead Cell Stain Kit (Invitrogen) according to manufacturer's protocol. The percentage of fluorescent positive cells was determined by flow cytometry and calculated using WinList 3.0. The effect of the compounds on tested leukemia cells viability was evaluated by CellTiter Glo Luminescent Cell Viability Assay (Promega). Cells were plated in 12-well plates at 0.5×10^6 cells/well and treated with various concentrations of the compounds and incubated for 3 days. Cell viability was determined by measuring intracellular ATP levels with the Cell Titer-Glo reagent and reading the luminescence with the Synergy H1 Hybrid BioTek plate reader. Percent cell growth was calculated relative to DMSO treated cells and IC_{50} values were calculated by non-linear regression analysis using GraphPad Prism 6.0 Software.

Determination of caspase acitivity

HL-60 cells were seeded in 12-well plates at 0.5×10^6 cells/well. After 20 hrs treatment with different concentrations of the compounds, caspase 3 activity was determined using the

fluorometric substrates DEVD-AFC following the protocol of the Caspase-3 Fluorometric Assay Kit (BioVision). Caspase 3 activity is reported as the fold change relative to DMSO treated cells.

Analysis of apoptosis

To determine the induction of apoptosis, HL-60 cells were plated in 12-well plates at 0.5×10^6 cells/well and treated with various concentrations of tested compounds. After 15 hours cells were harvested, washed with PBS and treated with Annexin-V FITC and propidium iodide using BD Annexin V FITC Assay kit (BD Biosciences Pharmingen). The percentage of cells undergoing apoptosis was assessed by flow cytometry within 1 h and analysed using WinList 3.0.

2.10 Contributions

Fardokht Abulwerdi designed, synthesized and characterized all the compounds and intermediates except the intermediate for analog **23**, which was synthesized and characterized by Dr. Lei Miao, as well as expressed and purified labeled Mcl-1, prepared NMR samples and analyzed HSQC NMR data with supervision from Dr. Nikolovska-Coleska and Dr. Hollis Showalter. Ahmed Mady performed all the biochemical and cellular experiments except for the cell growth inhibition studies and caspase activation in leukemia cells which were performed by Jordan Gavin. Dr. Chenzhong Liao performed all the molecular docking studies and contributed to the design of analogs. Dr. Chenxi Shen performed pull-down assay. Dr. Tomasz Cierpicki reassigned the backbone of Mcl-1 for the NMR studies. All the proteins used for biochemical assays were expressed and purified in Dr. Jeanne Stuckey lab at LSI. Efficacy studies were performed in Dr. Ramzi Mohammad lab at Wayne State University.

2.11 References

1.   Hanahan, D.; Weinberg, R. A. Hallmarks of cancer: the next generation. *Cell* **2011,** 144, 646-74.
2.   Hanahan, D.; Weinberg, R. A. The hallmarks of cancer. *Cell* **2000,** 100, 57-70.
3.   Fulda, S.; Debatin, K. M. Extrinsic versus intrinsic apoptosis pathways in anticancer chemotherapy. *Oncogene* **2006,** 25, 4798-811.
4.   Youle, R. J.; Strasser, A. The BCL-2 protein family: opposing activities that mediate cell death. *Nat Rev Mol Cell Biol* **2008,** 9, 47-59.
5.   Bajwa, N.; Liao, C.; Nikolovska-Coleska, Z. Inhibitors of the anti-apoptotic Bcl-2 proteins: a patent review. *Expert Opin Ther Pat* **2012,** 22, 37-55.
6.   Lessene, G.; Czabotar, P. E.; Colman, P. M. BCL-2 family antagonists for cancer therapy. *Nat Rev Drug Discov* **2008,** 7, 989-1000.
7.   Vogler, M.; Dinsdale, D.; Dyer, M. J.; Cohen, G. M. Bcl-2 inhibitors: small molecules with a big impact on cancer therapy. *Cell Death Differ* **2009,** 16, 360-7.
8.   Souers, A. J.; Leverson, J. D.; Boghaert, E. R.; Ackler, S. L.; Catron, N. D.; Chen, J.; Dayton, B. D.; Ding, H.; Enschede, S. H.; Fairbrother, W. J.; Huang, D. C.; Hymowitz, S. G.; Jin, S.; Khaw, S. L.; Kovar, P. J.; Lam, L. T.; Lee, J.; Maecker, H. L.; Marsh, K. C.; Mason, K. D.; Mitten, M. J.; Nimmer, P. M.; Oleksijew, A.; Park, C. H.; Park, C. M.; Phillips, D. C.; Roberts, A. W.; Sampath, D.; Seymour, J. F.; Smith, M. L.; Sullivan, G. M.; Tahir, S. K.; Tse, C.; Wendt, M. D.; Xiao, Y.; Xue, J. C.; Zhang, H.; Humerickhouse, R. A.; Rosenberg, S. H.; Elmore, S. W. ABT-199, a potent and selective BCL-2 inhibitor, achieves antitumor activity while sparing platelets. *Nat Med* **2013,** 19, 202-8.
9.   Lessene, G.; Czabotar, P. E.; Sleebs, B. E.; Zobel, K.; Lowes, K. N.; Adams, J. M.; Baell, J. B.; Colman, P. M.; Deshayes, K.; Fairbrother, W. J.; Flygare, J. A.; Gibbons, P.; Kersten, W. J.; Kulasegaram, S.; Moss, R. M.; Parisot, J. P.; Smith, B. J.; Street, I. P.; Yang, H.; Huang, D. C.; Watson, K. G. Structure-guided design of a selective BCL-X(L) inhibitor. *Nat Chem Biol* **2013,** 9, 390-7.
10.   Zhou, H.; Aguilar, A.; Chen, J.; Bai, L.; Liu, L.; Meagher, J. L.; Yang, C. Y.; McEachern, D.; Cong, X.; Stuckey, J. A.; Wang, S. Structure-based design of potent Bcl-2/Bcl-xL inhibitors with strong in vivo antitumor activity. *J Med Chem* **2012,** 55, 6149-61.
11.   Zhou, H.; Chen, J.; Meagher, J. L.; Yang, C. Y.; Aguilar, A.; Liu, L.; Bai, L.; Cong, X.; Cai, Q.; Fang, X.; Stuckey, J. A.; Wang, S. Design of Bcl-2 and Bcl-xL inhibitors with subnanomolar binding affinities based upon a new scaffold. *J Med Chem* **2012,** 55, 4664-82.
12.   Tse, C.; Shoemaker, A. R.; Adickes, J.; Anderson, M. G.; Chen, J.; Jin, S.; Johnson, E. F.; Marsh, K. C.; Mitten, M. J.; Nimmer, P.; Roberts, L.; Tahir, S. K.; Xiao, Y.; Yang, X.; Zhang, H.; Fesik, S.; Rosenberg, S. H.; Elmore, S. W. ABT-263: a potent and orally bioavailable Bcl-2 family inhibitor. *Cancer Res* **2008,** 68, 3421-8.
13.   Roberts, A. W.; Seymour, J. F.; Brown, J. R.; Wierda, W. G.; Kipps, T. J.; Khaw, S. L.; Carney, D. A.; He, S. Z.; Huang, D. C.; Xiong, H.; Cui, Y.; Busman, T. A.; McKeegan, E. M.; Krivoshik, A. P.; Enschede, S. H.; Humerickhouse, R. Substantial susceptibility of chronic lymphocytic leukemia to BCL2 inhibition: results of a phase I study of navitoclax in patients with relapsed or refractory disease. *J Clin Oncol* **2012,** 30, 488-96.

14. van Delft, M. F.; Wei, A. H.; Mason, K. D.; Vandenberg, C. J.; Chen, L.; Czabotar, P. E.; Willis, S. N.; Scott, C. L.; Day, C. L.; Cory, S.; Adams, J. M.; Roberts, A. W.; Huang, D. C. The BH3 mimetic ABT-737 targets selective Bcl-2 proteins and efficiently induces apoptosis via Bak/Bax if Mcl-1 is neutralized. *Cancer Cell* **2006,** 10, 389-99.

15. Konopleva, M.; Contractor, R.; Tsao, T.; Samudio, I.; Ruvolo, P. P.; Kitada, S.; Deng, X.; Zhai, D.; Shi, Y. X.; Sneed, T.; Verhaegen, M.; Soengas, M.; Ruvolo, V. R.; McQueen, T.; Schober, W. D.; Watt, J. C.; Jiffar, T.; Ling, X.; Marini, F. C.; Harris, D.; Dietrich, M.; Estrov, Z.; McCubrey, J.; May, W. S.; Reed, J. C.; Andreeff, M. Mechanisms of apoptosis sensitivity and resistance to the BH3 mimetic ABT-737 in acute myeloid leukemia. *Cancer Cell* **2006,** 10, 375-88.

16. Chauhan, D.; Velankar, M.; Brahmandam, M.; Hideshima, T.; Podar, K.; Richardson, P.; Schlossman, R.; Ghobrial, I.; Raje, N.; Munshi, N.; Anderson, K. C. A novel Bcl-2/Bcl-X(L)/Bcl-w inhibitor ABT-737 as therapy in multiple myeloma. *Oncogene* **2007,** 26, 2374-80.

17. Chen, S.; Dai, Y.; Harada, H.; Dent, P.; Grant, S. Mcl-1 down-regulation potentiates ABT-737 lethality by cooperatively inducing Bak activation and Bax translocation. *Cancer Res* **2007,** 67, 782-91.

18. Lin, X.; Morgan-Lappe, S.; Huang, X.; Li, L.; Zakula, D. M.; Vernetti, L. A.; Fesik, S. W.; Shen, Y. 'Seed' analysis of off-target siRNAs reveals an essential role of Mcl-1 in resistance to the small-molecule Bcl-2/Bcl-XL inhibitor ABT-737. *Oncogene* **2007,** 26, 3972-9.

19. Moulding, D. A.; Giles, R. V.; Spiller, D. G.; White, M. R.; Tidd, D. M.; Edwards, S. W. Apoptosis is rapidly triggered by antisense depletion of MCL-1 in differentiating U937 cells. *Blood* **2000,** 96, 1756-63.

20. Marsden, V. S.; Strasser, A. Control of apoptosis in the immune system: Bcl-2, BH3-only proteins and more. *Annu Rev Immunol* **2003,** 21, 71-105.

21. MacCallum, D. E.; Melville, J.; Frame, S.; Watt, K.; Anderson, S.; Gianella-Borradori, A.; Lane, D. P.; Green, S. R. Seliciclib (CYC202, R-Roscovitine) induces cell death in multiple myeloma cells by inhibition of RNA polymerase II-dependent transcription and down-regulation of Mcl-1. *Cancer Res* **2005,** 65, 5399-407.

22. Zhang, B.; Gojo, I.; Fenton, R. G. Myeloid cell factor-1 is a critical survival factor for multiple myeloma. *Blood* **2002,** 99, 1885-93.

23. Michels, J.; O'Neill, J. W.; Dallman, C. L.; Mouzakiti, A.; Habens, F.; Brimmell, M.; Zhang, K. Y.; Craig, R. W.; Marcusson, E. G.; Johnson, P. W.; Packham, G. Mcl-1 is required for Akata6 B-lymphoma cell survival and is converted to a cell death molecule by efficient caspase-mediated cleavage. *Oncogene* **2004,** 23, 4818-27.

24. Song, L.; Coppola, D.; Livingston, S.; Cress, D.; Haura, E. B. Mcl-1 regulates survival and sensitivity to diverse apoptotic stimuli in human non-small cell lung cancer cells. *Cancer Biol Ther* **2005,** 4, 267-76.

25. Qin, J. Z.; Xin, H.; Sitailo, L. A.; Denning, M. F.; Nickoloff, B. J. Enhanced killing of melanoma cells by simultaneously targeting Mcl-1 and NOXA. *Cancer Res* **2006,** 66, 9636-45.

26. Miyamoto, Y.; Hosotani, R.; Wada, M.; Lee, J. U.; Koshiba, T.; Fujimoto, K.; Tsuji, S.; Nakajima, S.; Doi, R.; Kato, M.; Shimada, Y.; Imamura, M. Immunohistochemical analysis of Bcl-2, Bax, Bcl-X, and Mcl-1 expression in pancreatic cancers. *Oncology* **1999,** 56, 73-82.

27. Ren, L. N.; Li, Q. F.; Xiao, F. J.; Yan, J.; Yang, Y. F.; Wang, L. S.; Guo, X. Z.; Wang, H. Endocrine glands-derived vascular endothelial growth factor protects pancreatic cancer cells from apoptosis via upregulation of the myeloid cell leukemia-1 protein. *Biochem Biophys Res Commun* **2009,** 386, 35-9.

28. Cavarretta, I. T.; Neuwirt, H.; Untergasser, G.; Moser, P. L.; Zaki, M. H.; Steiner, H.; Rumpold, H.; Fuchs, D.; Hobisch, A.; Nemeth, J. A.; Culig, Z. The antiapoptotic effect of IL-6 autocrine loop in a cellular model of advanced prostate cancer is mediated by Mcl-1. *Oncogene* **2007,** 26, 2822-32.

29. Chung, T. K.; Cheung, T. H.; Lo, W. K.; Yim, S. F.; Yu, M. Y.; Krajewski, S.; Reed, J. C.; Wong, Y. F. Expression of apoptotic regulators and their significance in cervical cancer. *Cancer Lett* **2002,** 180, 63-8.

30. Sieghart, W.; Losert, D.; Strommer, S.; Cejka, D.; Schmid, K.; Rasoul-Rockenschaub, S.; Bodingbauer, M.; Crevenna, R.; Monia, B. P.; Peck-Radosavljevic, M.; Wacheck, V. Mcl-1 overexpression in hepatocellular carcinoma: a potential target for antisense therapy. *J Hepatol* **2006,** 44, 151-7.

31. Cho-Vega, J. H.; Rassidakis, G. Z.; Admirand, J. H.; Oyarzo, M.; Ramalingam, P.; Paraguya, A.; McDonnell, T. J.; Amin, H. M.; Medeiros, L. J. MCL-1 expression in B-cell non-Hodgkin's lymphomas. *Hum Pathol* **2004,** 35, 1095-100.

32. Khoury, J. D.; Medeiros, L. J.; Rassidakis, G. Z.; McDonnell, T. J.; Abruzzo, L. V.; Lai, R. Expression of Mcl-1 in mantle cell lymphoma is associated with high-grade morphology, a high proliferative state, and p53 overexpression. *J Pathol* **2003,** 199, 90-7.

33. Backus, H. H.; van Riel, J. M.; van Groeningen, C. J.; Vos, W.; Dukers, D. F.; Bloemena, E.; Wouters, D.; Pinedo, H. M.; Peters, G. J. Rb, mcl-1 and p53 expression correlate with clinical outcome in patients with liver metastases from colorectal cancer. *Ann Oncol* **2001,** 12, 779-85.

34. Wuilleme-Toumi, S.; Robillard, N.; Gomez, P.; Moreau, P.; Le Gouill, S.; Avet-Loiseau, H.; Harousseau, J. L.; Amiot, M.; Bataille, R. Mcl-1 is overexpressed in multiple myeloma and associated with relapse and shorter survival. *Leukemia* **2005,** 19, 1248-52.

35. Kaufmann, S. H.; Karp, J. E.; Svingen, P. A.; Krajewski, S.; Burke, P. J.; Gore, S. D.; Reed, J. C. Elevated expression of the apoptotic regulator Mcl-1 at the time of leukemic relapse. *Blood* **1998,** 91, 991-1000.

36. Kitada, S.; Andersen, J.; Akar, S.; Zapata, J. M.; Takayama, S.; Krajewski, S.; Wang, H. G.; Zhang, X.; Bullrich, F.; Croce, C. M.; Rai, K.; Hines, J.; Reed, J. C. Expression of apoptosis-regulating proteins in chronic lymphocytic leukemia: correlations with In vitro and In vivo chemoresponses. *Blood* **1998,** 91, 3379-89.

37. Gomez-Bougie, P.; Bataille, R.; Amiot, M. The imbalance between Bim and Mcl-1 expression controls the survival of human myeloma cells. *Eur J Immunol* **2004,** 34, 3156-64.

38. Gomez-Bougie, P.; Wuilleme-Toumi, S.; Menoret, E.; Trichet, V.; Robillard, N.; Philippe, M.; Bataille, R.; Amiot, M. Noxa up-regulation and Mcl-1 cleavage are associated to apoptosis induction by bortezomib in multiple myeloma. *Cancer Res* **2007,** 67, 5418-24.

39. Hussain, S. R.; Cheney, C. M.; Johnson, A. J.; Lin, T. S.; Grever, M. R.; Caligiuri, M. A.; Lucas, D. M.; Byrd, J. C. Mcl-1 is a relevant therapeutic target in acute and chronic lymphoid malignancies: down-regulation enhances rituximab-mediated apoptosis and complement-dependent cytotoxicity. *Clin Cancer Res* **2007,** 13, 2144-50.

40.   Thallinger, C.; Wolschek, M. F.; Wacheck, V.; Maierhofer, H.; Gunsberg, P.; Polterauer, P.; Pehamberger, H.; Monia, B. P.; Selzer, E.; Wolff, K.; Jansen, B. Mcl-1 antisense therapy chemosensitizes human melanoma in a SCID mouse xenotransplantation model. *J Invest Dermatol* **2003,** 120, 1081-6.

41.   Wei, S. H.; Dong, K.; Lin, F.; Wang, X.; Li, B.; Shen, J. J.; Zhang, Q.; Wang, R.; Zhang, H. Z. Inducing apoptosis and enhancing chemosensitivity to gemcitabine via RNA interference targeting Mcl-1 gene in pancreatic carcinoma cell. *Cancer Chemother Pharmacol* **2008,** 62, 1055-64.

42.   Guoan, X.; Hanning, W.; Kaiyun, C.; Hao, L. Adenovirus-mediated siRNA targeting Mcl-1 gene increases radiosensitivity of pancreatic carcinoma cells in vitro and in vivo. *Surgery* **2010,** 147, 553-61.

43.   Abulwerdi, F.; Liao, C.; Liu, M.; Azmi, A. S.; Aboukameel, A.; Mady, A. S.; Gulappa, T.; Cierpicki, T.; Owens, S.; Zhang, T.; Sun, D.; Stuckey, J. A.; Mohammad, R. M.; Nikolovska-Coleska, Z. A Novel Small-Molecule Inhibitor of Mcl-1 Blocks Pancreatic Cancer Growth In vitro and In vivo. *Mol Cancer Ther* **2013**.

44.   Tanaka, Y.; Aikawa, K.; Nishida, G.; Homma, M.; Sogabe, S.; Igaki, S.; Hayano, Y.; Sameshima, T.; Miyahisa, I.; Kawamoto, T.; Tawada, M.; Imai, Y.; Inazuka, M.; Cho, N.; Imaeda, Y.; Ishikawa, T. Discovery of Potent Mcl-1/Bcl-xL Dual Inhibitors by Using a Hybridization Strategy Based on Structural Analysis of Target Proteins. *J Med Chem* **2013**.

45.   Friberg, A.; Vigil, D.; Zhao, B.; Daniels, R. N.; Burke, J. P.; Garcia-Barrantes, P. M.; Camper, D.; Chauder, B. A.; Lee, T.; Olejniczak, E. T.; Fesik, S. W. Discovery of potent myeloid cell leukemia 1 (mcl-1) inhibitors using fragment-based methods and structure-based design. *J Med Chem* **2013,** 56, 15-30.

46.   Song, T.; Li, X.; Chang, X.; Liang, X.; Zhao, Y.; Wu, G.; Xie, S.; Su, P.; Wu, Z.; Feng, Y.; Zhang, Z. 3-Thiomorpholin-8-oxo-8H-acenaphtho [1,2-b] pyrrole-9-carbonitrile (S1) derivatives as pan-Bcl-2-inhibitors of Bcl-2, Bcl-xL and Mcl-1. *Bioorg Med Chem* **2013,** 21, 11-20.

47.   Cohen, N. A.; Stewart, M. L.; Gavathiotis, E.; Tepper, J. L.; Bruekner, S. R.; Koss, B.; Opferman, J. T.; Walensky, L. D. A Competitive Stapled Peptide Screen Identifies a Selective Small Molecule that Overcomes MCL-1-Dependent Leukemia Cell Survival. *Chem Biol* **2012,** 19, 1175-86.

48.   Doi, K.; Li, R.; Sung, S. S.; Wu, H.; Liu, Y.; Manieri, W.; Krishnegowda, G.; Awwad, A.; Dewey, A.; Liu, X.; Amin, S.; Cheng, C.; Qin, Y.; Schonbrunn, E.; Daughdrill, G.; Loughran, T. P., Jr.; Sebti, S.; Wang, H. G. Discovery of marinopyrrole A (maritoclax) as a selective Mcl-1 antagonist that overcomes ABT-737 resistance by binding to and targeting Mcl-1 for proteasomal degradation. *J Biol Chem* **2012,** 287, 10224-35.

49.   Rega, M. F.; Wu, B.; Wei, J.; Zhang, Z.; Cellitti, J. F.; Pellecchia, M. SAR by interligand nuclear overhauser effects (ILOEs) based discovery of acylsulfonamide compounds active against Bcl-x(L) and Mcl-1. *J Med Chem* **2011,** 54, 6000-13.

50.   Bernardo, P. H.; Sivaraman, T.; Wan, K. F.; Xu, J.; Krishnamoorthy, J.; Song, C. M.; Tian, L.; Chin, J. S.; Lim, D. S.; Mok, H. Y.; Yu, V. C.; Tong, J. C.; Chai, C. L. Structural insights into the design of small molecule inhibitors that selectively antagonize Mcl-1. *J Med Chem* **2010,** 53, 2314-8.

51.   Stewart, M. L.; Fire, E.; Keating, A. E.; Walensky, L. D. The MCL-1 BH3 helix is an exclusive MCL-1 inhibitor and apoptosis sensitizer. *Nat Chem Biol* **2010,** 6, 595-601.

52. Muppidi, A.; Doi, K.; Edwardraja, S.; Drake, E. J.; Gulick, A. M.; Wang, H. G.; Lin, Q. Rational design of proteolytically stable, cell-permeable peptide-based selective Mcl-1 inhibitors. *J Am Chem Soc* **2012,** 134, 14734-7.

53. Schrödinger Suite 2011 Induced Fit Docking protocol; Glide version 5.7, Schrödinger, LLC, New York, NY, 2009; Prime version 3.0, Schrödinger, LLC, New York, NY. **2011**.

54. Czabotar, P. E.; Lee, E. F.; van Delft, M. F.; Day, C. L.; Smith, B. J.; Huang, D. C.; Fairlie, W. D.; Hinds, M. G.; Colman, P. M. Structural insights into the degradation of Mcl-1 induced by BH3 domains. *Proc Natl Acad Sci U S A* **2007,** 104, 6217-22.

55. Lee, E. F.; Czabotar, P. E.; van Delft, M. F.; Michalak, E. M.; Boyle, M. J.; Willis, S. N.; Puthalakath, H.; Bouillet, P.; Colman, P. M.; Huang, D. C.; Fairlie, W. D. A novel BH3 ligand that selectively targets Mcl-1 reveals that apoptosis can proceed without Mcl-1 degradation. *J Cell Biol* **2008,** 180, 341-55.

56. Yang, C. Y.; Wang, S. M. Analysis of Flexibility and Hotspots in Bcl-xL and Mcl-1 Proteins for the Design of Selective Small-Molecule Inhibitors. *ACS Med Chem Lett* **2012,** 3, 308-312.

57. Liu, Q.; Moldoveanu, T.; Sprules, T.; Matta-Camacho, E.; Mansur-Azzam, N.; Gehring, K. Apoptotic regulation by MCL-1 through heterodimerization. *J Biol Chem* **2010,** 285, 19615-24.

58. Ge, Y.; Kazi, A.; Marsilio, F.; Luo, Y.; Jain, S.; Brooks, W.; Daniel, K. G.; Guida, W. C.; Sebti, S. M.; Lawrence, H. R. Discovery and synthesis of hydronaphthoquinones as novel proteasome inhibitors. *J Med Chem* **2012,** 55, 1978-98.

59. Castanet, A. S.; Colobert, F.; Broutin, P. E. Mild and regioselective iodination of electron-rich aromatics with N-iodosuccinimide and catalytic trifluoroacetic acid. *Tetrahedron Lett* **2002,** 43, 5047-5048.

60. Ciattini, P. G.; Morera, E.; Ortar, G. A New, Palladium-Catalyzed Synthesis of Aromatic Mercapturic Acid-Derivatives. *Tetrahedron Lett* **1995,** 36, 4133-4136.

61. Dai, W.; Petersen, J. L.; Wang, K. K. Synthesis of the parent and substituted tetracyclic ABCD ring cores of camptothecins via 1-(3-aryl-2-propynyl)- 1,6-dihydro-6-oxo-2-pyridinecarbonitriles. *Org Lett* **2006,** 8, 4665-7.

62. Eichman, C. C.; Stambuli, J. P. Zinc-mediated palladium-catalyzed formation of carbon-sulfur bonds. *J Org Chem* **2009,** 74, 4005-8.

63. Itoh, T.; Mase, T. A general palladium-catalyzed coupling of aryl bromides/triflates and thiols. *Org Lett* **2004,** 6, 4587-4590.

64. Mispelaere-Canivet, C.; Spindler, J. F.; Perrio, S.; Beslin, P. Pd-2(dba)(3)/Xantphos-catalyzed cross-coupling of thiols and aryl bromides/triflates. *Tetrahedron* **2005,** 61, 5253-5259.

65. Riesgo, E. C.; Jin, X.; Thummel, R. P. Introduction of Benzo[h]quinoline and 1,10-Phenanthroline Subunits by Friedlander Methodology. *J Org Chem* **1996,** 61, 3017-3022.

66. Ortar, G.; Cascio, M. G.; De Petrocellis, L.; Morera, E.; Rossi, F.; Schiano-Moriello, A.; Nalli, M.; de Novellis, V.; Woodward, D. F.; Maione, S.; Di Marzo, V. New N-arachidonoylserotonin analogues with potential "dual" mechanism of action against pain. *J Med Chem* **2007,** 50, 6554-69.

67. Beaudoin, S.; Kinsey, K. E.; Burns, J. F. Preparation of unsymmetrical sulfonylureas from N,N'-sulfuryldiimidazoles. *J Org Chem* **2003,** 68, 115-9.

68.   Greig, I. R.; Idris, A. I.; Ralston, S. H.; van't Hof, R. J. Development and characterization of biphenylsulfonamides as novel inhibitors of bone resorption. *J Med Chem* **2006,** 49, 7487-92.

69.   Li, X.; Chu, S.; Feher, V. A.; Khalili, M.; Nie, Z.; Margosiak, S.; Nikulin, V.; Levin, J.; Sprankle, K. G.; Tedder, M. E.; Almassy, R.; Appelt, K.; Yager, K. M. Structure-based design, synthesis, and antimicrobial activity of indazole-derived SAH/MTA nucleosidase inhibitors. *J Med Chem* **2003,** 46, 5663-73.

70.   Wagner, J.; von Matt, P.; Faller, B.; Cooke, N. G.; Albert, R.; Sedrani, R.; Wiegand, H.; Jean, C.; Beerli, C.; Weckbecker, G.; Evenou, J. P.; Zenke, G.; Cottens, S. Structure-activity relationship and pharmacokinetic studies of sotrastaurin (AEB071), a promising novel medicine for prevention of graft rejection and treatment of psoriasis. *J Med Chem* **2011,** 54, 6028-39.

71.   Ishizuka, N.; Matsumura, K.; Sakai, K.; Fujimoto, M.; Mihara, S.; Yamamori, T. Structure-activity relationships of a novel class of endothelin-A receptor antagonists and discovery of potent and selective receptor antagonist, 2-(benzo[1,3]dioxol-5-yl)-6-isopropyloxy-4-(4-methoxyphenyl)-2H-chromene-3-carbox ylic acid (S-1255). 1. Study on structure-activity relationships and basic structure crucial for ET(A) antagonism. *J Med Chem* **2002,** 45, 2041-55.

72.   England, D. B.; Kerr, M. A. Synthesis and cross-coupling reactions of substituted 5-triflyloxyindoles. *J Org Chem* **2005,** 70, 6519-22.

73.   Pandiarajan, K.; Kabilan, S.; Sankar, P.; Kolehmainen, E.; Nevalainen, T.; Kauppinen, R. Multinuclear Magnetic-Resonance Spectroscopic and Semiempirical Molecular-Orbital (Am1) Studies of Substituted Anisoles. *B Chem Soc Jpn* **1994,** 67, 2639-2646.

74.   Huang, W.; Shen, Q.; Wang, J.; Zhou, X. One-step synthesis of substituted dihydro- and tetrahydroisoquinolines by FeCl3.6H2O catalyzed intramolecular Friedel-Crafts reaction of benzylamino-substituted propargylic alcohols. *J Org Chem* **2008,** 73, 1586-9.

75.   Zhu, L.; Zhang, L. H. Specific para-hydroxylation of nitronaphthalenes with cumene hydroperoxide in basic aqueous media. *Tetrahedron Lett* **2000,** 41, 3519-3522.

76.   Hajduk, P. J.; Bures, M.; Praestgaard, J.; Fesik, S. W. Privileged molecules for protein binding identified from NMR-based screening. *J Med Chem* **2000,** 43, 3443-7.

77.   Medek, A.; Hajduk, P. J.; Mack, J.; Fesik, S. W. The use of differential chemical shifts for determining the binding site location and orientation of protein-bound ligands. *J Am Chem Soc* **2000,** 122, 1241-1242.

78.   Williamson, M. P. Using chemical shift perturbation to characterise ligand binding. *Prog Nucl Magn Reson Spectrosc* **2013,** 73, 1-16.

79.   Nikolovska-Coleska, Z.; Wang, R.; Fang, X.; Pan, H.; Tomita, Y.; Li, P.; Roller, P. P.; Krajewski, K.; Saito, N. G.; Stuckey, J. A.; Wang, S. Development and optimization of a binding assay for the XIAP BIR3 domain using fluorescence polarization. *Anal Biochem* **2004,** 332, 261-73.

80.   Smits, C.; Czabotar, P. E.; Hinds, M. G.; Day, C. L. Structural plasticity underpins promiscuous binding of the prosurvival protein A1. *Structure* **2008,** 16, 818-29.

81.   Wei, M. C.; Zong, W. X.; Cheng, E. H.; Lindsten, T.; Panoutsakopoulou, V.; Ross, A. J.; Roth, K. A.; MacGregor, G. R.; Thompson, C. B.; Korsmeyer, S. J. Proapoptotic BAX and BAK: a requisite gateway to mitochondrial dysfunction and death. *Science* **2001,** 292, 727-30.

82. Lindsten, T.; Thompson, C. B. Cell death in the absence of Bax and Bak. *Cell Death Differ* **2006,** 13, 1272-6.

83. Whitecross, K. F.; Alsop, A. E.; Cluse, L. A.; Wiegmans, A.; Banks, K. M.; Coomans, C.; Peart, M. J.; Newbold, A.; Lindemann, R. K.; Johnstone, R. W. Defining the target specificity of ABT-737 and synergistic antitumor activities in combination with histone deacetylase inhibitors. *Blood* **2009,** 113, 1982-91.

84. Glaser, S. P.; Lee, E. F.; Trounson, E.; Bouillet, P.; Wei, A.; Fairlie, W. D.; Izon, D. J.; Zuber, J.; Rappaport, A. R.; Herold, M. J.; Alexander, W. S.; Lowe, S. W.; Robb, L.; Strasser, A. Anti-apoptotic Mcl-1 is essential for the development and sustained growth of acute myeloid leukemia. *Genes Dev* **2012,** 26, 120-5.

85. Murugesan, N.; Hunt, J. T.; Stein, P. D. Preparation of phenylsulfonamidooxazole and -isoxazole endothelin antagonists. US5514696A, 1996.

86. Lewis, I. A.; Schommer, S. C.; Markley, J. L. rNMR: open source software for identifying and quantifying metabolites in NMR spectra. *Magn Reson Chem* **2009,** 47 Suppl 1, S123-6.

87. Goddard, T. D.; Kneller, D. G. SPARKY 3.

Chapter 3
Development of 1*H*-pyrazolo[3,4-b]pyridine analogs as a novel class of Mcl-1 inhibitors

3.1   Introduction

High throughput screen (HTS) approach is a known strategy for identification of potential lead compounds for further development[1]. To identify novel small-small molecule Mcl-1 inhibitors, a dual-readout HTS assay that combines two assay technologies, fluorescence polarization (FP) and Forster resonance energy transfer (FRET), was developed, optimized and miniaturized to a 1,536-well ultra-HTS format[2]. The assay was used to screen a library of 102,255 compounds at Emory University Molecular Libraries Screening Center using recombinant Mcl-1 and either a labeled Noxa or Bid BH3 derived peptides. The identified hits from the both primary screens were subjected to secondary dose-response tests and a total of 1214 (875 from Mcl-1/Noxa and 509 from Mcl-1/Bid) including 170 overlapping compounds were identified. All the dose-response curves were further deposited in the PubChem's BioAssay Database under AID 1417[3] and 1418[4].

A high hit rate in HTS campaigns can make the identification of the most promising hits a challenging task and thus novel strategies to simplify this process are desired. Therefore, we employed an integrated screening approach by combining in silico target-based screening for selection of the most promising hits. For this purpose, molecular docking using the crystal structure of Mcl-1 bound to mNoxa (PDB 2NLA)[5] was utilized and all identified hits were subjected to Schrödinger's Induced Fit Docking (IFD) protocol[6] at the BH3 binding site of Mcl-1. A pharmacophore model (Figure 3.1) was developed based on the interactions of mNoxa and Mcl-1 which included 3 hydrophobic and one hydrogen bond/electrostatic interactions. Compounds able to mimic at least two of the 4 conserved interactions of mNoxa with Mcl-1 were selected. This totaled 67 compounds from which 48 were purchased from commercial vendors. Notably, compounds with hydroxynaphthalenylsulfonamide scaffold of **59** class

(Chapter 2) were among selected compounds. All 48 compounds were subjected to rigorous biochemical and biophysical assays which included dose-response competitive FP and SPR assays against Mcl-1 and HSQC NMR studies. Compounds which gave consistent results in all the binding assays were considered as validated hits and those with promising chemical scaffolds were selected for further optimization.
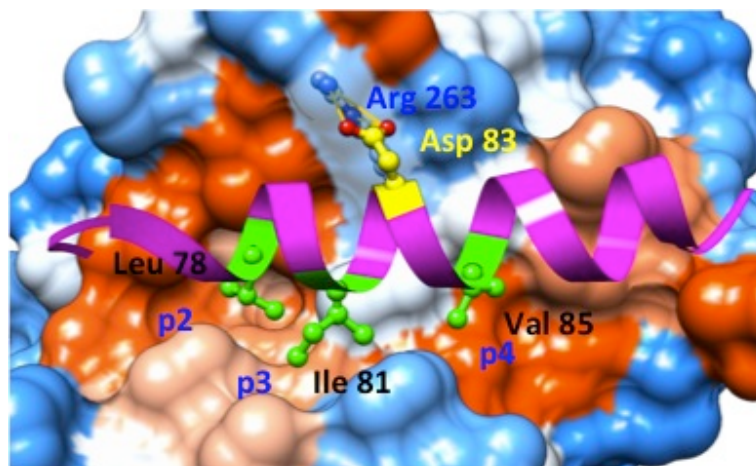

Figure 3.1. Pharmacophore model based on the interaction of mNoxa and Mcl-1. Crystal structure of mNoxa bound to Mcl-1 (PDB 2NLA) was used. Mcl-1 is shown in surface representation while mNoxa is shown as a purple ribbon. Three hydrophobic residues of mNoxa are shown in green and labeled in black. The charged residue is shown and labeled in yellow.

3.2   Identification of HTS lead 38 as a Mcl-1 inhibitor

Compound **38** (Figure 3.2A) was one of the validated hits which showed dose-dependent chemical shift changes of Mcl-1 residues in HSQC NMR experiments. Interestingly, compound **38** has structural features common to the **59** class (chapter 2) as well as to a newly published selective small-molecule Mcl-1 inhibitors[7] which include a bicyclic core (a 1*H*-pyrazolo[3,4-b]pyridine in **38**) and a carboxylic acid group. Compound **38** was resynthesized (analog **1**) and its potency was confirmed (K_i= 26 µM). Despite the low potency of this compound compared to the HTS lead **59** (K_i = 2 µM), the simplicity of synthetic modification for analog generation as well as its drug-like features as defined by Lipinski's Rule of Five[8] made it a good choice for further optimization. **38** has a favorable ligand efficiency of 12.9 which is calculated based on the equation below. Ligand efficiency (LE) as calculated below is also referred to as binding efficiency index (BEI)[9]. It has been documented that the optimum LE for small molecules targeting protein-protein interactions is around 12[10] and **38**'s LE nicely falls around this number.

$$LE = \frac{pK_i}{MW \ (kDa)}$$

For docking studies of **38**, a recently published Mcl-1 crystal structure in complex with a synthetic ligand (PDB 4HW2) was utilized[7]. The Gold-generated docking pose (Figure 3.2B) of **38** was further validated and confirmed by HSQC NMR studies of Mcl-1 in presence of 2-fold excess of **38**. Chemical shift perturbation (CSP) plot of compound **38** (Figure 3.2 C) showed moderate to significant perturbations of V249, M250 and M231, which are part of the p2 pocket of Mcl-1, consistent with the predicted binding model where 3-chlorophenyl of **38** binds to p2 hydrophobic pocket. Significant perturbations of L267 and R263 as well as residues in their vicinity (I264, V265) are also observed. L267 is predicted to interact with the 3-methyl while R263 forms an electrostatic interaction with 4-carboxylic acid of **38**. It should, however, be mentioned that the predicted distance for the electrostatic interaction is 4.2 Å, which is not optimal for a hydrogen bond. Finally, the 6-furyl is predicted to interact with residues in the p2/p3 pockets, mainly A227, F228, F270, G271 M231 which are moderately to significantly perturbed. In addition to the residues mentioned above which are predicted to interact with **38** by docking studies, significant chemical shift perturbations of V216, V220, Q221 (on C-terminal of α-helix 2), K234, L235 (on C-terminal of α-helix 3), N239 (on the disordered loop connecting α-helix 3 and 4) and V243 and V253 (on α-helix 4) are observed. Overall analysis of the chemical shift changes of **38** in complex with Mcl-1 shows that **38** affects the residues in the BH3-binding groove of Mcl-1 and provides a strong support for the binding of this compound to Mcl-1.
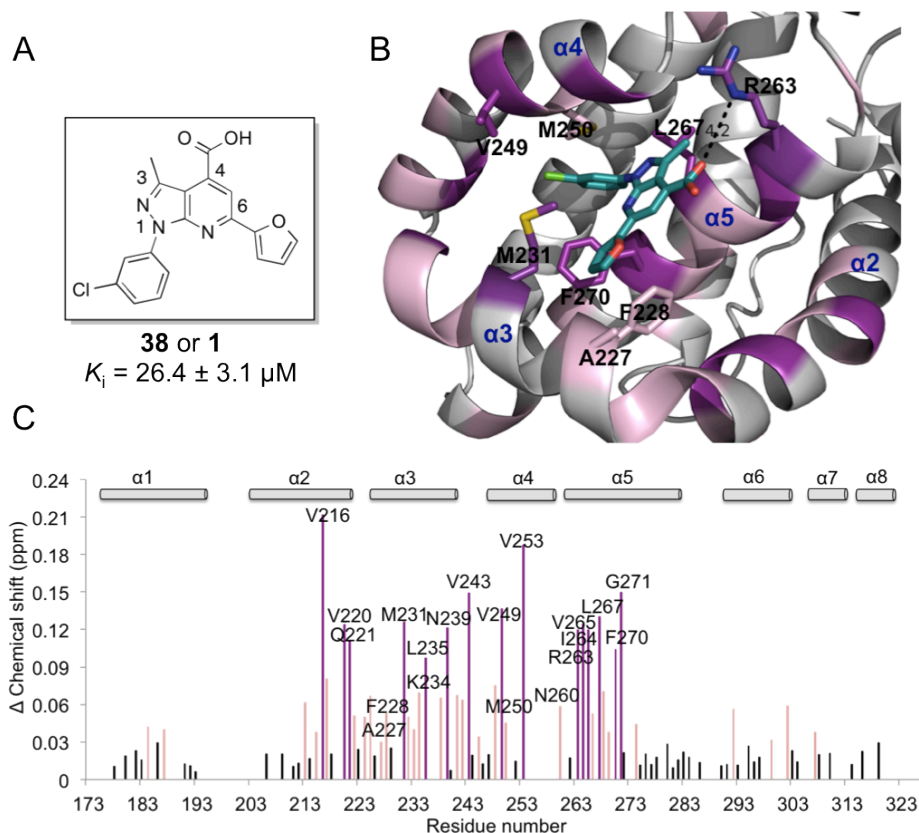
Figure 3.2. Docking and NMR studies of 38. (A) Structure of the HTS lead compound **38** or **1**. (B) Putative binding mode of **38** to Mcl-1 (4HW2). The surface of Mcl-1 is colored according to the chemical shift intensity. Residues of Mcl-1 labeled in black are predicted to interact with **38**. (C) Plot of chemical shift changes of Mcl-1 amide upon addition of **38** (Mcl-1:**38** ratio of 1:2) as a function of Mcl-1 residue numbers. Color legend: Significant shift (> 0.09 ppm) is represented with purple, moderate shift (≥ 0.03 ppm and ≤ 0.09 ppm) represented with pink.

The strong evidence of binding of **38** to Mcl-1 based on computational studies supported by NMR gave us the confidence to undertake the optimization of this class of compounds utilizing structure-based design strategy. Therefore an SAR plan was devised to make changes to the N-1 and C-6 aryl positions denoted as R and R' respectively (Scheme 3.1). We wished to achieve the following goals: 1) understand the contribution of R and R' to the overall binding of Mcl-1 and 2) incorporate moieties into R from the **59** class of compounds (R_1 substituents) (Chapter 2) that resulted in improved potency to increase the potency of this class of compounds.

3.3 Synthesis

A short, efficient and convergent synthesis of **38** class analogs was established based on literature methodology with the majority of compounds made utilizing Scheme 3.1.

Scheme 3.1. Generation of 1, 6-disubstituted-3-methyl-pyrazolopyridine-4-carboxylic acid analogs[a].

20-21   **22-31, 34**   **35-48** (Table 3.4)   **1-14** (Tables 3.1-3.3)
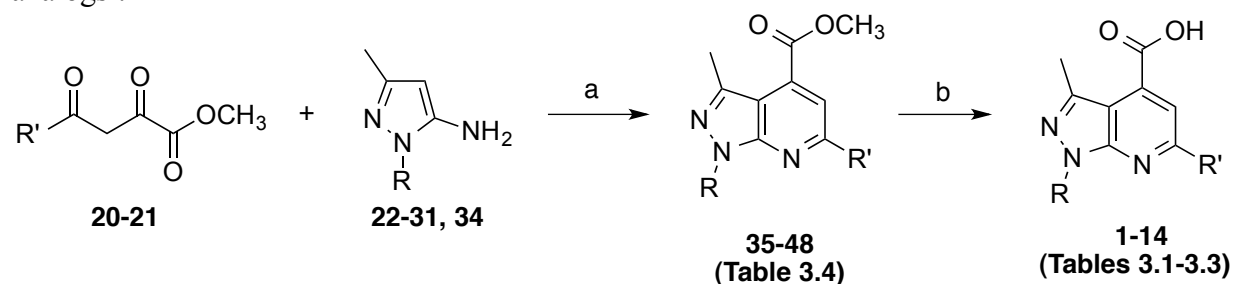
[a]Reagents and conditions: (a) AcOH, reflux, 2 h, 7%-97%; (b) KOH, iPrOH, reflux, 1 h, 20%-100%.

Acyl pyruvates **20** and **21** were obtained by Claisen condensation of 2-acetyl furan or acetone and diethyl oxalate[11] (Scheme 3.2). This introduced the first diversity point of the library which is termed R'.

Scheme 3.2. Synthesis of acylpyruvates **20** and **21**[a].

20-21
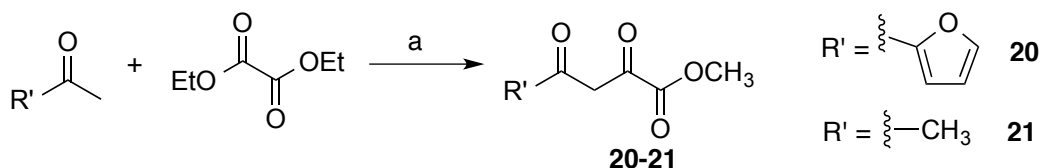
[a]Reagents and conditions: (a) Na, MeOH, rt, 1h, 26%-35%.

The second diversity point (R) was introduced with varying substitutions at the pyrazole N-1 position. Two sets of aminopyrazoles were prepared by two distinct approaches. The first series of aminopyrazoles (**22-25**) were obtained from a Michael addition of substituted hydrazines to 3-aminocrotononitrile[12] (Scheme 3.3).

109

Scheme 3.3. Synthesis of aminopyrazoles **22-25** from substituted hydrazines[a].
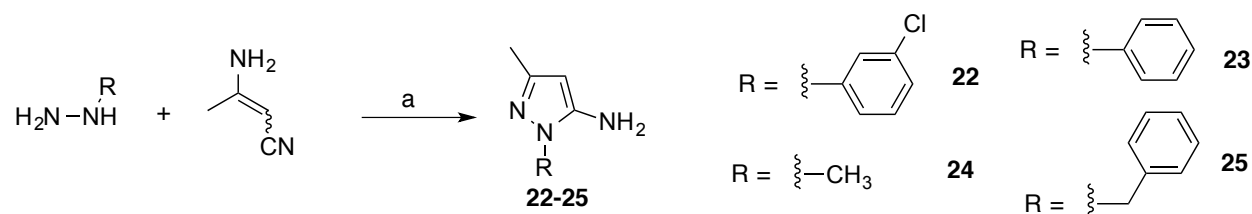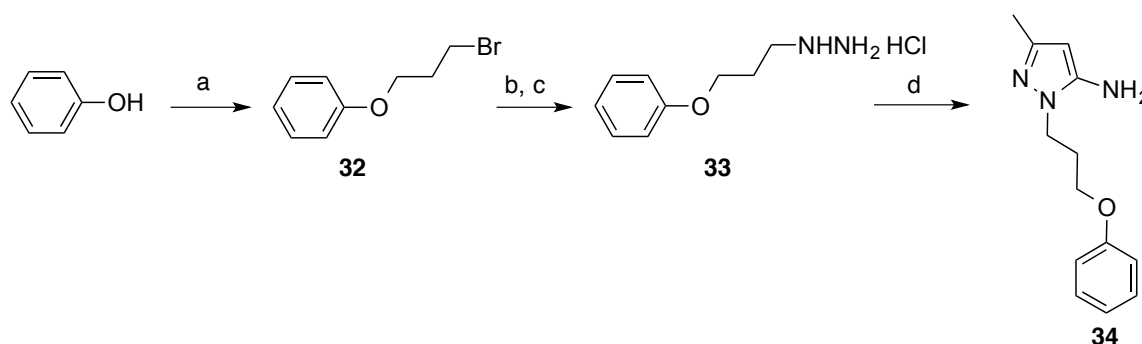

[a]Reagents and conditions: (a) 1N HCl, reflux, 3h, 20%-98%.

For analog **11 (311)**, the substituted hydrazine (**33**) was not available but was easily prepared (Scheme 3.4) by alkylation of 1-phenol by 1,3-dibromopropane[13] followed by displacement of bromide with hydrazine[14].

Scheme 3.4. Synthesis of aminopyrazole **34**[a].

[a]Reagents and conditions: (a) Br(CH$_2$)$_3$Br, K$_2$CO$_3$, acetone, reflux, 19 h, 77%; (b) H$_2$NNH$_2$. H$_2$O, EtOH, 80 °C, 3h 30 min; (c) 2N HCl, CH$_2$Cl$_2$, rt, overnight; (d) H$_2$N(CH$_3$)=CHCN, 1N HCl, reflux, 3 h, 48% over three steps.

When the substituted hydrazines were not commercially available or easily accessible, the multicomponent condensation of hydrazine, crotononitrile and arylaldehyde afforded the desired aminopyrazoles (**26-31**) (Scheme 3.5) as reported previously[15, 16]. The proposed mechanism by which this reaction works is as following: first, the Michael adduct is formed between reaction of crotononitrile and hydrazine. Treatment of this adduct with a desired arylaldehyde provides the intermediate imine (structure shown) which is not isolated, but is directly converted to the corresponding pyrazole via base-promoted cyclization and isomerization (Scheme 3.5). Having the desired acylpyruvates and aminopyrazoles in hand, the penultimate intermediates (**35-48**) were obtained from the reaction between these two building blocks in acetic acid[17] (Scheme 3.1).

110

Hydrolysis of ester using potassium hydroxide in 2-propanol provided the final analogs **1-14**[17] (Scheme 3.1).

**Scheme 3.5.** Synthesis of aminopyrazoles **26-31** from arylaldehydes[a].
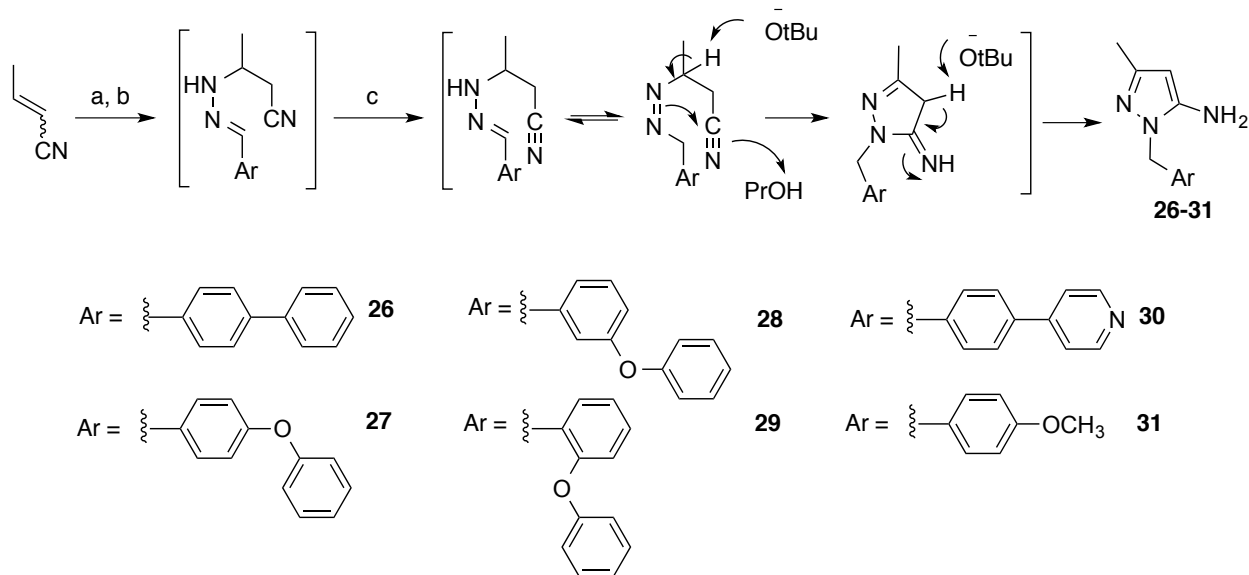
[a]Reagents and conditions: (a) H$_2$NNH$_2$. H$_2$O, THF, 40 °C, 2 h; (b) ArCHO, 40 °C, 2 h (c) *t*-BuONa, iPrOH, 100 °C, 2 h 30 min or *t*-BuONa, *n*-PrOH, 110 °C, 2 h 30 min, 20%-42% over three steps.

For analogs **15-19**, Scheme 3.6 was utilized. 3-methyl-1-(4-phenoxybenzyl)-1*H*-pyrazol-5-amine (**28**) was condensed with diethyl oxalacetate to provide ring-opened intermediate (structure not shown) which was cyclized to pyridinol **49** by refluxing in glacial acetic acid[18]. Chlorination of pyridone **49** with POCl$_3$ was not successful as previously reported[18]. Neither did the use of a stoichiometric amount of Vilsmeier reagent under mild conditions yield the desired product. However, use of a large excess of Vilsmeier reagent under reflux conditions[19] overnight cleanly provided **50** in high yield. Intermediate **50** then underwent Pd-catalyzed carbon-carbon coupling reactions[20-22] with phenylvinylboronic acid or phenylacetylene to provide **52** and **53** respectively. Intermediate **54** was obtained via hydrogenation[23] of **52**. Direct amination[23] of **50** with 2-aminomethylfuran or 4-(2-aminoethyl)morpholine under high temperature and long reaction time provided **51** and **55** respectively. Ester intermediates were hydrolyzed as previously described in Scheme 3.1 to provide acid analogs **15-19**.

Scheme 3.6. Generation of analogs **15-19**[a].
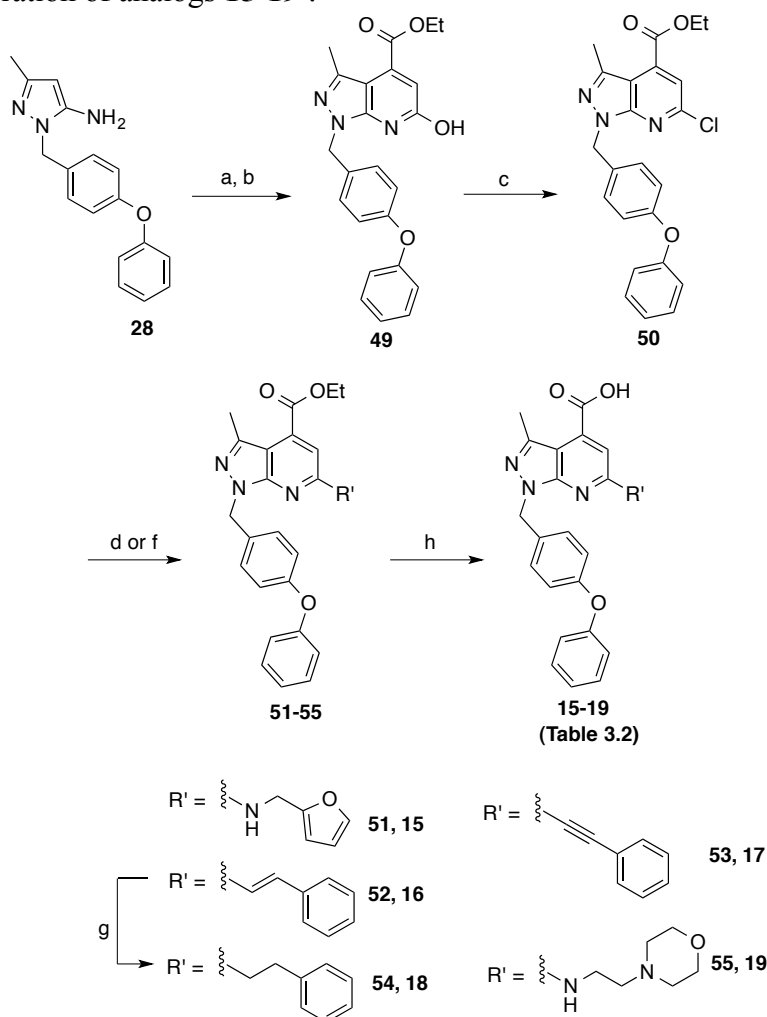
[a]Reagents and conditions: (a) $EtO_2CC(ONa)=CHCO_2Et$, toluene/glacial $AcOH/H_2O$, 80 °C, overnight; (b) glacial AcOH, reflux, 2 h, 67% over two steps; (c) $(COCl)_2$, DMF, 1,2 DCE, 0 °C to rt to reflux, overnight, quantitative; (d) for **52**: phenylvinylboronic acid, $Pd(PPh_3)_4$, Na_2CO_3, 1,4 dioxane/H_2O, 90 °C, overnight, 90% or for **53**: phenylacetylene, $Pd(PPh_3)_2Cl_2$, CuI, Et_3N/THF, 60 °C, overnight, 31%; (f) for **51**: 2-aminomethylfuran, iPrOH, 100 °C to 150 °C, 2 days, 30% or for **55**: 4-(2-aminoethyl)morpholine, iPrOH/NMP, 150 °C, overnight, 26%; (g) Pd/C, H_2 (1 atm), EtOH/THF, rt, overnight, 84%; (h) KOH, iPrOH/THF, reflux, 2 h, 39%-94% or for **15**: 1N NaOH, THF, reflux, 3 h, 61%.
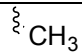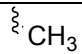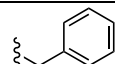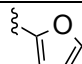
3.4   Structure-activity relationships

In an absence of a crystal structure of **38** with Mcl-1, we set to study the contributions of R and R' of **38** and gain further insight into their binding sites by systematically removing each group and study the obtained fragments (Table 3.1) in HSQC NMR. First, analog **2** was

synthesized in which a phenyl was substituted for the 3-chlorophenyl which led to 6-fold decrease in potency compared to **38**. Subsequently removal of either the phenyl at R or the furyl at R' or both, and their replacements with a methyl to give fragments **3-5** respectively, were studied. All three analogs did not bind up to 800 µM and showed little to no perturbations in HSQC NMR studies at 2-fold excess (final fragment concentration of 150 µM). This lack of perturbation is interesting as analog **2** (also a high micromolar binder) but having both aromatic groups at R and R', shows dose-dependent perturbations of Mcl-1 residues. This result confirms the importance of both aromatic rings at R and R' and their contributions to the overall potency. Next, the phenyl in **2** was replaced with a benzyl group in **6** which led to a 2-fold increase in potency. More importantly, the NMR studies (Figure 3.2) of these two analogs led to an important finding. When the chemical shift changes of **2** were subtracted from those caused by **6** and the residues were mapped onto the structure of Mcl-1 (Figure 3.3A-B), it became clear that the residues most affected by the changes between the two structures, mainly clustered on the C-terminal of α-helix 3 and α-helix 4, which are the residues lining the p2 pocket of Mcl-1. This finding indicates that the benzyl group of **6** inserts into the h2 pocket and forms additional hydrophobic interactions with p2 pocket.

Table 3.1. Binding affinities of **38** and fragments.

Cpd	R	R'	FP IC$_{50}$ ± SD (µM)	FP K_i ± SD (µM)	LE
1(38)	(3-chlorophenyl)	(furyl)	103.5 ± 12.4	26.4 ± 3.1	12.9
2	(phenyl)	(furyl)	580.9 ± 27.5	148.5 ± 7.0	12.0
3	CH$_3$	(furyl)	> 800	> 200	--
4	(phenyl)	CH$_3$	> 800	> 200	--

5	CH₃	CH₃	> 800	> 200	--
6	(benzyl)	(furanyl-O)	353.1 ± 21.7	90.2 ± 5.6	12.1

Figure 3.3. Mapping the binding site of R substituent. (A) Residues of Mcl-1 (PDB 4HW2) perturbed significantly in presence of **6** (green) and **2** (red) are shown and labeled. (B) Chemical shift perturbation (CSP) difference plot as generated by subtraction of CSP of **2** from **6** (Mcl-1:cpd ratio of 1:2). Significant CSP difference of >-0.015 ppm is highlighted in red and >0.015 ppm is highlighted in green.

Our NMR studies of **2** and **6** further validated our molecular docking model in which R is predicted to insert into the p2 pocket of Mcl-1. Therefore, we decided to synthesize analogs introducing R_1 substituents from our first class of Mcl-1 inhibitors that led to a gain in potency as R_1 was confirmed to also interact with h2 pocket of Mcl-1 (Table 3.2). *Para*-biphenylmethyl and *para*-phenoxybenzyl were introduced at R in **7** and **8**, which gratifyingly exhibited K_i of 4 μM and 2 μM, respectively, and an overall 7- to 12-fold improvement over **38**. Both **7** and **8** have improved LE values compared to **38** with **8** giving the best LE of 13.3 indicating a higher free energy of binding per atom. The molecular docking of **7** places the *para*-biphenylmethyl deeper

into the p2 pocket (Figure 3.4A) which is supported by the NMR studies showing moderate to significant perturbations of F228, M250, and F270 of p2 pocket, clearly demonstrating the importance of the hydrophobic interactions in this sub-pocket (Figure 3.4B).

Table 3.2. Binding affinities of analogs with variations at R.

Cpd	R	FP IC$_{50}$ ± SD (µM)	FP K_i ± SD (µM)	SPR IC$_{50}$ ± SD (µM)	LE	cLogP[a]
1(38)		103.5 ± 12.4	26.4 ± 3.1	160.0	12.9	3.71
7		14.8 ± 2.5	3.78 ± 0.63	11.6	13.2	4.82
8		8.6 ± 1.9	2.2 ± 0.5	6.3	13.3	4.68
9		54.6 ± 4.8	14.0 ± 1.25	19.4	11.4	--
10		239.6 ± 19.6	61.2 ± 5.0	80.1	9.9	--
11		> 200	> 51	--	--	3.61
12		> 800	> 200	--	--	3.02
13		608.1 ± 96.9	155.4 ± 24.7	--	10.1	--

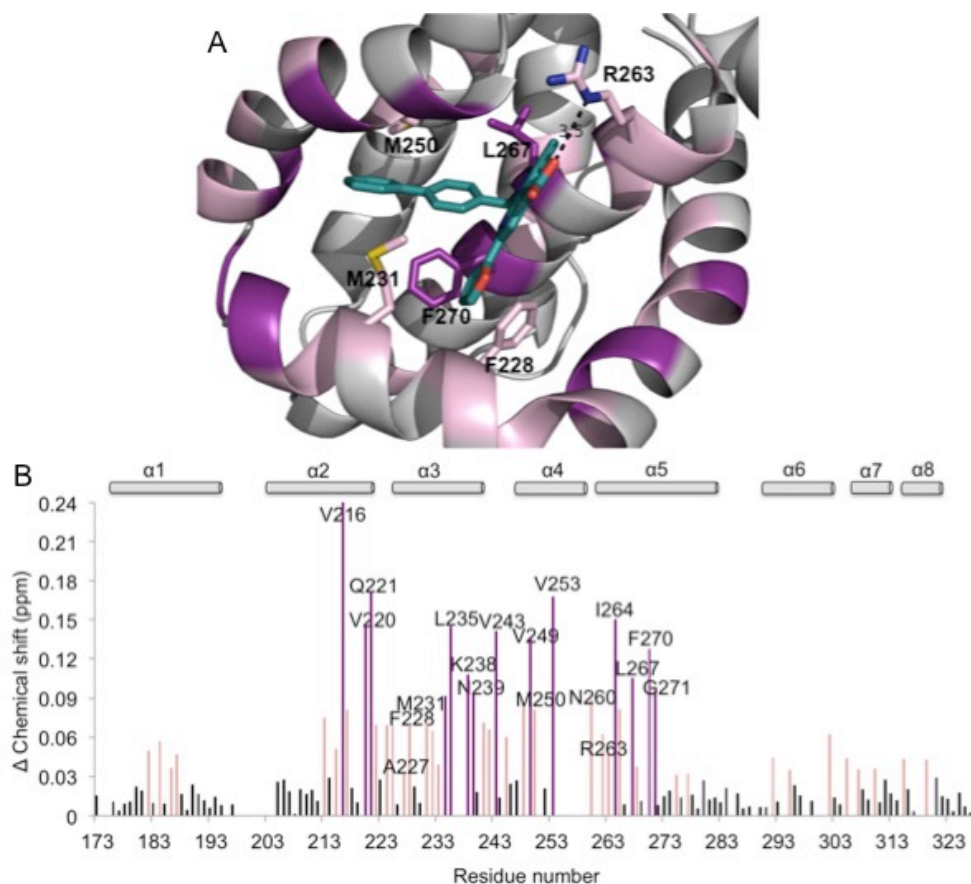[a] Calculated using MarvinSketch 6.2.4, ChemAxon.

Figure 3.4. Docking and NMR studies of 7. (A) Putative binding modes of **7** to Mcl-1 (4HW2). The surface of Mcl-1 is colored according to the chemical shift intensity. Residues of Mcl-1 labeled in black are predicted to interact with **7**. (B) Plot of chemical shift changes of Mcl-1 amide upon addition of **7** (Mcl-1:**7** ratio of 1:2) as a function of Mcl-1 residue numbers. Color legend: Significant shift (> 0.09 ppm) is represented with purple, moderate shift (≥ 0.03 ppm and ≤ 0.09 ppm) represented with pink.

The CSP plot of **8** (Figure 3.5A) also confirmed its binding to Mcl-1. To examine how the position of the distal phenyl ring in R substituent will affect the binding, compounds with *meta*-(**9**) and *ortho*-phenoxybenzyl substituents (**10**) were synthesized. Analog **9** showed a 6-fold decrease in binding compared to **8** while **10** decreased binding by a significant 27 fold indicating that there is a clear preference for the *para*-phenoxybenzyl in the pocket. The CSP plots derived from HSQC NMR (Figure 3.5A-C) of these three isomers supported the binding affinity data with **8** and **9** showing the highest magnitude of perturbations of residues. In addition, CSP demonstrated that the phenoxybenzyl substituent was placed in the p2 pocket through the chemical shift perturbations of V249, M250 and M231. In addition residues A227, F228, F270,

116

R263 and L267 are perturbed suggesting that carboxylic acid forms a hydrogen bond interaction and the 6-furyl is placed in the p3 pocket.
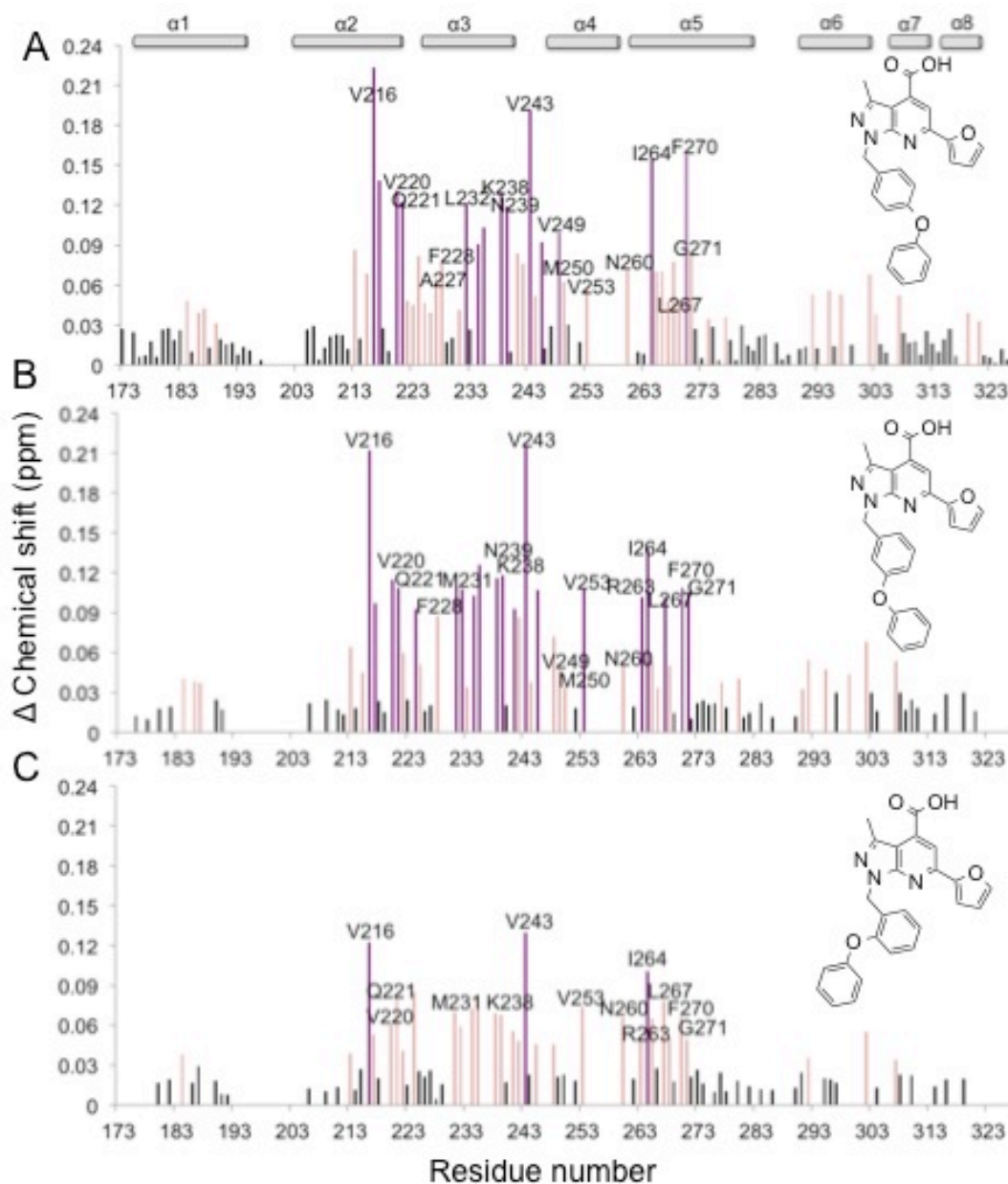
Figure 3.5. NMR studies of 8, 9, 10. (A) Plots of chemical shift changes of Mcl-1 amide upon addition of **8** (Mcl-1:**8** ratio of 1:2) (B) **9** (Mcl-1:**9** ratio of 1:2) (C) **10** (Mcl-1:**10** ratio of 1:2) as a function of Mcl-1 residue numbers. Color legend: Significant shift (> 0.09 ppm) is represented with purple, moderate shift (≥ 0.03 ppm and ≤ 0.09 ppm) represented with pink.

Attempts aimed at introducing polar groups and improving clogP by incorporation of a *para*-4-pyridinebenzyl substituent in **11** or a *para*-methoxybenzyl in **12** (Table 3.2) led to a decrease in binding affinity, clearly indicating that the pocket does not tolerate polar or

hydrophilic groups. Finally, in analog **13**, a propylphenoxy substituent was introduced at R. The design of this analog was based on the work of Friberg *et al.*[7] in which it was shown that flexible aryl groups off the bicyclic core occupied the p2 pocket of Mcl-1. In our case, this strategy did not work which can be explained by a different anchoring point of the flexible aryl due to core scaffold differences as well as differences in distance between the aryl and the carboxylic acid functions.

Next, we focused on the contribution of R' to the overall binding affinity (Table 3.3). While from our earlier studies of analog **2** and its fragment, **4**, missing the furyl at R', it became clear that removal of furyl resulted in drop in binding affinity. The low potencies of both analogs and lack of CSP with **4** did not allow for in-depth NMR studies and binding site mapping of furyl ring. Therefore, our most potent analog **8** from Table 3.2 was selected and a corresponding fragment **14**, where the furyl was replaced with a methyl, was synthesized and evaluated. Analog **14** decreased binding by a significant 20 fold compared to **8** further highlighting the importance of the furyl to the overall binding. The NMR studies of these two compounds did not provide a clear picture of the binding site of R' (Figure 3.6). The CSP difference plot of **14** and **8** (Figure 3.6B) showed that the residues affected by the furyl are spread along α-helices 2 to 5. The reason for this wide area to be affected can be explained because of the nature of R' substituent. A furyl at R' of **8** is much larger than a methyl in **14**, and its accommodation into the pocket requires conformational change by the protein which results in more perturbations.
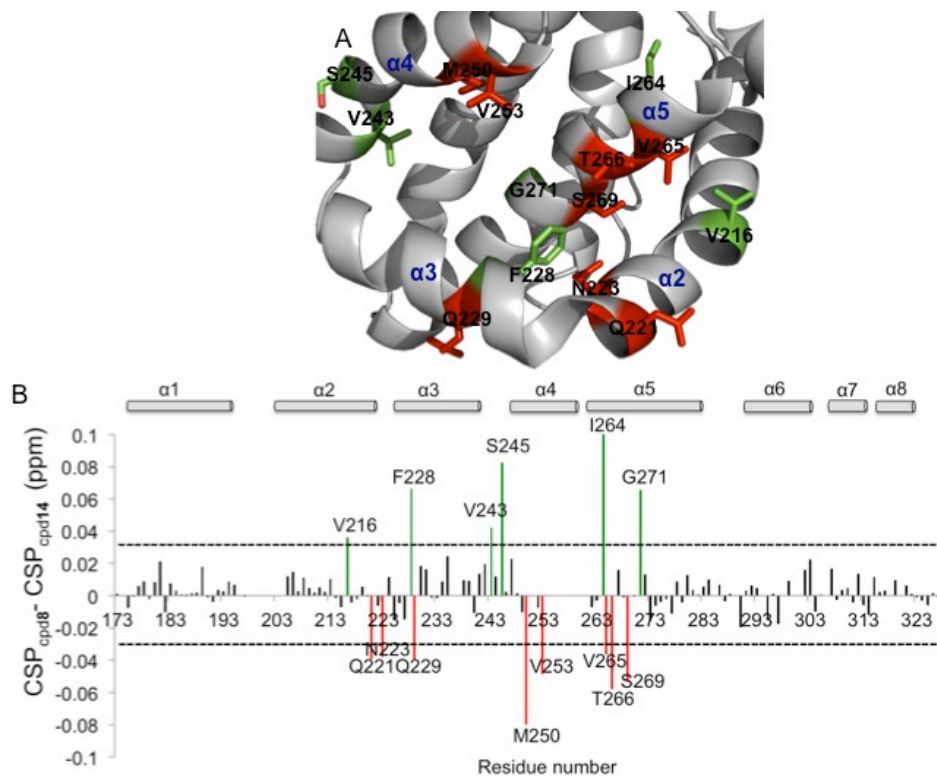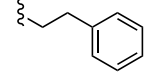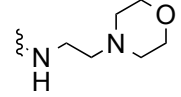
Figure 3.6. Mapping the binding site of R' substituent. (A) Residues of Mcl-1 (PDB 4HW2) perturbed significantly in presence of **8** (green) and **14** (red) are shown and labeled. (B) Chemical shift perturbation (CSP) difference plot as generated by subtraction of CSP of **14** from **8** (Mcl-1:cpd ratio of 1:2). Significant CSP difference of >-0.03 ppm is highlighted in red and >0.03 ppm is highlighted in green.

Since *para*-phenoxybenzyl at R (**8**) provided the most potent analog from our series with R variations as well as exhibited an acceptable clogP, we decided to retain that moiety at R and optimize R'. Based on the docking poses of earlier analogs, while the furan was predicted to interact with residues in p3 pocket, its direct attachment to the bicyclic core made its placement in p3 pocket dependent on the R substituent. Therefore, incorporation of linkers to provide more degrees of freedom and a better placement in the p3 pocket were assessed. Our attempts at homologation of the furyl group were not successful using our synthetic Scheme 3.1; however, using a different chemistry (Scheme 3.6), analog **15** with an aminomethyl furan at R' was obtained. This analog exhibited a K_i = 42 μM and a 5-fold decrease in binding compared to **8**. The decrease in binding affinity can be attributed to the introduction of a polar amine linker or an unfavorable direction of the furan ring in the p3 pocket. Next, analogs **16-18** with a phenyl in place of furyl and aliphatic linkers with different directional geometries were synthesized. All

three analogs **16-18** have improved potencies compared to **15**, which confirms that aliphatic linkers are preferred, but they show 2- to 3-fold loss of binding affinity compared to **8**. A more unexpected result for us was the similar potencies of these three analogs. While the ethyl linker in **18** is flexible and would allow for the phenyl to find its most favorable conformation, the trans ethenyl linker in **16** or the ethynyl linker in **17** with their linear geometry would provide very distinct and different orientations of the phenyl group. We contribute these to the different modes of binding of these analogs as predicted by their docking poses (Figure 3.7) in which **16** only provided a flipped pose (Figure 3.7A) compared to **17** and **18** (Figure 3.7B). Our attempts to validate the docking poses with NMR studies were not successful as all three analogs are quite lipophilic and were marginally soluble in our NMR assay resulting in poor quality spectra. Additionally, incorporation of a polar, hydrophilic group in **19** led to a decrease in binding by 14-fold compared to **8**, once again illustrating the hydrophobic nature of the pocket.

Table 3.3. Binding affinities of analogs with variations at R'.

Cpd	R'	FP IC$_{50}$ ± SD (µM)	FP K_i ± SD (µM)	LE	cLogP[a]
14	CH$_3$	175.6 ± 11.3	44.9 ± 2.9	11.6	3.71
15		42.3 ± 3.7	10.8 ± 1.0	10.9	4.44
16		13.0 ± 1.0	3.3 ± 0.2	11.9	6.16
17		17.7 ± 3.2	4.5 ± 0.8	11.6	6.09

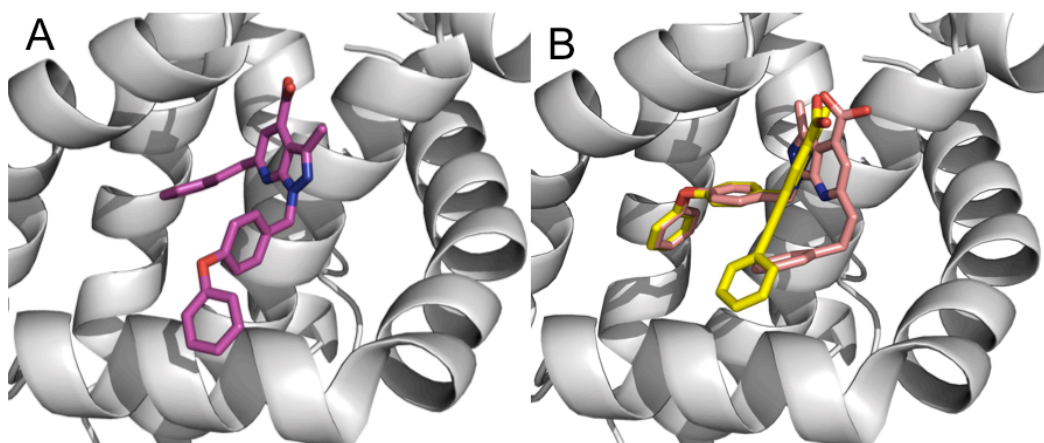| 18		22.6 ± 2.1	5.8 ± 0.5	11.3	5.99
19		193.8 ± 8.4	49.5 ± 2.1	8.82	3.45
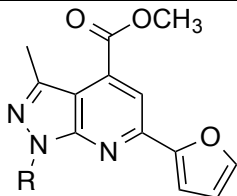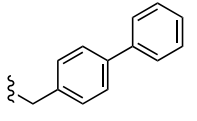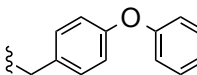
Figure 3.7. Docking poses of 16, 17, 18. (A) Putative binding pose of **16**. (B) Overlaid putative binding mode of **17** (yellow) and **18** (light pink).

Next, the contribution of the 4-carboxylic acid, which is predicted to form an electrostatic interaction with R263 of Mcl-1, was investigated. The potency of methyl ester intermediates **39** and **40** were assessed in FP-based assay. However, it was noted that the methyl ester analogs were fluorescent and therefore, FP-based assay cannot be used for determination of their binding affinity. In addition, HSQC NMR studies of the ester analogs were not successful due to their inferior solubility at high concentration in our NMR assay. Thus, competitive surface plasmon resonance (SPR)-based assay was used, which is not interfered by the intrinsic fluorescence of small molecules, to determine binding affinities of these analogs. As was expected, **39** and **40** resulted in decreased binding compared to their corresponding free acid parents (analogs **7** and **8** respectively). **40** with an $IC_{50} = 37$ μM exhibited a 6-fold loss of binding compared to **8** illustrating the importance of the carboxylic acid to the overall binding to Mcl-1.

Table 3.4. Binding affinities of esters **39** and **40**.

Cpd	R	SPR[a] IC_{50} (µM)	cLogP[b]
39	(biphenylmethyl group)	> 50	5.17
40	(phenoxybenzyl group)	37.2	5.02

[a] Values are the mean of two experiments. [b] Calculated using MarvinSketch 6.2.4, ChemAxon.

3.5   Selectivity studies

The selectivity profile of analogs **8**, **16-18** was determined against four other Bcl-2 anti-apoptotic proteins (Bcl-2, Bcl-X_L, Bcl-w, Bfl-1/A1) utilizing a competitive FP-based assays, and K_i values were calculated using equations developed previously[24] (Table 3.5).

Table 3.5. Selectivity of selected analogs against Bcl-2 anti-apoptotic proteins.

Cpd	Mcl-1 $K_i \pm$ SD (µM)	Bfl-1/A1 $K_i \pm$ SD (µM)	Bcl-2 $K_i \pm$ SD (µM)	Bcl-w $K_i \pm$ SD (µM)	Bcl-X_L $K_i \pm$ SD (µM)
8	2.2 ± 0.5	> 20*	16.2	> 17*	> 23*
16	3.3 ± 0.2	10.0 ± 3.2	4.6 ± 0.8	12.1 ± 1.8	23.2 ± 0.1
17	4.5 ± 0.8	> 20*	10.9	> 17*	> 23*
18	5.8 ± 0.5	> 20*	8.5	> 17*	> 23*

*Compounds were tested up to 100 µM.

Analogs **8**, **17**, **18** inhibited Mcl-1 most potently with K_i values from 2.2 µM to 5.8 µM, followed by Bcl-2 with K_i values from 8.5 µM to 16.2 µM. While **8** showed more potent inhibition of Mcl-1 with an 8-fold selectivity over Bcl-2, **17** and **18** inhibited both proteins

equipotently. All three analogs showed no inhibition of Bfl-1/A1, Bcl-w, and Bcl-X$_L$ up to 100 μM.

Interestingly, analog **16** showed inhibition of all four anti-apoptotic proteins with a slight selectivity for Mcl-1, Bfl-1/A1 and Bcl-2 (K_i values ≈ 4 μM) over Bcl-w (3 fold) and Bcl-X$_L$ (6 fold). Analog **16** shares a similar substituent at R with **17** and **18** and only differs in the geometry of two-carbon linker bearing a phenyl at R'. These three analogs exhibited similar binding affinities to Mcl-1 despite their distinct and different orientations of R' group as discussed above, which we speculated can be due to the predicted flipped binding pose of **16** (Figure 3.7A). Therefore, it is possible that the different selectivity profile of **16** over **17** and **18** is due to its different binding mode. Further studies, however, are needed to confirm the binding results and provide evidence for analog **16** binding pose.

3.6 Conclusions

A novel class of small-molecule Mcl-1 inhibitors based on a HTS lead **38** was developed. Systematic removal of side chains of **38** and detailed NMR analysis of the obtained fragments mapped the binding site of this class of inhibitors in the BH3-binding groove of Mcl-1. The structure-based lead optimization was guided by computational modeling supported by NMR studies. In addition our knowledge gained through the development of the **59** class of Mcl-1 inhibitors (Chapter 2) was also applied to design more potent analogs. Utilizing an efficient synthetic route, 19 analogs were synthesized and their binding affinity was determined by FP- and SPR-based assays. An initial SAR was established, and a more potent analog **8** with an K_i of 2 μM and 12-fold improvement in binding potency compared to **38** was developed. Analog **8** also showed improved ligand efficiency compared to the lead compound **38** illustrating that a gain in molecular weight of **8** over **38** is justified by its improved binding affinity. Selectivity profile of the most potent analog **8** further illustrated that it inhibited Mcl-1 most potently, followed by Bcl-2, but it did not show binding to A1, Bcl-w and Bcl-X$_L$ up to 100 μM. Interestingly, compound **16** showed similar binding affinity against Mcl-1 and Bcl-2, followed by A1 and Bcl-w with only 3-fold decrease in binding affinity, and an 8-fold less binding affinity to Bcl-X$_L$ suggesting that **16** is a pan inhibitor. Further studies are needed to confirm the selectivity results. Overall, **38** class of compounds with 1*H*-pyrazolo[3,4-b]pyridine scaffold is a promising class of Mcl-1 inhibitors which can be developed as dual Mcl-1 and Bcl-2 inhibitors.

3.7 Experimental

Chemistry

All anhydrous reactions were run under an atmosphere of dry nitrogen. Reagents were used as supplied without further purification. Reactions were monitored by TLC using precoated silica gel 60 F254 plates. Silica gel chromatography was performed with silica gel (220–240 mesh) obtained from Silicycle. Purities of final compounds were assessed by analytical HPLC performed on a Shimadzu system with a Restek Ultra C18 (4.6 x 150 mm, 5μm particle size) column or an Agilent 1100 series with an Agilent Zorbax Eclipse Plus−C18 column and a gradient of acetonitrile with 0.1 vol% TFA (10-90%) in water with 0.1 vol% TFA. All NMR spectra were obtained in DMSO-d_6 or CDCl$_3$ and results were recorded at 400 MHz on a Varian 400 instrument or at 500 MHz on a Varian 500 instrument. Mass spectrometry analysis was performed using a Waters LCT time-of-flight mass spectrometry instrument utilizing electrospray ionization operating in positive-ion (ESI+) or negative-ion (ESI-) modes where indicated.

**A representative procedure for synthesis of acyl pyruvates.**
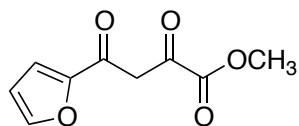
Methyl 4-(furan-2-yl)-2,4-dioxobutanoate (20).[11] To a stirred solution of MeOH (150 mL) at room temperature under nitrogen, freshly cut Na (1.81g, 78.7 mmol) was added in pieces and with care. After all the sodium dissolved, a mixture of 2-acetylfuran (6 mL, 59.8 mmol) and diethyl oxalate (8.14 mL, 59.9 mmol) was added dropwise over a period of 3 min at room temperature. The resulting mixture was continued to stir. Brown precipitates formed after 20 min stir. The mixture was stirred for a total of 1h. The reaction mixture was cooled to 0°C, and a mixture of concentrated H$_2$SO$_4$ and ice was added. Some solid precipitated at this point which was filtered off but was not the desired product by 1H NMR. The filterate was extracted with CH$_2$Cl$_2$ (50 mL x 2). The combined organic layers were washed with brine, dried (Na$_2$SO$_4$), filtered, and concentrated under reduced pressure. The crude was recrystallized from hot iPrOH to give the title compound (4.15 g, 35%) as a dark brown solid. ^{1}H NMR (400 MHz, CDCl$_3$) δ 7.67-7.65 (m, 1H), 7.33 (d, *J* = 3.6 Hz, 1H), 6.93 (s, 1H), 6.60 (dd, *J* = 3.5, 1.5 Hz, 1H), 3.91 (s,

3H). ^{13}C NMR (100 MHz, CDCl$_3$) δ 181.01, 165.39, 162.43, 150.82, 147.73, 118.58, 113.14, 99.17, 53.18.
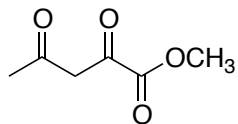

Methyl 2,4-dioxopentanoate (21). Synthesized using the procedure for **20** except acetone was used as one of the starting material. Crude was subjected to flash column chromatography on silica gel to provide the title compound (1.36 g, 26%) as a white gel. ^{1}H NMR (500 MHz, CDCl$_3$) δ 6.38 (s, 1H), 3.90 (s, 3H), 2.26 (s, 3H). ^{13}C NMR (125 MHz, CDCl$_3$) δ 199.96, 166.58, 162.48, 102.20, 53.10, 27.61.

A representative procedure for synthesis of aminopyrazoles from substituted hydrazines.
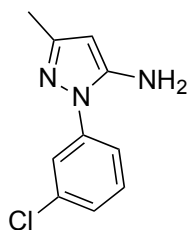
1-(3-Chlorophenyl)-3-methyl-1*H*-pyrazol-5-amine (22).[12] A solution of 3-aminocrotonitrile (mixture of cis and trans) (1.50 g, 17.5 mmol) and 3-chlorophenylhydrazine hydrochloride (3.0 g, 16.2 mmol) in 25 mL of 1N HCl was heated to reflux for 3 h under nitrogen. The reaction mixture was diluted with H$_2$O (30 mL) and extracted with EtOAc (20 mL x 2). The combined organic layers were washed with brine, dried (Na$_2$SO$_4$), filtered, and concentrated under reduced pressure. The crude was recrystallized from hot iPrOH to give the title compound (677 mg, 20%) as a beige fluffy solid. ^{1}H NMR (500 MHz, CDCl$_3$) δ 7.62 (s, 1H), 7.48 (d, *J* = 8.0 Hz, 1H), 7.37 (t, *J* = 8.0 Hz, 1H), 7.28 (d, *J* = 9.5 Hz, 1H), 5.46 (s, 1H), 2.22 (s, 3H). ^{13}C NMR (125 MHz, CDCl$_3$) δ 149.95, 145.30, 139.87, 135.05, 130.32, 126.86, 123.67, 121.28, 91.41, 13.89.
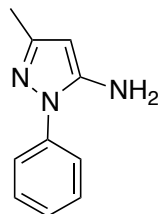
3-Methyl-1-phenyl-1*H*-pyrazol-5-amine (23). Synthesized using the procedure for **22** except phenyl hydrazine was used as the hydrazine. Recrystallization of crude from hot EtOH provided the title compound (1.28 g, 37%) as pink crystals. ^{1}H NMR (400 MHz, CDCl$_3$) δ 7.54 (s, 1H), 7.51 (s, 1H), 7.44 (t, *J* = 7.5 Hz, 2H), 7.30 (t, *J* = 7.4 Hz, 1H), 5.43 (s, 1H), 3.77 (s, 2H), 2.22 (s, 3H). ^{13}C NMR (100 MHz, CDCl$_3$) δ 149.37, 145.21, 138.65, 129.38, 126.99, 123.77, 90.68, 13.93.
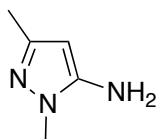
1,3-Dimethyl-1*H*-pyrazol-5-amine (24). Synthesized using the procedure for **22** except methyl hydrazine was used as the hydrazine. Recrystallization of crude from hot CH$_2$Cl$_2$ provided the title compound (908 mg, 45%) as clear crystals. ^{1}H NMR (400 MHz, CDCl$_3$) δ 5.30 (s, 1H), 3.55 (s, 3H), 2.11 (s, 3H). ^{13}C NMR (100 MHz, CDCl$_3$) δ 147.16, 144.96, 90.79, 33.83, 13.78.
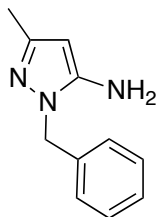
1-Benzyl-3-methyl-1*H*-pyrazol-5-amine (25). Synthesized using the procedure for **22** except benzyl hydrazine dihydrochloride was used as the hydrazine. After the reaction mixture was stopped and cooled to room temperature, solid precipitated which was filtered off and dried in vacuum oven to provide the title compound (3.6 g, 98%) as a white solid. ^{1}H NMR (400 MHz, DMSO-d$_6$) δ 7.40-7.34 (m, 2H), 7.34-7.27 (m, 3H), 5.57 (s, 1H), 5.35 (s, 2H), 2.18 (s, 3H). ^{13}C NMR (100 MHz, CDCl$_3$) δ 151.48, 146.65, 135.16, 129.19, 128.61, 128.00, 91.19, 49.13, 11.44.

A representative procedure for synthesis of aminopyrazoles from arylaldehydes.
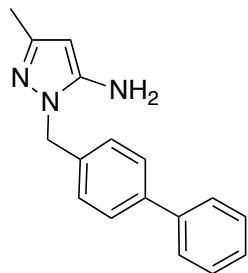
1-([1,1'-Biphenyl]-4-ylmethyl)-3-methyl-1*H*-pyrazol-5-amine (26).[16] To a solution of hydrazine monohydrate (hydrazine 78-82%) (0.51 ml, 10.5 mmol) in THF (2 mL), crotononitrile (mixture of cis and trans) (0.82 ml, 10.1 mmol) was added dropwise. The mixture was stirred at 40 ^{0}C for 2 h. The mixture was allowed to cool to room temperature and biphenyl-4-carboxaldehyde (1.82 g, 10.0 mmol) was added. The mixture was stirred at 40 ^{0}C for 2 h. The mixture was concentrated under reduced pressure. To the resulting yellow solid was added iPrOH (15 mL) and the suspension was transferred to a pressure vessel. *t*-BuONa (993 mg, 10.3 mmol) was added and the mixture was stirred at 100 ^{0}C for 2 h 30 min. The mixture was allowed to cool to room temperature and diluted with water (50 mL). The mixture was extracted with Et$_2$O (50 mL x 2). The combined organic layers were extracted with IN aq. HCl (2 x 30 mL). The combined aqueous phases were basified to pH 14 with 50 % aq. NaOH and extracted with Et$_2$O (50 mL x 2). The combined organic layers were washed with brine, dried (Na$_2$SO$_4$), filtered, and concentrated under reduced pressure to provide the title compound (885 mg, 34% over three steps) as a yellow solid. Crude was used in the next reaction without further purification. ^{1}H NMR (500 MHz, DMSO-d$_6$) δ 7.68-7.61 (m, 4H), 7.45 (t, *J* = 7.5 Hz, 2H), 7.39 (d, *J* = 7.9 Hz, 2H), 7.37-7.33 (m, 1H), 5.59 (s, 1H), 5.38 (s, 2H), 2.20 (s, 3H). ^{13}C NMR (125 MHz, DMSO-d$_6$) δ 151.46, 146.77, 140.52, 139.98, 134.32, 129.40, 128.62, 128.09, 127.51, 127.14, 91.23, 48.92, 11.54.
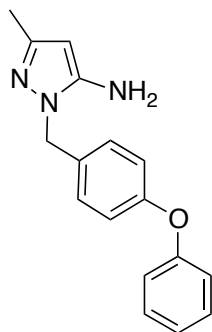
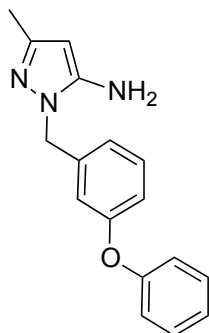**3-Methyl-1-(4-phenoxybenzyl)-1*H*-pyrazol-5-amine (27).** Synthesized using the procedure for **26** except 4-phenoxybenzaldehyde was used as the aldehyde. Title compound (994 mg, 35% over three steps) was obtained as a yellow solid. ^{1}H NMR (500 MHz, DMSO-d$_6$) δ 7.38 (dd, *J* = 17.2, 8.5 Hz, 4H), 7.17-7.13 (m, 1H), 7.03-6.98 (m, 4H), 5.58 (s, 1H), 5.32 (s, 2H), 2.19 (s, 3H). ^{13}C NMR (125 MHz, DMSO-d$_6$) δ 157.12, 156.73, 151.33, 146.70, 130.56, 130.06, 130.04, 124.17, 119.24, 119.12, 91.24, 48.61, 11.51.

A modified procedure for synthesis of aminopyrazoles from arylaldehydes.

3-Methyl-1-(3-phenoxybenzyl)-1*H*-pyrazol-5-amine (28).[15] To a solution of hydrazine monohydrate (hydrazine 78-82%) (0.80 ml, 16.5 mmol) in THF (3 mL), crotononitrile (mixture of cis and trans) (1.1 ml, 13.5 mmol) was added dropwise. The mixture was stirred at 40 ^{0}C for 2 h. The mixture was allowed to cool to room temperature and 3-phenoxybenzaldehyde (2.14 ml, 12 mmol) was added dropwise. The mixture was stirred at 40 ^{0}C for 2 h. The mixture was concentrated under reduced pressure. To the resulting intermediate was added nPrOH (10 mL) and the suspension was transferred to a pressure vessel. *t*-BuONa (1.41 g, 14.7 mmol) was added and the mixture was stirred at 110 ^{0}C for 2 h 30 min. The mixture was allowed to cool to room temperature and diluted with water (50 mL). The mixture was extracted with Et$_2$O (50 mL x 2). The combined organic layers were extracted with 1N aq. HCl (2 x 30 mL). The combined aqueous phases were basified to pH 14 with 50 % aq. NaOH and extracted with Et$_2$O (50 mL x 2). The combined organic layers were washed with brine, dried (Na$_2$SO$_4$), filtered, and concentrated under reduced pressure to provide the title compound (670 mg, 20% over three steps) as an orange oil. Crude was used in the next reaction without further purification. ^{1}H NMR (500 MHz, CDCl$_3$) δ 7.32 (t, *J* = 7.0 Hz, 2H), 7.25 (t, *J* = 7.8 Hz, 1H), 7.10 (t, *J* = 6.9 Hz, 1H), 6.98 (d, *J* = 7.8 Hz, 2H), 6.85 (t, *J* = 7.6 Hz, 2H), 6.80 (s, 1H), 5.37 (d, *J* = 2.6 Hz, 1H), 5.10 (s, 2H), 2.17 (s, 3H). ^{13}C NMR (125 MHz, CDCl$_3$) δ 157.81, 156.75, 147.74, 145.05, 139.08, 130.19, 129.75, 123.46, 121.22, 119.04, 117.63, 116.99, 91.65, 50.86, 13.92.
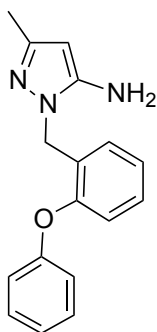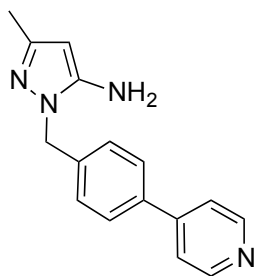
3-Methyl-1-(2-phenoxybenzyl)-1*H*-pyrazol-5-amine (29). Synthesized using the procedure for **28** except 2-phenoxybenzaldehyde was used as the aldehyde. Title compound (485 mg, 34% over three steps) was obtained as an off-white solid. Crude was used in the next reaction without further purification. ^{1}H NMR (500 MHz, CDCl$_3$) δ 7.34 (t, J = 7.1 Hz, 2H), 7.24-7.17 (m, 2H), 7.12 (t, J = 7.1 Hz, 1H), 7.08 (t, J = 7.5 Hz, 1H), 6.96 (d, J = 7.9 Hz, 2H), 6.84 (d, J = 8.1 Hz, 1H), 5.32 (s, 1H), 5.15 (s, 2H), 3.63 (s, 2H), 2.17 (s, 3H). ^{13}C NMR (126 MHz, CDCl$_3$) δ 156.75, 153.93, 147.82, 145.11, 129.94, 129.69, 129.09, 127.98, 124.16, 123.61, 118.48, 118.38, 90.68, 45.69, 14.00.

3-Methyl-1-(4-(pyridin-4-yl)benzyl)-1*H*-pyrazol-5-amine   (30). Synthesized using the procedure for **28** except 4-pyridine-4-benzaldehyde was used as the aldehyde. The title compound (274 mg, 20% over three steps) was obtained as a white solid. Crude was used in the next reaction without further purification. ^{1}H NMR (500 MHz, CDCl$_3$) δ 8.63 (d, J = 4.5 Hz, 2H), 7.58 (d, J = 8.1 Hz, 2H), 7.45 (d, J = 4.5 Hz, 2H), 7.26 (d, J = 7.3 Hz, 2H), 5.42 (s, 1H), 5.19 (s, 2H), 3.38 (s, 2H), 2.20 (s, 3H). ^{13}C NMR (125 MHz, CDCl$_3$) δ 150.26, 147.88, 147.72, 144.98, 138.06, 137.49, 127.48, 121.48, 91.83, 50.82, 13.97.
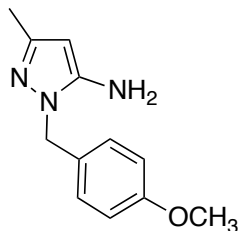
1-(4-Methoxybenzyl)-3-methyl-1*H*-pyrazol-5-amine (31). Synthesized using the procedure for **26** except *p*-anisaldehyde was used as the aldehyde. Title compound (910 mg, 42% over three steps) was obtained as a yellow oil which solidified upon standing. Crude was used in the next reaction without further purification. ^{1}H NMR (500 MHz, DMSO-d$_6$) δ 7.09 (d, J = 8.3 Hz, 2H), 6.84 (d, J = 8.3 Hz, 2H), 5.10 (s, 2H), 5.07 (s, 1H), 4.90 (s, 2H), 3.70 (s, 3H), 1.94 (s, 3H). ^{13}C

NMR (125 MHz, DMSO-d$_6$) δ 158.73, 147.58, 146.13, 130.82, 129.05, 114.05, 88.29, 55.49, 49.31, 14.30.
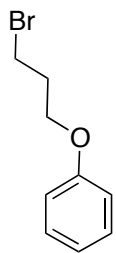
(3-Bromopropoxy)benzene (32).[13] 1-Phenol (1.03 g, 10.9 mmol), 1,3-dibromopropane (16 mL, 158 mmol), and K$_2$CO$_3$ (7.43 g, 53.8 mmol) were combined and suspended in acetone (100 mL). The mixture was stirred under reflux for 19 h, then filtered to remove the base and concentrated under reduced pressure. The crude was placed on high vacuum and provide the title compound (1.81 g, 77%) as a clear oil. Crude was used in the next reaction without further purification. ^{1}H NMR (400 MHz, CDCl$_3$) δ 7.29 (t, J = 7.6 Hz, 2H), 6.96 (t, J = 7.8 Hz, 1H), 6.91 (d, J = 7.8 Hz, 2H), 4.10 (t, J = 5.8 Hz, 2H), 3.61 (t, J = 6.1 Hz, 2H), 2.37-2.28 (m, 2H). ^{13}C NMR (100 MHz, CDCl$_3$) δ 158.62, 129.48, 120.89, 114.47, 65.12, 32.39, 30.12.
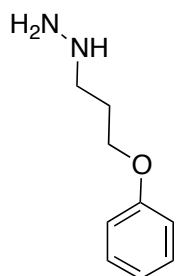
(3-Phenoxypropyl)hydrazine hydrochloride (33).[14] **32** (1.80 g, 8.4 mmol) was dissolved in EtOH (9 mL) followed by addition of hydrazine monohydrate (hydrazine 78-82%) (4.5 ml, 93 mmol). The solution was heated at 80 °C for 3h 30 min. After cooling to room temperature, the reaction mixture was concentrated under reduced pressure and the crude was treated with 2N HCl (7 mL) and dichloromethane (4 mL) while stirring at room temperature overnight. The crude was placed on high vacuum to remove solvent and then used without further purification in the next reaction.
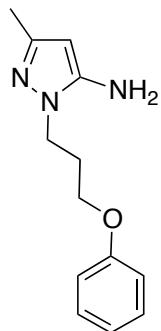
3-Methyl-1-(3-phenoxypropyl)-1*H*-pyrazol-5-amine (34). Synthesized using the procedure for **22** except **33** was used as crude and as the hydrazine. After the reaction mixture was stopped and cooled down to room temperature, the reaction mixture was diluted with H_2O and extracted with EtOAC (2x). Combined organic layers were washed with brine, dried (Na_2SO_4), filtered, and concentrated under reduced pressure. Crude was subjected to flash column chromatography on silica gel to provide the title compound (663 mg, 48% over two steps) as a yellow oil. ^{1}H NMR (400 MHz, CDCl$_3$) δ 7.23 (t, *J* = 7.2 Hz, 2H), 6.92 (t, *J* = 7.0 Hz, 1H), 6.84 (d, *J* = 8.0 Hz, 2H), 5.21 (s, 1H), 4.03 (t, *J* = 6.2 Hz, 2H), 3.84 (t, *J* = 5.6 Hz, 2H), 3.65 (s, 2H), 2.22-2.14 (m, 2H), 2.11 (s, 3H). ^{13}C NMR (100 MHz, CDCl$_3$) δ 158.19, 147.73, 145.69, 129.59, 121.12, 114.43, 90.07, 63.94, 42.66, 29.16, 13.92.

A representative procedure for synthesis of esters.
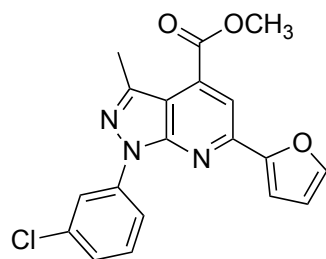
Methyl 1-(3-chlorophenyl)-6-(furan-2-yl)-3-methyl-1*H*-pyrazolo[3,4-*b*]pyridine-4-carboxylate (35).[17] A solution of **22** (306 mg, 1.47 mmol) and **20** (295 mg, 1.50 mmol) in glacial AcOH (10 mL) was heated to reflux for 3 h. When the reaction mixture was cooled down to room temperature, yellow precipitates formed which were filtered and washed with H_2O. Filtercake was placed in a vacuum oven to give the title compound (470 mg, 87%) as a yellow solid. ^{1}H NMR (500 MHz, CDCl$_3$) δ 8.48 (s, 1H), 8.29 (d, *J* = 9.1 Hz, 1H), 8.06 (s, 1H), 7.62 (s, 1H), 7.43 (t, *J* = 8.1 Hz, 1H), 7.28-7.23 (m, 2H), 6.63-6.59 (m, 1H), 4.06 (s, 3H), 2.75 (s, 3H).

¹³C NMR (125 MHz, CDCl₃) δ 165.53, 152.95, 151.82, 148.42, 144.43, 143.32, 140.31, 134.59, 133.91, 129.93, 125.41, 120.77, 118.52, 113.87, 112.57, 112.24, 110.94, 52.73, 16.21.
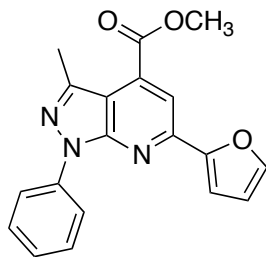
Methyl 6-(furan-2-yl)-3-methyl-1-phenyl-1*H*-pyrazolo[3,4-*b*]pyridine-4-carboxylate (36). Synthesized using the procedure for **35** except **23** was used as the amine. After reaction mixture was stopped and cooled down to room temperature, yellow precipitates formed which were filtered, washed with H₂O and dried in vacuum oven to give the title compound (971 mg, 97%) as a yellow solid. ¹H NMR (400 MHz, CDCl₃) δ 8.29 (d, *J* = 8.6 Hz, 2H), 8.05 (s, 1H), 7.59 (s, 1H), 7.52 (t, *J* = 7.7 Hz, 2H), 7.29 (t, *J* = 7.2 Hz, 1H), 7.23 (s, 1H), 6.58 (s, 1H), 4.04 (s, 3H), 2.76 (s, 3H). ¹³C NMR (100 MHz, CDCl₃) δ 165.73, 153.12, 151.69, 148.28, 144.27, 142.68, 139.24, 133.75, 128.94, 125.73, 121.17, 113.67, 112.45, 111.91, 110.70, 52.68, 16.19.
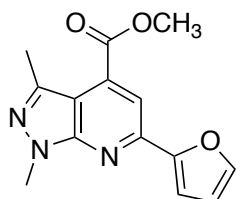
Methyl 6-(furan-2-yl)-1,3-dimethyl-1*H*-pyrazolo[3,4-*b*]pyridine-4-carboxylate (37). Synthesized using the procedure for **35** except **24** was used as the pyrazole amine. Crude was subjected to flash column chromatography on silica gel to provide the title compound (616mg, 76%) as a light pink solid. ¹H NMR (400 MHz, CDCl₃) δ 7.93 (s, 1H), 7.59-7.56 (m, 1H), 7.17 (d, *J* = 3.4 Hz, 1H), 6.55 (dd, *J* = 3.4, 1.7 Hz, 1H), 4.07 (s, 3H), 3.99 (s, 3H), 2.65 (s, 3H). ¹³C NMR (100 MHz, CDCl₃) δ 165.82, 153.11, 152.14, 147.83, 144.15, 140.61, 133.27, 113.10, 112.33, 110.30, 109.86, 52.52, 33.62, 16.00.

Methyl 1-benzyl-6-(furan-2-yl)-3-methyl-1*H*-pyrazolo[3,4-*b*]pyridine-4-carboxylate (38). Synthesized using the procedure for **35** except **25** was used as the pyrazole amine. Crude was subjected to flash column chromatography on silica gel to provide the title compound (97 mg, 9%) as a light yellow solid. ^{1}H NMR (400 MHz, CDCl$_3$) δ 8.06 (s, 1H), 7.67 (s, 1H), 7.33 (d, *J* = 7.2 Hz, 2H), 7.28 (t, *J* = 7.2 Hz, 2H), 7.26-7.21 (m, 1H), 7.08-7.04 (m, 1H), 6.61 (dd, *J* = 3.5, 1.8 Hz, 1H), 5.73 (s, 2H), 4.04 (s, 3H), 2.72 (s, 3H). ^{13}C NMR (100 MHz, CDCl$_3$) δ 165.99, 152.08, 150.69, 146.13, 144.45, 141.45, 137.02, 133.86, 128.53, 127.97, 127.62, 114.14, 112.40, 112.23, 111.85, 53.00, 50.45, 16.69.
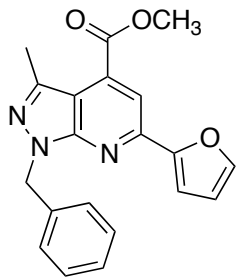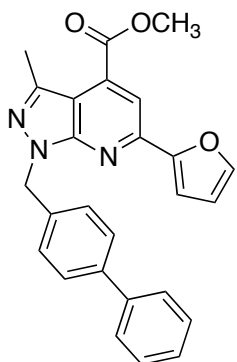

Methyl 1-([1,1'-biphenyl]-4-ylmethyl)-6-(furan-2-yl)-3-methyl-1*H*-pyrazolo[3,4-*b*]pyridine-4-carboxylate (39). Synthesized using the procedure for **35** except **26** was used as the pyrazole amine. Crude was subjected to flash column chromatography on silica gel to provide the title compound (87 mg, 7%) as an off-white solid. ^{1}H NMR (500 MHz, CDCl$_3$) δ 8.10 (s, 1H), 7.70 (s, 1H), 7.54 (t, *J* = 7.5 Hz, 4H), 7.42 (dd, *J* = 14.2, 7.9 Hz, 4H), 7.32 (t, *J* = 7.4 Hz, 1H), 7.08 (d, *J* = 3.4 Hz, 1H), 6.64 (dd, *J* = 3.4, 1.7 Hz, 1H), 5.79 (s, 2H), 4.07 (s, 3H), 2.76 (s, 3H). ^{13}C NMR (125 MHz, CDCl$_3$) δ 166.00, 152.12, 150.72, 146.21, 144.47, 141.55, 140.79, 140.60, 136.05, 133.93, 128.71, 128.46, 127.33, 127.24, 127.06, 114.20, 112.42, 112.26, 111.92, 53.01, 50.20, 16.71.
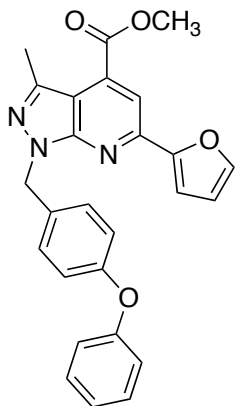
Methyl 6-(furan-2-yl)-3-methyl-1-(4-phenoxybenzyl)-1*H*-pyrazolo[3,4-*b*]pyridine-4-carboxylate (40). Synthesized using the procedure for **35** except **27** was used as the pyrazole amine. Crude was subjected to flash column chromatography on silica gel to provide the title compound (478 mg, 43%) as a yellow oil. ^{1}H NMR (500 MHz, CDCl$_3$) δ 8.03 (s, 1H), 7.61 (s, 1H), 7.37 (d, *J* = 8.3 Hz, 2H), 7.30 (t, *J* = 7.7 Hz, 2H), 7.25 (d, *J* = 3.4 Hz, 1H), 7.08 (t, *J* = 7.4 Hz, 1H), 6.97 (d, *J* = 8.4 Hz, 2H), 6.93 (d, *J* = 8.3 Hz, 2H), 6.61-6.58 (m, 1H), 5.66 (s, 2H), 4.04 (s, 3H), 2.70 (s, 3H). ^{13}C NMR (125 MHz, CDCl$_3$) δ 165.91, 157.01, 156.82, 153.27, 152.10, 148.09, 144.18, 141.35, 133.53, 132.00, 129.70, 129.59, 123.29, 118.95, 118.79, 113.33, 112.41, 110.37, 110.19, 52.59, 49.88, 16.12.
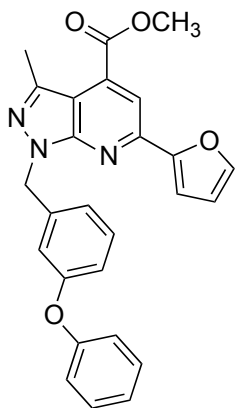
Methyl 6-(furan-2-yl)-3-methyl-1-(3-phenoxybenzyl)-1*H*-pyrazolo[3,4-*b*]pyridine-4-carboxylate (41). Synthesized using the procedure for **35** except **28** was used as the pyrazole amine. Crude was subjected to flash column chromatography on silica gel to provide the title compound (563 mg, 82%) as a yellow viscous oil. ^{1}H NMR (400 MHz, CDCl$_3$) δ 8.01 (s, 1H), 7.58 (s, 1H), 7.30-7.20 (m, 3H), 7.18-7.14 (m, 1H), 7.09-7.02 (m, 2H), 7.00 (s, 1H), 6.97-6.92 (m, 2H), 6.89-6.83 (m, 1H), 6.57 (s, 1H), 5.65 (s, 2H), 4.03 (s, 3H), 2.69 (s, 3H). ^{13}C NMR (100

MHz, CDCl₃) δ 165.89, 157.48, 156.78, 153.17, 152.21, 148.11, 147.73, 144.13, 141.47, 139.13, 133.52, 129.84, 129.66, 123.32, 122.47, 119.03, 118.18, 117.69, 113.36, 112.40, 110.42, 52.59, 50.11, 16.11. ESI MS: m/z 440.1 (M+H)$^{+}$.
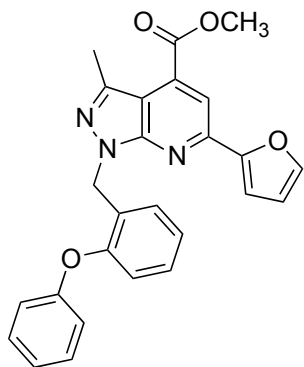

Methyl 6-(furan-2-yl)-3-methyl-1-(2-phenoxybenzyl)-1*H*-pyrazolo[3,4-*b*]pyridine-4-carboxylate (42). Synthesized using the procedure for **35** except **29** was used as the pyrazole amine. Crude was subjected to flash column chromatography on silica gel to provide the title compound (551 mg, 81%) as a yellow oil which formed a foam upon standing. ¹H NMR (500 MHz, CDCl₃) δ 7.98 (s, 1H), 7.57 (s, 1H), 7.27-7.18 (m, 3H), 7.13-7.10 (m, 1H), 7.09-7.05 (m, 1H), 7.05-6.99 (m, 2H), 6.90 (t, *J* = 7.1 Hz, 3H), 6.56-6.53 (m, 1H), 5.80 (s, 2H), 4.03 (s, 3H), 2.66 (s, 3H). ¹³C NMR (125 MHz, CDCl₃) δ 165.95, 157.40, 154.05, 153.25, 152.40, 147.97, 144.01, 141.35, 133.34, 129.48, 129.39, 128.98, 128.84, 123.88, 122.70, 119.32, 117.90, 113.19, 112.32, 110.35, 109.99, 52.53, 45.19, 16.09.

Methyl 6-(furan-2-yl)-3-methyl-1-(4-(pyridin-4-yl)benzyl)-1*H*-pyrazolo[3,4-*b*]pyridine-4-carboxylate (43). Synthesized using the procedure for **35** except **30** was used as the pyrazole amine. Crude was subjected to flash column chromatography on silica gel to provide the title compound (261 mg, 62%) as an off-white solid. ¹H NMR (500 MHz, CDCl₃) δ 8.64-8.58 (m, 2H), 8.03 (s, 1H), 7.60 (s, 1H), 7.55 (d, *J* = 7.8 Hz, 2H), 7.46 (d, *J* = 7.8 Hz, 2H), 7.45-7.40 (m,

2H), 7.27-7.22 (m, 1H), 6.58 (s, 1H), 5.73 (s, 2H), 4.03 (s, 3H), 2.69 (s, 3H). ^{13}C NMR (125 MHz, CDCl$_3$) δ 165.84, 153.21, 152.25, 150.19, 148.18, 147.87, 144.21, 141.62, 138.19, 137.46, 133.62, 128.70, 127.21, 121.49, 113.42, 112.40, 110.42, 110.21, 52.59, 50.00, 16.10.

Methyl 6-(furan-2-yl)-1-(4-methoxybenzyl)-3-methyl-1H-pyrazolo[3,4-b]pyridine-4-carboxylate (44). Synthesized using the procedure for **35** except **31** was used as the pyrazole amine. Crude was subjected to flash column chromatography on silica gel to provide the title compound (458 mg, 40%) as a light yellow solid. ^{1}H NMR (400 MHz, CDCl$_3$) δ 8.00 (s, 1H), 7.59 (s, 1H), 7.33 (d, J = 7.1 Hz, 2H), 7.27- 7.20 (m, 1H), 6.81 (d, J = 7.1 Hz, 2H), 6.62-6.55 (m, 1H), 5.61 (s, 2H), 4.01 (s, 3H), 3.74 (s, 3H), 2.67 (s, 3H). ^{13}C NMR (100 MHz, CDCl$_3$) δ 165.94, 159.07, 153.31, 152.01, 147.98, 144.10, 141.16, 133.43, 129.45, 129.37, 113.89, 113.22, 112.38, 110.26, 110.17, 55.21, 52.56, 49.93, 16.11.
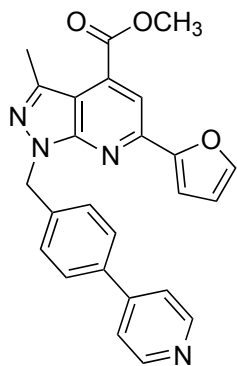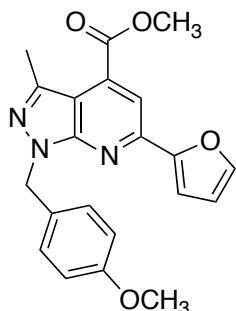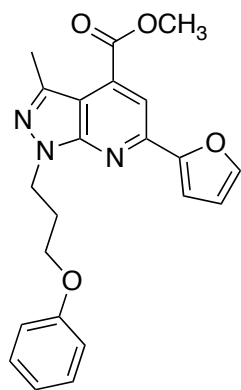

Methyl 6-(furan-2-yl)-3-methyl-1-(3-phenoxypropyl)-1H-pyrazolo[3,4-b]pyridine-4-carboxylate (45). Synthesized using the procedure for **35** except **32** was used as the pyrazole amine. Crude was subjected to flash column chromatography on silica gel to provide the title compound (388 mg, 35%) as an off-white solid. ^{1}H NMR (500 MHz, CDCl$_3$) δ 7.99 (s, 1H), 7.58 (s, 1H), 7.27-7.21 (m, 2H), 7.10 (s, 1H), 6.91 (t, J = 6.9 Hz, 1H), 6.87 (d, J = 8.7 Hz, 2H), 6.55 (dd, J = 3.3, 1.7 Hz, 1H), 4.72 (t, J = 6.8 Hz, 2H), 4.04 (s, 3H), 4.03-4.01 (m, 2H), 2.70 (s, 3H), 2.45 (p, J = 6.4 Hz, 2H). ^{13}C NMR (125 MHz, CDCl$_3$) δ 165.96, 158.82, 153.18, 152.21, 147.93,

144.06, 140.90, 133.39, 129.34, 120.62, 114.52, 113.21, 112.36, 110.29, 110.02, 65.08, 52.57, 43.83, 29.58, 16.06.

Methyl 3,6-dimethyl-1-phenyl-1*H*-pyrazolo[3,4-*b*]pyridine-4-carboxylate (46). Synthesized using the procedure for **35** except **21** and **23** were used as the starting materials. Crude was subjected to flash column chromatography on silica gel to provide the title compound (309 mg, 36%) as a light yellow solid. ^{1}H NMR (400 MHz, CDCl$_3$) δ 8.23 (d, *J* = 7.6 Hz, 2H), 7.53-7.46 (m, 3H), 7.31-7.24 (m, 1H), 4.01 (s, 3H), 2.74 (s, 3H), 2.72 (s, 3H). ^{13}C NMR (100 MHz, CDCl$_3$) δ 166.04, 158.80, 151.85, 142.31, 139.23, 132.97, 128.94, 125.77, 121.38, 118.13, 111.10, 52.56, 24.91, 16.15.

Methyl 1,3,6-trimethyl-1*H*-pyrazolo[3,4-*b*]pyridine-4-carboxylate (47). Synthesized using the procedure for **35** except **21** and **24** were used as the starting materials. Crude was subjected to flash column chromatography on silica gel to provide the title compound (266 mg, 40%) as a white solid. ^{1}H NMR (400 MHz, CDCl$_3$) δ 7.41 (s, 1H), 4.06 (s, 3H), 3.99 (s, 3H), 2.68 (s, 3H), 2.65 (s, 3H). ^{13}C NMR (100 MHz, CDCl$_3$) δ 166.20, 158.21, 152.29, 140.27, 132.69, 117.38, 109.19, 52.44, 33.61, 24.70, 15.96.

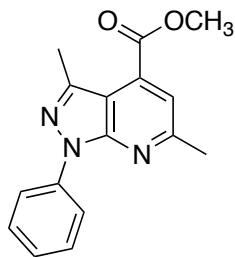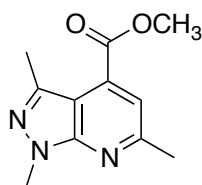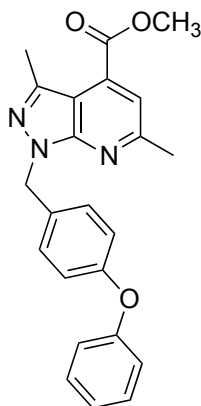**Methyl 3,6-dimethyl-1-(4-phenoxybenzyl)-1*H*-pyrazolo[3,4-*b*]pyridine-4-carboxylate (48).** Synthesized using the procedure for **35** except **20** and **27** were used as starting materials. Crude was subjected to flash column chromatography on silica gel to provide the title compound (67 mg, 12%) as a yellow oil. ^{1}H NMR (500 MHz, CDCl$_3$) δ 7.45 (s, 1H), 7.33-7.28 (m, 4H), 7.08 (t, *J* = 7.4 Hz, 1H), 6.98 (d, *J* = 7.7 Hz, 2H), 6.92 (d, *J* = 7.3 Hz, 2H), 5.63 (s, 2H), 4.01 (s, 3H), 2.71 (s, 3H), 2.68 (s, 3H). ^{13}C NMR (125 MHz, CDCl$_3$) δ 166.21, 158.43, 157.06, 156.71, 152.26, 140.98, 132.78, 132.14, 129.68, 129.35, 123.25, 118.91, 118.79, 117.65, 109.33, 52.45, 49.62, 24.77, 16.08.
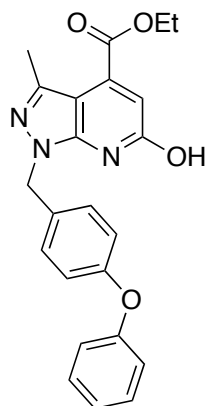
Ethyl 6-hydroxy-3-methyl-1-(4-phenoxybenzyl)-1*H*-pyrazolo[3,4-*b*]pyridine-4-carboxylate (49).[18] A solution of diethyl oxaloacetate sodium salt (516 mg, 2.46 mmol) and **28** (646 mg, 2.31 mmol) in a mixture of toluene: H$_2$O: glacial AcOH (5 mL/5 mL/0.5 mL) was heated at 80 °C overnight. The mixture was diluted with H$_2$O (20 mL) and extracted with EtOAc (20 mL x 2). Combined organic layers were washed with brine, dried (Na$_2$SO$_4$), filtered and concentrated under reduced pressure to provide the desired crude. Crude was used in the next reaction without further purification.

A suspension of diethyl 2-(5-amino-3-methyl-1-(4-phenoxybenzyl)-1*H*-pyrazol-4-yl)-2-hydroxysuccinate (crude from above) (2.31 mmol) from x in glacial AcOH (14 mL) was refluxed for 2 h. The mixture was concentrated under reduced pressure as much as possible. Then MeOH was added and the product crystallized as a white solid which was filtered, washed with cold MeOH and dried in a vacuum oven to provide the title compound (628 mg, 67% over two steps) as a tan solid. ^{1}H NMR (500 MHz, CDCl$_3$) δ 7.40 (d, *J* = 8.3 Hz, 2H), 7.31 (t, *J* = 7.3 Hz, 2H), 7.09 (t, *J* = 7.4 Hz, 1H), 6.97 (d, *J* = 8.0 Hz, 2H), 6.92 (d, *J* = 8.4 Hz, 2H), 6.78 (s, 1H), 5.50 (s, 2H), 4.44 (q, *J* = 7.1 Hz, 2H), 2.53 (s, 3H), 1.43 (t, *J* = 7.1 Hz, 3H). ^{13}C NMR (125 MHz, CDCl$_3$) δ 164.83, 164.75, 157.17, 156.81, 143.45, 143.12, 139.06, 130.59, 129.72, 129.51, 123.43, 119.11, 118.70, 113.27, 103.16, 62.13, 50.60, 15.44, 14.16. ESI MS: m/z 404.1 (M+H)$^+$.
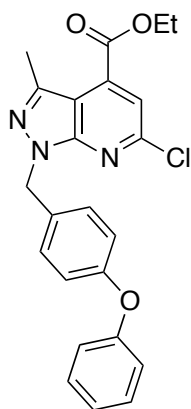
Ethyl 6-chloro-3-methyl-1-(4-phenoxybenzyl)-1*H*-pyrazolo[3,4-*b*]pyridine-4-carboxylate (50).[19] Fresh Vilsmeier's reagent was prepared as follows: to a stirring solution of 1,2 DCE (4 mL) was added DMF (0.2 mL, 2.6 mmol). The resulting solution was cooled down to 0 oC and (COCl)$_2$ (0.22 mL, 2.6 mmol) was added dropwise. The viscous suspension was stirred at room temperature for 10 min, and then **49** (104 mg, 0.26 mmol) was added to the mixture. The suspension was heated to reflux overnight. The mixture was diluted with H$_2$O (10 mL) and extracted with EtOAc (15mL x 2). The organic layers were washed with brine, dried (Na$_2$SO$_4$) and concentrated under reduced pressure to provide the title compound (120 mg, quantitative yield) as a yellow oil. Crude was used in the next reaction without further purification. ^{1}H NMR (500 MHz, CDCl$_3$) δ 7.56 (s, 1H), 7.31 (t, *J* = 8.2 Hz, 4H), 7.08 (t, *J* = 7.4 Hz, 1H), 6.97 (d, *J* = 7.7 Hz, 2H), 6.93 (d, *J* = 8.5 Hz, 2H), 5.59 (s, 2H), 4.48 (q, *J* = 7.1 Hz, 2H), 2.69 (s, 3H), 1.46 (t, *J* = 7.1 Hz, 3H). ^{13}C NMR (125 MHz, CDCl$_3$) δ 164.34, 157.00, 156.91, 151.20, 150.30, 141.77,

135.67, 131.25, 129.71, 129.54, 123.37, 119.00, 118.78, 117.69, 110.41, 62.31, 50.03, 16.16, 14.20.
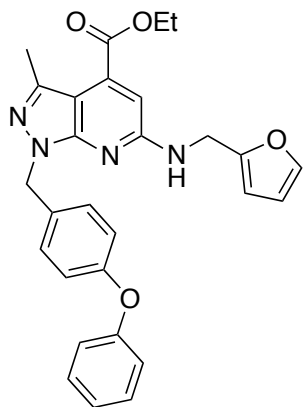
Ethyl 6-((furan-2-ylmethyl)amino)-3-methyl-1-(4-phenoxybenzyl)-1*H*-pyrazolo[3,4-*b*]pyridine-4-carboxylate (51).[23] A pressure vessel was charged with **50** (119 mg, 0.28 mmol), 2-aminomethylfuran (0.12 mL, 1. 36 mmol) and iPrOH (4mL). The vessel was sealed and the reaction mixture was heated at 100 °C overnight. An additional 1 mL (11.3 mmol) of amine was added and the mixture was heated at 150 °C overnight. The reaction mixture was diluted with H_2O (10 mL) and extracted with EtOAc (15 mL x 2). Combined organic layers were washed with brine, dried (Na_2SO_4) and concentrated under reduced pressure. Crude was subjected to flash column chromatography on silica gel to provide the title compound (40 mg, 30%) as an orange oil. ^{1}H NMR (400 MHz, CDCl$_3$) δ 7.36-7.24 (m, 5H), 7.07 (t, *J* = 7.3 Hz, 1H), 6.97 (d, *J* = 8.2 Hz, 2H), 6.91 (d, *J* = 8.2 Hz, 2H), 6.80 (s, 1H), 6.30 (s, 1H), 6.22 (s, 1H), 5.47 (s, 2H), 5.14 (t, *J* = 5.4 Hz, 1H), 4.68 (d, *J* = 5.5 Hz, 2H), 4.43 (q, *J* = 7.1 Hz, 2H), 2.58 (s, 3H), 1.42 (t, *J* = 7.1 Hz, 3H). ^{13}C NMR (100 MHz, CDCl$_3$) δ 165.83, 157.16, 156.86, 156.51, 152.16, 152.06, 141.97, 141.27, 134.71, 132.57, 129.67, 129.44, 123.17, 118.82, 110.40, 107.27, 106.91, 104.45, 61.66, 49.53, 38.75, 16.15, 14.23. ESI MS: m/z 483.1 (M+H)$^+$.
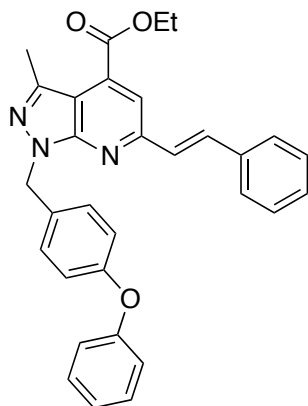
(*E*)-Ethyl 3-methyl-1-(4-phenoxybenzyl)-6-styryl-1*H*-pyrazolo[3,4-*b*]pyridine-4-carboxylate (52).[20, 21] To a mixture of **50** (205 mg, 0.49 mmol), Pd(PPh$_3$)$_4$ (27 mg, 0.02 mmol) and (E)-2-phenylvinylboronic acid (112 mg, 0.74 mmol) in 1,4-dioxane: H$_2$O (3mL/2mL) was added Na$_2$CO$_3$ (153 mg, 1.45 mmol), followed by stirring at 90 °C overnight. To the reaction mixture was added H$_2$O (10 mL) and the aqueous layer was extracted with EtOAc (10 mL x 2). The combined organic layer was washed with brine, dried (Na$_2$SO$_4$), filtered and concentrated under reduced pressure. Crude was subjected to flash column chromatography on silica gel to provide the title compound (216 mg, 90%) as a light yellow oil which solidified upon standing. ^{1}H NMR (500 MHz, CDCl$_3$) δ 7.80 (d, *J* = 16.1 Hz, 1H), 7.74 (s, 1H), 7.63 (d, *J* = 7.6 Hz, 2H), 7.41 (t, *J* = 7.6 Hz, 2H), 7.39-7.33 (m, 3H), 7.30 (t, *J* = 7.7 Hz, 3H), 7.07 (t, *J* = 7.4 Hz, 1H), 6.98 (d, *J* = 8.6 Hz, 2H), 6.95 (d, *J* = 8.3 Hz, 2H), 5.69 (s, 2H), 4.51 (q, *J* = 7.1 Hz, 2H), 2.71 (s, 3H), 1.49 (t, *J* = 7.0 Hz, 3H). ^{13}C NMR (125 MHz, CDCl$_3$) δ 165.76, 157.04, 156.79, 154.93, 152.39, 141.19, 136.28, 134.74, 133.60, 132.13, 129.69, 129.50, 128.81, 127.69, 127.33, 123.28, 118.94, 118.82, 116.48, 110.28, 61.93, 49.80, 16.30, 14.30.
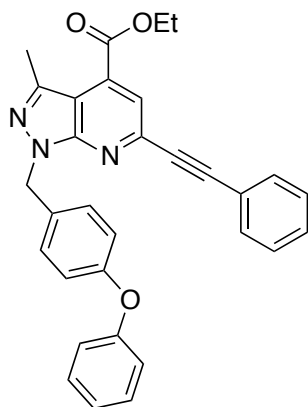
Ethyl 3-methyl-1-(4-phenoxybenzyl)-6-(phenylethynyl)-1*H*-pyrazolo[3,4-*b*]pyridine-4-carboxylate (53).[22] A mixture of **50** (95 mg, 0.22 mmol), Pd(PPh$_3$)$_2$Cl$_2$ (16 mg, 0.02 mmol), and CuI (8.6 mg, 0.04 mmol) in Et$_3$N (0.5 mL) and dry THF (1 mL) was added dropwise to a solution of phenylacetylene (40 µL, 0.36 mmol) in Et$_3$N (0.5 mL) under nitrogen at room temperature. Reaction mixture was heated to 60°C and stirred overnight then diluted with EtOAc (10 mL) and washed with saturated aqueous NH$_4$Cl (15 mL x 2) and brine (15 mL). The organic layer was dried (Na$_2$SO$_4$), filtered, concentrated under reduced pressure. The crude was purified by flash column chromatography on silica gel to give the title compound (33 mg, 31%) as an orange oil. ^{1}H NMR (500 MHz, CDCl$_3$) δ 7.81 (s, 1H), 7.68-7.63 (m, 2H), 7.42-7.37 (m, 3H), 7.35-7.29 (m, 4H), 7.08 (t, *J* = 7.6 Hz, 1H), 6.97 (d, *J* = 8.4 Hz, 2H), 6.93 (d, *J* = 8.4 Hz, 2H), 5.68 (s, 2H), 4.50 (q, *J* = 7.1 Hz, 2H), 2.72 (s, 3H), 1.47 (t, *J* = 7.1 Hz, 3H). ^{13}C NMR (125 MHz, CDCl$_3$) δ 165.08, 157.02, 156.83, 152.00, 141.84, 141.44, 133.56, 132.20, 131.77, 129.69, 129.47, 129.36, 128.45, 123.28, 121.86, 121.06, 118.94, 118.81, 110.56, 90.88, 88.87, 62.09, 49.81, 16.24, 14.26.
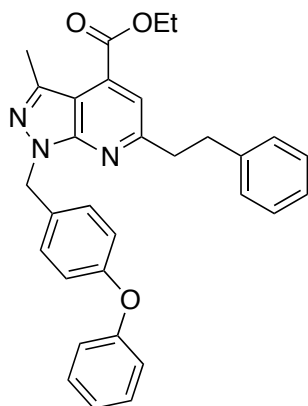
Ethyl 3-methyl-6-phenethyl-1-(4-phenoxybenzyl)-1*H*-pyrazolo[3,4-*b*]pyridine-4-carboxylate (54).[23] To a suspension of 10% Pd/C (70 mg) in EtOH (5 mL) was added **52** (186 mg, 0.38 mmol) dissolved in THF (1.5 mL). The suspension was stirred under an atmosphere of hydrogen (ca. 1 atm, balloon) overnight. The suspension was filtered through a pad of celite and the filtrate was concentrated under reduced pressure to provide the title compound (159 mg, 84%) as a light brown oil. Crude was used in the next reaction without further purification. ^{1}H NMR (500 MHz, CDCl$_3$) δ 7.44 (s, 1H), 7.36-7.31 (m, 3H), 7.31-7.26 (m, 3H), 7.26-7.22 (m, 2H), 7.19 (t, *J* = 7.0 Hz, 1H), 7.09 (t, *J* = 7.4 Hz, 1H), 7.00 (d, *J* = 7.9 Hz, 2H), 6.95 (d, *J* = 8.5 Hz, 2H), 5.67 (s, 2H), 4.49 (q, *J* = 7.1 Hz, 2H), 3.35-3.27 (m, 2H), 3.24-3.17 (m, 2H), 2.73 (s, 3H), 1.47 (t, *J* = 7.1 Hz,

3H). ^{13}C NMR (125 MHz, CDCl$_3$) δ 165.85, 161.09, 157.08, 156.78, 152.23, 141.30, 140.97, 133.36, 132.21, 129.72, 129.55, 128.49, 128.41, 126.04, 123.30, 118.95, 118.80, 117.33, 109.68, 61.83, 49.83, 39.82, 35.23, 16.31, 14.30. ESI MS: m/z 516.9 (M+H)$^+$.
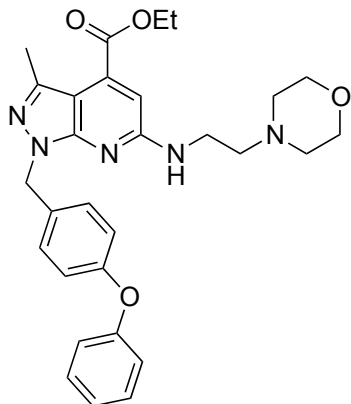

Ethyl 3-methyl-6-((2-morpholinoethyl)amino)-1-(4-phenoxybenzyl)-1*H*-pyrazolo[3,4-*b*]pyridine-4-carboxylate (55).[23] A pressure vessel was charged with **50** (121 mg, 0.29 mmol), 4-(2-aminoethyl)morpholine (1.0 mL, 7.6 mmol) and iPrOH (3 mL) and NMP (1 mL). The vessel was sealed and the reaction mixture was heated at 150 °C overnight. The reaction mixture was diluted with EtOAc (20 mL) and washed with H$_2$O (10 mL x 3) to remove NMP. Combined organic layers were washed with brine, dried (Na$_2$SO$_4$), filtered, and concentrated under reduced pressure. Crude was subjected to flash column chromatography on silica gel to provide the title compound (40 mg, 26%) as a yellow oil. ^{1}H NMR (500 MHz, CDCl$_3$) δ 7.29 (q, *J* = 7.1, 6.6 Hz, 4H), 7.07 (t, *J* = 7.1 Hz, 1H), 6.96 (d, *J* = 8.6 Hz, 2H), 6.91 (d, *J* = 8.3 Hz, 2H), 6.78 (s, 1H), 5.46 (s, 2H), 4.43 (q, *J* = 7.1 Hz, 2H), 3.76-3.70 (m, 4H), 3.55 (q, *J* = 5.0 Hz, 2H), 2.63 (t, *J* = 5.7 Hz, 2H), 2.58 (s, 3H), 2.49 (s, 4H), 1.42 (t, *J* = 7.1 Hz, 3H).^{13}C NMR (126 MHz, CDCl$_3$) δ 166.00, 157.47, 157.15, 156.51, 152.39, 141.23, 134.44, 132.67, 129.66, 129.31, 123.18, 118.83, 118.77, 107.03, 103.90, 66.92, 61.62, 57.03, 53.40, 49.37, 37.75, 16.16, 14.26.

A representative procedure for synthesis of carboxylic acids.

143
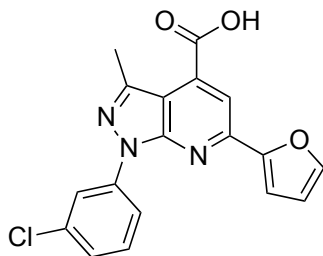
1-(3-Chlorophenyl)-6-(furan-2-yl)-3-methyl-1*H*-pyrazolo[3,4-*b*]pyridine-4-carboxylic   acid (1).[17] A solution of ester **35** (108 mg, 0.29 mmol) and KOH (29 mg, 0.52 mmol) in iPrOH (6 mL) was refluxed for 1 h 30 min. Reaction mixture was diluted with H_2O (10 mL) and washed with EtOAc (10 mL x 2). Aqueous layer was acidified with 1N HCl and extracted with EtOAc (10 mL x 2). Combined organic extracts were washed with brine, dried (Na_2SO_4), filtered, and concentrated under reduced pressure to give **1** (88 mg, 86%) as a bright yellow solid. 99% pure by HPLC. ^{1}H NMR (400 MHz, DMSO-d$_6$) δ 8.35 (s, 1H), 8.29 (d, *J* = 8.5 Hz, 1H), 7.96 (s, 1H), 7.92 (s, 1H), 7.55 (t, *J* = 8.1 Hz, 1H), 7.37-7.31 (m, 2H), 6.76-6.71 (m, 1H), 2.62 (s, 3H). ^{13}C NMR (100 MHz, DMSO-d$_6$) δ 166.48, 152.40, 151.70, 148.29, 146.21, 143.65, 140.42, 136.54, 133.86, 131.32, 125.57, 119.83, 118.66, 113.69, 113.32, 112.21, 112.10, 16.20. ESI MS: m/z 354.0 (M+H)[+].
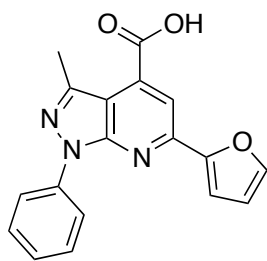
6-(Furan-2-yl)-3-methyl-1-phenyl-1*H*-pyrazolo[3,4-*b*]pyridine-4-carboxylic   acid   (2). Synthesized using the procedure for **1** except ester **36** was used as the starting material. The title compound (288 mg, 90%) was obtained as a white solid. 100% pure by HPLC. ^{1}H NMR (400 MHz, DMSO-d$_6$) δ 8.26 (d, *J* = 7.7 Hz, 2H), 7.95 (s, 2H), 7.55 (t, *J* = 7.5 Hz, 2H), 7.39 (s, 1H), 7.32 (t, *J* = 7.4 Hz, 1H), 6.73 (s, 1H), 2.65 (s, 3H). ^{13}C NMR (100 MHz, DMSO-d$_6$) δ 166.68, 152.54, 151.60, 148.24, 146.07, 142.86, 139.27, 136.37, 129.60, 126.17, 120.94, 113.46, 113.27, 112.07, 111.82, 16.17. ESI MS: m/z 320.1 (M+H)[+].
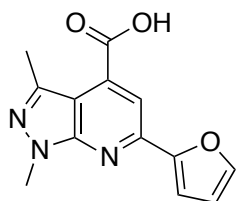
6-(Furan-2-yl)-1,3-dimethyl-1*H*-pyrazolo[3,4-*b*]pyridine-4-carboxylic acid (3). Synthesized using the procedure for **1** except ester **37** was used as the starting material. After the work up and acidifying the aqueous layer with 1N HCl, solid precipitated which was filtered off and dried on high vacuum to provide the title compound (203 mg, 79%) as a beige solid. 100% pure by

HPLC. ^{1}H NMR (400 MHz, DMSO-d$_6$) δ 13.91 (s, 1H), 7.91 (s, 1H), 7.85 (s, 1H), 7.33 (d, J = 2.9 Hz, 1H), 6.72-6.67 (m, 1H), 3.98 (s, 3H), 2.55 (s, 3H). ^{13}C NMR (100 MHz, DMSO-d$_6$) δ 166.91, 152.73, 152.00, 147.61, 145.67, 140.08, 135.59, 113.13, 112.56, 111.40, 109.74, 33.82, 15.92. ESI MS: m/z 258.0 (M+H)$^+$.

3,6-Dimethyl-1-phenyl-1H-pyrazolo[3,4-b]pyridine-4-carboxylic acid (4). Synthesized using the procedure for **1** except ester **46** was used as the starting material. After the work up and acidifying the aqueous layer with 1N HCl, solid precipitated which was filtered off and dried on high vacuum to provide the title compound (165 mg, 81%) as a light yellow solid. 100% pure by HPLC. ^{1}H NMR (400 MHz, DMSO-d$_6$) δ 13.90 (s, 1H), 8.19 (d, J = 7.7 Hz, 2H), 7.56-7.48 (m, 3H), 7.29 (t, J = 7.3 Hz, 1H), 2.65 (s, 3H), 2.63 (s, 3H). ^{13}C NMR (100 MHz, DMSO-d$_6$) δ 167.04, 159.52, 151.67, 142.43, 139.35, 135.32, 129.49, 126.12, 121.13, 118.29, 111.04, 24.92, 16.12. ESI MS: m/z 268.1 (M+H)$^+$.

1,3,6-Trimethyl-1H-pyrazolo[3,4-b]pyridine-4-carboxylic acid (12). Synthesized using the procedure for **1** except ester **47** was used as the starting material. The title compound (157 mg, 84%) was obtained as a white solid. 95% pure by HPLC. ^{1}H NMR (400 MHz, DMSO-d$_6$) δ 7.37 (s, 1H), 3.92 (s, 3H), 2.60 (s, 3H), 2.53 (s, 3H). ^{13}C NMR (100 MHz, CDCl$_3$) δ 167.25, 158.47, 152.04, 139.56, 134.57, 117.22, 108.94, 33.73, 24.66, 15.89. ESI MS: m/z 206.1 (M+H)$^+$.
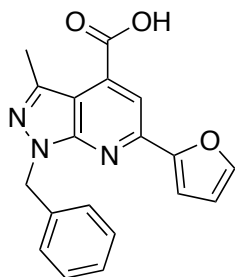
1-Benzyl-6-(furan-2-yl)-3-methyl-1*H*-pyrazolo[3,4-*b*]pyridine-4-carboxylic acid (6). Synthesized using the procedure for **1** except ester **38** was used as the starting material. The title compound (67 mg, quantitative yield) was obtained as a light yellow solid. 100% pure by HPLC. ^{1}H NMR (500 MHz, DMSO-d$_6$) δ 8.08-8.03 (m, 1H), 8.03-7.98 (m, 1H), 7.43 (s, 1H), 7.33-7.27 (m, 2H), 7.27-7.20 (m, 3H), 6.78 (s, 1H), 5.67 (s, 2H), 2.65 (s, 3H). ^{13}C NMR (125 MHz, DMSO-d$_6$) δ 166.49, 151.92, 150.08, 147.52, 146.28, 140.99, 137.81, 133.82, 128.98, 127.93, 113.74, 113.56, 113.34, 110.95, 50.03, 16.86. ESI MS: m/z 334.2 (M+H)$^+$.
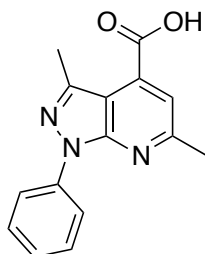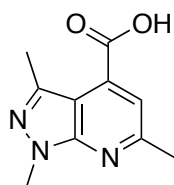

1-([1,1'-Biphenyl]-4-ylmethyl)-6-(furan-2-yl)-3-methyl-1*H*-pyrazolo[3,4-*b*]pyridine-4-carboxylic acid (7). Synthesized using the procedure for **1** except ester **39** was used as the starting material. The title compound (58 mg, 87%) was obtained as a light yellow solid. 100% pure by HPLC. ^{1}H NMR (500 MHz, DMSO-d$_6$) δ 13.47 (s, 1H), 8.04 (d, *J* = 16.4 Hz, 1H), 7.59 (d, *J* = 7.4 Hz, 5H), 7.45-7.39 (m, 3H), 7.33 (d, *J* = 7.6 Hz, 3H), 6.78 (s, 1H), 5.72 (s, 2H), 2.67 (s, 3H). ^{13}C NMR (125 MHz, DMSO-d$_6$) δ 166.48, 151.95, 150.09, 147.53, 146.30, 141.05, 140.19, 139.91, 136.98, 133.86, 129.34, 128.57, 127.89, 127.35, 127.07, 113.77, 113.60, 113.35, 111.00, 49.75, 16.89. ESI MS: m/z 410.2 (M+H)$^+$.

6-(Furan-2-yl)-3-methyl-1-(4-phenoxybenzyl)-1*H*-pyrazolo[3,4-*b*]pyridine-4-carboxylic acid (8). Synthesized using the procedure for **1** except ester **40** was used as the starting material. The title compound (63 mg, 43%) was obtained as an orange solid. 99% pure by HPLC. ^{1}H NMR (500 MHz, DMSO-d$_6$) δ 7.94 (s, 1H), 7.91 (s, 1H), 7.40 (d, *J* = 3.4 Hz, 1H), 7.34 (t, *J* = 7.8 Hz, 2H), 7.31 (d, *J* = 8.4 Hz, 2H), 7.10 (t, *J* = 7.2 Hz, 1H), 6.95 (t, *J* = 8.1 Hz, 4H), 6.74-6.71 (m, 1H), 5.61 (s, 2H), 2.59 (s, 3H). ^{13}C NMR (125 MHz, DMSO-d$_6$) δ 166.87, 156.95, 156.51, 152.71, 151.97, 147.92, 145.83, 140.95, 135.93, 132.85, 130.46, 129.94, 123.92, 119.10, 119.04, 113.21, 112.86, 111.69, 109.96, 49.50, 16.04. ESI MS: m/z 426.0 (M+H)$^+$.
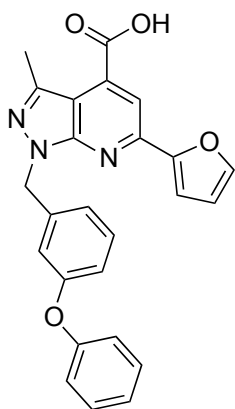
6-(Furan-2-yl)-3-methyl-1-(3-phenoxybenzyl)-1*H*-pyrazolo[3,4-*b*]pyridine-4-carboxylic acid (9). Synthesized using the procedure for **1** except ester **41** was used as the starting material. The title compound (84 mg, 86%) was obtained as a light orange solid. 99% pure by HPLC. ^{1}H NMR (500 MHz, DMSO-d$_6$) δ 7.91 (s, 1H), 7.89 (s, 1H), 7.33-7.26 (m, 4H), 7.09 (t, *J* = 7.4 Hz, 1H), 6.97 (d, *J* = 7.6 Hz, 1H), 6.93 (d, *J* = 8.3 Hz, 2H), 6.88 (s, 1H), 6.85 (d, *J* = 9.8 Hz, 1H), 6.72-6.69 (m, 1H), 5.60 (s, 2H), 2.56 (s, 3H). ^{13}C NMR (125 MHz, DMSO-d$_6$) δ 166.83, 157.39, 156.47, 152.64, 152.08, 147.91, 145.80, 141.07, 140.01, 135.92, 130.63, 130.41, 124.11, 122.72, 119.34, 117.73, 117.65, 113.17, 112.89, 111.65, 109.95, 49.77, 16.01. ESI MS: m/z 426.2 (M+H)$^+$.
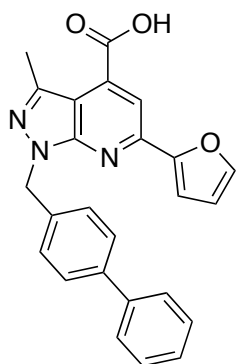
6-(Furan-2-yl)-3-methyl-1-(2-phenoxybenzyl)-1*H*-pyrazolo[3,4-*b*]pyridine-4-carboxylic acid (10). Synthesized using the procedure for **1** except ester **42** was used as the starting material. The title compound (86 mg, quantitative yield) was obtained as a yellow oil which solidified upon standing. 100% pure by HPLC. ^{1}H NMR (500 MHz, DMSO-d$_6$) δ 13.88 (s, 1H), 7.90 (s, 1H), 7.84 (s, 1H), 7.31-7.20 (m, 4H), 7.11-7.06 (m, 2H), 7.01 (t, *J* = 7.4 Hz, 1H), 6.89 (d, *J* = 8.0 Hz, 1H), 6.80 (d, *J* = 7.7 Hz, 2H), 6.70-6.66 (m, 1H), 5.65 (s, 2H), 2.53 (s, 3H). ^{13}C NMR (125 MHz, DMSO-d$_6$) δ 166.84, 157.37, 153.97, 152.72, 152.16, 147.73, 145.69, 140.97, 135.69, 130.19, 130.12, 129.76, 129.16, 124.60, 123.28, 119.94, 117.86, 113.11, 112.76, 111.43, 109.86, 45.04, 16.02. ESI MS: m/z 426.1 (M+H)$^+$.
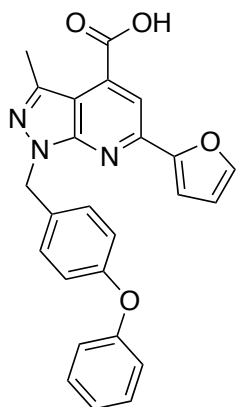

6-(Furan-2-yl)-3-methyl-1-(4-(pyridin-4-yl)benzyl)-1*H*-pyrazolo[3,4-*b*]pyridine-4-carboxylic acid (11). Synthesized using the procedure for **1** except ester **43** was used as the starting material. The title compound (31 mg, 32%) was obtained as an off-white solid. ^{1}H NMR (400 MHz, DMSO-d$_6$) δ 8.68 (d, *J* = 5.8 Hz, 2H), 7.94 (s, 1H), 7.92 (s, 1H), 7.85-7.80 (m, 3H), 7.79 (s, 1H), 7.42 (s, 1H), 7.40 (s, 2H), 6.74-6.70 (m, 1H), 5.71 (s, 2H), 2.59 (s, 3H). ^{13}C NMR (100 MHz, DMSO-d$_6$) δ 166.85, 152.65, 152.12, 149.44, 148.39, 147.99, 145.89, 141.18, 139.74, 136.00, 128.91, 127.90, 122.31, 113.22, 112.97, 111.79, 109.99, 49.69, 16.06. ESI MS: m/z 411.1 (M+H)$^+$.

148

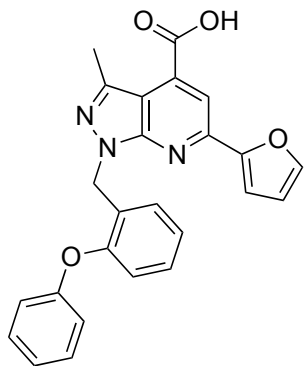**6-(Furan-2-yl)-1-(4-methoxybenzyl)-3-methyl-1*H*-pyrazolo[3,4-*b*]pyridine-4-carboxylic acid (12).** Synthesized using the procedure for **1** except ester **44** was used as the starting material. The title compound (158 mg, 99%) was obtained as an off-white solid. 100% pure by HPLC. ^{1}H NMR (500 MHz, DMSO-d$_6$) δ 13.92 (s, 1H), 7.94 (s, 1H), 7.88 (s, 1H), 7.39 (s, 1H), 7.24 (d, *J* = 6.9 Hz, 2H), 6.85 (d, *J* = 6.8 Hz, 2H), 6.72 (s, 1H), 5.54 (s, 2H), 3.68 (s, 3H), 2.57 (s, 3H). ^{13}C NMR (125 MHz, DMSO-d$_6$) δ 166.90, 159.13, 152.77, 151.87, 147.81, 145.78, 140.74, 135.94, 129.79, 129.59, 114.35, 113.19, 112.74, 111.58, 109.96, 55.49, 49.63, 16.01. ESI MS: m/z 364.2 (M+H)$^+$.
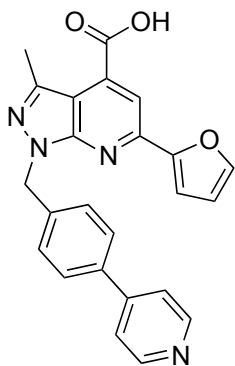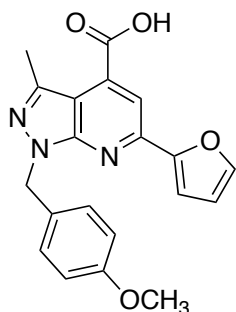

6-(Furan-2-yl)-3-methyl-1-(3-phenoxypropyl)-1*H*-pyrazolo[3,4-*b*]pyridine-4-carboxylic acid (13). Synthesized using the procedure for **1** except ester **45** was used as the starting material. The title compound (122 mg, 81%) was obtained as a yellow solid. 99% pure by HPLC. ^{1}H NMR (400 MHz, DMSO-d$_6$) δ 13.91 (s, 1H), 7.90 (s, 1H), 7.84 (s, 1H), 7.25-7.16 (m, 3H), 6.90-6.81 (m, 3H), 6.70-6.63 (m, 1H), 4.58 (t, *J* = 6.4 Hz, 2H), 3.97 (t, *J* = 5.2 Hz, 2H), 2.57 (s, 3H), 2.35-2.24 (m, 2H). ^{13}C NMR (101 DMSO-d$_6$) δ 166.93, 158.83, 152.70, 152.02, 147.61, 145.64, 140.43, 135.68, 129.81, 120.92, 114.83, 113.10, 112.66, 111.37, 109.87, 65.17, 43.71, 29.32, 16.04. ESI MS: m/z 378.2 (M+H)$^+$.
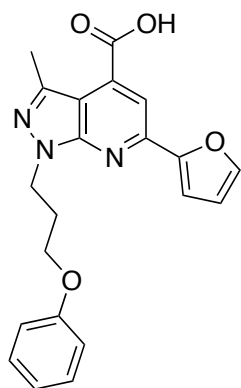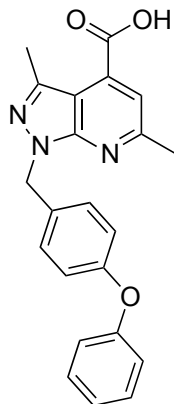
3,6-Dimethyl-1-(4-phenoxybenzyl)-1*H*-pyrazolo[3,4-*b*]pyridine-4-carboxylic acid (14). Synthesized using the procedure for **1** except ester **48** was used as the starting material. The title compound (11 mg, 20%) was obtained as an off-white solid. 97% pure by HPLC. ^{1}H NMR (400 MHz, DMSO-d$_6$) δ 7.42 (s, 1H), 7.34 (t, *J* = 7.6 Hz, 2H), 7.22 (d, *J* = 8.1 Hz, 2H), 7.10 (t, *J* = 6.8 Hz, 1H), 6.98-6.88 (m, 4H), 5.55 (s, 2H), 2.63 (s, 3H), 2.55 (s, 3H). ^{13}C NMR (100 MHz, DMSO-d$_6$) δ 167.28, 158.92, 156.97, 156.39, 152.02, 140.48, 133.05, 130.46, 129.66, 123.90, 119.09, 119.00, 117.53, 109.99, 109.14, 49.25, 24.80, 15.98. ESI MS: m/z 374.0 (M+H)[+].

6-((Furan-2-ylmethyl)amino)-3-methyl-1-(4-phenoxybenzyl)-1*H*-pyrazolo[3,4-*b*]pyridine-4-carboxylic acid (15).[18] A solution of ester **51** (40 mg, 0.08 mmol) and 1N NaOH (3.5 mL, 3.5 mmol) in THF (1.5 mL) was refluxed for 3 h. Reaction mixture was diluted with water (10 mL) and washed with EtOAc (10 mL x 2). Aqueous layer was acidified with 1N HCl and extracted with EtOAc (10 mL x 2). Combined organic extracts were washed with brine, dried (Na$_2$SO$_4$) and filtered. The solvent was removed under reduced pressure to give the title compound (22 mg, 61%) as an orange solid. 99% pure by HPLC. ^{1}H NMR (500 MHz, DMSO-d$_6$) δ 7.79 (t, *J* = 5.1 Hz, 1H), 7.54 (s, 1H), 7.34 (t, *J* = 7.6 Hz, 2H), 7.27 (d, *J* = 8.1 Hz, 2H), 7.10 (t, *J* = 6.8 Hz, 1H),

6.95 (d, *J* = 7.9 Hz, 2H), 6.90 (d, *J* = 8.3 Hz, 2H), 6.86 (s, 1H), 6.33 (s, 1H), 6.25 (s, 1H), 5.35 (s, 2H), 4.57 (d, *J* = 5.2 Hz, 2H), 2.41 (s, 3H). ^{13}C NMR (125 MHz, DMSO-d$_6$) δ 167.35, 157.85, 157.05, 156.29, 153.26, 152.02, 142.37, 140.38, 135.41, 133.48, 130.46, 130.44, 130.08, 123.85, 118.98, 118.97, 110.81, 107.38, 103.37, 49.09, 37.87, 15.96. ESI MS: m/z 455.0 (M+H)[+].

A modified procedure for synthesis of carboxylic acids.
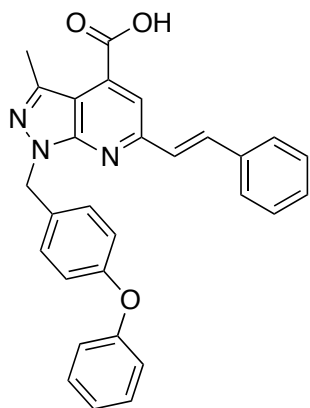
(*E*)-3-methyl-1-(4-phenoxybenzyl)-6-styryl-1*H*-pyrazolo[3,4-*b*]pyridine-4-carboxylic acid (16). A solution of ester **52** (56 mg, 0.11 mmol) and KOH (19 mg, 0.34 mmol) in iPrOH:THF (2 mL/ 1mL) was refluxed at 87 °C for 2 h. Reaction mixture was diluted with water (10 mL) and washed with EtOAc (10 mL x 2). Aqueous layer was acidified with 1N HCl and extracted with EtOAc (10 mL x 2). Combined organic extracts were washed with brine, dried (Na$_2$SO$_4$) and filtered. The solvent was removed under reduced pressure to give the title compound (45 mg, 94%) as a yellow solid. 88% pure by HPLC. ^{1}H NMR (500 MHz, DMSO-d$_6$) δ 13.86 (s, 1H), 7.87 (d, *J* = 16.2 Hz, 1H), 7.81 (s, 1H), 7.74 (d, *J* = 7.8 Hz, 2H), 7.52 (d, *J* = 16.2 Hz, 1H), 7.42 (t, *J* = 7.5 Hz, 2H), 7.37-7.29 (m, 5H), 7.09 (t, *J* = 7.4 Hz, 1H), 6.98-6.92 (m, 4H), 5.64 (s, 2H), 2.58 (s, 3H). ^{13}C NMR (125 MHz, DMSO-d$_6$) δ 167.16, 156.97, 156.47, 155.22, 152.20, 140.74, 136.47, 135.39, 134.92, 133.00, 130.46, 129.90, 129.30, 128.04, 127.87, 123.90, 119.11, 119.02, 116.60, 110.13, 49.41, 16.02. ESI MS: m/z 462.0 (M+H)[+].

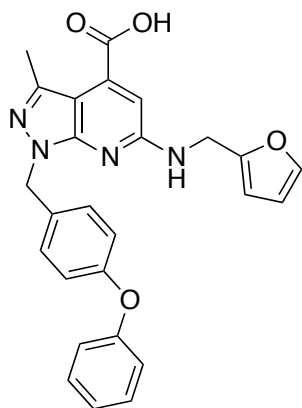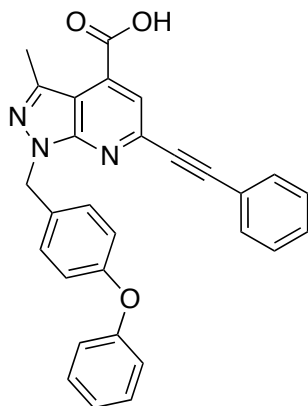**3-Methyl-1-(4-phenoxybenzyl)-6-(phenylethynyl)-1*H*-pyrazolo[3,4-*b*]pyridine-4-carboxylic acid (17).** Synthesized using the procedure for **16** except ester **53** was used as the starting material. The title compound (13 mg, 39%) was obtained as a light brown solid. 98% pure by HPLC. ^{1}H NMR (500 MHz, DMSO-d_6) δ 7.75 (s, 1H), 7.69 (d, *J* = 7.1 Hz, 2H), 7.51-7.45 (m, 3H), 7.35 (t, *J* = 7.6 Hz, 2H), 7.24 (d, *J* = 8.3 Hz, 2H), 7.10 (t, *J* = 6.9 Hz, 1H), 6.96 (t, *J* = 8.4 Hz, 4H), 5.63 (s, 2H), 2.61 (s, 3H). ^{13}C NMR (125 MHz, DMSO-d_6) δ 166.45, 156.94, 156.51, 151.85, 141.39, 141.14, 132.72, 132.43, 130.46, 130.35, 129.62, 129.37, 123.93, 121.34, 120.69, 119.13, 119.05, 110.56, 90.88, 89.26, 49.53, 15.97. ESI MS: m/z 460.0 (M+H)$^+$.
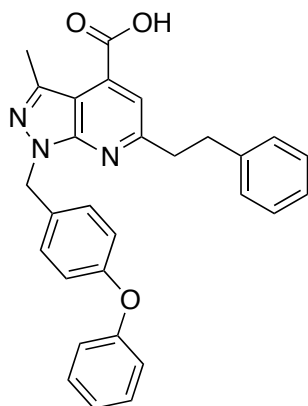
3-Methyl-6-phenethyl-1-(4-phenoxybenzyl)-1*H*-pyrazolo[3,4-*b*]pyridine-4-carboxylic   acid (18). Synthesized using the procedure for **16** except ester **54** was used as the starting material. The title compound (67 mg, 91%) was obtained as a white solid. 96% pure by HPLC. ^{1}H NMR (500 MHz, DMSO-d_6) δ 13.75 (s, 1H), 7.44 (s, 1H), 7.34 (t, *J* = 7.5 Hz, 2H), 7.24 (d, *J* = 8.0 Hz, 2H), 7.22-7.17 (m, 4H), 7.11 (t, *J* = 6.8 Hz, 2H), 6.95 (d, *J* = 8.2 Hz, 2H), 6.91 (d, *J* = 8.0 Hz, 2H), 5.57 (s, 2H), 3.24 (t, *J* = 7.6 Hz, 2H), 3.09 (t, *J* = 7.5 Hz, 2H), 2.55 (s, 3H). ^{13}C NMR (125 MHz, DMSO-d_6) δ 167.24, 161.61, 156.94, 156.49, 151.91, 141.54, 140.43, 134.92, 132.98,

130.46, 129.89, 128.85, 128.64, 126.26, 123.95, 119.08, 119.00, 117.34, 109.43, 49.45, 34.84, 15.99. ESI MS: m/z 464.1 $(M+H)^+$.
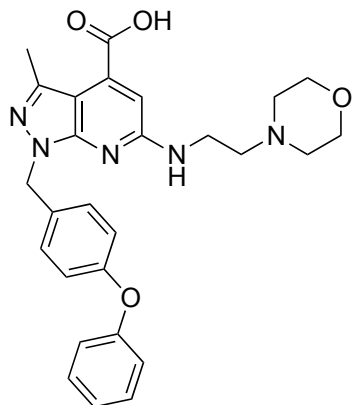
3-Methyl-6-((2-morpholinoethyl)amino)-1-(4-phenoxybenzyl)-1*H*-pyrazolo[3,4-*b*]pyridine-4-carboxylic acid (19). Synthesized using the procedure for **1** except ester **55** was used as the starting material. The title compound (35 mg, 89%) was obtained as a white solid. 100% pure by HPLC. ¹H NMR (400 MHz, DMSO-d₆) δ 13.50 (s, 1H), 11.03 (s, 1H), 7.79-7.71 (m, 1H), 7.39-7.32 (m, 2H), 7.32-7.26 (m, 2H), 7.14-7.07 (m, 1H), 6.99-6.90 (m, 3H), 6.81 (s, 1H), 5.40 (s, 2H), 4.05-3.97 (m, 2H), 3.84-3.73 (m, 3H), 3.40-3.26 (m, 3H), 2.42 (s, 3H), 1.97 (s, 2H), 1.19-1.12 (m, 2H). ¹³C NMR (100 MHz, DMSO-d₆) δ 167.26, 157.73, 157.04, 156.29, 151.98, 140.48, 135.53, 133.48, 130.47, 129.99, 123.88, 119.05, 118.97, 107.78, 103.53, 63.55, 60.20, 55.24, 51.64, 49.09, 21.22, 16.00, 14.54. ESI MS: m/z 488.0 $(M+H)^+$.

Protein purification

His-tagged proteins containing Mcl-1 (residues 171–327), Bcl-2 (residues 1-202 with inserted Bcl-X$_L$ sequence from residues 35 to 50), Bcl-X$_L$ (residues 1-209 lacking its C-terminal transmembrane domain with a deletion of the flexible loop region 45 – 85), Bcl-w (residues 1-155), A1/Bfl-1 (residues 1-151), were expressed from the pHis-TEV vector (a modified pET vector) in *E. coli* BL21 (DE3) cells. Cells were grown at 37 ºC in 2×YT containing antibiotics to an OD$_{600}$ density of 0.6. Protein expression was induced by 0.4 mM IPTG at 37 ºC for 4 hours. Cells were lysed in 50 mM Tris pH 8.0 buffer containing 500 mM NaCl, 0.1% bME and 40 µl of Leupectin/Aprotin. All proteins were purified from the soluble fraction using Ni-NTA resin (QIAGEN), following the manufacturer's instructions. Mcl-1 was further purified on a Source Q15 column (Amersham Biosciences) in 25 mM Tris pH 8.0 buffer, with NaCl gradient. Bcl-2

and Bcl-X_L were purified on a Superdex75 column (Amersham Biosciences) in 25 mM Tris pH 8.0 buffers containing 150 mM NaCl and 2 mM DTT and at -80 °C in presence of 25% Glycerol.

Determination of the K_d values of fluorescent probes to anti-apoptotic proteins

Fluorescein tagged BID BH3 (Bcl-2 Homology 3) peptide was used as a fluorescent probe in the FP-based binding assays. Two fluorescent labeled BID BH3 peptide probes were used: i) fluorescein tagged BID peptide (Flu-BID), labeled with fluorescein on the N-terminus of the BH3 peptide (79-99); ii) the second tracer was purchased from Abgent (Catalog # SP2121a), named as FAM-BID, where the BH3 peptide (80-99) is labeled with 5-FAM. Their K_d values were determined to all members of the Bcl-2 family proteins with a fixed concentration of the tracer (2 nM of Flu-BID and FAM-BID) and different concentrations of the tested proteins, in a final volume of 125 μl in the assay buffer (100 mM potassium phosphate, pH 7.5, 100 μg/ml bovine γ-globulin, 0.02% sodium azide, Invitrogen, with 0.01% Triton X-100 and 4% DMSO). Plates were mixed and incubated at room temperature for 2 hours and the polarization values in millipolarization units (mP) were measured at an excitation wavelength of 485 nm and an emission wavelength of 530 nm. Equilibrium dissociation constants (K_d) were calculated by fitting the sigmoidal dose-dependent FP increases as a function of protein concentrations using Graphpad Prism 6.0 software. Based upon analysis of the dynamic ranges for the signals and their K_d values, Flu-BID was selected as the tracer in the Mcl-1 and Bcl-2 competitive binding assays, while FAM-BID was selected as the tracer for the rest of the proteins, A1/Bfl-1, Bcl-w and Bcl-xL. The K_d value of Flu-BID to Mcl-1 was 34 ± 3.5 nM, and to Bcl-2 was 20 ± 0.86 nM and the K_d values of FAM-BID to A1/Bfl-1 was 0.83 ± 0.06 nM, to Bcl-w was 5.5 ± 1.6 nM, and to Bcl-xL was 10 ± 4.0 nM respectively, in our saturation experiments.

Fluorescence polarization-based binding assays

Sensitive and quantitative FP-based binding assays were developed and optimized to determine the binding affinities of small-molecule inhibitors to the recombinant Mcl-1, A1/Bfl-1, Bcl-w, Bcl-2, and Bcl-xL proteins. Protocols for expression and purification of used anti-apoptotic proteins and determination of Kd values of fluorescent probes to proteins are provided in the Supporting Information. Based on the K_d values, the concentrations of the proteins used in the competitive binding experiments were 90 nM for Mcl-1, 40 nM for Bcl-w, 50 nM for Bcl-x$_{L, 60}$

nM for Bcl-2, and 4 nM for A1/Bfl-1. The fluorescent probes, Flu-BID and FAM-BID were fixed at 2 nM for all assays except for A1/Bfl-1 where FAM-BID was used at 1 nM. 5 μL of the tested compound in DMSO and 120 μL of protein/probe complex in the assay buffer (100 mM potassium phosphate, pH 7.5; 100 μg/ml bovine gamma globulin; 0.02% sodium azide, purchased from Invitrogen, Life Technologies) were added to assay plates (Microfluor 2Black, Thermo Scientific), incubated at room temperature for 3 h and the polarization values (mP) were measured at an excitation wavelength at 485 nm and an emission wavelength at 530 nm using the plate reader Synergy H1 Hybrid, BioTek. IC_{50} values were determined by nonlinear regression fitting of the competition curves (GraphPad Prism 6.0 Software). The K_i values were calculated as described previously[24].

Solution competitive surface plasmon resonance-based assay using immobilized biotin-labeled Bim BH3 peptide

The solution competitive SPR-based assay was performed on Biacore 2000. N terminal biotin-labeled Bim BH3 peptide (141 - 166 amino acids), was immobilized on streptavidin (SA) chip giving density of 1400 RU (Response Units). The pre-incubated Mcl-1 protein (20 nM) with tested small-molecule inhibitors for at least 30 minutes was injected over the surfaces of the chip. Response units were measured at 15 seconds in the dissociation phase and the specific binding was calculated by subtracting the control surface (Fc1) signal from the surfaces with immobilized biotin-labeled Bim BH3. IC_{50} values were determined by non-linear least squares analysis using GraphPad Prism 6.0 software.

Molecular modeling

Crystal structure of Mcl-1 in complex with mNoxa BH3 peptide (PDB entry 2NLA) and in silico Schrödinger's IFD were used to model the binding poses of our designed compounds with Mcl-1. IFD is allowing incorporation of the protein and ligand flexibility in the docking protocol, which is consisted of the following steps: (i) constrained minimization of the protein with an RMSD cutoff of 0.18 Å; (ii) initial Glide docking of the ligand using a softened potential (Van der Waals radii scaling); (iii) one round of Prime side-chain prediction for each protein/ligand complex, on residues within defined distance of any ligand pose; (iv) prime minimization of the same set of residues and the ligand for each protein/ligand complex pose; (v) Glide re-docking of

each protein/ligand complex structure within a specified energy of the lowest energy structure; (vi) estimation of the binding energy (IFDScore) for each output pose. All docking calculations were run in the extra precision (XP) mode of Glide. The center of the grid box of the Mcl-1 was defined by the Val 249 (in h1), Phe 270 (in h2), Val 220 (in h3/h4) and Val 216 (in h4). The size of the grid box was set to 15 Å. Default values were used for all other parameters. Schrödinger's MC/SD dynamic simulation performs constant temperature calculations that take advantage of the strengths of Monte Carlo methods for quickly introducing large changes in a few degree of freedom, and stochastic dynamics for its effective local sampling of collective motions. The MC/SD dynamic simulation time in our study was set to 100 ps by allowing movement of the docked ligand and the residues which is less than 6 Å to the ligand. The force field used was set to OPLS_2001. Default values were used for all other parameters.

NMR studies

[15]N-labeled or ^{15}N, ^{13}C-labeled Mcl-1 proteins for NMR studies were prepared and purified using the same protocol as for unlabeled protein with the exception that the bacteria were grown on M9 minimal media supported with 3 g/ L of ^{13}C-glucose and/or 1 g/L of ([15]NH$_4$)$_2$SO$_4$. [15]N, ^{13}C-labeled Mcl-1 was used for backbone reassignment and 80% of residues were reassigned based on the work by Liu *et al*[26]. Protein samples were prepared in a 20 mM sodium phosphate, 150 mM NaCl and 1 mM DTT solution at pH 7 in 7% D$_2$O. The binding mode of the compounds has been characterized by recording ^{1}H,^{15}N -HSQC experiments with a 138 µL solution of uniformly ^{15}N-labeled Mcl-1 (75µM) in the absence and presence of added compounds with the indicated molar ratio concentrations. All Spectra were acquired at 30 °C on a Bruker 600 MHz NMR spectrometer equipped with a cryogenic probe, processed using Bruker TopSpin and rNMR[25], and were analyzed with Sparky[27]. Plots of chemical shift changes were calculated as $((\Delta^1H \text{ ppm})^2 + (0.2(\Delta^{15}N \text{ ppm}))^2)^{0.5}$ of Mcl-1 amide upon addition of compound. The absence of a bar in a chemical shift plot indicates no chemical shift difference, or the presence of a proline or residue that is overlapped or not assigned.

3.8   Contributions

Fardokht Abulwerdi designed, synthesized and characterized all the compounds and as well as expressed and purified labeled Mcl-1, prepared NMR samples and analyzed HSQC NMR data with supervision from Dr. Nikolovska-Coleska and Dr. Hollis Showalter. Ahmed Mady performed all the biochemical experiments. Dr. Chenzhong Liao performed the in silico target-based screen and identified the potential leads. Dr. Andrej Perdih performed all the molecular docking studies. All the proteins used for biochemical assays were expressed and purified in Dr. Jeanne Stuckey lab at LSI.

3.9   References

1.   Macarron, R.; Banks, M. N.; Bojanic, D.; Burns, D. J.; Cirovic, D. A.; Garyantes, T.; Green, D. V.; Hertzberg, R. P.; Janzen, W. P.; Paslay, J. W.; Schopfer, U.; Sittampalam, G. S. Impact of high-throughput screening in biomedical research. *Nat Rev Drug Discov* **2011,** 10, 188-95.
2.   Du, Y.; Nikolovska-Coleska, Z.; Qui, M.; Li, L.; Lewis, I.; Dingledine, R.; Stuckey, J. A.; Krajewski, K.; Roller, P. P.; Wang, S.; Fu, H. A dual-readout F2 assay that combines fluorescence resonance energy transfer and fluorescence polarization for monitoring bimolecular interactions. *Assay Drug Dev Technol* **2011,** 9, 382-93.
3.   http://pubchem.ncbi.nlm.nih.gov/assay/assay.cgi?aid=1417.
4.   http://pubchem.ncbi.nlm.nih.gov/assay/assay.cgi?aid=1418.
5.   Czabotar, P. E.; Lee, E. F.; van Delft, M. F.; Day, C. L.; Smith, B. J.; Huang, D. C.; Fairlie, W. D.; Hinds, M. G.; Colman, P. M. Structural insights into the degradation of Mcl-1 induced by BH3 domains. *Proc Natl Acad Sci U S A* **2007,** 104, 6217-22.
6.   Schrödinger Suite 2011 Induced Fit Docking protocol; Glide version 5.7, Schrödinger, LLC, New York, NY, 2009; Prime version 3.0, Schrödinger, LLC, New York, NY. **2011**.
7.   Friberg, A.; Vigil, D.; Zhao, B.; Daniels, R. N.; Burke, J. P.; Garcia-Barrantes, P. M.; Camper, D.; Chauder, B. A.; Lee, T.; Olejniczak, E. T.; Fesik, S. W. Discovery of potent myeloid cell leukemia 1 (Mcl-1) inhibitors using fragment-based methods and structure-based design. *J Med Chem* **2013,** 56, 15-30.
8.   Lipinski, C. A.; Lombardo, F.; Dominy, B. W.; Feeney, P. J. Experimental and computational approaches to estimate solubility and permeability in drug discovery and development settings. *Adv Drug Deliv Rev* **2001,** 46, 3-26.
9.   Abad-Zapatero, C.; Metz, J. T. Ligand efficiency indices as guideposts for drug discovery. *Drug Discov Today* **2005,** 10, 464-9.
10.   Hajduk, P. J. Fragment-based drug design: how big is too big? *J Med Chem* **2006,** 49, 6972-6.
11.   Ghosh, A. K.; Xi, K.; Ratia, K.; Santarsiero, B. D.; Fu, W.; Harcourt, B. H.; Rota, P. A.; Baker, S. C.; Johnson, M. E.; Mesecar, A. D. Design and synthesis of peptidomimetic severe acute respiratory syndrome chymotrypsin-like protease inhibitors. *J Med Chem* **2005,** 48, 6767-71.

12. Ganesan, A.; Heathcock, C. H. Synthesis of Unsymmetrical Pyrazines by Reaction of an Oxadiazinone with Enamines. *Journal of Organic Chemistry* **1993,** 58, 6155-6157.

13. Martins, A.; Marquardt, U.; Kasravi, N.; Alberico, D.; Lautens, M. Synthesis of substituted benzoxacycles via a domino ortho-alkylation/Heck coupling sequence. *J Org Chem* **2006,** 71, 4937-42.

14. Khire, U.; Zhang, C.; Kluender, H. C. E.; Mugge, I.; Hong, Z.; Shao, J.; Bifulco, N.; Trail, P. A.; Dumas, J.; Lavoie, R. C.; Liu, X.-G.; Agarwal, V.; Verma, S. K.; Wang, L. Preparation of 1-[2-(aryloxy)ethyl]-1H-pyrazoles useful in the treatment of hyper-proliferative disorders. WO2003027074A1, 2003.

15. Misra, R. N.; Rawlins, D. B.; Xiao, H. Y.; Shan, W.; Bursuker, I.; Kellar, K. A.; Mulheron, J. G.; Sack, J. S.; Tokarski, J. S.; Kimball, S. D.; Webster, K. R. 1H-Pyrazolo[3,4-b]pyridine inhibitors of cyclin-dependent kinases. *Bioorg Med Chem Lett* **2003,** 13, 1133-6.

16. Aissaoui, H.; Boss, C.; Brotschi, C.; Gatfield, J.; Koberstein, R.; Siegrist, R.; Sifferlen, T.; Williams, J. T. Tetrazole derivatives as orexin receptor antagonists and their preparation, pharmaceutical compositions and use in the treatment of diseases. WO2009150614A1, 2009.

17. Volochnyuk, D. M.; Ryabukhin, S. V.; Plaskon, A. S.; Dmytriv, Y. V.; Grygorenko, O. O.; Mykhailiuk, P. K.; Krotko, D. G.; Pushechnikov, A.; Tolmachev, A. A. Approach to the library of fused pyridine-4-carboxylic acids by Combes-type reaction of acyl pyruvates and electron-rich amino heterocycles. *J Comb Chem* **2010,** 12, 510-7.

18. Neres, J.; Engelhart, C. A.; Drake, E. J.; Wilson, D. J.; Fu, P.; Boshoff, H. I.; Barry, C. E., 3rd; Gulick, A. M.; Aldrich, C. C. Non-nucleoside inhibitors of BasE, an adenylating enzyme in the siderophore biosynthetic pathway of the opportunistic pathogen Acinetobacter baumannii. *J Med Chem* **2013,** 56, 2385-405.

19. Sercel, A. D.; Sanchez, J. P.; Showalter, H. D. H. Simple synthesis of 4-substituted 1(2H)-Isoquinolinones via electrophilic trapping of lithiated mono- and dianion precursors. *Synthetic Communications* **2007,** 37, 4199-4208.

20. Greig, I. R.; Idris, A. I.; Ralston, S. H.; van't Hof, R. J. Development and characterization of biphenylsulfonamides as novel inhibitors of bone resorption. *J Med Chem* **2006,** 49, 7487-92.

21. Li, X.; Chu, S.; Feher, V. A.; Khalili, M.; Nie, Z.; Margosiak, S.; Nikulin, V.; Levin, J.; Sprankle, K. G.; Tedder, M. E.; Almassy, R.; Appelt, K.; Yager, K. M. Structure-based design, synthesis, and antimicrobial activity of indazole-derived SAH/MTA nucleosidase inhibitors. *J Med Chem* **2003,** 46, 5663-73.

22. Dai, W.; Petersen, J. L.; Wang, K. K. Synthesis of the parent and substituted tetracyclic ABCD ring cores of camptothecins via 1-(3-aryl-2-propynyl)- 1,6-dihydro-6-oxo-2-pyridinecarbonitriles. *Org Lett* **2006,** 8, 4665-7.

23. Burgess, J. L.; Johnson, N. W.; Knight, S. D.; Lafrance, L. V., III; Miller, W. H.; Newlander, K. A.; Romeril, S. P.; Rouse, M. B.; Suarez, D.; Tian, X.; Verma, S. K. Preparation of azaindole carboxamide derivatives as EZH2 inhibitors for the treatment of cancer. WO2013039988A1, 2013.

24. Nikolovska-Coleska, Z.; Wang, R.; Fang, X.; Pan, H.; Tomita, Y.; Li, P.; Roller, P. P.; Krajewski, K.; Saito, N. G.; Stuckey, J. A.; Wang, S. Development and optimization of a binding assay for the XIAP BIR3 domain using fluorescence polarization. *Anal Biochem* **2004,** 332, 261-73.

25. Lewis, I. A.; Schommer, S. C.; Markley, J. L. rNMR: open source software for identifying and quantifying metabolites in NMR spectra. *Magn Reson Chem* **2009,** 47 Suppl 1, S123-6.

26. Liu, Q.; Moldoveanu, T.; Sprules, T.; Matta-Camacho, E.; Mansur-Azzam, N.; Gehring, K. Apoptotic regulation by MCL-1 through heterodimerization. *J Biol Chem* **2010,** 285, 19615-24.

27. Goddard, T. D.; Kneller, D. G. SPARKY 3.

Chapter 4
Summary and future directions

4.1   Summary

Apoptosis, an evolutionary-conserved genetic program for the removal of unwanted cells, is triggered by the extrinsic or the intrinsic (mitochondrial) apoptotic pathways. Bcl-2 family of proteins regulate the mitochondrial apoptotic pathway through a network of protein-protein interactions (PPIs) between the anti- and pro-apoptotic members. Myeloid cell leukemia-1 (Mcl-1) is a potent anti-apoptotic protein, and together with Bcl-X_L, Bcl-2, Bcl-w, Bcl-b and Bfl-1/A1, belongs to the pro-survival Bcl-2 subfamily. Structural studies of pro-survival members show that these proteins share up to four conserved helical domains known as Bcl-2 homology (BH) domains of which BH1-3 are involved in forming a well-defined, hydrophobic cleft on the surface of pro-survival members known as BH3-binding site. This conserved binding site interacts and sequesters the BH3 domain of pro-apoptotic proteins and is essential for the anti-apoptotic function of anti-apoptotic members.

Functional studies have demonstrated that Mcl-1 is capable of blocking apoptosis induced by various apoptotic stimuli, including chemotherapy and radiation[1,2] while its down-regulation enhances the induction of apoptosis[3-5]. Thus, Mcl-1 represents an attractive molecular target for developing a new class of anti-cancer therapy for treatment of cancer and overcoming resistance to apoptosis. In addition, Mcl-1's structural differences (e.g. larger size, electropositive BH3-binding site, etc) as compared to other anti-apoptotic members as well as its short half-life and tight regulation at the transcriptional and post-translational levels suggest that Mcl-1 has a distinct and non-redundant function, and its activities can be modulated to allow for different cellular functions[6, 7].

Binding studies have shown that interactions between Bcl-2 family proteins appear to be selective and specific[8] (Figure 1.5, Chapter 1). The selective binding of pro-survival Bcl-2

proteins to their pro-apoptotic BH3-only ligands strongly suggests that specific targeting is possible and that highly specific small molecules can be designed. Indeed, there are several successful examples[9-11] of potent small molecules, binding to the BH3-binding groove of a subset (Bcl-2/Bcl-X_L) or a single (Bcl-2 or Bcl-X_L) anti-apoptotic protein(s), that are being advanced in clinical trials. However, development of selective and potent small molecules against Mcl-1 has proved difficult and lagged behind.

The research described in this dissertation aimed at developing novel small-molecule inhibitors of Mcl-1. We utilized a traditional approach of high throughput screening (HTS) to identify small molecules capable of binding to Mcl-1 and disrupt its interaction with BH3 peptides. HTS has been a common and popular way to identify small molecules as starting points for further development[12]. To triage the HTS hits and select the most promising compounds for follow-up evaluation, structural knowledge of the interaction between Mcl-1 and BH3 peptides coupled with molecular docking and supported by protein NMR spectroscopy were utilized, and compounds were selected based on the their ability to mimic the conserved interactions between Mcl-1 and BH3-only proteins.

Chapter 2 described the development of a class of selective Mcl-1 inhibitors based on the first HTS lead, compound **59**, bearing a hydroxynaphthalenylsulfonamide scaffold. Structure-based design supported by NMR led to the design of new analogs, which were synthesized through a modular and efficient synthetic route. A library of more than 40 analogs of **59** with variations at four sites was generated and a SAR was established through two orthogonal biochemical assays. A potent and selective inhibitor, compound **21**, was identified which binds to Mcl-1 with a K_i of 180 nM and an overall 9-fold improvement in potency over **59.** Compound **21** maintained the specificity profile of **59** and selectively inhibited Mcl-1 over the other anti-apoptotic members. Compound **21** selectively sensitizes Eμ-myc lymphomas overexpressing Mcl-1, but not Eμ-myc lymphomas overexpressing Bcl-2 which correlates well with its *in vitro* biochemical inhibition and selectivity profile. Furthermore, it was demonstrated that **21** disrupts the interaction of endogenous Mcl-1 and biotinylated Noxa-BH3 peptide and causes cell death through a Bak/Bax-dependent mechanism. Treatment of human leukemic cell lines with compound **21** resulted in dose-dependent cell death, through activation of caspase-3 and induction of apoptosis. Additionally, another potent analog from this series, **10**, was used as a chemical tool to validate Mcl-1 as a potential therapeutic target in pancreatic cancer (PC). The

in vitro and *in vivo* efficacy studies in a panel of pancreatic cancer cell lines and PC xenograft model, showed single-agent antitumor activity, demonstrating the therapeutic potential of Mcl-1 inhibitors against PC[13].

Chapter 3 described the development of a second class of Mcl-1 inhibitors based on a second HTS lead, compound **38**, with a 1*H*-pyrazolo[3,4-b]pyridine scaffold. Systematic removal of side chains of **38** and detailed NMR studies of the fragments mapped the binding site of this class of compounds in the Mcl-1 BH3-binding site. Through structure-based design and our knowledge from the first class of Mcl-1 inhibitors, analogs were deigned and synthesized using a short and convergent synthetic route. An initial SAR was established and analog **8** (K_i = 2.2 μM) with an overall 12-fold improvement in binding affinity over **38** was developed. **8** inhibits Mcl-1 most potently with an 8-fold selectivity over Bcl-2, and shows no inhibition of Bfl-1/A1, Bcl-w, and Bcl-X_L up to 100 μM.

4.2   Significance of the study

This work showcases a successful use of structure-based design in conjunction with a series of biochemical and biophysical techniques toward developing small molecules as PPI inhibitors for a challenging target such as Mcl-1. More specifically the following scientific contributions were made.

-A novel synthetic route was established for the synthesis of **59** class of compounds with a hydroxynaphthalenylsulfonamide scaffold.

-Two classes of novel Mcl-1 inhibitors with hydroxynaphthalenylsulfonamide and 1*H*-pyrazolo[3,4-b]pyridine scaffolds were developed.

-Over 150 compounds including intermediates were synthesized and characterized.

-Binding of potent inhibitors to Mcl-1 was verified and further mapped to the BH3-binding site of Mcl-1.

-Binding of both classes of inhibitors to Mcl-1 was further analyzed by computational studies and validated by NMR studies.

-SARs of both classes of analogs were established and more potent analogs were identified.

-Selectivity profile of inhibitors was determined against five anti-apoptotic proteins.

-Most potent inhibitors were characterized in cell-based assays and the mechanism of induction of apoptosis was elucidated.

-Efficacy of most potent inhibitors were studied in human leukemia and pancreatic cancers.

Overall through this work, the importance of targeting Mcl-1 in cancer with small molecules to overcome the Mcl-1-mediated resistance to cell death was highlighted. Finally, both classes of compounds can be further optimized and potentially lead to drug candidates for cancers that rely on Mcl-1 or can be used as probes to elucidate the role of Mcl-1 in cancer and normal physiology.

4.3   Future directions

Crystallography studies

To optimize both classes of Mcl-1 inhibitors for improved potency, potent analogs with acceptable physicochemical properties from each class should be selected for crystallography trials. Indeed crystallography trials are ongoing in collaboration with the Center for Structural Biology at UM with inhibitors from both classes. Crystallography studies with Mcl-1 in the presence of a small molecule have been challenging compared to Bcl-2 and Bcl-X$_L$ possibly due its higher degree of plasticity over other anti-apoptotic proteins. However, recently two crystal structures of Mcl-1 in complex with small molecules[14, 15] have been solved. We also obtained a crystal structure of Mcl-1 bound to a small-molecule inhibitor form a different chemical class using higher concentrations of polyethylene glycol and a more alkaline pH, which produced crystals with sharp edges and clean faces. Similar conditions have been applied to the classes developed here and produced crystals for Mcl-1 bound to **37**, from our **59** series, and **8**, belonging to the **38** series. Currently we are screening around these conditions to obtain diffraction-quality crystals. A co-crystal of Mcl-1 bound to our inhibitor can provide a molecular picture of binding of our inhibitor to Mcl-1 and further guide the design of potent analogs.

Improving the binding affinity through targeting p4 pocket

Most of the binding affinity of potent analogs developed through this work comes from the hydrophobic interactions within the p2 and p3 pockets of Mcl-1. Structural data comparison of ABT-737 (Bcl-X$_L$/Bcl-2 selective), ABT-199 (Bcl-2 selective) and WEHI-539 (Bcl-X$_L$

selective), show that all three inhibitors bind to the p2 and p4 pockets of their respective protein(s) and therefore exhibit sub-nanomolar potency[16]. Thus, one strategy to improve potency of our inhibitors is to reach into the p4 pocket of Mcl-1. For this purpose, NMR or in silico fragment-based screening[17-19] can be utilized in the presence of an inhibitor from either class to identify fragments that bind to p4 pocket. Once fragments were identified from either strategy and their binding was validated, medicinal chemistry efforts can be utilized to link the desired fragment to the current scaffolds which is by itself a challenging task and can be greatly circumvented through structural information.

Studies toward understanding the selectivity of inhibitors

Understanding the binding determinants that dictate similarities and differences among BH3-binding sites of anti-apoptotic proteins presents a significant drug design challenge[20]. Through this work, we developed two classes of Mcl-1 inhibitors with different selectivity profiles against the anti-apoptotic proteins. While inhibitors from **59** class show high selectivity in binding to Mcl-1 over other anti-apoptotic members, **38** class of compounds, show a mixed profile of selectivity. For example, analog **8** shows a slight 8-fold selectivity for Mcl-1 over Bcl-2, but both **17** and **18** equipotently inhibit both proteins. Interestingly, **16** is a pan inhibitor of all anti-apoptotic proteins. The selectivity profile observed for both classes of inhibitors is interesting and requires further studies to fully understand their binding to Bcl-2 anti-apoptotic proteins. Point mutation(s) of the proteins coupled with computational modeling can help in identifying the binding determinants of different anti-apoptotic proteins and to assist in the design of analogs with tailored specificity toward each anti-apoptotic member. It is still unclear whether selective or pan inhibition of anti-apoptotic proteins is desirable for cancer therapy. Thus, development of such molecules can shed light on this question.

Overall, the work presented in this dissertation contributes to our understanding of developing selective Mcl-1 inhibitors. The continued development of such inhibitors can elucidate the role of Mcl-1 in cancer and identify a subset of cancers most susceptible to Mcl-1 inhibition which can further lead to more effective targeted therapies.

4.4 References

1. Beroukhim, R.; Mermel, C. H.; Porter, D.; Wei, G.; Raychaudhuri, S.; Donovan, J.; Barretina, J.; Boehm, J. S.; Dobson, J.; Urashima, M.; Mc Henry, K. T.; Pinchback, R. M.; Ligon, A. H.; Cho, Y. J.; Haery, L.; Greulich, H.; Reich, M.; Winckler, W.; Lawrence, M. S.; Weir, B. A.; Tanaka, K. E.; Chiang, D. Y.; Bass, A. J.; Loo, A.; Hoffman, C.; Prensner, J.; Liefeld, T.; Gao, Q.; Yecies, D.; Signoretti, S.; Maher, E.; Kaye, F. J.; Sasaki, H.; Tepper, J. E.; Fletcher, J. A.; Tabernero, J.; Baselga, J.; Tsao, M. S.; Demichelis, F.; Rubin, M. A.; Janne, P. A.; Daly, M. J.; Nucera, C.; Levine, R. L.; Ebert, B. L.; Gabriel, S.; Rustgi, A. K.; Antonescu, C. R.; Ladanyi, M.; Letai, A.; Garraway, L. A.; Loda, M.; Beer, D. G.; True, L. D.; Okamoto, A.; Pomeroy, S. L.; Singer, S.; Golub, T. R.; Lander, E. S.; Getz, G.; Sellers, W. R.; Meyerson, M. The landscape of somatic copy-number alteration across human cancers. *Nature* **2010,** 463, 899-905.
2. Zhou, P.; Qian, L.; Kozopas, K. M.; Craig, R. W. Mcl-1, a Bcl-2 family member, delays the death of hematopoietic cells under a variety of apoptosis-inducing conditions. *Blood* **1997,** 89, 630-43.
3. Guoan, X.; Hanning, W.; Kaiyun, C.; Hao, L. Adenovirus-mediated siRNA targeting Mcl-1 gene increases radiosensitivity of pancreatic carcinoma cells in vitro and in vivo. *Surgery* **2010,** 147, 553-61.
4. Hussain, S. R.; Cheney, C. M.; Johnson, A. J.; Lin, T. S.; Grever, M. R.; Caligiuri, M. A.; Lucas, D. M.; Byrd, J. C. Mcl-1 is a relevant therapeutic target in acute and chronic lymphoid malignancies: down-regulation enhances rituximab-mediated apoptosis and complement-dependent cytotoxicity. *Clin Cancer Res* **2007,** 13, 2144-50.
5. Wei, S. H.; Dong, K.; Lin, F.; Wang, X.; Li, B.; Shen, J. J.; Zhang, Q.; Wang, R.; Zhang, H. Z. Inducing apoptosis and enhancing chemosensitivity to gemcitabine via RNA interference targeting Mcl-1 gene in pancreatic carcinoma cell. *Cancer Chemother Pharmacol* **2008,** 62, 1055-64.
6. Akgul, C. Mcl-1 is a potential therapeutic target in multiple types of cancer. *Cell Mol Life Sci* **2009,** 66, 1326-36.
7. Quinn, B. A.; Dash, R.; Azab, B.; Sarkar, S.; Das, S. K.; Kumar, S.; Oyesanya, R. A.; Dasgupta, S.; Dent, P.; Grant, S.; Rahmani, M.; Curiel, D. T.; Dmitriev, I.; Hedvat, M.; Wei, J.; Wu, B.; Stebbins, J. L.; Reed, J. C.; Pellecchia, M.; Sarkar, D.; Fisher, P. B. Targeting Mcl-1 for the therapy of cancer. *Expert Opin Investig Drugs* **2011,** 20, 1397-411.
8. Chen, L.; Willis, S. N.; Wei, A.; Smith, B. J.; Fletcher, J. I.; Hinds, M. G.; Colman, P. M.; Day, C. L.; Adams, J. M.; Huang, D. C. Differential targeting of prosurvival Bcl-2 proteins by their BH3-only ligands allows complementary apoptotic function. *Mol Cell* **2005,** 17, 393-403.
9. Oltersdorf, T.; Elmore, S. W.; Shoemaker, A. R.; Armstrong, R. C.; Augeri, D. J.; Belli, B. A.; Bruncko, M.; Deckwerth, T. L.; Dinges, J.; Hajduk, P. J.; Joseph, M. K.; Kitada, S.; Korsmeyer, S. J.; Kunzer, A. R.; Letai, A.; Li, C.; Mitten, M. J.; Nettesheim, D. G.; Ng, S.; Nimmer, P. M.; O'Connor, J. M.; Oleksijew, A.; Petros, A. M.; Reed, J. C.; Shen, W.; Tahir, S. K.; Thompson, C. B.; Tomaselli, K. J.; Wang, B.; Wendt, M. D.; Zhang, H.; Fesik, S. W.; Rosenberg, S. H. An inhibitor of Bcl-2 family proteins induces regression of solid tumours. *Nature* **2005,** 435, 677-81.
10. Souers, A. J.; Leverson, J. D.; Boghaert, E. R.; Ackler, S. L.; Catron, N. D.; Chen, J.; Dayton, B. D.; Ding, H.; Enschede, S. H.; Fairbrother, W. J.; Huang, D. C.; Hymowitz, S.

G.; Jin, S.; Khaw, S. L.; Kovar, P. J.; Lam, L. T.; Lee, J.; Maecker, H. L.; Marsh, K. C.; Mason, K. D.; Mitten, M. J.; Nimmer, P. M.; Oleksijew, A.; Park, C. H.; Park, C. M.; Phillips, D. C.; Roberts, A. W.; Sampath, D.; Seymour, J. F.; Smith, M. L.; Sullivan, G. M.; Tahir, S. K.; Tse, C.; Wendt, M. D.; Xiao, Y.; Xue, J. C.; Zhang, H.; Humerickhouse, R. A.; Rosenberg, S. H.; Elmore, S. W. ABT-199, a potent and selective BCL-2 inhibitor, achieves antitumor activity while sparing platelets. *Nat Med* **2013,** 19, 202-8.

11. Lessene, G.; Czabotar, P. E.; Sleebs, B. E.; Zobel, K.; Lowes, K. N.; Adams, J. M.; Baell, J. B.; Colman, P. M.; Deshayes, K.; Fairbrother, W. J.; Flygare, J. A.; Gibbons, P.; Kersten, W. J.; Kulasegaram, S.; Moss, R. M.; Parisot, J. P.; Smith, B. J.; Street, I. P.; Yang, H.; Huang, D. C.; Watson, K. G. Structure-guided design of a selective BCL-X(L) inhibitor. *Nat Chem Biol* **2013,** 9, 390-7.

12. Macarron, R.; Banks, M. N.; Bojanic, D.; Burns, D. J.; Cirovic, D. A.; Garyantes, T.; Green, D. V.; Hertzberg, R. P.; Janzen, W. P.; Paslay, J. W.; Schopfer, U.; Sittampalam, G. S. Impact of high-throughput screening in biomedical research. *Nat Rev Drug Discov* **2011,** 10, 188-95.

13. Abulwerdi, F.; Liao, C.; Liu, M.; Azmi, A. S.; Aboukameel, A.; Mady, A. S.; Gulappa, T.; Cierpicki, T.; Owens, S.; Zhang, T.; Sun, D.; Stuckey, J. A.; Mohammad, R. M.; Nikolovska-Coleska, Z. A Novel Small-Molecule Inhibitor of Mcl-1 Blocks Pancreatic Cancer Growth In vitro and In vivo. *Mol Cancer Ther* **2013**.

14. Friberg, A.; Vigil, D.; Zhao, B.; Daniels, R. N.; Burke, J. P.; Garcia-Barrantes, P. M.; Camper, D.; Chauder, B. A.; Lee, T.; Olejniczak, E. T.; Fesik, S. W. Discovery of potent myeloid cell leukemia 1 (Mcl-1) inhibitors using fragment-based methods and structure-based design. *J Med Chem* **2013,** 56, 15-30.

15. Tanaka, Y.; Aikawa, K.; Nishida, G.; Homma, M.; Sogabe, S.; Igaki, S.; Hayano, Y.; Sameshima, T.; Miyahisa, I.; Kawamoto, T.; Tawada, M.; Imai, Y.; Inazuka, M.; Cho, N.; Imaeda, Y.; Ishikawa, T. Discovery of Potent Mcl-1/Bcl-xL Dual Inhibitors by Using a Hybridization Strategy Based on Structural Analysis of Target Proteins. *J Med Chem* **2013,** 56, 9635-45.

16. Czabotar, P. E.; Lessene, G.; Strasser, A.; Adams, J. M. Control of apoptosis by the BCL-2 protein family: implications for physiology and therapy. *Nat Rev Mol Cell Biol* **2013,** 15, 49-63.

17. Shuker, S. B.; Hajduk, P. J.; Meadows, R. P.; Fesik, S. W. Discovering high-affinity ligands for proteins: SAR by NMR. *Science* **1996,** 274, 1531-4.

18. Hajduk, P. J.; Greer, J. A decade of fragment-based drug design: strategic advances and lessons learned. *Nat Rev Drug Discov* **2007,** 6, 211-9.

19. Zoete, V.; Grosdidier, A.; Michielin, O. Docking, virtual high throughput screening and in silico fragment-based drug design. *J Cell Mol Med* **2009,** 13, 238-48.

20. Juin, P.; Geneste, O.; Gautier, F.; Depil, S.; Campone, M. Decoding and unlocking the BCL-2 dependency of cancer cells. *Nat Rev Cancer* **2013,** 13, 455-65.

Appendix
Development of second-generation 59 inhibitors of Mcl-1

A.1   Introduction

Despite the favorable properties of our **59** series of analogs (Chapter 2) with a hydroxynaphthalenylsulfonamide scaffold as defined by Lipinki's Rule of Five[1], the hydronaphthoiminoquinone part of the scaffold is prone to oxidation over time to a naphthoiminoquinone (Figure A.1A). While we never noticed any differences in our binding/NMR studies using old or freshly prepared stocks, we were pleased to see identification of compounds with naphthoiminoquinone as Mcl-1 inhibitors in the HTS leads identified from our screening effort at Emory University (Chapter 3). Additionally, compounds with naphthoiminoquinone scaffold have been identified recently as selective Mcl-1 inhibitors by Cohen *et al*[2].
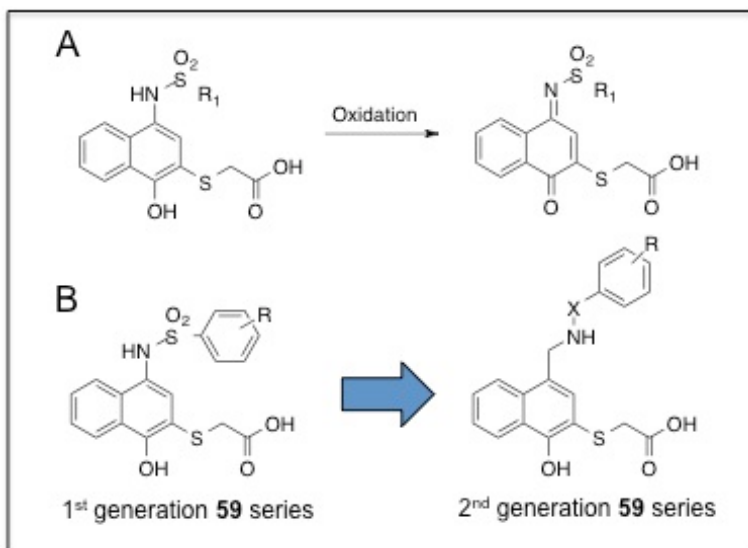

Figure A.1. Development of 2nd generation 59 series. A) Oxidation of hydronaphthoiminoquinone to naphthoiminoquinone B) General structures for 1st and 2nd generation **59** series.

Therefore, we set to develop second-generation analogs of our hydronaphthoiminoquinone series that would maintain similar potency to the first generation analogs but display an improved stability toward oxidation. We envisioned synthesizing compounds with the general structure as shown in Figure A.1 B in which a methylene linker is added in between the naphthalene scaffold and the amine which is linked to an aryl group by an aliphatic linker (X). The inspiration for the design of this compound with a flexible linker came from a recent work by Friberg *et al*[3]. in which selective Mcl-1 inhibitors have been developed. The structural features of Friberg inhibitors include substituted aryls which are linked to a core scaffold (an indole or a benzothiophene) by a flexible ether linkage. An example of such an inhibitor crystallized in complex with Mcl-1 is compound **53** (Figure A.2 A). The crystal structure of **53** in complex with Mcl-1 (PDB 4HW2) showed that the substituted aryl group inserts into the p2 pocket of Mcl-1 (Figure A.2 B). Utilizing the same crystal structure, a docking pose of the proposed analog **I-1** (Figure A.2 C) predicted that the phenyl is placed in the p2 pocket while the carboxylate is predicted to form an electrostatic interaction with R263 (Figure A.2 D). Interestingly, the naphthalene core is placed away from the p3 pocket and closer toward the opening of the p2 pocket. Encouraged by our computational studies, we developed a synthetic route to synthesize compound **I-1** and its analogs. Synthesized analogs were then assessed in our competitive fluorescence polarization (FP)-based assay against Mcl-1 to determine their binding affinities.
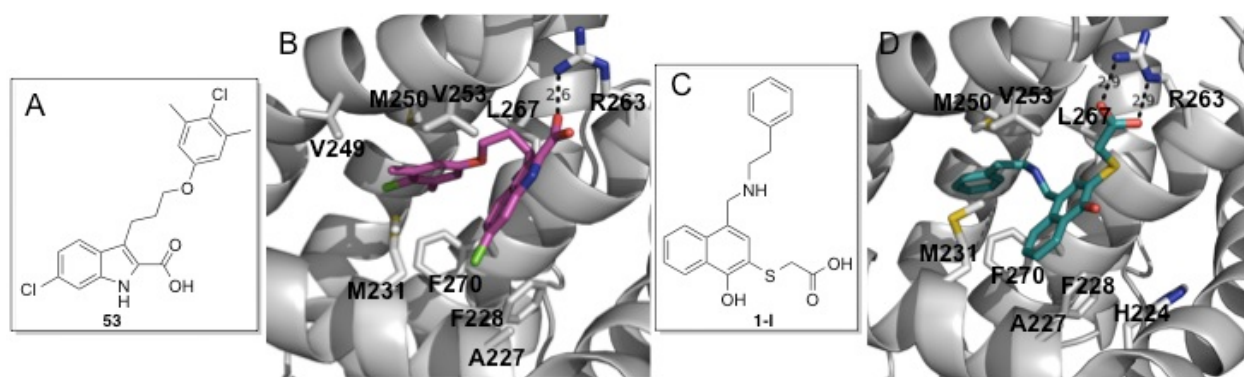

Figure A.2. Comparison of crystal structure of 53 and docking pose of 1-I. A) Structure of compound **53** B) Crystal structure of **53** in complex with Mcl-1 (4HW2). C) Structure of compound **1-I** D) Putative binding pose of **1-I** (4HW2)

A.2   Synthesis

To synthesize **I-1** and its analogs, Scheme A.1 was utilized. 4-methoxy-1-naphthaldehyde was first subjected to *N*-iodosuccinamide to provide **3** via electrophilic aromatic substitution (S_EAr). Intermediate **3** underwent reductive amination[4] with the desired amines, which were either available commercially or synthesized using Scheme A.2, to provide the corresponding imine which was reduced using sodium borohydride. Intermediates **4** were subjected to C-S coupling with methyl thioglycolate using conditions reported previously[5]. Intermediates **5** were subjected to boron tribromide to provide analogs **1-I** through **1-IV** with a free hydroxyl and a carboxylic acid. To preserve the methyl ester in analog **2-IV**, analog **5-IV** was subjected to boron tribromide followed by a quench with MeOH.

**Scheme A.1.** Synthesis of analogs **1-I–1-IV**[a].
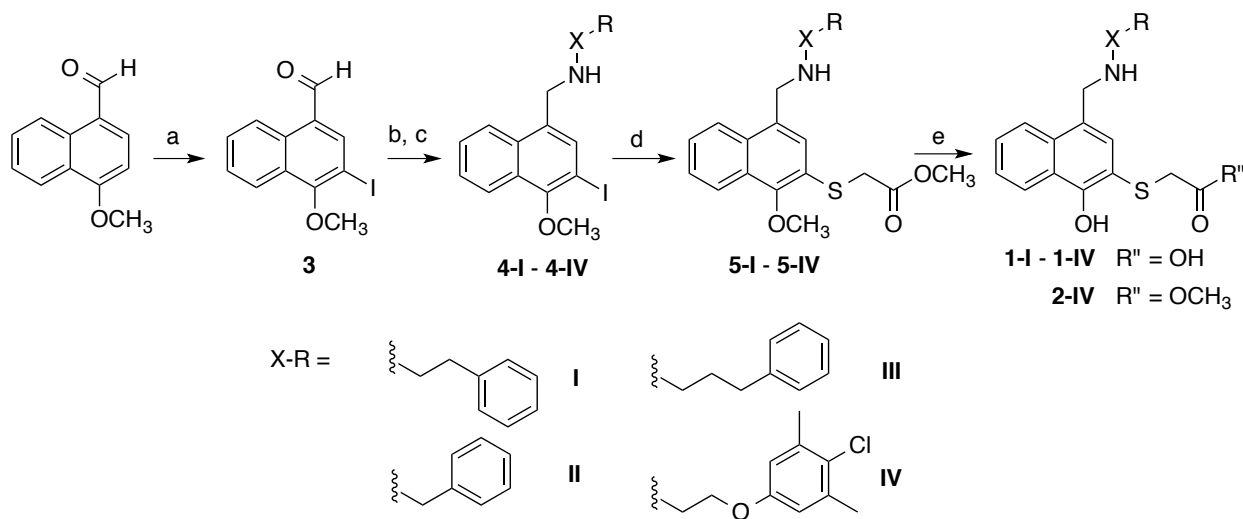
[a]Reagents and conditions: (a) NIS, TFA, reflux, 8 h, 77%; (b) phenylethylamine or benzylamine or phenylpropylamine or **6**, EtOH, reflux, 2 h; (c) NaBH$_4$, EtOH, reflux, 1 h, 47%-88% over two steps; (d) HSCH$_2$COOCH3, Pd$_2$(dba)$_3$, Xantphos, DIEA, 1,4-dioxane, 95 $^{\circ}$C, 2 h, 62%-82%; (e) BBr$_3$, CH$_2$Cl$_2$, 0 $^{\circ}$C to rt, 1 h, 8%-60% or BBr$_3$, CH$_2$Cl$_2$, 0 $^{\circ}$C to rt, 1 h, quench with MeOH at 0 $^{\circ}$C, 73%.

As mentioned previously, most of the amines were available commercially except 2-(4-chloro-3,5-dimethylphenoxy)ethanamine which was synthesized using Scheme A.2. 4-Chloro-3,5-dimethylphenol was subjected to Mitsunobu conditions[6] in the presence of 2-bromoethanol

to provide intermediate **6**. Displacement of bromide in **6** with an azide[7] and reduction of the azide to an amine using tin chloride[8] provided the desired amine **7**.

Scheme A.2. Synthesis of amine **7**[a].
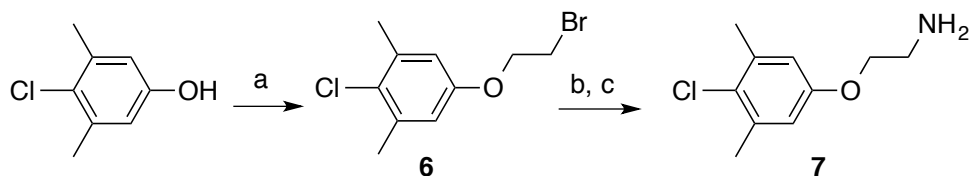
[a]Reagents and conditions: (a) 2-BrCH$_2$CH$_2$OH, PPh$_3$, DIAD, THF, 0°C to rt, overnight, 68%; (b) NaN$_3$, DMF, 60 °C, overnight, 97%; (c) SnCl$_2$, MeOH, rt, 1 h, 98%.

A.3   Results

Compound **I-1** was the first proposed compound with a phenylethyl at X-R that was synthesized using Scheme I.1 and gratifyingly it exhibited an IC$_{50}$ of 13 μM (Table A.1) which was comparable to analog **3** from our first-generation **59** series (Chapter 2) with a phenylsulfonamido group suggesting that our linking strategy works. Encouraged by our results, we wished to vary the length of the aliphatic linker and determine the optimum length. For that purpose, analogs **1-II** and **1-III** having one and three methylene(s), respectively, in between the amine and the phenyl ring were synthesized and evaluated. Interestingly both displayed similar binding affinities compared to **I-1**. These findings can be explained based on an overlay of the predicted docking poses of analogs **1-I**, **1-II**, and **1-III** (Figure A.3 A) suggesting that the phenyl in these analogs reaches the same distance despite the variation in the length of the linker.

Table A.1. Binding affinities of **1-I** and its analogs.

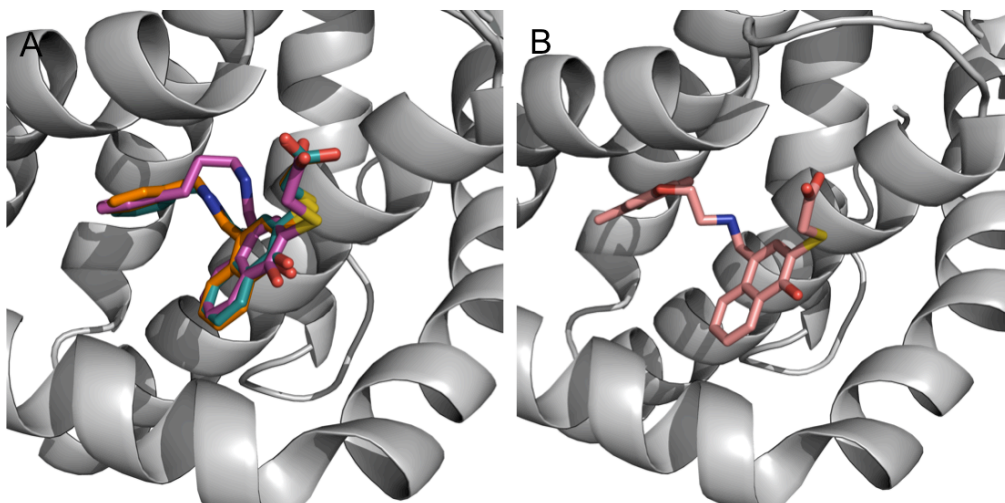| Cpd	X-R	R'	R"	FP IC$_{50}$ ± SD (μM)
Analog **3**				13.02 ± 1.62
1-I		-OH	-OH	13.2 ± 1.7
1-II		-OH	-OH	15.9
1-III		-OH	-OH	18.0
5-IV		-OCH$_3$	-OCH$_3$	613.9
1-IV		-OH	-OH	28.1
2-IV		-OCH$_3$	-OH	> 100

Figure A.3. Docking poses of analogs 1-I, 1-II, 1-III and 1-IV. (A) Overlay of putative binding poses of **1-I** (dark green), **1-II** (orange), **1-III** (magenta). (B) Putative binding mode of **1-IV**.

The predicted binding poses of second-generation **59** analogs suggested that the aryl group at R inserts into the p2 pocket of Mcl-1 and based on our previous knowledge from **59** as well as **38** classes of compounds, the majority of the gain in binding affinity came from introduction of halogenated aromatic or bi-aromatic rings. Furthermore, Friberg and coworkers reported improved potencies for their analogs when 3,5-dimethyl-4-chloro-phenyl or naphthyl were introduced in place of a phenyl. Therefore, to improve the potency, analog **1-IV** with a 3,5-dimethyl-4-chloro-phenoxyethyl at X-R was synthesized and evaluated. However, surprisingly this analog did not show any improvement in binding compared to **1-I** despite its favorable docking pose (Figure A.3 B). Furthermore, to our surprise, analog **1-IV** proved to be quite unstable even at -20 $^{\circ}$C and underwent chemical transformation.
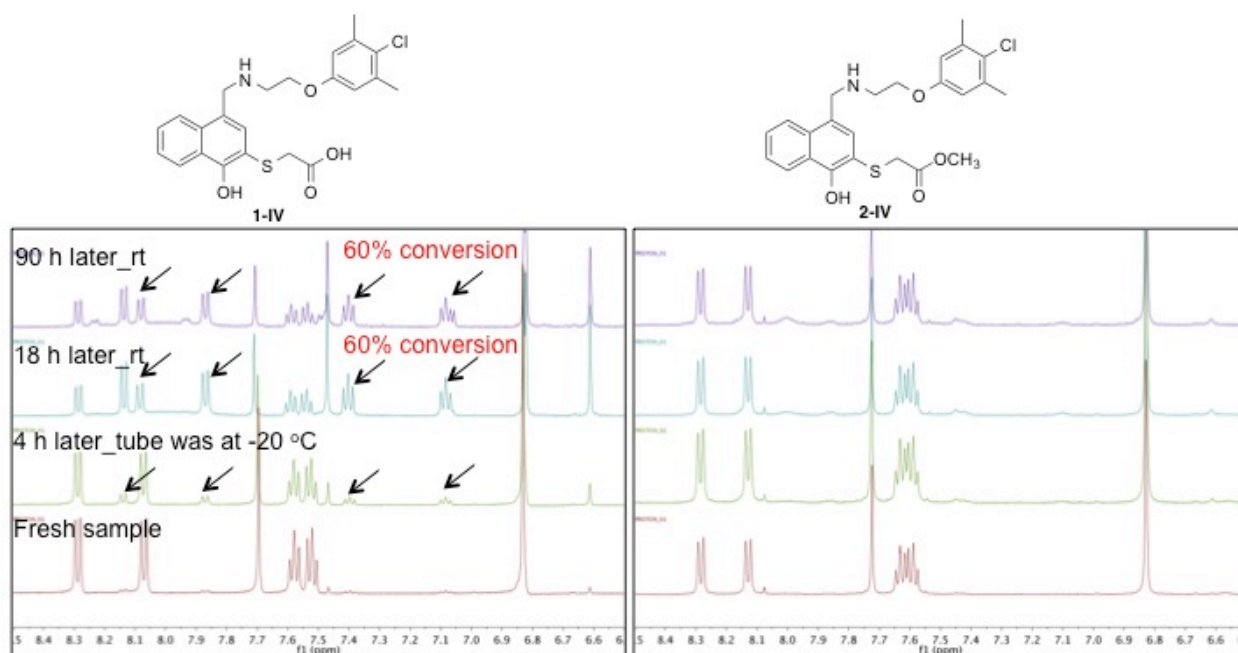
Figure A.4. Stability studies with 1-IV and 2-IV. 1D HNMR of analogs **1-IV** (left) and **2-IV** (right) in DMSO-d$_6$. Arrows point to newly forming peaks.

1D HNMR study of a sample of analog **1-IV** in deuterated DMSO kept at -20 $^{\circ}$C and then at room temperature showed that this compound undergoes chemical transformation by the appearance of a new set of peaks (Figure A.4). This transformation however appeared to stop at 60% conversion of **1-IV** to a new species and did not proceed further from comparison of a sample stored at room temperature for 18 h and 90 h. Interestingly, the transformation did not take place with analog **2-IV** (Figure A.4) suggesting that the free acid plays a role in this transformation possibly by providing a proton source for the amine to generate an ammonium species, which is an excellent leaving group. A possible mechanism of unraveling of **1-IV** has been proposed which involves fragmentation to quinomethide as well as the amine (Figure A.5 A). In-depth studies are needed to prove this mechanism; however, preliminary studies with liquid chromatography/mass spectrometry (LCMS) supported our proposed mechanism. LCMS chromatogram of the NMR sample of **1-IV** after 90 h period resulted in two peaks with a ratio of 1 (30%) to 2 (60%) (Figure A.5 B) matching the percentage conversion seen in 1D HNMR spectrum for the desired product versus the newly formed species. Additionally, MS analysis of the aforementioned peaks resulted in molecular mass of the desired product for the smaller peak (Figure A.5 C) and the molecular masses of the fragments in the larger peak (Figure A.5 D).
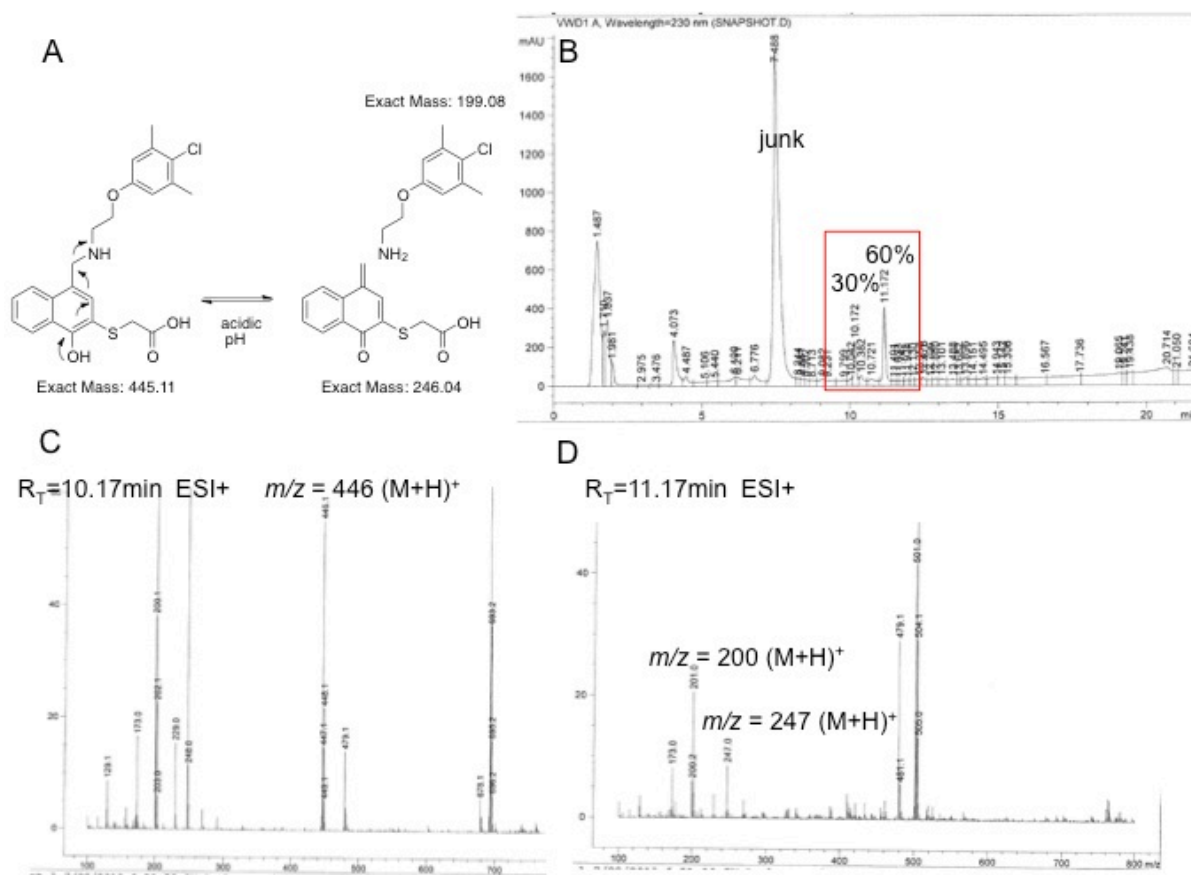
173

Figure A.5. LCMS trace of 1-IV after 90 h monitor. (A) Proposed mechanism for unraveling of **1-IV**. (B) LCMS chromatogram of NMR sample of 1-IV after 90 h period. (C) MS trace of the smaller peak at 10.17 min. (D) MS trace of the larger peak at 11.17 min.

It should be mentioned that NMR studies of other earlier analogs also resulted in the same type of conversion observed with **1-IV** indicating that this transformation is universal to this scaffold.
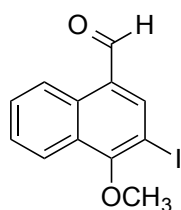
A.4   Conclusions

A second-generation **59** class of compounds was designed to improve the stability of the oxidation-prone hydronaphthoiminoquinone scaffold of **59** class. The design idea involved removal of the sulfonamide linker of first-generation compounds and introduction of an aliphatic amine linker inspired by the design of the recently reported selective Mcl-1 inhibitors. The proposed analog **1-I** provided a favorable docking pose and therefore was synthesized and resulted in reasonable potency compared to a similar analog from first-generation series. The impact of the length of the linker was briefly studied and did not greatly affect the potency.

However, additional elaboration of the phenyl ring of **1-I** to increase hydrophobic interactions at the p2 pocket of Mcl-1 and improve potency in analog **1-IV** was not successful. 1D NMR studies of analog **1-IV** showed that this analog is inherently unstable. A possible unraveling mechanism for this class of analogs was proposed which is supported by LCMS data.

A.5   Experimental

Chemistry

All anhydrous reactions were run under an atmosphere of dry nitrogen. Reagents were used as supplied without further purification. Reactions were monitored by TLC using precoated silica gel 60 F254 plates. Silica gel chromatography was performed with silica gel (220–240 mesh) obtained from Silicycle. Purities of final compounds were assessed by analytical HPLC performed on a Shimadzu system with a Restek Ultra C18 (4.6 x 150 mm, 5μm particle size) column or an Agilent 1100 series with an Agilent Zorbax Eclipse Plus−C18 column and a gradient of acetonitrile with 0.1 vol% TFA (10-90%) in water with 0.1 vol% TFA. Semi-preparative HPLC was performed on a Shimadzu system with a Restek Ultra C18 (21.2 x 150 mm, 5μm particle size) column. All NMR spectra were obtained in DMSO-d_6 or CDCl$_3$ and results were recorded at 400 MHz on a Varian 400 instrument or at 500 MHz on a Varian 500 instrument. Mass spectrometry analysis was performed using a Waters LCT time-of-flight mass spectrometry instrument utilizing electrospray ionization operating in positive-ion (ESI+) or negative-ion (ESI-) modes where indicated.


3-Iodo-4-methoxy-1-naphthaldehyde (3). A mixture of commercially available 1-methoxy-4-naphthaldehyde (504 mg, 2.7 mmol), N-iodosuccinimide (704 mg, 3.1 mmol) in TFA (10 mL) was heated to reflux and stirred for 8 h under nitrogen. The reaction mixture was diluted with EtOAc (20 mL), washed with saturated aqueous Na$_2$S$_2$O$_3$ solution (20 mL), saturated aqueous NaHCO$_3$ (20 mL x 2), and brine (20 mL). The organic layer was dried (MgSO$_4$), filtered and silica was added to filtrate and the solvent was removed under reduced pressure. The adsorbed crude residue was purified by flash column chromatography (hexane/EtOAc 96:4) on silica gel

to give **3** (648 mg, 77%) as a tan solid. ^{1}H NMR (400 MHz, CDCl$_3$) δ 10.23 (s, 1H), 9.22 (d, $J =$ 8.48 Hz, 1H), 8.26 (s, 1H), 8.18 (d, $J =$ 8.48 Hz, 1H), 7.71 (t, $J =$ 7.63 Hz, 1H), 7.62 (t, $J =$ 7.63 Hz, 1H), 4.04 (s, 3H); ^{13}C NMR (100 MHz, CDCl$_3$) δ 191.28, 162.11, 146.45, 131.97, 129.69, 129.44, 128.64, 127.75, 125.41, 122.73, 85.22, 62.06; ESI MS: m/z 313.0 (M+H)$^+$.
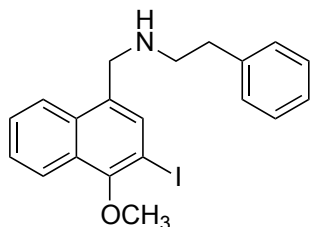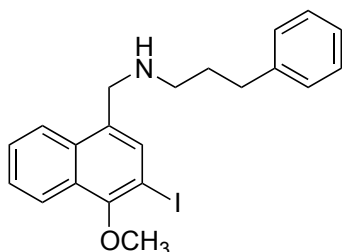

N-((3-Iodo-4-methoxynaphthalen-1-yl)methyl)-2-phenylethanamine (4-I).[4] To a stirring solution of **3** (106 mg, 0.34 mmol) dissolved in absolute EtOH was added phenylethylamine (44 µL, 0.35 mmol) at room temperature. The mixture was heated to reflux for 2 h. The reaction mixture was cooled down to room temperature and NaBH$_4$ (32 mg, 0.84 mmol) was added. The mixture was again heated to reflux for 1 h. The solvent was removed under reduced pressure. The residue was diluted with EtOAc (10 mL) and washed with aqueous 1N NaOH (5 mL x 2) and brine (10 mL). Organic layer was dried (Na$_2$SO$_4$), filtered and concentrated under reduced pressure to give the title compound (125 mg, 88%) as a yellow oil. The crude was used in the next reaction without further purification. ^{1}H NMR (500 MHz, CDCl$_3$) δ 8.16 (dd, $J =$ 6.4, 3.2 Hz, 1H), 8.03 (dd, $J =$ 6.3, 3.2 Hz, 1H), 7.79 (s, 1H), 7.54 (dd, $J =$ 6.4, 3.2 Hz, 2H), 7.32 (t, $J =$ 7.4 Hz, 2H), 7.26-7.22 (m, 3H), 4.16 (s, 2H), 3.98 (s, 3H), 3.04 (t, $J =$ 7.1 Hz, 2H), 2.89 (t, $J =$ 7.1 Hz, 2H). ^{13}C taken on 400 varian: ^{13}C NMR (100 MHz, CDCl$_3$) δ 155.92, 139.92, 134.86, 134.07, 132.95, 128.75, 128.54, 128.51, 126.82, 126.46, 126.23, 124.33, 122.94, 86.68, 61.66, 51.07, 50.69, 36.36.
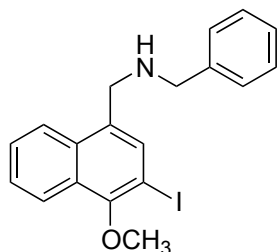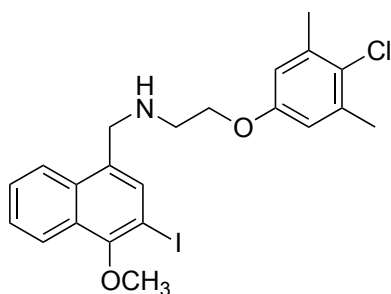

N-Benzyl-1-(3-Iodo-4-methoxynaphthalen-1-yl)methanamine (4-II). Synthesized using the procedure for **4-I** except benzylamine was used as the amine. The crude was subjected to flash column chromatography on silica gel to provide the title compound (197 mg, 76%) as a yellow

oil. ^{1}H NMR (400 MHz, CDCl$_3$) δ 8.16-8.10 (m, 1H), 8.08-8.01 (m, 1H), 7.80 (s, 1H), 7.57-7.50 (m, 2H), 7.41-7.33 (m, 3H), 7.31-7.24 (m, 1H), 4.13 (s, 2H), 3.96 (s, 3H), 3.91 (s, 2H). ^{13}C NMR (100 MHz, CDCl$_3$) δ 155.96, 140.06, 135.05, 134.02, 133.01, 128.52, 128.46, 128.24, 127.10, 126.79, 126.46, 124.44, 122.92, 86.55, 61.65, 53.76, 50.03.

N-((3-Iodo-4-methoxynaphthalen-1-yl)methyl)-3-phenylpropan-1-amine (4-III). Synthesized using the procedure for **4-I** except phenylpropylamine was used as the amine. The crude was subjected to flash column chromatography on silica gel to provide the title compound (216 mg, 78%) as a yellow oil. ^{1}H NMR (400 MHz, CDCl$_3$) δ 8.15 (d, J = 7.1 Hz, 1H), 8.08 (d, J = 7.7 Hz, 1H), 7.77 (s, 1H), 7.55 (p, J = 5.9 Hz, 2H), 7.28 (q, J = 6.5, 5.1 Hz, 2H), 7.22-7.15 (m, 3H), 4.12 (s, 2H), 3.97 (s, 3H), 2.77 (t, J = 7.1 Hz, 2H), 2.73-2.66 (m, 2H), 1.88 (p, J = 7.2 Hz, 2H). ^{13}C NMR (100 MHz, CDCl$_3$) δ 155.91, 142.07, 134.92, 134.27, 132.98, 128.53, 128.41, 128.35, 126.82, 126.45, 125.80, 124.39, 122.95, 86.62, 61.65, 50.89, 49.45, 33.62, 31.69.


2-(4-Chloro-3,5-dimethylphenoxy)-N-((3-iodo-4-methoxynaphthalen-1 yl)methyl)ethanamine (4-IV). Synthesized using the procedure for **4-I** except **7** was used as the amine. The crude was subjected to flash column chromatography on silica gel to provide the title compound (235 mg, 47%) as an orange oil. ^{1}H NMR (500 MHz, CDCl$_3$) δ 8.09-8.05 (m, 1H), 8.05-8.00 (m, 1H), 7.76 (s, 1H), 7.50-7.43 (m, 2H), 6.57 (s, 2H), 4.10 (s, 2H), 3.96 (t, J = 5.1 Hz, 2H), 3.89 (s, 3H), 2.99 (t, J = 5.0 Hz, 2H). ^{13}C NMR (125 MHz, CDCl$_3$) δ 156.55, 155.94, 136.91, 134.83, 133.91, 132.92, 128.47, 126.72, 126.39, 126.22, 124.36, 122.85, 114.49, 86.58, 67.42, 61.49, 50.47, 48.53, 20.91.
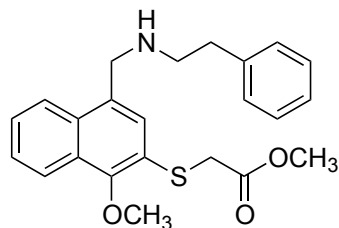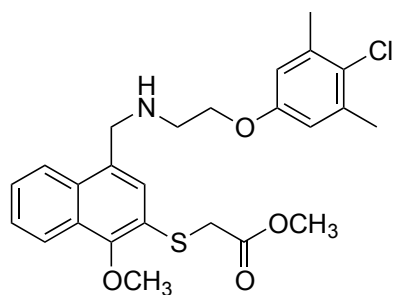
Methyl 2-((1-methoxy-4-((phenethylamino)methyl)naphthalen-2-yl)thio)acetate (5-I). To a solution of **4-I** (120 mg, 0.29 mmol) dissolved in dry 1,4-dioxane (2 mL) was added DIEA (101 μL, 0.58 mmol) at room temperature. The mixture was evacuated and backfilled with nitrogen (3 cycles) followed by addition of $Pd_2(dba)_3$ (15 mg, 0.016 mmol) and Xantphos (18 mg, 0.030 mmol). The reaction mixture was stirred for 5 min at room temperature then methyl thioglycolate (27 μM, 0.29 mmol) was added. The mixture was heated to 95 ^{o}C for 2 h. The reaction mixture was cooled down to room temperature and solvent was removed under reduced pressure. The residue was adsorbed onto silica gel and subjected to flash column chromatography on silica gel to provide the title compound (80 mg, 69%) as a red oil. ^{1}H NMR (500 MHz, CDCl$_3$) δ 8.13 (d, J = 8.0 Hz, 1H), 8.02 (d, J = 8.4 Hz, 1H), 7.56-7.51 (m, 2H), 7.49 (s, 2H), 7.31 (t, J = 7.4 Hz, 2H), 7.24 (q, J = 8.1, 7.3 Hz, 2H), 4.19 (s, 2H), 4.01 (s, 3H), 3.78 (s, 2H), 3.66 (s, 3H), 3.03 (t, J = 7.1 Hz, 2H), 2.89 (t, J = 7.1 Hz, 2H). ^{13}C NMR (125 MHz, CDCl$_3$) δ 170.23, 154.63, 140.01, 132.74, 132.36, 128.75, 128.59, 128.47, 128.02, 126.50, 126.27, 126.17, 124.10, 122.59, 122.49, 61.40, 52.48, 51.18, 51.04, 36.38, 35.45.
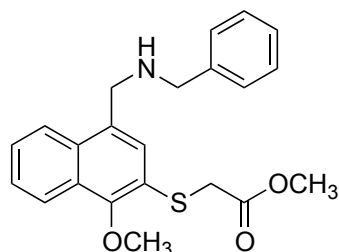

Methyl 2-((4-((benzylamino)methyl)-1-methoxynaphthalen-2-yl)thio)acetate (5-II). Synthesized using the procedure for **5-I** except **4-II** was used as the starting material. The crude was subjected to flash column chromatography on silica gel to provide the title compound (109 mg, 62%) as a red oil. ^{1}H NMR (500 MHz, CDCl$_3$) δ 8.12 (d, J = 8.0 Hz, 1H), 8.04 (d, J = 7.0 Hz, 1H), 7.55-7.48 (m, 3H), 7.41-7.37 (m, 2H), 7.35 (t, J = 7.5 Hz, 2H), 7.30-7.25 (m, 1H), 4.18 (s, 2H), 4.00 (s, 3H), 3.92 (s, 2H), 3.77 (s, 2H), 3.67 (s, 3H).^{13}C NMR (125 MHz, CDCl$_3$) δ 170.21, 154.77, 140.16, 132.65, 132.45, 128.62, 128.42, 128.33, 128.22, 127.04, 126.49, 126.27, 124.21, 122.58, 122.42, 61.40, 53.65, 52.48, 50.46, 35.51.
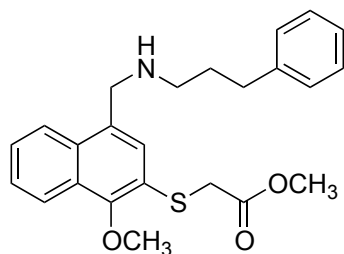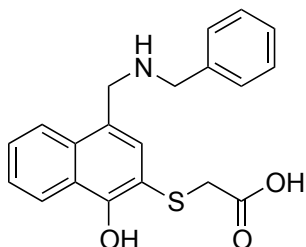
Methyl 2-((1-methoxy-4-(((3-phenylpropyl)amino)methyl)naphthalen-2-yl)thio)acetate (5-III). Synthesized using the procedure for **5-I** except **4-III** was used as the starting material. The crude was subjected to flash column chromatography on silica gel to provide the title compound (153 mg, 82%) as a brown oil. ^{1}H NMR (500 MHz, CDCl$_3$) δ 8.17-8.12 (m, 1H), 8.12-8.06 (m, 1H), 7.58-7.52 (m, 2H), 7.52-7.48 (m, 1H), 7.31-7.26 (m, 2H), 7.23-7.17 (m, 3H), 4.18 (s, 2H), 4.02 (s, 3H), 3.79 (s, 2H), 3.69 (s, 3H), 2.83-2.75 (m, 2H), 2.74-2.67 (m, 2H), 1.94-1.86 (m, 2H). ^{13}C NMR (125 MHz, CDCl$_3$) δ 170.24, 154.69, 142.09, 132.82, 132.40, 128.63, 128.41, 128.33, 128.21, 126.55, 126.30, 125.78, 124.15, 122.63, 122.49, 61.41, 52.51, 51.28, 49.31, 35.50, 33.62, 31.69.
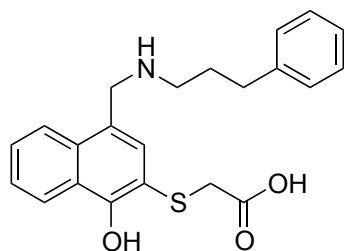

Methyl 2-((4-(((2-(4-chloro-3,5-dimethylphenoxy)ethyl)amino)methyl)-1-methoxynaphthalen-2-yl)thio)acetate (5-IV). Synthesized using the procedure for **5-I** except **4-IV** was used as the starting material. The crude was subjected to flash column chromatography on silica gel to provide the title compound (148 mg, 66%) as a yellow oil. ^{1}H NMR (500 MHz, CDCl$_3$) δ 8.15-8.11 (m, 1H), 8.11-8.07 (m, 1H), 7.56-7.49 (m, 3H), 6.64 (s, 2H), 4.24 (s, 2H), 4.08 (t, J = 5.1 Hz, 2H), 4.00 (s, 3H), 3.78 (s, 2H), 3.68 (s, 3H), 3.10 (t, J = 5.1 Hz, 2H), 2.33 (s, 6H). ^{13}C NMR (125 MHz, CDCl$_3$) δ 170.22, 156.57, 154.80, 137.07, 132.50, 132.39, 128.64, 128.26, 126.55, 126.36, 126.30, 124.10, 122.63, 122.45, 114.52, 67.49, 61.41, 52.48, 51.01, 48.52, 35.49, 20.93.
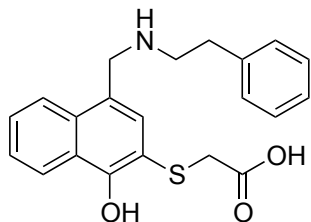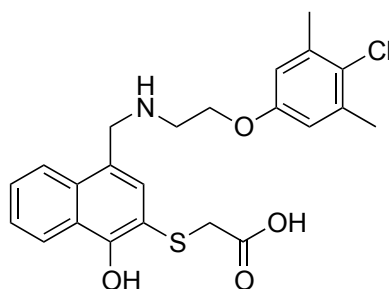
2-((1-Hydroxy-4-((phenethylamino)methyl)naphthalen-2-yl)thio)acetic acid (1-I). To a stirred solution of **5-I** (79 mg, 0.20 mmol) dissolved in dry CH_2Cl_2 (1.5 mL) was added BBr_3 (1 M in CH_2Cl_2, 0.60 mL, 0.60 mmol) dropwise at 0°C under nitrogen. The mixture was allowed to warm up to room temperature. After 1hr stir, the mixture was cooled down to 0°C and quenched with H_2O (2 mL). The reaction mixture was diluted with more H_2O (10 mL) and extracted with EtOAc (10 mL x 2). The combined organic extracts were washed with brine (15 mL), dried (Na_2SO_4), filtered, and the solvent was removed under reduced pressure. The crude was purified using a C_{18} reverse phase semipreparative HPLC column with solvent A (0.1% of TFA in water) and solvent B (0.1% of TFA in CH_3CN) as eluents to give the title compound (36 mg**, 49%**) as a white solid. 99% pure by HPLC. ^{1}H NMR (400 MHz, DMSO-d$_6$) δ 8.28 (d, J = 8.3 Hz, 1H), 8.10 (d, J = 8.4 Hz, 1H), 7.69 (s, 1H), 7.61 (t, J = 7.5 Hz, 1H), 7.54 (t, J = 7.6 Hz, 1H), 7.36-7.29 (m, 2H), 7.28-7.20 (m, 3H), 4.52 (s, 2H), 3.55 (s, 2H), 3.31-3.23 (m, 2H), 3.00-2.89 (m, 2H). ESI MS: m/z 368.2 (M+H)$^+$.

2-((4-((Benzylamino)methyl)-1-hydroxynaphthalen-2-yl)thio)acetic acid (1-II). Synthesized using the procedure for **1-I** except **5-II** was used as the starting material. The title compound (8 mg, 9%) as a white solid after HPLC purification. 90% pure by HPLC. ^{1}H NMR (500 MHz, DMSO-d$_6$) δ 8.27 (d, J = 8.3 Hz, 1H), 8.03 (d, J = 8.3 Hz, 1H), 7.71 (s, 1H), 7.65-7.60 (m, 1H), 7.60-7.56 (m, 1H), 7.53 (d, J = 7.1 Hz, 2H), 7.44 (q, J = 6.2 Hz, 3H), 4.54 (s, 2H), 4.29 (s, 2H), 3.71 (s, 2H). ESI MS: m/z 354.3 (M+H)$^+$.

2-((1-Hydroxy-4-(((3-phenylpropyl)amino)methyl)naphthalen-2-yl)thio)acetic acid (1-III). Synthesized using the procedure for **1-I** except **5-III** was used as the starting material. The title compound (6 mg, 8%) as a white solid after HPLC purification. 97% pure by HPLC. ^{1}H NMR (500 MHz, DMSO-d$_6$) δ 8.27 (d, J = 7.3 Hz, 1H), 8.11 (d, J = 7.7 Hz, 1H), 7.71 (s, 1H), 7.64 (t, J = 8.1 Hz, 1H), 7.58 (t, J = 6.4 Hz, 1H), 7.30 (t, J = 6.1 Hz, 2H), 7.23-7.17 (m, 3H), 4.51 (s, 2H), 3.68 (s, 2H), 3.03 (s, 2H), 2.64 (t, J = 7.9 Hz, 2H), 1.99-1.88 (m, 2H). ESI MS: m/z 382.3 (M+H)$^+$.

2-((4-(((2-(4-Chloro-3,5-dimethylphenoxy)ethyl)amino)methyl)-1-hydroxynaphthalen-2-yl)thio)acetic acid (1-IV). Synthesized using the procedure for **1-I** except **5-IV** was used as the starting material. The title compound (28 mg, 60%) as a white solid after HPLC purification. ^{1}H NMR (500 MHz, DMSO-d$_6$) δ 8.29 (d, J = 8.3 Hz, 1H), 8.07 (d, J = 8.4 Hz, 1H), 7.69 (s, 1H), 7.58 (t, J = 7.5 Hz, 1H), 7.55-7.50 (m, 1H), 6.83 (s, 2H), 4.55 (s, 2H), 4.24 (t, J = 5.0 Hz, 2H), 3.48 (s, 2H), 3.44-3.39 (m, 2H), 2.29 (s, 6H). ESI MS: m/z 446.1 (M+H)$^+$.
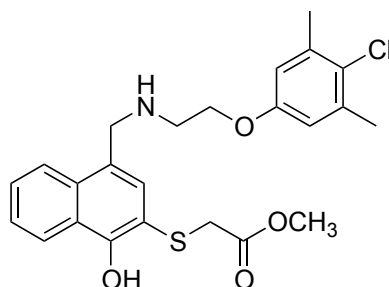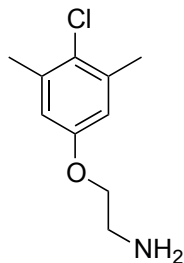

Methyl 2-((4-(((2-(4-chloro-3,5-dimethylphenoxy)ethyl)amino)methyl)-1-hydroxynaphthalen-2-yl)thio)acetate (2-IV). To a stirred solution of **5-IV** (50 mg, 0.10 mmol) dissolved in dry CH$_2$Cl$_2$ (1 mL) was added BBr$_3$ (1 M in CH$_2$Cl$_2$, 0.32 mL, 0.0.32 mmol)

dropwise at 0°C under nitrogen. The mixture was allowed to warm up to room temperature. The starting material was entirely consumed as determined by TLC after 1 h. The mixture was again cooled down to 0°C and MeOH (2 mL) was added. After addition, the mixture was allowed to warm up to room temperature and stirred for 1 h till a new spot formed as monitored by TLC. The reaction mixture was diluted with H_2O (10 mL) and extracted with EtOAc (10 mL x 2). The combined organic extracts were washed with brine (15 mL), dried (Na_2SO_4), filtered, and the solvent was removed under reduced pressure. The crude was purified using a C_{18} reverse phase semipreparative HPLC column with solvent A (0.1% of TFA in water) and solvent B (0.1% of TFA in CH_3CN) as eluents to give the title compound (34 mg, 73%) as a white solid. 97% pure by HPLC. ^{1}H NMR (500 MHz, DMSO-d_6) δ 8.28 (d, J = 8.2 Hz, 1H), 8.13 (d, J = 8.4 Hz, 1H), 7.72 (s, 1H), 7.65-7.61 (m, 1H), 7.61-7.57 (m, 1H), 6.83 (s, 2H), 4.61 (s, 2H), 4.25 (t, J = 4.9 Hz, 2H), 3.76 (s, 2H), 3.58 (s, 3H), 3.47-3.41 (m, 2H), 2.29 (s, 6H). ^{13}C NMR (125 MHz, DMSO-d_6) δ 170.39, 156.19, 154.87, 137.13, 135.05, 132.72, 127.93, 126.33, 126.16, 125.46, 124.32, 123.46, 119.85, 115.35, 112.86, 63.93, 52.68, 47.23, 46.20, 36.48, 20.92. ESI MS: m/z 460.0 $(M+H)^+$.
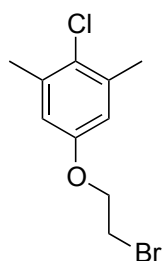

5-(2-Bromoethoxy)-2-chloro-1,3-dimethylbenzene (6).[6] To a stirring solution of 4-chloro-3,5-dimethylphenol (1 g, 6.26 mmol) in dry THF (23 mL) was added 2-bromoethanol (0.7 mL, 9.40 mmol) followed by PPh3 (2.53 g, 9.40 mmol) at room temperature. The reaction mixture was cooled down to 0°C and a solution of DIAD (1.95 mL, 9.40 mmol) in dry THF (2mL) was added dropwise over 3 min. The reaction mixture was warm up to room temperature and stirred overnight. The reaction mixture was diluted with H_2O (50 mL) and extracted with CH_2Cl_2 (40 mL x 2). Combined organic extracts were washed with brine, dried (Na_2SO_4), filtered and concentrated under reduced pressure. The crude residue was treated with a mixture of Et_2O and hexanes to crash triphenyl phosphine oxide which was filtered off. The crude was next subjected to flash column chromatography on silica gel to provide the title compound (1.12 g, 68%) as an oil which solidified to a white solid upon standing. ^{1}H NMR (500 MHz, CDCl$_3$) δ 6.66 (s, 2H),

4.25 (t, J = 6.3 Hz, 2H), 3.62 (t, J = 6.3 Hz, 2H), 2.36 (s, 6H). ^{13}C NMR (125 MHz, CDCl$_3$) δ 155.85, 137.30, 126.98, 114.76, 68.00, 29.08, 20.95.

2-(4-Chloro-3,5-dimethylphenoxy)ethanamine (7).
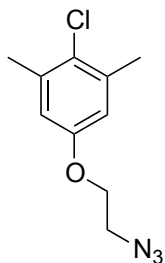
As previously reported[7], to a solution of **6** (505 mg, 1.92 mmol) in DMF (8 ml) was added NaN$_3$ (374 mg, 5.75 mmmol) and the reaction mixture stirred at 60 °C overnight at which time the reaction mixture was cooled down to room temperature. The reaction mixture was diluted with H$_2$O (30 ml) and extracted with Et$_2$O (30 ml x 2). The organic extracts were combined, washed with brine, dried (Na$_2$SO$_4$), filtered and concentrated under reduced pressure to provide 5-(2-azidoethoxy)-2-chloro-1,3-dimethylbenzene (421 mg, 97%) as a clear oil. The crude was used in the next reaction without further purification. ^{1}H NMR (500 MHz, CDCl$_3$) δ 6.66 (s, 2H), 4.07 (t, J = 4.9 Hz, 2H), 3.55 (t, J = 4.9 Hz, 2H), 2.36 (s, 7H). ^{13}C NMR (125 MHz, CDCl$_3$) δ 156.08, 137.18, 126.80, 114.56, 67.08, 50.16, 20.87.

As previously reported[8], to a stirring solution of SnCl$_2$ (700 mg, 3.69 mmol) in dry MeOH (3 mL) was added 5-(2-azidoethoxy)-2-chloro-1,3-dimethylbenzene (102 mg, 0.45 mmol) dissolved in dry MeOH (1 mL) dropwise at room temperature. The mixture was stirred at room temperature for 1 h. The reaction mixture was concentrated under reduced pressure. To the residue was added cold H$_2$O (10 mL) and the mixture was basified with 50% aqueous solution of NaOH. White solid (tin salts) precipitated and filtered. After filtration, the filtrate was diluted with more H$_2$O (20 mL) and extracted with EtOAc (15 mL x 2). The organic extracts were washed with brine, dried (Na$_2$SO$_4$), filtered and concentrated under reduced pressure to provide

the title compound (88 mg, 98%) as a yellow gel. Crude was used in the next step without further purification. ^{1}H NMR (500 MHz, CDCl$_3$) δ 6.60 (s, 2H), 3.87 (t, J = 5.1 Hz, 2H), 3.00 (t, J = 4.9 Hz, 2H), 2.29 (s, 6H). ^{13}C NMR (125 MHz, CDCl$_3$) δ 156.66, 137.07, 126.31, 114.49, 70.17, 41.48, 20.91.

Protein purification

His-tagged proteins containing Mcl-1 (residues 171–327) was expressed from the pHis-TEV vector (a modified pET vector) in *E. coli* BL21 (DE3) cells. Cells were grown at 37 ºC in 2×YT containing antibiotics to an OD$_{600}$ density of 0.6. Protein expression was induced by 0.4 mM IPTG at 37 ºC for 4 hours. Cells were lysed in 50 mM Tris pH 8.0 buffer containing 500 mM NaCl, 0.1% bME and 40 μl of Leupectin/Aprotin. Mcl-1 was purified from the soluble fraction using Ni-NTA resin (QIAGEN), following the manufacturer's instructions. Mcl-1 was further purified on a Source Q15 column (Amersham Biosciences) in 25 mM Tris pH 8.0 buffer, with NaCl gradient. Mcl-1 was stored in 25 mM Tris pH 8.0 buffers containing 150 mM NaCl and 2 mM DTT and at -80 ºC in presence of 25% Glycerol.

Determination of the K_d values of fluorescent probe to Mcl-1

Fluorescein tagged BID peptide (Flu-BID), labeled with fluorescein on the N-terminus of the BH3 peptide (79-99) was used as a fluorescent probe in the FP-based binding assays. The K_d value of the tracer was determined Mcl-1 with a fixed concentration of the tracer (2 nM of Flu-BID) and different concentrations of the tested proteins, in a final volume of 125 μl in the assay buffer (100 mM potassium phosphate, pH 7.5, 100 μg/ml bovine γ-globulin, 0.02% sodium azide, Invitrogen, with 0.01% Triton X-100 and 4% DMSO). Plates were mixed and incubated at room temperature for 2 hours and the polarization values in millipolarization units (mP) were measured at an excitation wavelength of 485 nm and an emission wavelength of 530 nm. Equilibrium dissociation constants (K_d) were calculated by fitting the sigmoidal dose-dependent FP increases as a function of protein concentrations using Graphpad Prism 6.0 software. The K_d value of Flu-BID to Mcl-1 was determined to be 34 ± 3.5 nM in our saturation experiments.

Fluorescence polarization-based binding assays

Sensitive and quantitative FP-based binding assays were developed and optimized to determine the binding affinities of small-molecule inhibitors to the recombinant Mcl-1. Based on the K_d value, the concentrations of the proteins used in the competitive binding experiment was 90 nM for Mcl-1. The fluorescent probes, Flu-BID was fixed at 2 nM. 5 μL of the tested compound in DMSO and 120 μL of protein/probe complex in the assay buffer (100 mM potassium phosphate, pH 7.5; 100 μg/ml bovine gamma globulin; 0.02% sodium azide, purchased from Invitrogen, Life Technologies) were added to assay plates (Microfluor 2Black, Thermo Scientific), incubated at room temperature for 3 h and the polarization values (mP) were measured at an excitation wavelength at 485 nm and an emission wavelength at 530 nm using the plate reader Synergy H1 Hybrid, BioTek. IC_{50} values were determined by nonlinear regression fitting of the competition curves (GraphPad Prism 6.0 Software).

Molecular modeling

Molecular docking calculations were performed using GOLD molecular docking tool[9]. To begin with, in accordance with required guidelines, molecular docking software tool GOLD was validated[10]. For this purpose, initial conformation of the ligand bound in the Mcl-1 active site (PDB: 4HW2) was extracted from its active site and subsequently docked using GOLD molecular docking package. The ligand binding site was defined as a 10 Å cavity around the ligand present in the 4HW2 strcture. The remaining waters and part of the ligand present in the unit cell were deleted for docking purposes. Hydrogen atoms were added to the Mcl-1 protein molecule using GOLD with default settings of the amino acid protonation pattern. Side chains of amino acids were treated as rigid entities. In the validation procedure ligand present in the crystal structure was docked 10 times into the defined binding site by applying the following parameters of the GOLD genetic algorithm (GA) (population size = 100, selection pressure = 1.1, no. of operations = 100000, no. of islands = 5, niche size = 2, migrate = 10, mutate = 95, crossover = 95) along with different scoring functions available in GOLD to provide initial measurement of binding affinity of the produced Mcl-1: ligand complex. The best agreement between the crystallized and docked pose was obtained using ChemPLP scoring function and it was used further for molecular docking calculations of the selected compounds from this study using the same docking settings.

A.6   Contributions

Fardokht Abulwerdi designed, synthesized and characterized all the compounds and intermediates with supervision from Dr. Nikolovska-Coleska and Dr. Hollis Showalter. Ahmed Mady performed all the biochemical experiments. Dr. Andrej Perdih performed all the molecular docking studies. The protein used for biochemical assays was expressed and purified in Dr. Jeanne Stuckey lab at LSI.

A.7   References

1.   Lipinski, C. A.; Lombardo, F.; Dominy, B. W.; Feeney, P. J., *Adv Drug Deliv Rev* 2001, *46* (1-3), 3-26.
2.   Cohen, N. A.; Stewart, M. L.; Gavathiotis, E.; Tepper, J. L.; Bruekner, S. R.; Koss, B.; Opferman, J. T.; Walensky, L. D., *Chem Biol* 2012, *19* (9), 1175-86.
3.   Friberg, A.; Vigil, D.; Zhao, B.; Daniels, R. N.; Burke, J. P.; Garcia-Barrantes, P. M.; Camper, D.; Chauder, B. A.; Lee, T.; Olejniczak, E. T.; Fesik, S. W., *J Med Chem* 2013, *56* (1), 15-30.
4.   Gotz, M. G.; James, K. E.; Hansell, E.; Dvorak, J.; Seshaadri, A.; Sojka, D.; Kopacek, P.; McKerrow, J. H.; Caffrey, C. R.; Powers, J. C., *J Med Chem* 2008, *51* (9), 2816-32.
5.   Itoh, T.; Mase, T., *Org Lett* 2004, *6* (24), 4587-90.
6.   Sen, S. E.; Roach, S. L., *Synthesis-Stuttgart* 1995, (7), 756-758.
7.   Raju, M. V.; Lin, H. C., *Org Lett* 2013, *15* (6), 1274-7.
8.   Pisani, L.; Muncipinto, G.; Miscioscia, T. F.; Nicolotti, O.; Leonetti, F.; Catto, M.; Caccia, C.; Salvati, P.; Soto-Otero, R.; Mendez-Alvarez, E.; Passeleu, C.; Carotti, A., *J Med Chem* 2009, *52* (21), 6685-706.
9.   Jones, G.; Willett, P.; Glen, R. C.; Leach, A. R.; Taylor, R., *J Mol Biol* 1997, *267* (3), 727-48.
10.   Kirchmair, J.; Markt, P.; Distinto, S.; Wolber, G.; Langer, T., *J Comput Aided Mol Des* 2008, *22* (3-4), 213-28.